

Characterisation of Host- Parasite- Microbiota Interactions that Drive Hatching in *Trichuris* Species

Tapoka Thulisile Mkandawire

Murray Edwards College



University of Cambridge & Wellcome Sanger Institute

November 2021

This dissertation is submitted for the degree of Doctor of Philosophy Supervised by

Dr María A. Duque Correa & Dr Matthew Berriman

Parasite Genomics Laboratory

Funded by the Wellcome Sanger Institute

Declaration

This dissertation is the result of my own work and includes nothing that is the outcome of work done in collaboration except as declared in the preface and specified in the text. It is not substantially the same as any that I have submitted, or, is being concurrently submitted for a degree or diploma or other qualification at the University of Cambridge or any other University or similar institution except as declared in the preface and specified in the text. I further state that no substantial part of my dissertation has already been submitted, or, is being concurrently submitted for any such degree, diploma or other qualification at the University of Cambridge or any other University or similar institution except as declared in the Preface and specified in the text. It does not exceed the word limit of 60,000 words (excluding bibliography, figures, and appendixes) as prescribed by the Degree Committee for the Faculty of Biology at the University of Cambridge.

Tapoka Thulisile Mkandawire November 2021

Abstract

Characterisation of Host- Parasite- Microbiota Interactions that Drive Hatching in *Trichuris* Species

Tapoka Thulisile Mkandawire

Trichuris trichiura infections account for 400 million individuals infected across the tropics and subtropics, making it a key neglected tropical disease (NTD). Infection occurs upon ingestion of whipworm eggs that hatch in the caecum and proximal colon, liberating larvae that establish in the intestinal epithelia. Trichuriasis has been studied in murine and porcine models of infection, with *Trichuris muris* and *Trichuris suis* respectively; revealing the role of the host intestinal microbiota in inducing hatching of whipworm eggs. However, the mechanisms behind the interactions between *Trichuris* species and the host microbiota that result in hatching, particularly in *T. trichiura*, remain unexplained. Understanding hatching could lead to greater control in the lab in maintaining *T. trichiura* life cycles, allowing us to use alternate more accessible hosts to study the human whipworm. I hypothesised that hatching in *Trichuris* spp, which is centered around the polar plugs of the egg, occurs as a result of physical interaction between the bacteria of the host microbiota and the parasite egg, and enzymatic activity that results in the degradation of the polar plugs and the liberation of the larvae. I isolated intrinsic and extrinsic factors that govern hatching in *Trichuris* species. In studying intrinsic factors in *T. muris* I discovered alterations in gene expression during embryonation that facilitate hatching, in particular serine proteases. I also examined the composition of the polar plugs to understand how they might be degraded in eclosion. In studying extrinsic factors in *T. muris*, *T. suis*, and *T. trichiura* I discovered that trichuris species preferentially respond to the microbiota from the parasite niche– the caecal mucosa, and that bacterial induced hatching of *Trichuris* species can be mediated by protease inhibitors. Furthermore, this study presents the first time a humanised microbiota model has been used to study *in vitro* hatching and *in vivo* infections of *T. trichiura*. In this study I isolated gastrointestinal samples that induce parasite hatching, and utilised metagenomic analyses to identify members of porcine, human, and humanised murine, microbiomes that could be responsible for inducing hatching of *T. suis* and *T. trichiura*, respectively.

Dedication

To the ones who taught me how to be resilient

*“The toughest wood with brightest blaze will greet:
The hardest nut contains the sweetest meat;
So wisdom, gained by light of midnight oil,
Gives richest recompense to patient toil.”*

Charles Eugene Banks

Acknowledgements

The PhD is never a journey taken alone and I have been surrounded and supported by many professionally and personally. Thank you to my supervisory team and my thesis committee for all the invaluable insight and wisdom that have truly made this a learning and growing experience. Thank you to my collaborators for the opportunities that have expanded my horizons and skill toolkit. Thank you to Wellcome for the funding and to all the Sanger Institute research and support teams, making it possible to generate and process all this data. Thank you to my colleagues across the institute for all the questions answered and projects worked on, from: parasitology and microbiology, through to public engagement and entrepreneurship. Finally thank you to all the volunteers who have kindly donated samples to my study making this work possible.

Incredible thanks to my family for the continued and unwavering support, and ultimately the inspiration and nurturing that led me down this scientific career path. Thanks to friends old and new, Cambridge has brought many fast friends into my life. I'm grateful for: the camaraderie of the Sanger PhD and MPhil cohorts I have gotten to know, the sisterhood at Murray Edwards College, and living in the same city as my best friend. As well as the delightful connections I made on exchange in Denmark; teaching gin at the Cambridge Distillery and Gin Laboratory; and teaching biology at SnapRevise. Final big thanks goes to my Manchester crew, whose love has never felt far, particularly over the last couple years through the magic of zoom.

Publications

Mkandawire, T. T., Grencis, R. K., Berriman, M., Duque-Correa, M. A.,
Hatching of parasitic nematode eggs: a crucial step determining infection,
Trends in Parasitology (2021).

Forster, S. C., Kumar, N., Anonye, B. A., Almeida, A., Viciani, E., Stares, M. D., Dunn, M.,
Mkandawire, T. T., Zhu, A., Shao, Y, Pike, L. J., Louie, T., Browne, H. P., Mitchell, A. L.,
Neville, B. A., Finn, R. D. & Lawley, T. D. A human gut bacterial genome and culture
collection for improved metagenomic analyses. Nature Biotechnology 37, 186-192 (2019).

Forster, S. C., Liu, J., Kumar, N., Gulliver, E., Gould, J., Escobar-Zepeda, A., **Mkandawire,**
T. T., Pike, L. J., Stares, M. D., Shao, Y., Browne, H. P., Neville, B. A., & Lawley, T. D. In
vitro demonstration of broad host range mobile genetic elements transferring antibiotic
resistance from the human microbiome. (*Under review*)
bioRxiv <https://doi.org/10.1101/2022.01.18.476738>

Table of contents

Declaration	2
Abstract	3
Dedication	4
Acknowledgements	5
Publications	6
Chapter 1- Introduction to Hatching in Nematodes	21
1.1 Introduction to Phylum Nematoda	21
1.2 The Importance of Parasitic Nematodes	22
1.3 Canonical Nematode Life Cycle	22
Figure 1.1. The Canonical Nematode Life Cycle.	23
1.4 The Structure and Function of the Nematode Egg	23
Table 1.1 Summary of nematode egg composition across representative species from major nematode clades	24
1.5 Nematode Hatching Cascade	25
Figure 1.2. Nematode Egg Hatching Cascade.	25
Table 1.2. Hatching-inducing factors and larval responses of <i>C. elegans</i> and key parasitic species from major nematode clades	28
1.6 Intrinsic and extrinsic hatching-inducing factors	33
1.7 <i>Trichuris</i> Life Cycle	36
Figure 1.3. The life cycle of <i>Trichuris trichiura</i> .	36
1.8 <i>Trichuris</i> Egg Structure and Composition	37
Figure 1.4. Embryonated <i>Trichuris muris</i> eggs.	38
1.9 Hatching in <i>Trichuris</i> Species	38
Figure 1.5. Hatching progression in <i>T. muris</i> .	40
1.10 Aims Of The Thesis And Contribution To The Field	41
1.11 Chapter Summaries	43
Chapter 3: Mechanistic study of bacterial–parasite interactions responsible for the induction of egg hatching in <i>T. muris</i> by <i>E. coli</i>	43

Chapter 4: Identification of extrinsic factors for hatching <i>Trichuris</i> spp	43
Chapter 5: Metagenomic analysis to identify bacterial species involved in hatching across <i>Trichuris</i> species.	43
Chapter 2- Materials and Methods	45
2.1 Bacterial culture	45
2.2 Parasite egg sources	45
2.3 <i>In vitro</i> <i>T. muris</i> egg hatching assays with <i>E. coli</i> MG1655, Keio Knockout Strains, <i>P. aeruginosa</i> , <i>S. aureus</i> , and <i>S. typhimurium</i> .	46
Table 2.1 Protease inhibitors and their working concentrations	46
cComplete™, Mini, EDTA-free Protease Inhibitor Cocktail	46
2.4 <i>In vitro</i> hatching assays with gastrointestinal tract samples	47
2.5 Mouse models and infections	48
2.5.1 Mice	48
2.5.2 Infection of SCID mice for <i>T. muris</i> maintenance	48
2.5.3 <i>T. muris</i> study of embryonation	48
2.5.4 Infection of humanised microbiota mice and WT C57BL/6 murine microbiota mice	49
2.6 Detection of parasite specific antibodies	49
2.7 Confocal and electron microscopy	49
2.7.1 Scanning electron microscopy	49
2.7.2 Confocal microscopy	50
2.8 Nucleic acid and protein extractions	50
2.8.1 RNA extraction	50
2.7.2 DNA extractions from gastrointestinal tract samples for metagenomic sequencing	51
2.8.3 Protein extraction	51
2.9 Library preparation and sequencing	51
2.9.1 RNAseq Library preparation and sequencing	52
2.9.2 Metagenomic and whole genome library preparation and sequencing	52
2.9.3 Peptide preparation and mass spectrometry	52
2.10 RNAseq analysis	52
2.11 Proteomic analysis	53

2.12 Metagenomic analysis	53
2.12.1 Identification and visualisation of genes in the Human Gastrointestinal Bacteria (HBC) Culture Collection	53
2.12.2 Taxonomic classification and differential analysis of metagenomic reads from gastrointestinal tract samples	54
2.12.3 Assembly of metagenomic genomes from metagenomic reads	54
Chapter 3- Mechanistic study of bacterial–parasite interactions responsible for the induction of egg hatching in <i>T. muris</i> by <i>E. coli</i>	57
3.1 Introduction	57
Table 3.1 Genes of the <i>fim</i> operon	58
Figure 3.1- Rough and smooth <i>E. coli</i> K12 MG1655 display differing colony morphologies and interactions with <i>T. muris</i> eggs.	60
Figure 3.2- Cartoon depicting the hypothesis of the minimum requirements for hatching.	62
3.2 The role of fimbriae in hatching of <i>T. muris</i> in the presence of <i>E. coli</i>	63
Figure 3.3. Bacterial colony morphology impacts levels of <i>T. muris</i> egg hatching induced by <i>E. coli</i> K12.	64
Figure 3.4. <i>fim</i> gene knockouts display reduced capability to induce hatching of <i>T. muris</i> eggs.	65
3.3 SEM on <i>T. muris</i> and <i>E. coli</i> , <i>S. typhimurium</i> , and <i>P. aeruginosa</i> co cultures.	65
Figure 3.5. Smooth <i>E. coli</i> K12 MG1655 display fimbriae when proximal to the <i>T. muris</i> polar plug.	67
Figure 3.6. <i>S. typhimurium</i> display fimbriae when proximal to the <i>T. muris</i> polar plug and do not attach to distal regions of the egg.	67
Figure 3.7. <i>P. aeruginosa</i> displays attachment pili when proximal to the <i>T. muris</i> polar plug.	68
3.4 Characterising the role of proteases in bacteria mediated hatching of <i>T. muris</i> eggs	68
Figure 3.8. Protease inhibitors mediate a reversible interruption of <i>E.coli</i> induced hatching of <i>T. muris</i> eggs.	69
Figure 3.9. Protease inhibitors mediate a titratable interruption of <i>E.coli</i> induced hatching of <i>T. muris</i> eggs.	71

Figure 3.10. <i>E. coli</i> induced hatching of <i>T. muris</i> eggs is ablated by the addition of a protease inhibitor cocktail, or serine protease inhibitor Pefabloc TM .	Error!
Bookmark not defined.	
Figure 3.11. <i>E. coli</i> K12 serine protease gene knockout <i>clpP</i> displays reduced capability to induce hatching of <i>T. muris</i> eggs.	74
Figure 3.12. <i>E. coli</i> K12 cysteine protease gene knockouts <i>hchA</i> and <i>ydhO</i> display reduced capability to induce hatching of <i>T. muris</i> eggs.	Error! Bookmark not defined.
Figure 3.13. Protease inhibitors interrupt bacterial mediated hatching of <i>T. muris</i> eggs.	76
3.5 The composition of the polar plug	77
Figure 3.14. Unique peptides of the polar plug inferred by subtractive proteomic analysis.	78
Table 3.2 Putative components of the polar plugs of <i>T. muris</i> eggs	79
3.6 Bacteria induced hatching of <i>T. muris</i> occurs after a minimum amount of embryonation	80
Figure 3.15. A minimum of 7 weeks of embryonation is required to observe <i>E. coli</i> induction of <i>T. muris</i> egg hatching. .	81
3.7 Changes in gene expression of <i>T. muris</i> occurring during embryonation	82
Figure 3.16. Immature and fully mature <i>T. muris</i> eggs have distinct RNA expression profiles.	83
Table 3.3 Top 20 genes expressed in immature and fully mature eggs	84
3.8 Discussion and Conclusions	87
Chapter 4- Identification of extrinsic host microbiota factors for hatching <i>Trichuris</i> spp	96
4.1 Introduction	
Figure 4.1. The distribution of bacteria and resources along the longitudinal and transverse axes of the gastrointestinal tract.	96
4.2 Inhibition of proteases impacts in vitro hatching of <i>T. muris</i> eggs with murine microbiota and humanised microbiota mice gastrointestinal tract samples	99
Figure 4.2. Hatching of <i>T. muris</i> with gastrointestinal tract samples from murine microbiota mice or mice with humanised microbiota is mediated by protease inhibitors.	102

4.3 Gastrointestinal tract samples from pigs display differing capabilities to induce hatching of <i>T. suis</i> and <i>T. muris</i> <i>in vitro</i> .	102
Figure 4.3 Greater levels of <i>T. muris</i> and <i>T. suis</i> egg hatching observed with porcine caecal mucosal scrapings.	103
4.4 In vitro hatching of <i>T. trichiura</i> eggs with Human Colon Biopsies	104
Figure 4.4. Hatching of <i>T. trichiura</i> eggs induced by human mucosal gastrointestinal tract contents is mediated by proteases.	105
4.5 Gastrointestinal tract samples from humanised microbiota mice induce <i>in vitro</i> hatching of <i>T. trichiura</i> eggs.	106
Figure 4.5. gastrointestinal tract samples collected from two humanised mice models display differing capability to induce hatching of <i>T. trichiura</i> <i>in vitro</i> .	108
4.6 In vivo study of <i>T. trichiura</i> and <i>T. muris</i> infections in murine microbiota and humanised microbiota mice	108
Figure 4.6. <i>T. trichiura</i> can establish an infection in humanised-microbiota mouse models.	110
Figure 4.7. Two humanised microbiota mice models display differing antibody responses to infections with <i>T. muris</i> and <i>T. trichiura</i> .	111
4.7 Discussion and Conclusions	112
Chapter 5- Metagenomic analysis to identify bacterial species involved in hatching across <i>Trichuris</i> species.	118
5.1 Introduction	118
Figure 5.1 Metagenomic analysis, workflow and tools.	122
5.2 Candidate genes important to hatching of whipworm eggs are found in human gut bacteria	123
Figure 5.2. The diversity of fimbrial and pili genes annotated in the HBC phylogram.	125
Table 5.1 Fimbrial and pili genes annotated in the HBC	126
Figure 5.3. <i>de novo</i> annotation increases the prediction of fimbrial genes in Firmicutes the HBC.	128
Figure 5.4. The distribution of serine protease genes involved in <i>T. muris</i> hatching in the HBC.	130
Figure 5.5. <i>de novo</i> annotation increases the prediction of serine protease genes in the HBC.	131

5.3 A differential analysis of relative taxonomic abundances in human biopsies capable of inducing hatching in <i>T. trichiura</i>	132
Figure 5.6 Genome assembly using MEGAHIT does not improve classification of gastrointestinal tract samples from humans.	133
Figure 5.7 Beta diversity of gastrointestinal tract samples from human biopsies reveals that a diverse collection of samples can induce hatching of <i>T. trichiura</i> .	134
Figure 5.8 The relative abundances of bacterial phyla in human gastrointestinal tract biopsies.	138
Table 5.2 Differentially abundant phyla in human biopsies isolated from the length of the lower gastrointestinal tract.	138
Table 5.3 Differentially abundant phyla and species in human biopsies capable of inducing <i>T. trichiura</i> hatching.	138
5.4 A differential analysis of relative taxonomic abundances in porcine gastrointestinal tract samples identifying hatching determinants in porcine caecal scrapings	141
Figure 5.9 Genome assembly using MEGAHIT improves classification of crude and cultured gastrointestinal tract samples from porcine caeca.	142
Figure 5.10 Beta diversity of gastrointestinal tract samples from pigs reveals that culturing is the greatest source of variation.	143
Figure 5.11 The relative abundance of bacterial phyla in porcine crude and cultured caecal samples.	147
Table 5.4 Differentially abundant phyla and species in porcine scrapings and contents isolated from the caecum.	147
Table 5.5 Differentially abundant phyla in crude porcine scrapings and contents and cultured metascrapes isolated from the caecum.	148
Table 5.6 Differentially abundant phyla in aerobically and anaerobically cultured metascrapes isolated from the porcine caecum.	148
5.5 A differential analysis of relative taxonomic abundances in naive humanised microbiota mice	149
Figure 5.12 Genome assembly using MEGAHIT improves classification of crude and cultured gastrointestinal tract samples from naive humanised microbiota mice and murine microbiota caeca.	150

Figure 5.13 Beta diversity of gastrointestinal tract samples from naive murine microbiota and humanised microbiota mice reveals samples capable of inducing hatching of <i>T. trichiura</i> form a distinct cluster.	151
Figure 5.14 Beta diversity of cultured gastrointestinal tract metascrapes from naive murine microbiota and humanised microbiota mice reveals that oxygen culturing conditions are the greatest source of variation.	152
Figure 5.15 The relative abundances of bacterial phyla in donor B humanised microbiota mice crude and cultured caecal samples.	156
Table 5.7 Differentially abundant phyla and species in donor B scrapings and contents isolated from the caecum.	156
Table 5.8 Differentially abundant phyla in crude donor B scrapings and contents and cultured metascrapes isolated from the caecum.	156
Table 5.9 Differentially abundant phyla in aerobically and anaerobically cultured metascrapes isolated from the caecum in donor B mice.	157
Figure 5.16 The relative abundances of bacterial phyla in donor A humanised microbiota mice crude and cultured caecal samples.	160
Table 5.10 Differentially abundant phyla in crude donor A scrapings and contents and cultured metascrapes isolated from the caecum.	160
Table 5.11 Differentially abundant phyla in aerobically and anaerobically cultured metascrapes isolated from the caecum in donor A mice.	161
5.6 A differential analysis of relative taxonomic abundances in infected humanised microbiota mice	162
Figure 5.17 Genome assembly using MEGAHIT improves classification of crude gastrointestinal tract samples from infected humanised microbiota mice and murine microbiota mice caeca.	163
Figure 5.18 Beta diversity of gastrointestinal tract samples from naive infected murine microbiota and humanised microbiota mice reveals that donor microbiota is the greatest source of variation.	165
Figure 5.19 The relative abundances of bacterial phyla in donor B and donor A humanised microbiota mice infected with <i>T. muris</i> and <i>T. trichiura</i> .	169
Table 5.12 Differentially abundant phyla and in naive humanised microbiota mice caecal contents and the caecal contents of mice infected with <i>T. muris</i> or <i>T. trichiura</i> .	169

Table 5.13 Differentially abundant phyla species in the caecal contents of mice capable of supporting a chronic <i>T. trichiura</i> infection.	170
5.7 Discussion and Conclusions	173
Chapter 6- Discussion and Future Directions	181
6.1 Key messages and future work	181
6.2 Concluding remarks	187
Bibliography	188

List of Figures

Figure 1.1. The Canonical Nematode Life Cycle.	23
Figure 1.2. Nematode Egg Hatching Cascade.	25
Figure 1.3. The life cycle of <i>Trichuris trichiura</i> .	36
Figure 1.4. Embryonated <i>Trichuris muris</i> eggs.	38
Figure 1.5. Hatching progression in <i>T. muris</i> .	40
Figure 3.1- Rough and smooth <i>E. coli</i> K12 MG1655 display differing colony morphologies and interactions with <i>T. muris</i> eggs.	60
Figure 3.2- Cartoon depicting the hypothesis of the minimum requirements for hatching.	62
Figure 3.3. Bacterial colony morphology impacts levels of <i>T. muris</i> egg hatching induced by <i>E. coli</i> K12.	64
Figure 3.4. <i>fim</i> gene knockouts display reduced capability to induce hatching of <i>T. muris</i> eggs.	65
Figure 3.5. Smooth <i>E. coli</i> K12 MG1655 display fimbriae when proximal to the <i>T. muris</i> polar plug.	67
Figure 3.6. <i>S. typhimurium</i> display fimbriae when proximal to the <i>T. muris</i> polar plug and do not attach to distal regions of the egg.	67
Figure 3.7. <i>P. aeruginosa</i> displays attachment pili when proximal to the <i>T. muris</i> polar plug.	68
Figure 3.8. Protease inhibitors mediate a reversible interruption of <i>E.coli</i> induced hatching of <i>T. muris</i> eggs.	69
Figure 3.9. Protease inhibitors mediate a titratable interruption of <i>E.coli</i> induced hatching of <i>T. muris</i> eggs.	71
Figure 3.10. <i>E.coli</i> induced hatching of <i>T. muris</i> eggs is ablated by the addition of a protease inhibitor cocktail, or serine protease inhibitor Pefabloc TM .	72
Figure 3.11. <i>E. coli</i> K12 serine protease gene knockout <i>clpP</i> displays reduced capability to induce hatching of <i>T. muris</i> eggs.	74
Figure 3.12. <i>E. coli</i> K12 cysteine protease gene knockouts <i>hchA</i> and <i>ydhO</i> display reduced capability to induce hatching of <i>T. muris</i> eggs.	75
Figure 3.13. Protease inhibitors interrupt bacterial mediated hatching of <i>T. muris</i> eggs.	76

Figure 3.14. Unique peptides of the polar plug inferred by subtractive proteomic analysis.	78
Figure 3.15. A minimum of 7 weeks of embryonation is required to observe <i>E. coli</i> induction of <i>T. muris</i> egg hatching. .	81
Figure 3.16. Immature and fully mature <i>T. muris</i> eggs have distinct RNA expression profiles.	
Figure 4.1. The distribution of bacteria and resources along the longitudinal and transverse axes of the gastrointestinal tract.	83
Figure 4.2. Hatching of <i>T. muris</i> with gastrointestinal tract samples from murine microbiota mice or mice with humanised microbiota is mediated by protease inhibitors.	103
Figure 4.3 Greater levels of <i>T. muris</i> and <i>T. suis</i> egg hatching observed with porcine caecal mucosal scrapings.	104
Figure 4.4. Hatching of <i>T. trichiura</i> eggs induced by human mucosal gastrointestinal tract contents is mediated by proteases.	106
Figure 4.5. gastrointestinal tract samples collected from two humanised mice models display differing capability to induce hatching of <i>T. trichiura in vitro</i> .	109
Figure 4.6. <i>T. trichiura</i> can establish an infection in humanised-microbiota mouse models.	111
Figure 4.7. Two humanised microbiota mice models display differing antibody responses to infections with <i>T. muris</i> and <i>T. trichiura</i> .	112
Figure 5.1 Metagenomic analysis, workflow and tools.	123
Figure 5.2. The diversity of fimbrial and pili genes annotated in the HBC phylogram.	126
Figure 5.3. de novo annotation increases the prediction of fimbrial genes in Firmicutes the HBC.	129
Figure 5.4. The distribution of serine protease genes involved in <i>T. muris</i> hatching in the HBC.	131
Figure 5.5. de novo annotation increases the prediction of serine protease genes in the HBC.	132
Figure 5.6 Genome assembly using MEGAHIT does not improve classification of gastrointestinal tract samples from humans.	134

Figure 5.7 Beta diversity of gastrointestinal tract samples from human biopsies reveals that a diverse collection of samples can induce hatching of <i>T. trichiura</i> .	135
Figure 5.8 The relative abundances of bacterial phyla in human gastrointestinal tract biopsies.	139
Figure 5.9 Genome assembly using MEGAHIT improves classification of crude and cultured gastrointestinal tract samples from porcine caeca.	143
Figure 5.10 Beta diversity of gastrointestinal tract samples from pigs reveals that culturing is the greatest source of variation.	144
Figure 5.11 The relative abundance of bacterial phyla in porcine crude and cultured caecal samples.	148
Figure 5.12 Genome assembly using MEGAHIT improves classification of crude and cultured gastrointestinal tract samples from naive humanised microbiota mice and murine microbiota caeca.	151
Figure 5.13 Beta diversity of gastrointestinal tract samples from naive murine microbiota and humanised microbiota mice reveals samples capable of inducing hatching of <i>T. trichiura</i> form a distinct cluster.	152
Figure 5.14 Beta diversity of cultured gastrointestinal tract metascrapes from naive murine microbiota and humanised microbiota mice reveals that oxygen culturing conditions are the greatest source of variation.	153
Figure 5.15 The relative abundances of bacterial phyla in donor B humanised microbiota mice crude and cultured caecal samples.	157
Figure 5.16 The relative abundances of bacterial phyla in donor A humanised microbiota mice crude and cultured caecal samples.	161
Figure 5.17 Genome assembly using MEGAHIT improves classification of crude gastrointestinal tract samples from infected humanised microbiota mice and murine microbiota mice caeca.	164
Figure 5.18 Beta diversity of gastrointestinal tract samples from naive infected murine microbiota and humanised microbiota mice reveals that donor microbiota is the greatest source of variation.	166
Figure 5.19 The relative abundances of bacterial phyla in donor B and donor A humanised microbiota mice infected with <i>T. muris</i> and <i>T. trichiura</i> .	170

List of Tables

Table 1.1 Summary of nematode egg composition across representative species from major nematode clades	24
Table 1.2. Hatching-inducing factors and larval responses of <i>C. elegans</i> and key parasitic species from major nematode clades	28
Table 2.1 Protease inhibitors and their working concentrations	46
Table 3.1 Genes of the <i>fim</i> operon	58
Table 3.2 Putative components of the polar plugs of <i>T. muris</i> eggs	79
Table 3.3 Top 20 genes expressed in immature and fully mature eggs	84
Table 5.1 Fimbrial and pili genes annotated in the HBC	127
Table 5.2 Differentially abundant phyla in human biopsies isolated from the length of the lower gastrointestinal tract.	139
Table 5.3 Differentially abundant phyla and species in human biopsies capable of inducing <i>T. trichiura</i> hatching.	139
Table 5.4 Differentially abundant phyla and species in porcine scrapings and contents isolated from the caecum.	148
Table 5.5 Differentially abundant phyla in crude porcine scrapings and contents and cultured metascrapes isolated from the caecum.	149
Table 5.6 Differentially abundant phyla in aerobically and anaerobically cultured metascrapes isolated from the porcine caecum.	149
Table 5.7 Differentially abundant phyla and species in donor B scrapings and contents isolated from the caecum.	157
Table 5.8 Differentially abundant phyla in crude donor B scrapings and contents and cultured metascrapes isolated from the caecum.	157
Table 5.9 Differentially abundant phyla in aerobically and anaerobically cultured metascrapes isolated from the caecum in donor B mice.	158
Table 5.10 Differentially abundant phyla in crude donor A scrapings and contents and cultured metascrapes isolated from the caecum.	161
Table 5.11 Differentially abundant phyla in aerobically and anaerobically cultured metascrapes isolated from the caecum in donor A mice.	161
Table 5.12 Differentially abundant phyla and in naive humanised microbiota mice caecal contents and the caecal contents of mice infected with <i>T. muris</i> or <i>T. trichiura</i> .	170

Table 5.13 Differentially abundant phyla species in the caecal contents of mice capable of supporting a chronic *T. trichiura* infection.

Chapter 1- Introduction to Hatching in Nematodes

Declaration of contributions

M. Duque-Correa and M. Berriman supervised this work. I performed all literature review and synthesis.

Publication

The following chapter has been published as:

“Hatching of Parasitic Nematode Eggs: A Crucial Step Determining Infection.”

Tapoka T Mkandawire; Richard K Grencis, Professor; Matthew Berriman, PhD; Maria A.

Duque-Correa, PhD

(Mkandawire et al. 2021)

The gastrointestinal tract is home to millions of organisms including parasites, bacteria, viruses, and fungi, each playing different roles. Members of the gut microbiota can have effects on diet and metabolism, immune signalling, as well as disease susceptibility and progression (Rinninella et al. 2019; Smallwood et al. 2017; Duque-Correa et al. 2019; Nayfach et al. 2019). Studies have shown that complex relationships exist between hosts, parasites, and the microbiota, with nematodes, like the whipworm, requiring interactions with the host microbiota to complete key transitions in the life cycle (Hayes et al. 2010; White et al. 2018; Vejzagić, Thamsborg, et al. 2015). While we know that whipworms interact with the host microbiota, we have not yet fully characterised the interactions between the human whipworm, and the human intestinal microbiota. Understanding the molecular mechanisms parasites can use to invade and exploit the host, not only increases our fundamental understanding of their biology. It also allows us to understand and develop strategies against infections, and may one day lead to novel immunotherapeutics (Smits et al. 2010). Current advances in molecular biology and in microbiome analysis are perfectly positioned to facilitate investigations into host- parasite- microbiota interactions.

1.1 Introduction to Phylum Nematoda

Nematoda is a speciose phylum occupying most environmental habitats, from alpine grasslands to marine sediment, as well as colonising plants and animals, including 43,945 known vertebrate hosts (Dobson et al. 2008; Kergunteuil et al. 2016; Blaxter and Koutsovoulos

2015). 23,000 nematode species have been described but it is estimated that the phylum comprises up to 1 million species (Blaxter and Koutsovoulos 2015; Lambdhead 1993). With their relatively simple body plans and life cycles, they are a highly successful group of animals. Nematodes are a major component of soil, indeed the best known species *Caenorhabditis elegans*, resides in the soil. *C. elegans* was the first animal to have its whole genome sequenced, and is an extensively used model organism (Blaxter and Koutsovoulos 2015). Nematoda can also exist in extreme environments; for example, Rhabditida and Plectida have been isolated from permafrost and were still viable after an estimated 30,000-40,000 years (Shatilovich et al. 2018). Additionally, the *Auanema* spp. have extreme arsenic resistance and were isolated from Mono Lake CA, US (Sapir 2021; Shih et al. 2019). Another notable feature of the phylum is parasitism, and nematodes are responsible for over 1 billion human infections (Jourdan et al. 2018).

1.2 The Importance of Parasitic Nematodes

Parasitism has arisen independently across Nematoda and has resulted in the average mammalian or avian host harbouring at least three parasitic nematode species (Dobson et al. 2008; Blaxter and Koutsovoulos 2015). Infections cause an enormous impact on human, animal, and plant health and have gross medical, social and economic repercussions. In terms of human health, it has been estimated that approximately 1.45 billion people are infected with at least one soil transmitted helminth (STH), accounting for an average of 4.98 million years lived with disability (YLDs) (Nicol et al. 2011; Jourdan et al. 2018; Pullan et al. 2014). STHs are gastrointestinal parasitic nematodes that infect humans. This group includes giant roundworms (*Ascaris lumbricoides*), whipworms (*Trichuris trichiura*), hookworms (*Necator americanus* and *Ancylostoma duodenale*), and threadworms (*Strongyloides stercoralis*) (Jourdan et al. 2018; Pullan et al. 2014). In regards to animal health, all livestock farmed with pasture-grazing are exposed to gastrointestinal nematodes and the resistance of these parasites to certain classes of anthelmintics costs the European livestock industry €38 million annually (Charlier et al. 2020). Agriculturally, annual crop production losses to nematodes are estimated to be between 8.8–14.6% (Nicol et al. 2011).

1.3 Canonical Nematode Life Cycle

Unlike Platyhelminthes, the other phylum containing human-parasitic worms, Nematoda is unusual because the majority of members undergo life cycles that have several key transitions in common (Figure 1.1) (Lee 2002b). The canonical nematode life cycle starts with embryonation inside an egg, giving rise to a first-stage (L1) larva. The larva grows and moults

through three subsequent larval stages (L2-L4), each time increasing in size and shedding its cuticle, with a final moult resulting in a sexually reproductive adult (Figure 1.1). Variations to this canonical scheme are seen across several species, for instance certain *Xiphinema* spp. only have three juvenile stages (Robbins et al. 1996; Halbrendt and Brown 1992). Additionally, the first moult for several plant nematodes, such as *Meloidogyne* spp. and *Globodera* spp., occurs inside the egg, as does the first two moults for *Ascaris* species. (Lee 2002a; Maung 1978; Bird 1977; Chitwood and Perry 2009; Baldwin and Handoo 2018). Free-living species hatch seemingly spontaneously in the environment; however, hatching is likely still governed by a specific internal switch or external cue that is more challenging to isolate (Van Gundy 1965). Conversely, for parasitic nematodes, there is often a clear stimulus for their “non-spontaneous” hatching. Hatching of embryonated eggs can occur either inside a host, as happens in *Ascaris* spp. or in the environment, as occurs with the hookworms and threadworms that hatch and develop through to the L3 stage before infecting a new host (Panesar and Croll 1980; Geenen et al. 1999; Croll 1974; Viney 1994). Finally, to create new eggs and complete the life cycle, fully developed adults typically reproduce sexually (Lee 2002b), but notable exceptions include parthenogenetic reproduction from adult female root-knot nematodes (*Meloidogyne* spp.) and threadworms (*Strongyloides* spp.) (Castagnone-Sereno 2006; Chitwood and Perry 2009; Viney 1994).

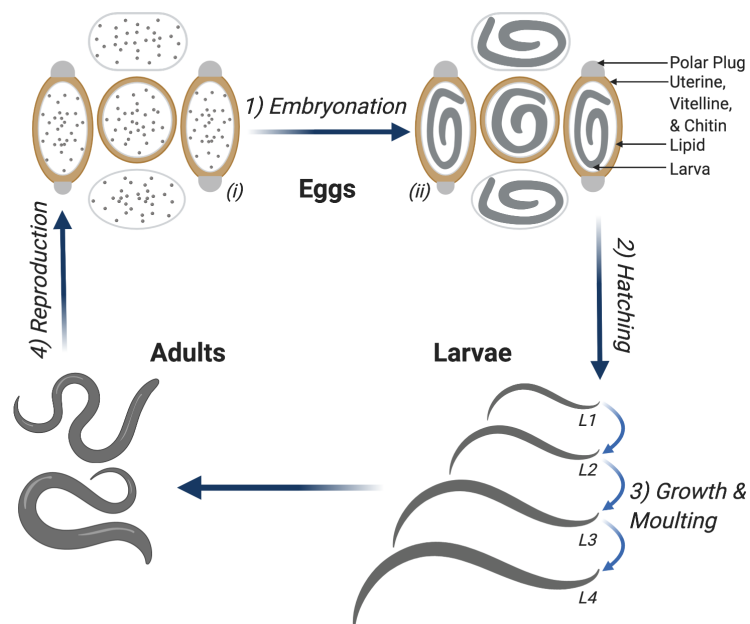


Figure 1.1. The Canonical Nematode Life Cycle. Key stages in a nematode life cycle are shown: 1) eggs transition from (i) unembryonated to (ii) embryonated states; 2) eggs hatch; 3) larvae transition from L1-L4 stages by growing and undergoing successive moults; and 4) adults reproduce generating new eggs and completing the cycle. (Image created with BioRender.com).

1.4 The Structure and Function of the Nematode Egg

The role of the egg in the nematode life cycle is multifaceted (Stein and Golden 2018; D. Wharton 1980). Firstly, the egg provides a contained environment in which embryonation, and occasionally moulting, can occur. Secondly, the nematode eggshell acts as a protective shield and both its structure and composition contribute to this function. Specifically, the components of the eggshell form a multi-layered and resilient barrier composed of lipid, chitin, vitelline (mainly glycoproteins) and, in some species, uterine layers (Figure 1.1 , Table 1.1) (D. Wharton 1980). The arrangement of these layers makes the eggshell resistant to stress but also selectively permeable (D. Wharton 1980; Quilès, Balandier, and Capizzi-Banas 2006). Thus, eggs persist in the environment for long periods of time; for example, *Ascaris suum* eggs remain viable in the environment for up to 10 years (Lindgren et al. 2020; Muller 1953). On the other hand, the selective permeability of nematode eggs allows them to receive cues from and respond to the outside environment thereby preventing premature hatching, but triggering it under favourable conditions (Johnston and Dennis 2012). Finally, the eggshell serves as a vehicle for the larva to reach the site of hatching and infection (Wharton 1980).

Table 1.1 Summary of nematode egg composition across representative species from major nematode clades

Clade ¹	Order	Species	Uterine layer	Vitelline layer	Chitinous layer	Lipid layer	Reference
			Present (+) or Absent (–)				
I	Trichurida	<i>Trichuris suis</i>	–	+	+	+	(Wharton and Jenkins 1978; Beer 1973b)
III	Oxyurida	<i>Enterobius vermicularis</i>	+	+	+	+	(Inatomi 1957; Jacobs, Jones, and Others 1939)
	Ascaridida	<i>Ascaris lumbricoides</i>	+	+	+	+	(Meng et al. 1981)
IV	Tylenchida	<i>Globodera rostochiensis</i>	–	+	+	+	(Clarke, Cox, and Shepherd 1967; Bird and McClure 1976)
V	Strongylida	<i>Haemonchus contortus</i>	–	+	+	+	(Waller 1971)
¹ Phylogenetic clades as defined by Blaxter et al (Blaxter et al. 1998)							

1.5 Nematode Hatching Cascade

In addition to the commonalities found in the life cycle, the process of hatching is broadly conserved across nematode species, and progresses through the following cascade: (1) induction via intrinsic and extrinsic factors that promote changes in the eggshell and volume of the eggs, (2) changes in larval behaviour and activity, and (3) larval eclosion (Figure 1.2) (Perry 2002). The current wealth of knowledge in hatching in nematodes is summarised using key representatives from the phylum, for which specific hatching factors and the effect they have on hatching have been described (Table 1.2).

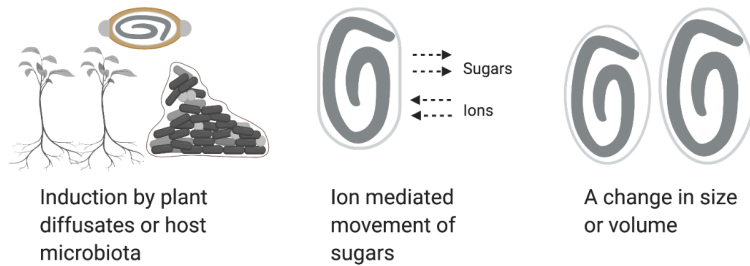
Much work has gone into describing hatching in nematodes particularly those with large health and economic repercussions, however there are still some key gaps in the knowledge. Induction of hatching has been investigated primarily in parasitic nematodes, in which host cues lead to an ion-mediated exchange of water and sugars across the eggshell, altering osmotic pressure, the flexibility of the eggshell, and the size of the egg (Figure 1.2) (Perry 2002). For instance, in the potato-cyst nematode *Globodera rostochiensis* calcium mediates trehalose exchange across the eggshell during hatching induction (Perry 2002; Duceppe et al. 2017); and *Tylenchorhynchus maximus* eggs swell in the early stages of hatching (Figure 1.2) (Panesar and Croll 1981; Bridge 1974). Surprisingly, the factors that induce hatching in *C. elegans* are not known; however, the eggs of *C. elegans* exhibit weakening and digestion of the eggshell during hatching (Perry 2002; Hall, Herndon, and Altun 2017a).

Larval movement and metabolic activity increase as hatching progresses, following distinct patterns of widespread or local exploration (Figure 1.2)(Perry 2002). Widespread exploration, or unfocussed movement that includes head waving and whole body rolling, occurs well before eclosion. For example, in *T. maximus* continuous movement is observed for up to three days before hatching (Bridge 1974). Local exploration immediately precedes eclosion, and consists of targeted and localised thrusting of the larval head or tail, secretions from the pharyngeal glands, and propulsion of the larval worm's stylet (oral spear) to cut through the shell, strategies employed by *Aphelenchus avenae*, and *Meloidogyne* spp (Perry 2002; Taylor 1962; Curtis, Robinson, and Perry 2009). In *G. rostochiensis*, local exploration is used to both propel and guide the stylet to create a perforated slit in one region of the eggshell (Perry 2002; Bridge 1974). In some nematode species, the larva also produces enzymes to weaken the integrity of the eggshell. These enzymes are released through activation of the pharyngeal glands (Perry 2002). Pharyngeal pumping has been observed in *A. avenae*, *G. rostochiensis*, and *C. elegans*, and enzymes including chitinases, lipases and proteases have been found in the perivitelline fluid (extracellular fluid in the nematode egg that surrounds the embryo) or

hatching fluid (secretions released into the hatching media) of *Ascaris lumbricoides*, *Haemonchus contortus*, and *Ancylostoma ceylanicum* (Perry 2002; Taylor 1962; Rogers 1958; Rogers and Brooks 1977; Doncaster and Shepherd 1967; Abriola et al. 2019; Chen et al. 2021).

The last step of the hatching process is eclosion, where occasionally, the whole egg shell degrades as has been observed in *A. lumbricoides* (Rogers 1958). More commonly, nematode species exit the egg head first, some simply by pushing their head against the eggshell like *C. elegans* where distortion of the eggshell is observed around the head prior to eclosion (Hall, Herndon, and Altun 2017a). Some species identify specific eclosion sites: *Capillaria* species, in addition to utilising a stylet, exit the egg through the polar plugs, and *Enterobius vermicularis* egresses through a thinned region of the eggshell (Perry 2002; Wehr 1939; Inatomi 1957). Finally, an alternative method, only observed to date in a few species, is posterior-driven eclosion. *A. ceylanicum* and *Ancylostoma tubaeforme* occasionally perforate the shell with their tail, before reversing to emerge head first (Matthews 1985); and *Haemonchus contortus* and *Heterodera iri* utilise their sharp tail to perforate the shell and emerge tail first (Silverman and Campbell 1959; Laughlin, Lugthart, and Vargas 1974; Rogers and Brooks 1977).

Step I: induction via intrinsic/extrinsic factors



Step II: changes in behaviour



Step III: eclosion

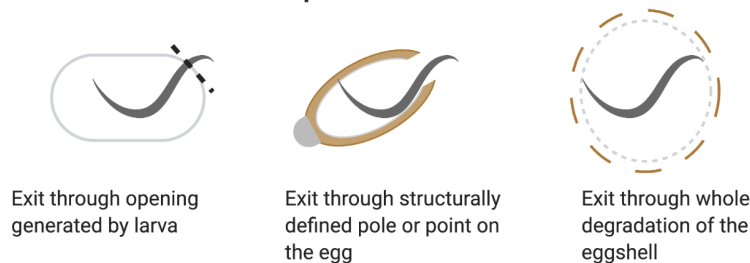


Figure 1.2. Nematode Egg Hatching Cascade. Hatching is the mechanism by which larvae are released from the eggs. The hatching cascade begins with induction via intrinsic or extrinsic factors that promote changes in the eggshell including increased flexibility and permeability and alterations on the egg osmotic pressure and volume. These include host or environmental molecules; the ion mediated exchange of sugars such as trehalose; and uptake of water and rehydration. These changes activate the larva to increase its movement in both a random and targeted manner, through induction of head waving, stylet propulsion and enzyme secretion. The final step is eclosion, the exit of the larvae from the eggshell that happens through an orifice in the egg generated by the larvae, via the polar plug, or through the complete degradation of the eggshell. (Image created with BioRender.com)

Table 1.2. Hatching-inducing factors and larval responses of *C. elegans* and key parasitic species from major nematode clades

Clade ¹	Species	Host	Intrinsic Factors and Larval Responses	Host Factors	Physicochemical/ Environmental Factors
I	<i>Trichuris muris</i>	<i>Mus musculus</i>	Larval movement aids hatching. Larvae use stylet to perforate polar plug (Panesar and Croll 1981)	Eggs hatch in the host caecum and proximal colon where host gut microbiota is required to induce hatching (Panesar and Croll 1980; White et al. 2018) Incubation of eggs with <i>Escherichia coli</i> , <i>Salmonella typhimurium</i> , <i>Pseudomonas aeruginosa</i> , and <i>Staphylococcus aureus</i> induces hatching <i>in vitro</i> via accumulation around polar plugs (Hayes et al. 2010)	Hatching occurs at 37°C (Panesar and Croll 1981) Incubation with sodium hypochlorite for 2 hours at 37°C with 5% carbon dioxide, followed by incubation in RPMI media at 37°C with 5% carbon dioxide results in hatching after 4-5 days (White et al. 2018)
	<i>Trichuris suis</i>	<i>Sus domesticus</i>		Eggs hatch in response to mucosal scrapings from the host gastrointestinal tract (Vejzagić, Thamsborg, et al. 2015)	Embryonation is impaired below 5°C and above 40°C. Hatching induced by stirring eggs with glass beads and HCl. Hatching occurs at 37°C (Vejzagić et al. 2016; Vejzagić, Thamsborg, et al. 2015)
	<i>Trichuris trichiura</i>	<i>Homo sapiens</i>			Oxygen is continually up taken during embryonation, and rapid changes in its availability or low starting concentrations impede development (Nolf 1932)
I	<i>Capillaria obsignata</i> *	<i>Gallus gallus domesticus</i>	L1 have a distinct stylet used during hatching (Wehr 1939; Wakelin 1965)	Eggs hatch in the host small intestine (Tiersch et al. 2013; Wehr 1939)	Chemical solutions influence rate of embryonation and affect larval fitness/infectivity. For example, incubation in sulphuric

		<i>Columba livia domestica</i>			acid results in more embryonated eggs than incubation in water (Tiersch et al. 2013). In addition, potassium dichromate increases embryonation, but the infectivity of eggs embryonated in this way is low (Tiersch et al. 2013)
III	<i>Ascaris lumbricoides</i>	<i>H. sapiens</i>	“Hatching fluid” collected from eggs contains enzymes (Rogers 1958)		Carbon dioxide, sodium bicarbonate, and a reducing agent such as sodium dithionite are the minimum requirement for hatching (Rogers 1958)
	<i>Ascaris suum</i>	<i>S. domesticus</i>	Larvae need to be sufficiently embryonated to survive hatching (Geenen et al. 1999)	Bile has a positive effect on hatching at 5% concentration, at concentrations above 20% it is detrimental (Han et al. 2000)	High carbon dioxide concentration and mechanical stimulation induces hatching (Han et al. 2000)
IV	<i>Globodera rostochiensis</i>	<i>Solanum tuberosum</i>	Larvae can diapause or quiescence to pause development and prevent hatching in unfavourable environmental conditions (Masler and Perry 2018)	Natural hatching stimulant is potato root diffusate (Duceppe et al. 2017)	Calcium ions mediate the change in osmotic stress allowing movement of the sugar trehalose (Duceppe et al. 2017)
	<i>Globodera pallida</i>	<i>Solanum lycopersicum</i>	Change in osmotic stress ends larval dormancy,		

			concomitantly large changes in larval metabolism are observed (Duceppe et al. 2017)		
	<i>Heterodera glycines</i>	<i>Glycine max</i>	Larvae use directed stylet thrusts to create a series of perforations and eventually a slit in eggshell (Doncaster and Shepherd 1967)	Natural hatching stimulant is soybean root exudate (Thapa et al. 2017)	Hatching can be stimulated artificially using sodium metavanadate or zinc chloride (Doncaster and Shepherd 1967; Thapa et al. 2017)
	<i>Tylenchorhynchus maximus</i>	<i>Hordeum vulgare</i>	Larvae push head against and use stylet to rupture the eggshell (Bridge 1974)		
	<i>Meloidogyne incognita</i>	~3000 species of plants		Root diffusates from susceptible and resistant plants suppress hatching to different levels, due to varied phenol and ester content (Yang et al. 2016)	
	<i>Merlinius icarus</i>	<i>Lolium perenne</i>	Larvae push their heads against the eggshell and use their stylet to rupture the egg wall (Bridge 1974)		
	<i>Aphelenchus avenae</i>	~54 species of fungi	Larvae puncture the shell using their stylet (Taylor 1962)		Eggs require temperature in an optimal range 10°C - 38°C for successful hatching (Taylor 1962)
V	<i>Caenorhabditis</i>	Free-living	Larval movement inside the egg is observed		Changes in egg shell flexibility are observed, in particular

	<i>elegans</i>		before eclosion (Hall, Herndon, and Altun 2017b) Enzymes such as hch-1 are required for hatching (Hishida et al. 1996)		deformation at the anterior end (Hall, Herndon, and Altun 2017b)
	<i>Pristionchus pacificus</i>	Free-living		In certain strains (PS312, RLH163, PS1843, RS5194, RS5186), exposure to beetle pheromone ZDTO delays embryonation indirectly preventing hatching (Renahan and Hong 2017)	
	<i>Haemonchus contortus</i>	<i>Ovis aries</i>	Larvae use their sharp tails to rupture the eggshell before eclosion (Silverman and Campbell 1959) “Hatching fluid” collected from eggs contains a lipase that induces hatching (Rogers and Brooks 1977)		Hatching begins at temperatures above 9°C and occurs in the presence of water (Silverman and Campbell 1959)
	<i>Ancylostoma ceylanicum</i>	<i>Canis familiaris</i> <i>H. sapiens</i> <i>Mesocricetus auratus</i>	Chitinases are released by larvae during the hatching process (Abriola et al. 2019)	Host faecal material or live bacteria required to induce hatching and development from L1 to L3 stage (Reiss et al. 2007)	

	<i>Necator americanus</i>	<i>H. sapiens</i>	Larval movement begins as a response to changes in osmotic pressure (Croll 1974)		Optimal temperature, humidity and oxygen are required to induce hatching (Croll 1974)
¹ Phylogenetic clades as defined by Blaxter et al (Blaxter et al. 1998) * <i>Capillaria obsignata</i> also referred to as <i>Capillaria columbae</i> .					

1.6 Intrinsic and extrinsic hatching-inducing factors

Hatching in nematodes is traditionally considered to be “spontaneous” or “non-spontaneous” (Van Gundy 1965), and while the process of hatching is broadly conserved, there are a wide variety of factors that induce hatching and each species responds to specific ones (Table 1.2). These factors can be split into two large categories: intrinsic and extrinsic factors. Intrinsic larval factors are harder to identify as we lack an understanding of the genes governing embryonation and hatching in many nematode species. Pausing or arresting development is the primary intrinsic or larva-directed strategy for preventing untimely hatching, but this is often in response to an unsuitable external environment for hatching (Perry 2002). In cyst nematodes, entering diapause during the egg stage in response to unfavourable conditions has been well documented (Masler and Perry 2018). Temperature is the primary cue that initiates or relieves this state, allowing nematodes to hatch during favourable seasons (Masler and Perry 2018). In addition to a dependence on temperature to progress development, in *A. suum*, eggs that have not reached the stage of full embryonation cannot be induced to hatch successfully (Geenen et al. 1999); however, a genetic explanation for this observation remains outstanding. Host cues or food availability can also trigger developmental arrest. This is the case of *Pristionchus pacificus*, a free-living nematode that is, however, necromenically associated with several beetle species (Renahan and Hong 2017). Pheromones from living beetles halt *P. pacificus* embryonation, preventing untimely hatching in the absence of food (Renahan and Hong 2017).

In addition to disruptions in development preventing hatching, there are intrinsic factors that affect the progression of hatching. As larvae develop there are stage-specific changes in gene expression (Cotton et al. 2014; J. Wang, Garrey, and Davis 2014); some of the genes may be temporally expressed by the larvae to facilitate the progression of hatching. For example, in *C. elegans*, mutants for the *hch-1*, *vab-19*, *snx-3*, and *ddo-3* genes all exhibit delayed hatching as a phenotype (Brundage et al. 1996; Hishida et al. 1996; Ding et al. 2003; Saitoh et al. 2019). The most interesting of these is perhaps *hch-1* where the mutation gives a clear insight into the internal mechanism behind hatching in *C. elegans*. Specifically, the hatching cascade is induced and progresses but *hch-1* mutants are unable to complete eclosion as they do not express this gene, which encodes a putative hatching enzyme needed to degrade the eggshell (Hishida et al. 1996).

Extrinsic factors are particularly important for traditionally 'nonspontaneous' hatchers and can be host-derived, environmental, and physicochemical. Host cues are important for species that hatch inside their host, a strategy employed by animal-parasitic nematodes such as those of the *Ascaris* genera (Table 1.2). In the case of *A. suum*, hatching is induced by bile, a process that is replicated in the laboratory by exposing eggs to a bile concentration of 5%; however, higher bile concentrations have a detrimental effect on hatching (Table 1.2) (Han et al. 2000). The hookworm species *A. ceylanicum* can be hatched *in vitro* in either faecal charcoal culture or faeces coated filter paper strips, suggesting that the microbiota play role in hatching (Chiejina 1982; Navitsky et al. 1998). An agar plate method for *in vitro* culturing has been developed and confirmed the role of bacteria in hatching by demonstrating that eggs incubated with live *E. coli* culture produced viable infective larvae. This study revealed some insights into the molecular mechanisms of hatching of hookworms. Successful induction of hatching requires a live bacterial culture; growth media alone and growth media with heat killed *E. coli* do not produce viable larvae (Reiss et al. 2007).

Studies of plant-parasitic nematodes have shown that host cues can have positive, neutral, or negative hatching effects. Specifically, for members of the *Globodera* genus, hatching can be induced by plant diffusates, thus enabling the parasites to minimise time and resources spent on migration to reach their host (Ochola et al. 2020; Duceppe et al. 2017). Conversely, the majority of *Meloidogyne* species do not require host stimuli for hatching (Wesemael, Perry, and Moens 2006); hatching in *Meloidogyne chitwoodi* is neither positively or negatively affected by the presence of root diffusates (Wesemael, Perry, and Moens 2006). In *Meloidogyne incognita*, extracts from tomato roots have been shown to suppress hatching (G. Yang et al. 2016). The level of hatching suppression is dependent on the tomato plant's level of nematode resistance, and is reflected in the different proportions of phenols and esters contained in their diffusates, suggesting that these chemicals interfere with hatching pathways (G. Yang et al. 2016).

Environmental factors also influence hatching. Optimal pH, temperature, oxygen availability, and carbon dioxide levels all play a role, along with the texture, moisture, and microbial activity of the soil in the case of soil nematodes such as plant-parasitic nematodes and STHs (Perry 2002; Curtis, Robinson, and Perry 2009; Topalović and Vestergård 2021). Attempts to replicate these environmental factors in the laboratory have revealed the minimal physicochemical stimuli that induce hatching for some nematode species, including various chemicals and artificial mechanical action (Table 1.2).

Temperature plays a crucial role in embryonation and hatching; at nonoptimal temperatures, eggs fail to thrive from the outset. *A. avenae*, *Capillaria obsignata*, and *Trichuris* and *Ascaris* species exhibit poor embryonation and hatching if subjected to extreme cold or heat (Taylor 1962; Nolf 1932; Wakelin 1965; Curtis, Robinson, and Perry 2009). The composition of the air surrounding the eggs is another key hatching determinant. Specifically, the availability of moisture and gases such as carbon dioxide and oxygen are critical, with desiccation posing the greatest threat to *Ascaris* eggs (Nolf 1932; Caldwell and Caldwell 1928), and moisture being required by several species (Table 1.2) (Caldwell and Caldwell 1928). The gaseous requirements vary between nematodes. *T. trichiura* eggs continually take up oxygen during embryonation, and a drastic change in oxygen availability arrests development (Table 1.2) (Nolf 1932). In our own experience, we observe decreased hatching of *T. trichiura*, *T. suis* and *T. muris* in an anaerobic environment. In *Ascaris*, carbon dioxide is crucial to hatching, but *N. americanus* prefers oxygen in the environment (Table 1.2) (Nolf 1932; Croll 1974; Rogers 1958).

Investigations into the chemical stimuli that could serve as hatching factors have found that some biologically less obvious and unlikely compounds can serve as stimuli. Clarke and Shepherd tested over 400 chemicals while investigating the response of plant-parasitic *Heterodera* species to iron commonly present in soil, and discovered that zinc and vanadium are also able to induce hatching in these species (Clarke, Cox, and Shepherd 1967; Doncaster and Shepherd 1967; Thapa et al. 2017). Laboratory studies on the responses of nematodes to soil microbial products that aimed to identify nematicidal molecules revealed that some of these molecules induce increased rates of hatching in addition to larval mortality (Kerry and Hominick 2002). Specifically, 2,4-diacetylphloroglucinol produced by *Pseudomonas fluorescens*, and chitinases produced by *Streptomyces griseus*, augment hatching and larval mortality in *G. rostochiensis* and *Meloidogyne hapla*, respectively (Cronin et al. 1997; Mercer, Greenwood, and Grant 1992).

Physical perturbation designed to mimic the actions of peristalsis in the gastrointestinal tract can artificially induce hatching, as evidenced by hatching of *A. suum* ova by stirring with glass beads (Han et al. 2000). *A. suum* eggs can also be hatched using pressure between two coverslips (Geenen et al. 1999). The survival of larvae released by this procedure depends on their stage of development inside the egg, which correlates with their infectivity to mice (Geenen et al. 1999). Ultimately, the intrinsic and extrinsic factors are inextricably linked; and whether 'spontaneous' or 'nonspontaneous', hatching commencement and progression in nematodes is the result of active participation by larvae in response to stimuli.

1.7 *Trichuris* Life Cycle

T. trichiura infections cause Trichuriasis and account for 400 million individuals infected across the globe. Despite this large burden on global health, treatment and research has remained relatively underfunded and the WHO have defined it as a priority neglected tropical disease (NTD) (Else et al. 2020). *Trichuris* infections in animals are found across the globe and human infections were once ubiquitous but are now segregated to countries in the tropics and sub-tropics (Søe et al. 2015; Gildner and Casana 2021; Else et al. 2020). This is due to the nature of transmission in humans which occurs in regions with poor water sanitation and hygiene (WASH), and is particularly high where human waste is used as fertiliser or where untreated waste is released into the environment (“CDC, Parasites - Trichuriasis” 2019). Human infections can result in heavy or light worm burden and individuals in endemic regions often suffer from chronic infections due to frequent reinfections or incomplete clearance of the parasite (O’Dempsey 2010). Cases with light worm burdens are often asymptomatic, but heavy worm burden results in: *Trichuris* dysentery syndrome, diarrhoea, anaemia, fatigue, and in extreme cases, rectal prolapse (Shears et al. 2018; Jourdan et al. 2018).

Including the human infective species, there are over 70 members of the *Trichuris* genus, infecting a variety of domestic and wild hosts (Else et al. 2020). The murine and porcine whipworms, *T. muris* and *T. suis*, have provided key model systems to study (“CDC, Parasites - Trichuriasis” 2019) (Burden and Hammet 1976; Panesar 1981). In *Trichuris* species, transmission occurs through the oral-faecal route, and the life cycle begins with embryonation (“CDC, Parasites - Trichuriasis” 2019; Else et al. 2020). *Trichuris* eggs contaminate soil and water sources, where embryonation occurs in the absence of light and in response to temperature and moisture (Figure 1.3). Transmission to humans then occurs upon the ingestion of contaminated food and water. In pigs *T. suis* infections are of veterinary importance as transmission occurs during grazing and animals continually face exposure (Lindgren et al. 2020); and in mice, *T. muris* is transmitted in part because mice are coprophagic animals that re-ingest stool (Ebino 1993; Sakaguchi 2003). The majority of the life cycle— hatching, growth and moulting, and reproduction— occurs inside the host in the caecum and proximal colon. After hatching in response to the host microbiota, *Trichuris* first stage (L1) larvae invade the intestinal epithelial cells of the caecum forming syncytial tunnels where they grow and mature through a series of moults (Panesar 1981). Adult worms then reproduce, and females release eggs into the gastrointestinal tract to be passed in faeces (Panesar 1981; Else et al. 2020).

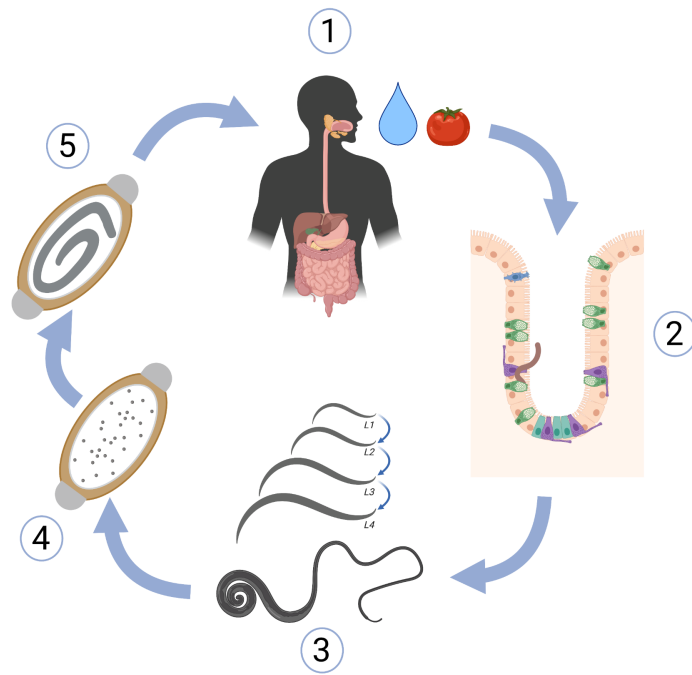


Figure 1.3. The life cycle of *T. trichiura*. During stage 1 eggs are ingested orally through contaminated food and water. At stage 2 eggs hatch releasing larvae into the caecum and proximal colon where they burrow into the intestinal epithelium. During stage 3 larvae grow and moulting takes place generating adult worms. Adult worms reproduce and the females lay eggs that are released into the environment through faeces in stage 4. The eggs then undergo embryonation in the soil developing into infective larvae in stage 5. Once embryonation is complete the eggs can be ingested completing the cycle. Image made with Biorender.com

1.8 *Trichuris* Egg Structure and Composition

Trichuris eggshells comprise three layers: a vitelline, a chitin, and a lipid layer (Wharton and Jenkins 1978) (Figure 1.4). The eggs are oval shaped with a defined point at each pole known as the polar or opercular plug (Nolf 1932). The composition of the polar plugs is not yet known conclusively; however, imaging studies suggest they are composed of an extension of the chitin in the eggshell that is less densely packed (Wharton and Jenkins 1978; Appleton and White 1989). The extended chitin forms a matrix of chitin fibres that suspends material with a reduced protein density (Wharton and Jenkins 1978). The molecules suspended in the chitin matrix are likely hydrophilic molecules, given the observation that the polar plugs swell during hatching (Panesar and Croll 1981). The eggs are incredibly resistant and thus persist in the environment for long periods of time; *T. suis* has been reported to maintain viability over 10 years (Lindgren et al. 2020; Burden, Hammet, and Brookes 1987).

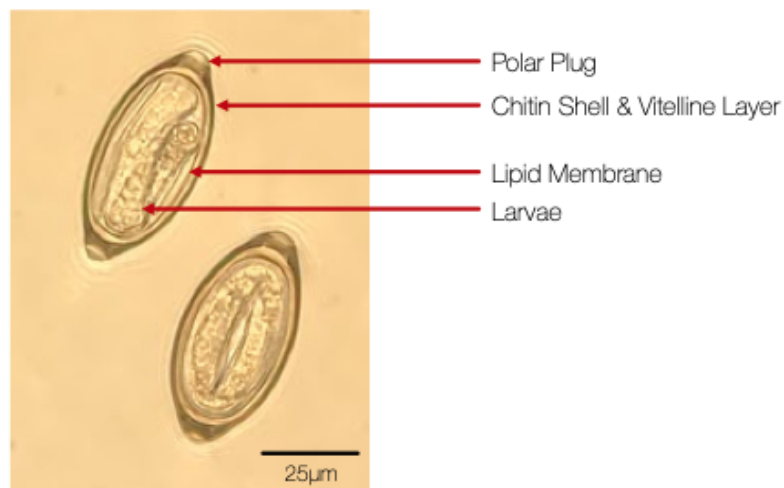


Figure 1.4. Embryonated *Trichuris muris* eggs. The key features of the egg structure have been labelled. There are two opercular plugs. The outer shell is formed of chitin and covered in a vitelline layer not visible at this magnification. The larvae are enclosed in an inner lipid membrane

1.9 Hatching in *Trichuris* Species

Studies on hatching of *Trichuris* species have focussed on *T. muris* strains that readily infect laboratory mice and can be reliably induced to hatch using bacteria: The Edinburgh, Japan, and Sobreda strains (Panesar and Croll 1981; Hayes et al. 2010; Koyama 2013; Bancroft, Else, and Grencis 1994; Wakelin 1969; Johnston et al. 2005; Bellaby et al. 1995). Studies in *T. muris* demonstrated that embryonation is temperature dependent, and development is arrested in eggs exposed to extreme temperatures (Nolf 1932; Vejzagić et al. 2016; Forman et al. 2021). As seen in other nematodes, induction of the hatching cascade begins with alterations in osmotic pressure in *T. muris*, eggs swell in the early stages of hatching (Panesar and Croll 1981). As hatching progresses, eclosion is facilitated by larval movement, in particular the action of the stylet against the polar plugs (Panesar and Croll 1981). Studies on the specific activation of hatching in response to the correct niche (the caecum and proximal colon) revealed that *T. muris* hatches in response to mouse caecal but not ileal contents (Panesar and Croll 1980). The specific involvement of the gastrointestinal microbiota in *T. muris* hatching was later confirmed by studies using antibiotics and germ free mice. The addition of antibiotics to gastrointestinal tract contents or bacterial cultures prevented the *in vitro* hatching of *T. muris* (Hayes et al. 2010; Koyama 2013); and antibiotic dosed or germ free mice are incapable of sustaining an infection (White et al. 2018). Germ-free mice are only able to sustain an infection once colonised with *Bacteroides thetaiotaomicron*, or *E. coli* strains (White et al. 2018; Venzon et al. 2021).

In vitro *T. muris* responds to monocultures of *E. coli*, *Pseudomonas aeruginosa*, *Staphylococcus aureus*, and *Salmonella typhimurium*, which facilitates the study of the egg and bacteria interactions and the molecular mechanisms involved in whipworm egg hatching

(Hayes et al. 2010). Specifically, Hayes, et al showed that direct contact between intact bacteria and whipworm eggs is required for hatching based on the observation that lysed bacteria, bacterial supernatants or transwell culture systems result in no hatching (Hayes et al. 2010). However, cultures containing live bacteria or bacteria killed by a bacteriostatic antibiotic are able to induce hatching (Hayes et al. 2010). Hayes et al showed the bacteria localising at the polar plug, and this contact or adhesion of the bacteria to the poles of the egg is facilitated by type 1 fimbriae expressed on the surface of *E. coli* strain Nissle.

Perturbing fimbriae was shown to affect hatching, knocking out the fimbrial gene *fimA* significantly reduced hatching, and knocking it back in recovered hatching (Hayes et al. 2010). Using scanning and transmission electron microscopy (SEM, TEM) Duque- Correa and Goulding visualised the interaction between *E. coli* K12 MG1655 and *T. muris* eggs (Figure 1.5) (Duque- Correa and Goulding 2017). The bacteria bind to the polar plug using fimbrial projections. As hatching progresses and the poles are degraded and the bacterial projections maintain contact with the polar plugs (Figure 1.5). Through the studies by Hayes, and (Duque- Correa and Goulding 2017) we know that bacterial surface projections facilitate adhesion to the *T. muris* egg at the start of hatching. However, the molecular mechanisms that facilitate induction and progression of hatching leading to the degradation of the polar plugs and eclosion remain unknown.

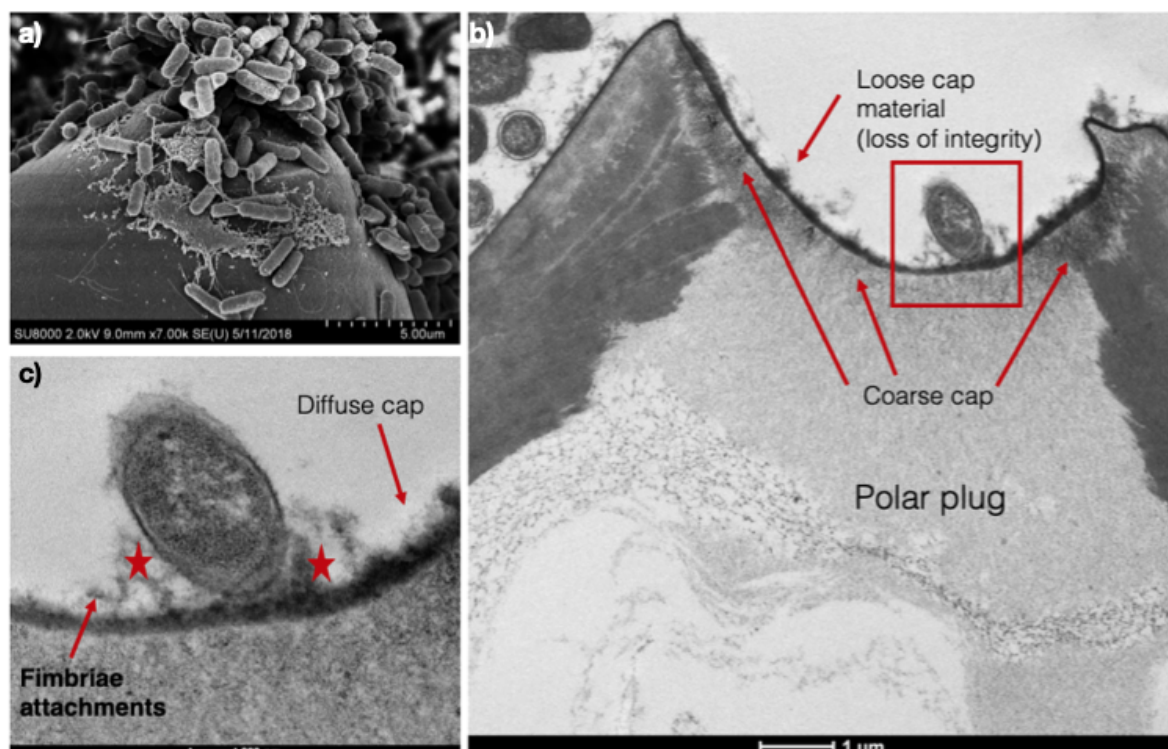


Figure 1.5. Hatching progression in *T. muris*. a) SEM micrograph displaying the aggregation of *E. coli* K12 MG1655 around the polar plug. b) & c) TEM micrographs displaying the interactions and between *E. coli* K12 MG1655 fimbriae and the polar plug, and the degradation and invagination of the plug (Duque- Correa and Goulding 2017)

Trichuris species have specific hatching requirements, for instance while *T. muris* eggs can be hatched in caecal contents, or co-cultures with different strains of *E. coli* and gram positive bacterial species (*Enterococcus caccae*, *Streptococcus hyointestinalis*, *Lactobacillus amylovorus*, *Lactobacillus murinus*, and *Lactobacillus reuteri*), *T. suis* eggs can not (Vejzagić, Adelfio, et al. 2015). Instead *in vitro* hatching of *T. suis* eggs is only observed with mucosal contents from the porcine caecum (Vejzagić, Thamsborg, et al. 2015). Microbiota from the parasite niche is the primary driver of hatching in *T. suis*, other attempts to recreate the gastrointestinal environment and simulate the parasite niche yielded mixed results. Mechanical stimulation with glass beads to mimic peristalsis complemented the levels of hatching induced by caecal scrapings, whereas the use of acids or anaerobic gas to mimic the chemical composition of the gut did not (Vejzagić, Thamsborg, et al. 2015). Knowledge of the specific members of the porcine microbiota that induce hatching of *T. suis*, and the mechanisms by which they induce hatching remains outstanding.

The factors that induce hatching of human-infective *T. trichiura* are currently unknown, and research progress has been hampered by the lack of a laboratory model. We are currently unable to hatch and propagate *T. trichiura* in the lab making it difficult to obtain purified egg cultures; eggs have to be isolated from infected non-human primates or individuals in endemic regions, who are often infected with several gastrointestinal parasites (Dige et al. 2017; Nolf 1932; Rivero et al. 2021; Rivero, Cutillas, and Callejón 2020). At present the only strategy for hatching *T. trichiura* eggs *in vitro* is by incubation with sodium hypochlorite (White et al. 2018). However, this method does not inform us of the intrinsic and extrinsic factors that lead to hatching, and is very much a “brute force” approach. The studies in *T. suis* and *T. muris* provide essential clues to the potential requirements for hatching of *T. trichiura*. Firstly, hatching is likely induced by commensal bacterial species found in the human gut microbiota of people globally. Secondly, the bacteria are likely to be associated with the mucosa of the caecum. Finally, these bacteria will need to be intact and likely expressing surface adhesion protein complexes such as type 1 fimbriae in order to establish contact with the eggs around the polar plugs to induce hatching.

1.10 Aims Of The Thesis And Contribution To The Field

To summarise key gaps in our knowledge: the factors required for inducing hatching of *T. trichiura* are unknown; we do not know the molecular basis for the bacterial or gastrointestinal tract contents mediated hatching of *T. muris*, *T. suis*, or *T. trichiura*; nor do we know the microbial composition of the parasite niche (caecal mucosa) and how the composition relates to hatching of *T. muris*, *T. suis*, or *T. trichiura*.

First, I hypothesise that hatching in *Trichuris*, which is centered around the polar plugs of the eggshell, occurs as a result of physical interaction between the bacteria of the parasite niche and the egg. Second, in addition to physical interaction, I hypothesise that hatching also requires enzymatic activity. Enzyme secretion in hatching in nematodes has previously been documented (Perry 2002; Rogers 1958; Abriola et al. 2019), and as hatching progresses in *T. muris* the polar plugs are visibly degraded and the larva ecloses (Figure 1.5). Last, I hypothesise that the parasite niche is defined by the respective host microbiota, in particular the bacterial species residing in the caecal mucosa, and whipworm species preferentially respond to bacteria from their host that express the necessary adhesins and enzymes. My goal is to address some of the knowledge gaps mentioned to understand the molecular basis of the parasite– microbiota interactions and determine the bacterial and larval molecules essential for the hatching of *Trichuris* species. Detailed in this thesis is the work undertaken to investigate my hypotheses. I used the *T. muris* and *E. coli* hatching system as a starting point to drill down into specific bacterial– egg interactions. Building on and extrapolating from these findings, I investigated which members of the murine, porcine and human microbiota are responsible for hatching of *Trichuris* species. This process is best described using the specific aims that make up the framework of my PhD and form the chapters of my thesis.

Aim 1. To identify the extrinsic factors– bacterial molecule(s) responsible for the *E. coli* – *T. muris* interaction that drives hatching; and identify intrinsic factors responsible for hatching of *T. muris*.

Aim 2. To identify extrinsic host factors in the gastrointestinal tract responsible for hatching of *T. muris*, *T. suis*, and *T. trichiura*.

Aim 3. To identify members of the gastrointestinal tract microbiota responsible for hatching of *T. trichiura*.

Through this sequence of work I aim to understand the molecular basis of hatching in *Trichuris* species, as well as making the following key contributions to the field.

- I. This study presents the first *in vitro* and *in vivo* models and protocols for hatching *T. trichiura* in a laboratory setting using biologically relevant samples and a laboratory model of the human gastrointestinal tract.
- II. This study presents a list of bacterial species from the porcine, human, and humanised murine microbiota that are implicated in the hatching of *T. suis* and *T. trichiura*. Draft genomes of these species have been generated for qualitative analysis.
- III. This study presents the first transcriptomic study of *T. muris* during embryonation. I identified 40 genes with increased expression in immature or mature eggs, this list includes genes of proteases potentially involved in hatching.
- IV. This study builds on and extends on the research conducted by Hayes in *T. muris*, and Vejzagic in *T. suis* (Hayes et al. 2010; Vejzagić, Thamsborg, et al. 2015). In this study, I re-examined the effects of fimbriae and fimbrial proteins on hatching and discovered that serine proteases are a key inducer of hatching in *T. muris*. In this study I re-examined the effects of porcine gastrointestinal tract mucosal samples on the hatching of *T. suis*, with the additional examination of the role of proteases during hatching and the identification of bacterial taxa.

In the long term, understanding hatching of whipworm eggs could lead to the refinement of current *T. muris* and *T. suis* laboratory life cycles, and the development of a laboratory model to sustain *T. trichiura*. Such a model would allow us to use laboratory animals to study the human whipworm. Access to material from all the lifecycle stages in the lab will greatly accelerate research into the basic and infection biology of *T. trichiura*. In turn this knowledge would drive forward translational research, for example: by providing novel therapeutic targets for drug development, facilitating improved parasite surveillance, or the development of new techniques to decontaminate the environment (Mkandawire et al. 2021). Eventually, model systems could be used for larger scale operations, such as the production of eggs for controlled infections (Dige et al. 2017), or the production of adult worms for future therapeutics (Eichenberger et al. 2018).

1.11 Chapter Summaries

Chapter 3: Mechanistic study of bacterial–parasite interactions responsible for the induction of egg hatching in *T. muris* by *E. coli*

The work presented in this chapter examines the role of specific E. coli classes of proteases and fimbriae and in the hatching of T. muris eggs. The role of proteases was characterised through screening the Keio collection of E. coli knockouts and hatching bacteria in the presence of protease inhibitors; and the role of fimbriae was characterised through imaging bacteria and egg co-cultures. Proteases were identified as crucial for hatching in T. muris. Transcriptomics was utilised to study gene expression in T. muris eggs during embryonation to identify intrinsic hatching factors, and putative protease genes were identified. Proteomics was used to characterise the composition of the T. muris polar plug and identify components that bacteria may bind to and may be enzymatically degraded during hatching. The polar plug was found to contain glycoproteins and lipopolysaccharides.

Chapter 4: Identification of extrinsic factors for hatching *Trichuris* spp

In this chapter to study extrinsic host factors samples were isolated from the host gastrointestinal tract and the effects on hatching of T. muris, T. suis, and T. trichiura observed. Trichuris species preferentially responded to samples collected from the caecal mucosa. The feasibility of using a humanised microbiota mouse model to recreate the T. trichiura life cycle in the lab was examined, revealing that humanised microbiota models can be used to induce hatching of T. trichiura in vitro and establish infections in vivo.

Chapter 5: Metagenomic analysis to identify bacterial species involved in hatching across *Trichuris* species.

The work presented in this chapter examines the abundance of E. coli genes identified in chapter 3 in a human gut microbiota reference database revealing that these genes are present in human gastrointestinal tract commensal species. The microbial composition of samples collected from the parasite niche in pigs, humans, mice, and humanised microbiota mice was analysed utilising the metadata from chapter 4 regarding the induction of hatching of the three Trichuris species. Candidate bacteria that can be studied for their ability to induce hatching of T. trichiura as monocultures were identified. The suitability of the bacterial candidates identified was discussed, and this list of candidates can be used for follow up in vitro studies and eventually generating in vivo models.

Chapter 2- Materials and Methods

2.1 Bacterial culture

Bacterial culture for aero-tolerant isolates (*E. coli*, *P. aeruginosa*, *S. aureus*, *S. typhimurium*, and gastrointestinal microbiota samples collected from mice, pigs, and humans) was carried out under standard aerobic conditions (37°C, 5% CO₂) in Luria Bertani (LB) medium broth and agar plates, liquid cultures were shaken at 180 rpm. Bacterial culture of Keio Collection knockouts (Yamamoto et al. 2009) was carried out under standard aerobic conditions in LB medium broth and agar plates supplemented with 25 µg/ml of kanamycin (Yamamoto et al. 2009), liquid cultures were shaken at 180 rpm. Aero-sensitive species (gastrointestinal microbiota samples collected from mice, pigs, and humans) were cultured under anaerobic conditions (37°C, Anaerobic gas =10% H₂, 10% CO₂, 80% N₂) in anaerobic gas jars (Thermo Scientific) or in a Whitley DG250 workstation at 37°C in Yeast extract-Casein hydrolysate-Fatty Acids (YCFA) medium broth and agar plates (Browne et al. 2016; Duncan et al. 2002).

2.2 Parasite egg sources

T. muris eggs of the Edinburgh strain were maintained as described in section 2.5.2 .

Embryonated *T. suis* eggs were kindly provided by P. Nejsum. Eggs were isolated from faeces of experimentally infected female Göttingen minipigs (Ellegaard Göttingen Minipigs A/S, Dalmose, DK). *T. suis* eggs were embryonated in 0.1 M sulphuric acid (to prevent any bacterial and fungal growth during storage) (Merck) for 100 days (±10 days) at 25 °C and then stored at 5 °C (2–8 °C).

T. trichiura eggs were isolated from the faeces of an infected individual (Dige et al. 2017) as described below and embryonated at 28°C for 3 weeks then stored at room temperature. Faeces were collected using the Fe-Col Basic Faecal collection kit (Alpha Laboratories), and 10 ml of 0.1 M sulphuric acid (Merck) was added to the collection tube to prevent bacterial and fungal growth during storage. Faecal acid slurry was diluted in 200 ml of distilled water and passed through a series of 100 µm, 70 µm and 40 µm pluriStrainers (pluriSelect) to remove faecal debris, before being collected on a 20 µm pluriStrainer. Next, eggs were cleaned of small faecal debris using a modified “ethyl acetate floatation” protocol (Choi et al. 2019). The modified flotation protocol is as follows: one volume of ethyl acetate (Sigma) was added to 3 volumes of egg suspension and thoroughly mixed. Debris was separated out by

centrifugation at 3220 g for 5 min at room temperature (room temperature). The aqueous phase containing debris was discarded and the egg pellet washed 3 times by centrifugation at 720 g for 10 min at room temperature with no brake.

2.3 *In vitro* *T. muris* egg hatching assays with *E. coli* MG1655, Keio Knockout Strains, *P. aeruginosa*, *S. aureus*, and *S. typhimurium*.

T. muris eggs were seeded in 96-well plates (Costar) at a density of 3000 eggs per ml (150 eggs in 50 µl) and co-cultured with 150 µl of an overnight bacterial culture. Each condition was run in triplicate. Plates were incubated for 2, 5 or 24 h under standard aerobic conditions (37°C, 5% CO₂). To investigate the effects of proteases, protease inhibitors (Roche) were prepared according to manufacturer's instructions and added to the eggs and bacteria co-cultures at the concentrations detailed in Table 2. To evaluate dose dependency, the protease inhibitor cocktail was added in a serial dilution (1x, 0.5x, 0.25x, 0.125x, 0.0625x working concentration).

To investigate if eggs could still be induced to hatch after exposure to the inhibitor cocktail, eggs were then washed twice in 25 ml of sterile water by centrifugation at 720 g for 10 min at room temperature. Eggs were re-seeded in a 96-well plate (Costar) at a density of 3000 eggs per ml and incubated with 150 µl of the same overnight bacterial culture that was previously used 24 h earlier (cultures were refrigerated overnight between experiments and then reactivated by shaking at 37°C 180 rpm for 20 min before incubating with eggs). Plates were incubated for further 24 h under standard aerobic conditions (37°C, 5% CO₂).

For all hatching experiments, results were reported as percentage hatching where:
Percentage Hatching = (hatched larvae/starting egg count) x 100

Table 2.1 Protease inhibitors and their working concentrations

Protease Inhibitor	Working Concentration
cOmplete™, Mini, EDTA-free Protease Inhibitor Cocktail	1x / 2x
Antipain	50 µg/ml
Chymostatin	60 µg/ml
E-64	10 µg/ml
Leupeptin	0.5 µg/ml
Pefabloc SC	1 mg/ml
Aprotinin	2 µg/ml

2.4 *In vitro* hatching assays with gastrointestinal tract samples

Gastrointestinal mucosal scrapings were prepared from porcine and murine caeca as described in previous studies (Vejzagić, Thamsborg, et al. 2015). The gastrointestinal tract was opened with curved surgical scissors, gastrointestinal luminal contents were scooped out and thoroughly mixed in 5 ml Roswell Park Memorial Institute Medium (RPMI-1640) containing 1% L- glutamine (Gibco). Empty tissue was washed with 10 ml warm phosphate buffered saline (PBS) (Gibco), and mucus was gently scraped from the tissue with a cell scraper (Costar) and thoroughly mixed in 5 ml of RPMI containing 1% L- glutamine (Gibco). Bacterial metascrapes from gastrointestinal tract samples were generated by plating thoroughly mixed gastrointestinal tract luminal contents or mucosal scrapings directly onto YCFA agar, and culturing under standard aerobic and anaerobic conditions. The growth was then mixed with 1 ml sterile PBS (Gibco), scraped off, and immediately frozen at -80°C until sequencing (Pike 2020).

Twelve subjects (completely randomised and anonymised) who were scheduled to undergo colonoscopy were recruited at Aarhus Universitet Hospitalet, Aarhus, Denmark. Inflammation state of the subjects' gastrointestinal tract was assessed at the time of collection by the attending gastroenterologist. Six 3 x 3 mm tissue sections were collected from each gastrointestinal tract site, placed in 1 ml of PBS, and processed immediately. Samples were homogenised by repeated pipetting (>200 times with a p1000 pipette) in RPMI containing 1% L- glutamine (Gibco). In order to use the minimum amount of media required for plating and sequencing samples, and avoid over diluting the samples, all homogenised samples were prepared in a volume of RPMI calculated as follows: Amount of RPMI= ((number of conditions in triplicate*150 µl)+ 600 µl). The study was implemented in accordance with the Danish Act on Research Ethics Review of Health Research Projects and the Data Protection Act. Informed consent was obtained from all participants involved in this study.

Eggs were seeded in 96-well plates at a density of 3000 eggs per ml (150 eggs in 50 µl) for *T. muris* and *T. suis* and 600 eggs per ml (30 eggs in 50 µl) for *T. trichiura*. Homogenised gastrointestinal tract scrapings or contents were added in a volume of 150 µl to each well. Plates were incubated for 24 h under either standard aerobic or anaerobic conditions in anaerobic gas jars or in a Whitley DG250 workstation. To investigate the effect of proteases on hatching, cOmplete™, Mini, EDTA-free Protease Inhibitor Cocktail (Roche) was prepared according to manufacturer's instructions and added to the appropriate wells at 2x working concentration (Table 2.1).

For all hatching experiments, results were reported as percentage hatching where:

Percentage Hatching = (hatched larvae/starting egg count) x 100

2.5 Mouse models and infections

2.5.1 Mice

Wild type (WT) C57BL/6N mice were maintained under specific pathogen-free (murine microbiota) conditions and contained a murine microbiota. Humanised microbiota mouse lines donor A and donor B were generated by oral gavage of germ free C57BL/6N mice with stool from healthy donors that had not been exposed to antibiotics for at least 6 months. Humanised microbiota mice were maintained behind containment (Forster et al. 2021). Severe combined immune deficiency (SCID) mice were maintained under murine microbiota conditions. All animals were maintained at a Home Office-approved facility (Sanger Institute Research Support Facility) within individually ventilated cages at $22^{\circ} \pm 1^{\circ}\text{C}$ and 65% humidity with a 12-hour light-dark cycle and had free access to food and water. All procedures carried out in accordance with the United Kingdom Animals (Scientific Procedures) Act of 1986 under the project license P77E8A062.

2.5.2 Infection of SCID mice for *T. muris* maintenance

Infections of *T. muris* were maintained in SCID mice which were infected with a high dose (400 eggs) by oral gavage under anesthesia. Adult worms were harvested at 35 days post infection (p.i) and adult worms placed in culture under standard aerobic conditions in RPMI containing 5% Penicillin and Streptomycin (pen/strep) (Gibco) and 10% fetal calf serum (FCS) (Gibco) for 4 or 24 h. Eggs were collected, washed and left to embryonate in distilled water for 8 weeks in the dark at room temperature (White et al. 2018; M. A. Duque-Correa et al. 2019).

2.5.3 *T. muris* study of embryonation

T. muris eggs were produced as described in section 2.5.2 and aliquots of ~500 eggs were collected weekly during embryonation to examine morphology by light microscopy using a Zeiss Axio Observer 5, to study *in vitro* response to bacteria during embryonation, and to examine gene expression utilising RNA sequencing (RNAseq) (Section 2.9).

2.5.4 Infection of humanised microbiota mice and WT C57BL/6 murine microbiota mice

Mice from two humanised microbiota mouse lines and WT C57BL/6 murine microbiota mice between 6 and 20 weeks old were infected with a low dose (20 eggs) of either *T. muris* and *T. trichiura* by oral gavage. At days 35 and 90 p.i., blood was obtained by cardiac puncture under terminal anesthesia, mice were cervically dislocated, and the mesenteric lymph nodes and caecum were collected. Serum was separated from the blood by centrifugation at 14,000g for 10 min at room temperature and tested for parasite specific antibodies by ELISA (section 2.5.5) (Houlden et al. 2015; White et al. 2018). Caecal contents were collected and immediately stored at -80°C until DNA extraction for metagenomic sequencing (Section 2.8.2). The caecum was slit longitudinally and adult worms were individually removed from the tissue and counted.

2.6 Detection of parasite specific antibodies

Analysis of the presence of parasite-specific IgG2a and IgG1 in mice serum was detected using biotinylated rat anti-mouse antibodies (BD Pharmingen) and conducted using ELISA. Briefly, immulon IV plates (Dynatech) were coated with 5 µg/ml *T. muris* excretory/secretory (E/S) antigen (kindly provided by Prof Richard Grencis at the University of Manchester) in carbonate/bicarbonate buffer (pH 9.6) (Sigma) overnight at 4°C. Plates were blocked with 3% bovine serum albumin (Sigma) in PBS and 0.05% Tween (Sigma). Serum was diluted 20-fold and then added in eight serial 2-fold dilutions to the plates and the optical density recorded.

2.7 Confocal and electron microscopy

2.7.1 Scanning electron microscopy

SEM was performed by D. Goulding as follows. *T. muris* eggs and bacterial strains were incubated in 0.5ml Eppendorf tubes at 37°C for 90 min. The eggs were washed in PBS 2 times by centrifugation at 280 g for 30 s at room temperature, fixed with 2% PFA (Thermo) and 2.5% glutaraldehyde (Sigma) in 0.1 M sodium cacodylate buffer (SCB) (Sigma) at pH 7.42 and immediately spun at 280 g for 2 min at room temperature. Tubes were left to stand for 2 h to fasten the eggs vertically in the bottom of the Eppendorf tubes. The eggs were carefully rinsed in SCB three times by centrifugation at 280 g for 5 min at room temperature, before fixing again in 1% osmium tetroxide in SCB for 2 h followed by layering of thiocarbohydrazide and osmium according to (Mallick and Wilson 1975). The eggs were then

dehydrated through an ethanol series from 30,50,70,90 to 3 times in 100% for an hour each. The tip of each Eppendorf was cut off and dried with the eggs inside in a Leica CPD300 before coating with 20nm of platinum in a Leica ACE600 evaporation unit. Finally, the cut tips were mounted eggs-up onto Hitachi SEM stubs with silver DAG and viewed in an Hitachi SU8030 scanning electron microscope.

2.7.2 Confocal microscopy

Confocal microscopy was performed by D. Goulding as follows. *T. muris* eggs and bacterial strains were incubated in 0.5ml Eppendorf tubes at 37°C for 90 min and then fixed in 3% PFA in PBS for 30 min. The eggs were then rinsed in PBS three times by centrifugation at 280 g for 5 min at room temperature and incubated in 5% foetal calf serum (Gibco) and 1% BSA (Sigma) in PBS (blocking medium) for 1 h at room temperature. Blocking medium was replaced with rabbit anti FimH (Cusabio), diluted 1:50 with blocking medium for 30 min at room temperature (all incubations at room temperature). The eggs were then rinsed in PBS three times by centrifugation at 280 g for 5 min at room temperature incubated in goat anti-rabbit conjugated to FITC (Abcam) diluted 1:50 with blocking medium for 1 h and rinsed in PBS three times by centrifugation at 280 g for 5 min at room temperature. The eggs were then incubated in ConA directly conjugated to Rhodamin (Vector Labs) diluted 1:50 with blocking medium for 1 h and rinsed in PBS three times by centrifugation at 280 g for 5 min at room temperature. The eggs were then gently mounted on a slide with coverslip in Prolong-gold antifade with DAPI (Thermo). The slide was imaged on a Leica SP8 confocal microscope.

2.8 Nucleic acid and protein extractions

2.8.1 RNA extraction

T. muris eggs were collected (Section 2.5.3) and stored at -80°C until RNA extraction. Eggs were washed 3 times in PBS containing SUPERase•In RNase Inhibitor (Thermo Fisher) at 1 U/μL and pelleted by centrifugation at 20,000g for 2 min at 4°C. Washed eggs were resuspended in 500 μl of Trizol LS (Thermo Fisher), placed in a tube containing acid washed 1.4mm ceramic beads (Roche), and homogenised in an MP Bio fast prep machine (MP Bio) at 6.0 m/s for 20 s. Samples were incubated at room temperature for 5 min with two inversions. Chloroform (267 μl) was then added, tubes were shaken, and samples incubated at room temperature for 3 min with 2 inversions. The aqueous phase containing the RNA was separated by centrifugation at 15,000g for 15 min at room temperature. Aqueous phase

was placed on a Zymo-Spin IC column (Zymo) to collect the RNA, and RNA was then eluted in 15 µl of RNase-free water (Ambion) and stored at -80°C until sequencing.

2.7.2 DNA extractions from gastrointestinal tract samples for metagenomic sequencing

Gastrointestinal tract scrapings and contents were collected as described in section 2.4 and immediately stored at -80°C until DNA extraction. DNA was extracted from the samples using FastDNA Spin Kit for Soil (MPBio) according to manufacturer's instructions and DNA stored at -20 °C until metagenomic sequencing.

2.8.3 Protein extraction

Whole *T. muris* eggs were obtained as described in Section 2.5.2. Bacterial hatching was performed as described in Section 2.3 to generate *T. muris* eggshells and larvae, eggshells and larvae were separated by 50%, 60% percoll gradient centrifugation at 300 g for 15 min at room temperature with no brake. Bleach hatched *T. muris* larvae were produced as previously described (White et al. 2018). Eggs were incubated with sodium hypochlorite for 2 h at 37°C with 5% carbon dioxide, dissolving the eggshell and leaving only the lipid membrane, followed by culture in RPMI media at 37°C with 5% carbon dioxide, for 4-5 days until eclosion. 500 eggs, eggshells, or larvae were placed in PBS (Gibco) with 1% Triton X 100. Samples were incubated at 37 °C for 30 min and then placed in a tube containing acid washed 1.4 mm ceramic beads (Roche). Samples were homogenised in an MP Bio fast prep machine (MP Bio) at 6.0 m/s for 60 s. Beads were allowed to settle before the supernatant was collected and placed in a fresh tube. For acetone precipitation 5 volumes of -20 °C acetone were added to the sample and samples were vortexed well. Following overnight storage of the samples at -20 °C, samples were vortexed again and then pelleted by centrifugation at 10, 000g for 10 min at 10 °C. Pellets were air dried for 5 min and stored at -20 °C.

2.9 Library preparation and sequencing

2.9.1 RNAseq Library preparation and sequencing

RNA mass was measured using the Bioanalyzer RNA 6000 Nano (Agilent) and 1-8 ng was present in each sample. RNAseq libraries were prepared using the NEBNext® Ultra™ II Directional RNA Library preparation kit (NEB) according to manufacturer's instructions with the TruSeq TSQ adapter (Integrated DNA technologies) and UDI tags (WSI). RNA libraries were sequenced using paired-end (2 × 75 bp) sequencing on the HiSeq 4000 platform (Illumina).

2.9.2 Metagenomic and whole genome library preparation and sequencing

DNA for metagenomics was prepared using the Ultra II DNA Library preparation kit (NEB) according to manufacturer's instructions with the TruSeq TSQ adapter (Integrated DNA technologies) and UDI tags (WSI). DNA concentrations were measured using the Agilent D5000 ScreenTape System (Agilent) and 40-100 ng was present in each sample. DNA samples were sequenced using paired-end (2 × 150 bp) metagenomics sequencing on the HiSeq 4000 platform (Illumina).

2.9.3 Peptide preparation and mass spectrometry

Peptide processing kindly provided by Prof Jyoti Choudhary, and Dr Lu Yu at the Institute for Cancer Research. Protein pellets were resuspended in triethylammonium bicarbonate (TEAB) and protein concentrations were measured by Pierce 660 nm Protein Assay (Thermo Fisher), 30-45 µg was present in each sample. Samples underwent tryptic digestion, alkylation, deglycosylation, and desalination; and peptides were analysed using liquid chromatography-tandem mass spectrometry LC-MS/MS.

2.10 RNAseq analysis

Reads were trimmed and mapped to the *T. muris* genome and annotations (WormBase ParaSite 11-Apr-2019) using tophat v2.1.1 (Trapnell, Pachter, and Salzberg 2009). Read counts were generated using htseq v0.13.5 (Anders, Pyl, and Huber 2014), differential analysis was performed using deseq 2 v1.34.0 (Love, Anders, and Huber 2014), and results were visualised in R v4.0.4 (Team 2020; Blighe, Rana, and Lewis 2019).

2.11 Proteomic analysis

Peptide identities were assigned using the Sequest HT search engine in Proteome Discoverer [™] (PD) 2.4 (analysis kindly provided by Prof Jyoti Choudhary, and Dr James Wright at the Institute for Cancer Research). Protein databases included the Institute for Cancer Research contaminant database, as well as protein databases for *T. muris* (WormBase ParaSite 2019), *T. suis* (WormBase ParaSite 2014b) and *T. trichiura* (WormBase ParaSite 2014a).

2.12 Metagenomic analysis

2.12.1 Identification and visualisation of genes in the Human Gastrointestinal Bacteria (HBC) Culture Collection

The HBC contains 737 whole-genome sequenced bacterial isolates from the faecal samples of healthy adults (Forster et al. 2019). These genomes were annotated using the Sanger Pathogen Informatics Pipeline annotation tool which searches the following databases to annotate sequences (Page et al. 2016; Seemann 2014).

- I. RefSeq databases (NCBI)
- II. UniprotKB (bacteria/virus databases)
- III. Protein Clusters (NCBI)
- IV. Conserved domain database (NCBI)
- V. Tigrfams (J. Craig Venter Institute)
- VI. pfam (part A) (EMBL-EBI)
- VII. rfam (EMBL-EBI)

The annotated genomes were searched for gene sequences comprising fimbriae and *E. coli* serine protease operons. *De novo* functional annotation of fimbriae and serine protease genes was performed using prodigal and eggNOG (Hyatt et al. 2010; Huerta-Cepas et al. 2019). Phylogenetic analysis was completed by extracting the amino acid sequence of 40 universal core marker genes from each genome in the collection using fetchMG (Ciccarelli et al. 2006; Kultima et al. 2012; Sorek et al. 2007). The protein sequences were concatenated and aligned with MAFFT v7.20 (Kato and Standley 2013), and maximum-likelihood trees were constructed using RAxML v8.2.8 (Stamatakis 2014) with the standard LG model and 100 rapid bootstrap replicates. Trees were visualized using FastTree followed by iTOL (Price, Dehal, and Arkin 2009; Letunic and Bork 2021).

2.12.2 Taxonomic classification and differential analysis of metagenomic reads from gastrointestinal tract samples

Metagenomic reads were trimmed and then aligned to the host genome using BWA- MEM v0.7.17 (H. Li and Durbin 2009) to remove host reads. The host genomes used were: human (Genome Reference Consortium Human Build 38), porcine (The Swine Genome Sequencing Consortium; Sscrofa 11), or murine (Genome Reference Consortium Mouse Build 38). Reference based strategies utilise a curated set of genomes to identify members of the microbiota in a given sample. Un-assembled reads were classified using Kraken2 (Wood, Lu, and Langmead 2019) with a curated human gut metagenome database: the Unified Human Gastrointestinal Genome (UHGG) (Almeida et al. 2021). Kraken 2 utilises databases to provide classification of organisms in a sample at each taxonomic level from kingdom through to species. In addition to classification, a matrix of the relative abundances of each taxon is generated. The relative abundances reported by Kraken 2 were utilised for differential analysis of the presence of different taxa, and data analysis was performed in R v4.0.4 (Team 2020). In order to visualise the beta diversity (differences in taxonomic composition between the different samples), Bray–Curtis similarities were plotted on Principal Coordinates Analysis (PCoA) graphs annotated with hatching metadata. Bray–Curtis distance matrices were generated using taxonomic relative abundances and vegan (Oksanen et al. 2007). In order to examine the abundance of the various phyla in the samples, abundance charts were plotted. Multivariate Association with Linear Models 2 (MaAsLin2) v1.80 (Mallick et al. 2021) was used to evaluate if the differences in composition at phylum and species levels were statistically significant in each of the various categories of metadata. MaAsLin2 is a modified general linear regression model for feature-wise multivariate modeling of associations between microbial meta’omic features and fixed or random effects. Using MaAsLin2 differentially abundant taxa were identified using the default parameters, aside from the q-value threshold, which was set at 0.05 (Mallick et al. 2021). According to default parameters, taxa were considered prevalent in a sample with an abundance >0 at least 10% of the time (Minimum prevalence= 0.1). Data were Log transformed (LOG) and normalised using Total Sum Scaling (TSS), and p values were corrected using Benjamini-Hochberg Procedure (BH)

2.12.3 Assembly of metagenomic genomes from metagenomic reads

Metagenome-assembled genomes (MAGs) were generated through a binning process, whereby reads or contigs are sorted into taxonomically similar pools, or bins, in order to reconstitute individual genomes. There are two thresholds to consider when creating MAGs:

completeness and contamination, which refer to how much of the complete genome is acceptable and how many misassigned reads are acceptable respectively. Acceptable thresholds for completeness begin at 50% for undefined samples generating low quality MAGs, and can be set as high as 95% for well characterised samples generating high quality MAGs (Uritskiy, DiRuggiero, and Taylor 2018; Saheb Kashaf et al. 2021). The MetaWRAP v1.3 (Uritskiy, DiRuggiero, and Taylor 2018) wrapper was used to generate MAGs using two assembly tools MEGAHIT v1.2.9 (D. Li et al. 2015) and metaSPAdes v. (Bankevich et al. 2012). Once MAGs were assembled, bin consolidation was used to sort MAGs and recover the best quality bins by combining the output of three binning tools: CONCOCT v1.1.0, MetaBat 2 v2.12.1 and MaxBin 2 v2.2.7 (Uritskiy, DiRuggiero, and Taylor 2018; D. Li et al. 2015; Alneberg et al. 2013; Kang et al. 2019; Wu, Simmons, and Singer 2016). Bins were refined using the MetaWRAP bin refinement module, with the CheckM v1.1.3 (Parks et al. 2015) bin quality thresholds set at 65% completeness and 5% contamination (Uritskiy, DiRuggiero, and Taylor 2018) to balance these stringencies and aim for shorter but less-contaminated genomes as the gastrointestinal samples were uncharacterised. Taxonomic identities were assigned using Kraken 2 and the MetaWRAP bin classification module and the MAG sequences banked for future qualitative analysis.

Chapter 3- Mechanistic study of bacterial–parasite interactions responsible for the induction of egg hatching in *T. muris* by *E. coli*

Declaration of contributions

M. Duque Correa and M. Berriman supervised this work. M. Duque Correa and D. Goulding provided images from the SEM and TEM of *T. muris* eggs hatching with *E. coli*. D. Goulding performed SEM and confocal imaging and analyses on *T. muris* egg hatching with *E. coli*, *P. aeruginosa*, *S. aureus* and *S. typhimurium*. Sanger Sequencing Pipelines performed RNAseq library prep and sequencing. Sanger Pathogen Informatics Pipelines provided informatics support. L. Yu, J. Wright and J. Choudhary performed protein digests, and peptide sequencing, and peptide analysis. I performed all inoculum preparations, hatching experiments, RNA extractions, protein extractions, and analyses.

Publication

3.1 Introduction

Hatching is a fundamental process in the life cycle of *Trichuris* species marking the start of an infection; it is governed by internal and external factors, however we do not know what extrinsic and intrinsic factors govern hatching in *T. trichiura* (Mkandawire et al. 2021). Understanding hatching will not only shed light on the basic biology of this parasite, it will facilitate infection biology and translational research. *In vitro* and *in vivo* maintenance of *T. trichiura* in the laboratory is not currently possible and presents a significant challenge in the study of these parasites. Unlike *T. suis*, which can infect pigs and humans, *T. trichiura* exhibits strong host specificity only infecting primates (Ghai et al. 2014). *T. trichiura* cannot be passaged in a tractable laboratory host. As a result, *T. trichiura* has only been studied when specimens could be isolated from naturally infected individuals or apes (Dige et al. 2017; Nolf 1932; Rivero et al. 2021; Rivero, Cutillas, and Callejón 2020). The majority of studies on whipworm infection have primarily used *T. muris* and *T. suis* infections of mice and pigs respectively, as model systems (Wakelin 1969; Houlden et al. 2015; Hayes et al. 2010; Burden and Hammet 1976; Beer 1973b; Vejzagić, Adelfio, et al. 2015). Key similarities between these three species of whipworm include: hatching in response gastrointestinal contents, and progression through the canonical nematode hatching cascade (Figure 1.2).

However, there are key differences that have made reproducing the conditions required to initiate hatching a challenge (Vejzagić, Adelfio, et al. 2015). *T. muris* hatching can be induced *in vitro* with a single bacterial strain (Hayes et al. 2010; Vejzagić, Adelfio, et al. 2015), and in the *T. suis* model, hatching can be induced using mucosal gastrointestinal tract samples (Vejzagić, Thamsborg, et al. 2015). In both *T. suis* (Vejzagić, Adelfio, et al. 2015) and *T. trichiura* bacteria that are capable of inducing hatching have not yet been identified.

T. muris was first shown to selectively hatch in the presence of caecal and colon contents, but not ileal contents suggesting that the microbiota is a key extrinsic factor for hatching (Panesar and Croll 1980). Studies using germ-free mice demonstrated that *T. muris* is dependent on bacteria to establish infections (White et al. 2018). *T. muris* hatching is routinely induced by *E. coli* (Hayes et al. 2010), and infections can be established in mono colonised mice (White et al. 2018). In addition to identifying *E.coli* as capable of inducing hatching Hayes *et al* also showed that type 1 bacterial fimbriae are required in hatching (Hayes et al. 2010). Fimbriae are filamentous adhesins utilised by bacteria to adhere to surfaces and are composed of fimbrial subunit proteins (attachment, length, tip, and localisation) encoded by several genes comprising the *fim* operon (Table 3.1) (Y.-W. Chen et al. 2014; Schwan 2011).

Table 3.1 Genes of the *fim* operon

Gene	Function
<i>fimA</i>	Pilin structural gene
<i>fimB</i>	<i>fimS</i> DNA positioning
<i>fimC</i>	Periplasmic chaperone protein
<i>fimD</i>	Surface localisation usher
<i>fimE</i>	<i>fimS</i> DNA positioning
<i>fimF</i>	Adhesin anchor
<i>fimG</i>	Adhesin anchor
<i>fimH</i>	Adhesin
<i>fimI</i>	Unknown
<i>fimS</i>	Invertible element

Despite Type 1 fimbriae being implicated in hatching, co-culturing *T. muris* eggs with a purified recombinant fimbrial subunit protein- *fimA*, did not induce hatching (Hayes et al. 2010). These results suggested that fimbrial proteins alone are not sufficient to induce hatching; hatching is only seen when the projections are fully assembled on the whole bacterium. Additionally, co-culturing *T. muris* eggs with *S. aureus* and *P. aeruginosa*,

bacterial strains that do not express fimbriae, still results in successful hatching, indicating that there are type 1 fimbriae independent routes to inducing hatching (Hayes et al. 2010).

In preliminary studies Duque- Correa and Goulding (Duque- Correa and Goulding 2017) observed that *E. coli* K12 MG1655 presents two colony morphologies- rough and smooth (Figure 3.1.a), that induce hatching to opposite levels. While co-cultures of *T. muris* eggs with smooth *E. coli* cultures resulted in high levels of hatching of *T. muris*, rough colonies induced no hatching (Duque- Correa and Goulding 2017). Variations in colony morphologies of *E. coli* have been previously attributed to type 1 fimbriae, with smooth colonies expressing fimbriae and rough colonies being afimbriate (Hasman, Schembri, and Klemm 2000; Y.-W. Chen et al. 2014). Fimbrial projections were observed on the bacteria in the smooth cultures, but not in the rough cultures using SEM and TEM to explore the interactions of bacteria with *T. muris* eggs (Figure 3.1b). These projections facilitated interactions with the eggs, leading to bacterial aggregates on the surface of the egg, particularly around the polar plugs with smooth cultures (Figure 3.1b). With rough cultures however, fewer bacteria are localised at the polar plug (Figure 3.1b). Eclosion was visualised by TEM and the bacterial projections maintain contact with the polar plugs as hatching progresses and eventually, the polar plug degrades and disappears resulting in larval exit (Figure 3.1c) (Duque- Correa and Goulding 2017).

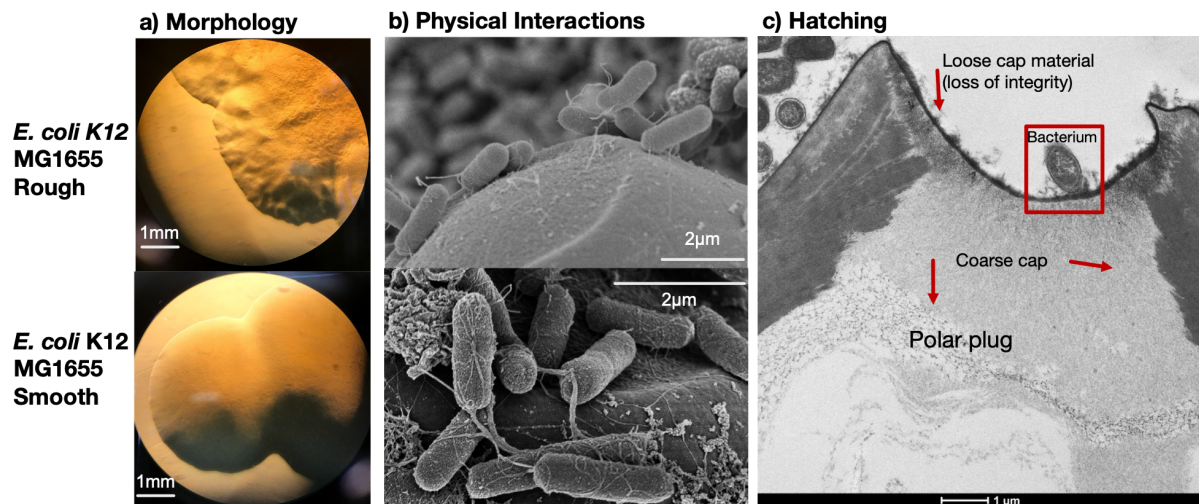


Figure 3.1- Rough and smooth *E. coli* K12 MG1655 display differing colony morphologies and interactions with *T. muris* eggs. a) Rough and smooth colony morphologies. Rough colonies have distinctly jagged edges and a matt finish. Smooth colonies are rounded and have a glossy finish. b) SEM micrographs displaying the aggregation of bacteria around the polar plug of *T. muris* eggs c) TEM micrographs displaying the interactions and between smooth bacteria and the plug, and the degradation and invagination of the plug (Duque- Correa and Goulding 2017)

In addition to extrinsic factors such as the microbiota, hatching is also driven by intrinsic factors such as embryonation and diapause; however, for many of these factors, a genetic explanation remains outstanding, due to difficulties in developing transgenic systems to study parasitic nematodes (Section 1.6). While it is not yet possible to generate *Trichuris* knockout worms, it is possible to sequence larvae and analyse temporal changes in gene expression. For instance, RNAseq has been used to evaluate the changes in gene expression during dormancy, embryonation and hatching of the cyst nematodes, providing invaluable insight into these processes (Duceppe et al. 2017; Cotton et al. 2014; Eves-van den Akker and Jones 2018). For example, revealing the genes responsible for calcium and water uptake at the initiation of hatching, genes related to pharyngeal pumping and peptidase genes (Duceppe et al. 2017; Eves-van den Akker and Jones 2018). Further evidence for the role of embryonation in hatching comes from studies in *Ascaris*. Immature *Ascaris* larvae cannot be induced to hatch using natural cues (Geenen et al. 1999), and when immature larvae were forced to hatch using physical methods that break the eggshell, the larvae were smaller, non motile, and considered non viable (Vejzagić, Thamsborg, et al. 2015; Geenen et al. 1999). The level of embryonation and the conditions under which it takes place not only affect the ability to hatch but also the subsequent infectivity of the larvae. In *Ascaris*, immature eggs are unable to establish an infection in mice (Geenen et al.

1999). In contrast in *T. muris* once immature larvae are motile in the egg an infection can be established in mice (Forman et al. 2021). In *Capillaria*, altering the culture medium in which eggs are embryonated changes both the proportion of eggs that embryonate and their infectivity (Tiersch et al. 2013). These studies indicate that the ability to hatch does change during embryonation and a differential analysis of gene expression may provide a genetic explanation. I hypothesised that there is a minimum amount of embryonation that must occur in order for the eggs to hatch in response to natural cues. Thus, to analyse these changes in *T. muris*, in the present chapter I evaluated gene expression during embryonation of *T. muris*.

Hatching is facilitated by the selective permeability (section 1.5) of nematode eggs which allows larvae to receive and respond to environmental cues (Johnston and Dennis 2012). In the case of *Trichuris*, while the microbiota may signal the arrival of the eggs in the ceacum and induce hatching, hatching only progresses with larval involvement. Specifically, previous studies showed that movement of the larvae, in particular movement of the oral spear (stylet) facilitates eclosion (Panesar and Croll 1981). Larval involvement can also come in the form of enzyme secretions released during pharyngeal pumping (Perry 2002). Enzymes have been isolated from the perivitelline fluid of several nematodes including *Ascaris*, *A. ceylanicum*, *H. contortus*, and *G. rostochiensis* (Perry 2002; Rogers 1958; Rogers and Brooks 1977; Doncaster and Shepherd 1967; Abriola et al. 2019; Q. Chen et al. 2021). Therefore, I hypothesised that larval enzymes are involved in chemically progressing hatching in addition to the physical aids i.e. bacterial fimbriae, and stylet propulsion. In this chapter I aimed to identify the larval enzymes using RNAseq across different developmental stages; to determine which transcripts are expressed in preparation for hatching. These enzymes may degrade the polar plugs in order to facilitate larval exit. As mentioned in Chapter 1 (section 1.8), the composition of the polar plugs of *Trichuris* eggs is poorly characterised. However, they are known to contain chitin fibres that form a diffuse matrix that suspends various molecules (Appleton and White 1989; Wharton and Jenkins 1978). In the present chapter, I used proteomics to better understand the composition of the polar plugs and identify molecules that may bind to bacteria and may be targeted by the proteases involved in hatching.

I hypothesised that induction of *T. muris* hatching is in part facilitated by a combination of physical interactions between bacteria and eggs and enzymatic activity concentrated around the polar plugs; as hatching progresses polar plugs are degraded and larvae eclose (Figure 3.2).

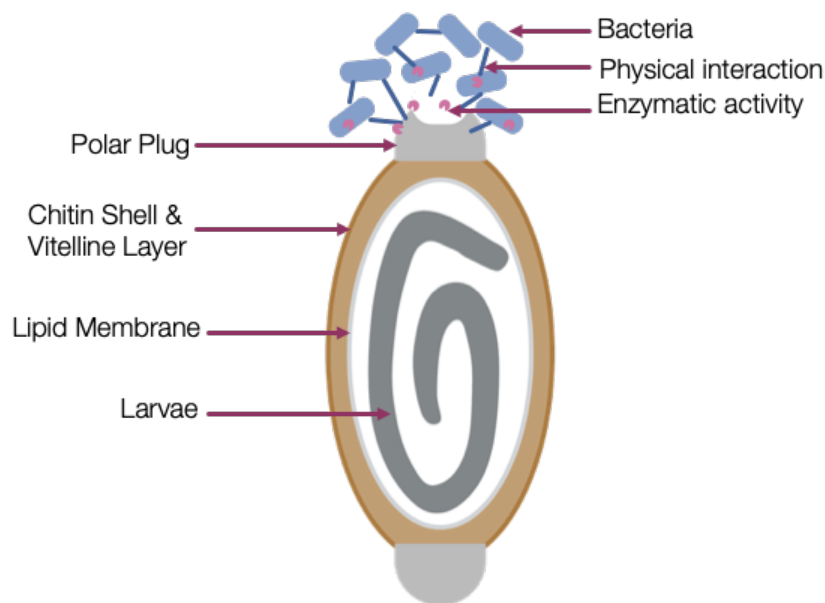


Figure 3.2- Cartoon depicting the hypothesis of the minimum requirements for hatching. Bacteria aggregate around the polar plugs, using physical interactions to adhere to one another and the eggs. As hatching progresses the polar plugs are degraded through enzymatic activity and disappear facilitating larval eclosion. (Image created using BioRender)

In this chapter, I aimed to further characterise the role of type 1 fimbriae from *E. coli* in *T. muris* hatching and further understand how fimbriae mediate the physical interaction between *E. coli* and the eggs using a whole *fim* operon knockout kindly supplied by Paul Orndorff (Hamrick et al. 2000), as well as knockout lines from the Keio Collection (Yamamoto et al. 2009). The Keio collection was generated to create a knockout library of all non-essential *E. coli* genes; all genes for which a clone was not recovered are considered essential to the survival of *E. coli* (Yamamoto et al. 2009). I then investigated the role of proteases in degradation of the polar plugs and hatching. I evaluated the effects of inhibiting proteases in the hatching reaction using commercially available inhibitors and Keio Collection knockouts for genes encoding both cysteine and serine proteases (Yamamoto et al. 2009). Finally, I used proteomics to better understand the composition of the polar plugs and identify molecules that may be targeted by the proteases involved in hatching and used RNAseq across different developmental stages, to determine which transcripts are expressed in preparation for hatching.

3.2 The role of fimbriae in hatching of *T. muris* in the presence of *E. coli*

To evaluate differences in hatching induction related to fimbriae expression, I first isolated rough and smooth colonies from the in-house lab strain *E. coli* K12 MG1655, as well as the Keio Collection parent strain *E. coli* K12 BW25113 and co-cultured them with *T. muris* eggs. I observed the following variable hatching phenotype: with smooth colonies of *E. coli* K12 MG1655, hatching ranged from 20 to 100% with a median of 50.7%; and with rough colonies of *E. coli* K12 MG1655, hatching ranged from 20% to 80% with a median 18.9% (Figure 3.3). This variation may be as a result of batch variation in the eggs used; previous in-house batch testing of eggs produced during routine parasite maintenance (data not shown) have revealed that different batches of eggs can be more or less effectively stimulated to hatch using *E. coli*. Additionally, bacteria are able to switch between rough and smooth colony types during the experiment, likely affecting the levels of hatching induced. Despite this, on average rough cultures induced less hatching compared to smooth cultures, indicating that variations in colony morphology, and by extension surface projections, have an effect on the ability of *E. coli* K12 to induce hatching.

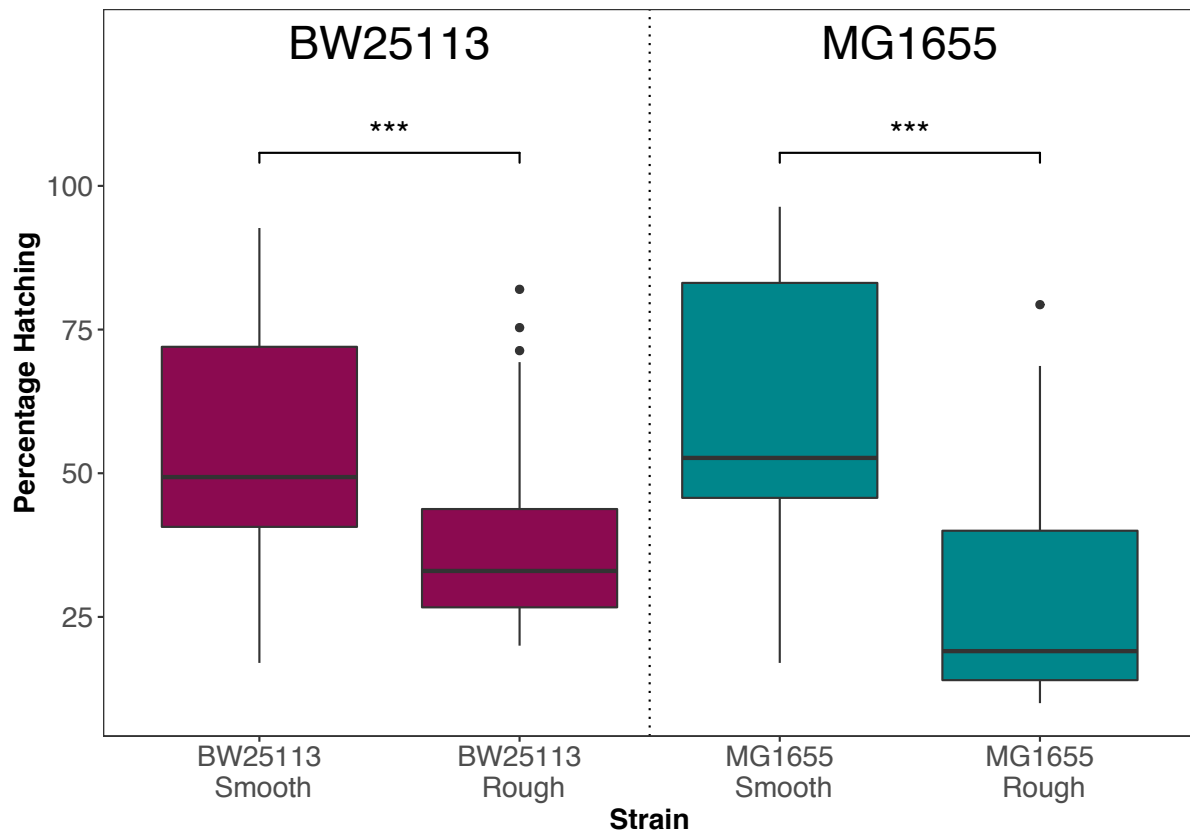


Figure 3.3. Bacterial colony morphology impacts levels of *T. muris* egg

hatching induced by *E. coli* K12. Hatching of *T. muris* eggs was induced using rough and smooth colonies of the *E. coli* strains K12 MG1655 and BW25113.

Percentage hatching was recorded after 24 h of co-culture. Hatching was completed in triplicate across 10 independent experiments (n=30). Median and interquartile range are shown, statistical differences were evaluated using the paired samples Wilcoxon test on comparisons (***) $p \leq 0.001$.

To better understand the role of type 1 fimbriae from *E. coli* K12 on the induction of *T. muris* hatching, I used single *fim* gene knockouts, the *fim* operon knockout, and rough and smooth bacteria (Figure 3.4). With the knockout strains, I observed a slight but non significant reduction in hatching, suggesting there are alternative mechanisms. In previous studies Hayes *et al* observed that hatching can be induced by both fimbriate and afimbriate bacteria. They observed a ~93% reduction in hatching of *T. muris* with a *fim A* knockout and a two-thirds reduction in hatching by inhibiting mannose dependent fimbriae (Hayes et al. 2010). In addition to demonstrating the role of fimbriae they showed that afimbriate strains *S. aureus* and *P. aeruginosa* induced hatching (Hayes et al. 2010). Together these results suggest that type 1 fimbriae alone are not responsible for hatching and there are alternative surface proteins that can provide the physical interaction between *Trichuris* eggs and bacteria.

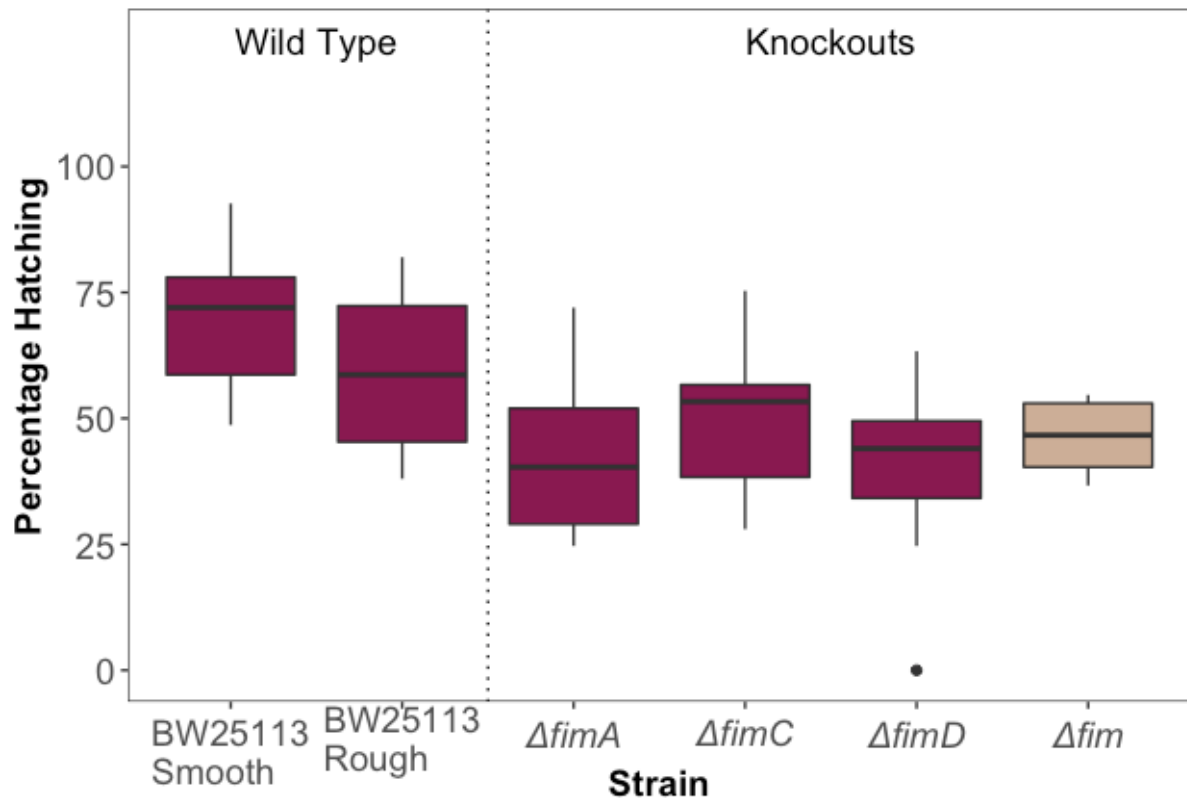


Figure 3.4. *fim* gene knockouts display reduced capability to induce hatching of *T. muris* eggs. Hatching of *T. muris* eggs was induced using *E. coli* K12 *fim* single-gene knockouts from the Keio collection ($\Delta fimA$, $\Delta fimC$, $\Delta fimD$); as well as a whole *fim* operon knockout (Δfim). Rough and smooth colonies of the parent strain of the Keio collection *E. coli* K12 BW25113 were used as a control for hatching. Percentage hatching was recorded after 24 h of co-culture. Hatching was completed in quadruplicate across 2 independent experiments (n=8), median and interquartile range are shown.

3.3 SEM on *T. muris* and *E. coli*, *S. typhimurium*, and *P. aeruginosa* co cultures.

In order to identify alternative surface proteins involved in hatching we investigated whether fimbriate (*E. coli*, *S. typhimurium*) and afimbriate (*P. aeruginosa*) bacteria formed fimbriae-like physical interactions around the surface of the eggs and the polar plug during hatching, similar to those of *E. coli*. SEM was conducted on *T. muris* co-cultures with each species and a pool of samples generated by imaging at three time points: 90, 120, and 150 min (Goulding 2021). As previously observed, smooth *E. coli* K12 MG1655 localised around the polar plug of the eggs (Figure 3.5). Bacterial localisation around the plug may be supported by the expression of fimbrial projections, which were more commonly observed on bacterial cells closer to the polar plug (Figure 3.5 b). This suggests that these fimbriae play a role in

hatching and the expression of fimbriae can be driven by proximity to the polar plugs, indeed no fimbriae were observed on the bacteria distal to the polar plug (Figure 3.5 c). Hatching specific expression of fimbriae may be driven by chemotaxis to the components of the plug that the fimbriae bind to. The type 1 fimbriae operon can be flexibly switched on and off to facilitate *E.coli* attachment; this phenomena has primarily been observed during urogenital epithelial attachment in infections (Y.-W. Chen et al. 2014; Lim et al. 1998). Together these results suggest that egg–bacteria interactions can result in expression of the molecules necessary to facilitate hatching. Similar to *E. coli*, co–culturing *T. muris* eggs with *S. typhimurium*, another type 1 fimbriae expressing strain, resulted in fimbriae–expressing bacteria being localised around the polar plug during hatching with very few bacteria found distal to the plug (Figure 3.6)(Goulding 2021).

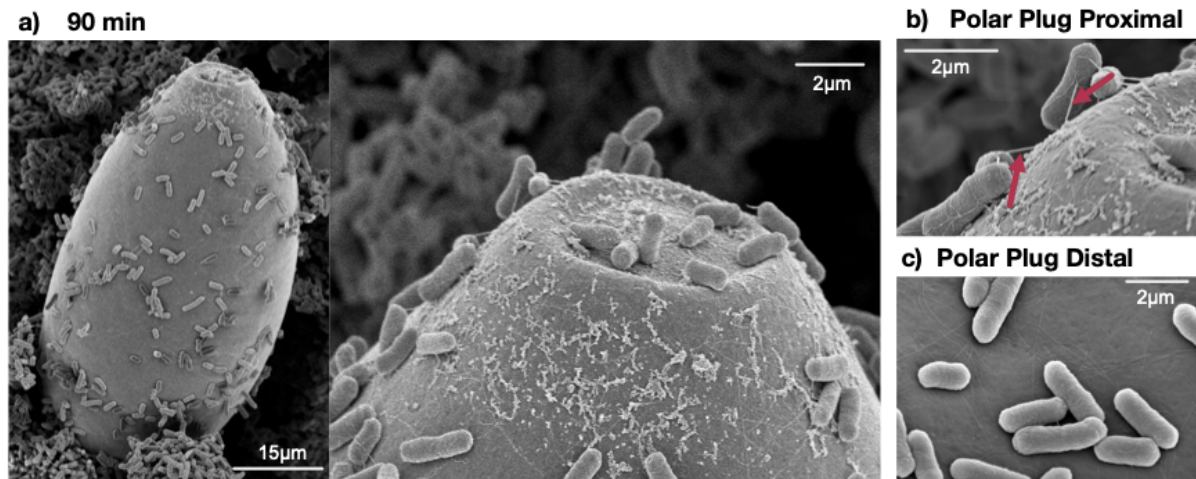


Figure 3.5. Smooth *E. coli* K12 MG1655 display fimbriae when proximal to the *T. muris* polar plug. a) Representative image of bacterial and egg co cultures collected at 90 min. b) SEM micrograph showing fimbriae expressing bacteria localised at the polar plug. c) SEM micrograph showing the lack of fimbriae on bacteria in areas further away from the plug (Goulding 2021).

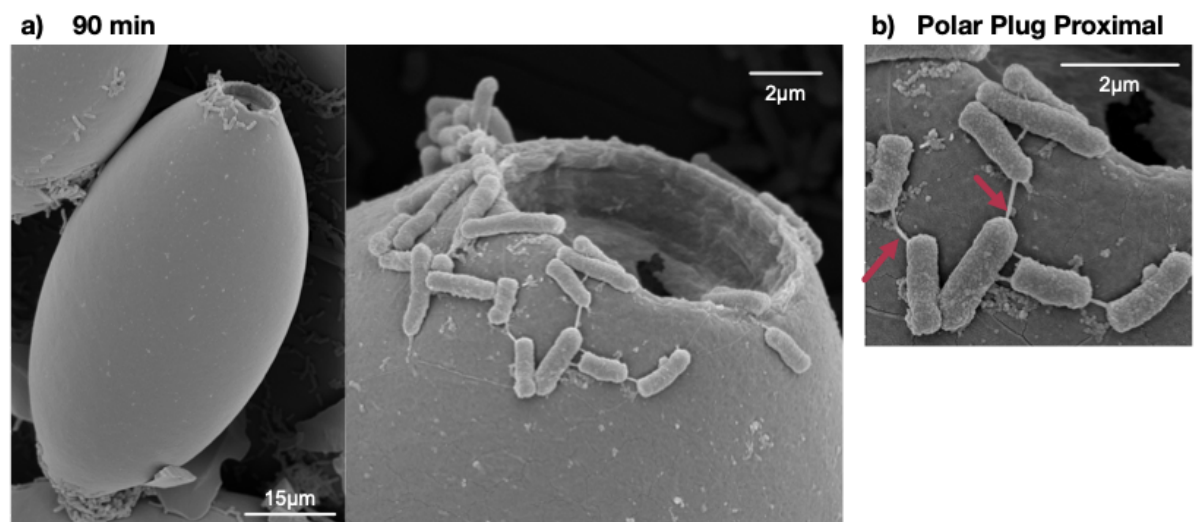


Figure 3.6. *S. typhimurium* display fimbriae when proximal to the *T. muris* polar plug and do not attach to distal regions of the egg. a) Representative images of bacterial and egg co cultures collected at 90 min. b) SEM micrograph showing fimbriae (arrow) of bacteria in areas proximal to the polar plug (Goulding 2021).

In the co-cultures of *T. muris* and *P. aeruginosa*, bacteria also localised around the polar plugs. Discernible projections could be seen on the surface of the bacteria; *P. aeruginosa* is an afimbriate strain, these images indicate that it expresses a different surface molecule to facilitate adherence to the polar plug (Figure 3.7). *P. aeruginosa* typically uses type IV pili to attach to surfaces (Crouzet et al. 2017).

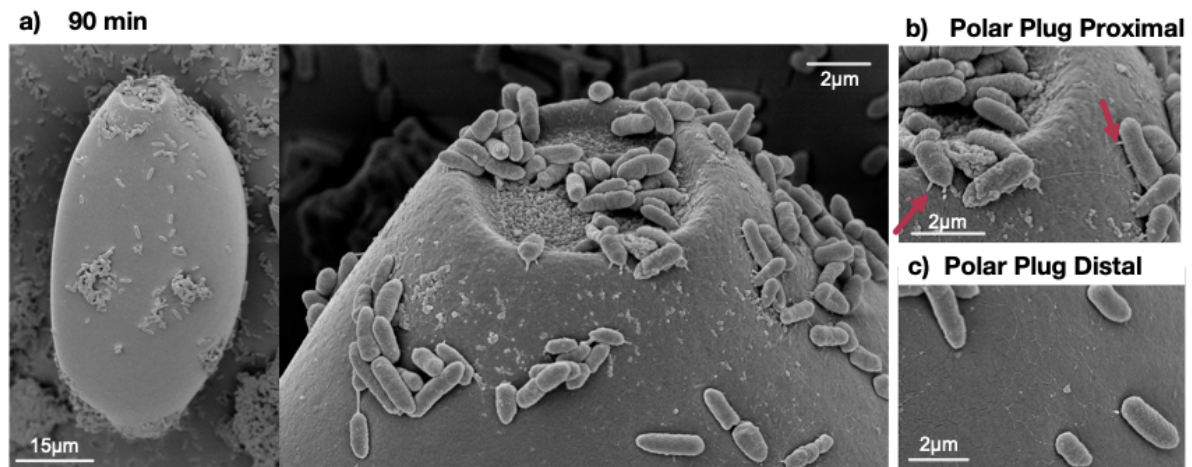


Figure 3.7. *P. aeruginosa* displays attachment pili when proximal to the *T. muris* polar plug. Representative images of bacterial and egg co-cultures collected at 90 min (a) SEM micrograph displaying bacteria with surface projections aggregated around the polar plugs prior to eclosion. (b) SEM micrograph showing fimbriae (arrow) of bacteria in areas proximal to the polar plug. (c) SEM micrograph showing the lack of fimbriae on bacteria in areas further away from the plug. *P. aeruginosa* is an afimbriate gram positive strain utilising an alternative attachment pilus (arrow) (Goulding 2021).

3.4 Characterising the role of proteases in bacteria mediated hatching of *T. muris* eggs

Considering that first, there is variation in the ways bacteria physically associate with the egg and, second, the presence or absence of individual physical–interaction proteins cannot alone explain the induction of hatching. I investigated the mechanism behind the degradation observed at the polar plugs and the potential role that proteases play. Hatching of *T. muris* was switched off by the addition of a protease inhibitor (Figure 3.8). I examined whether the effects of a cysteine and serine protease inhibitor cocktail could be reversed by washing the eggs and re-exposing them to the bacterial cultures, ensuring that the protease had no effect on larval viability. As shown in Figure 3.8 once the eggs were washed and re-incubated with

both rough and smooth *E. coli* K12 cultures of BW25113 and MG1655, hatching was observed at levels comparable to the control. This data demonstrated that the inhibitor did not irreversibly prevent hatching, perhaps by acting only on secreted proteases. In addition to demonstrating reversible inhibition, inhibition was shown to be dose- dependent with all four strains of *E. coli* K12 (Figure 3.9). Dilution of the protease inhibitor decreased its effects and this suggests that enzyme kinetics can be optimised to maximise inhibition of hatching.

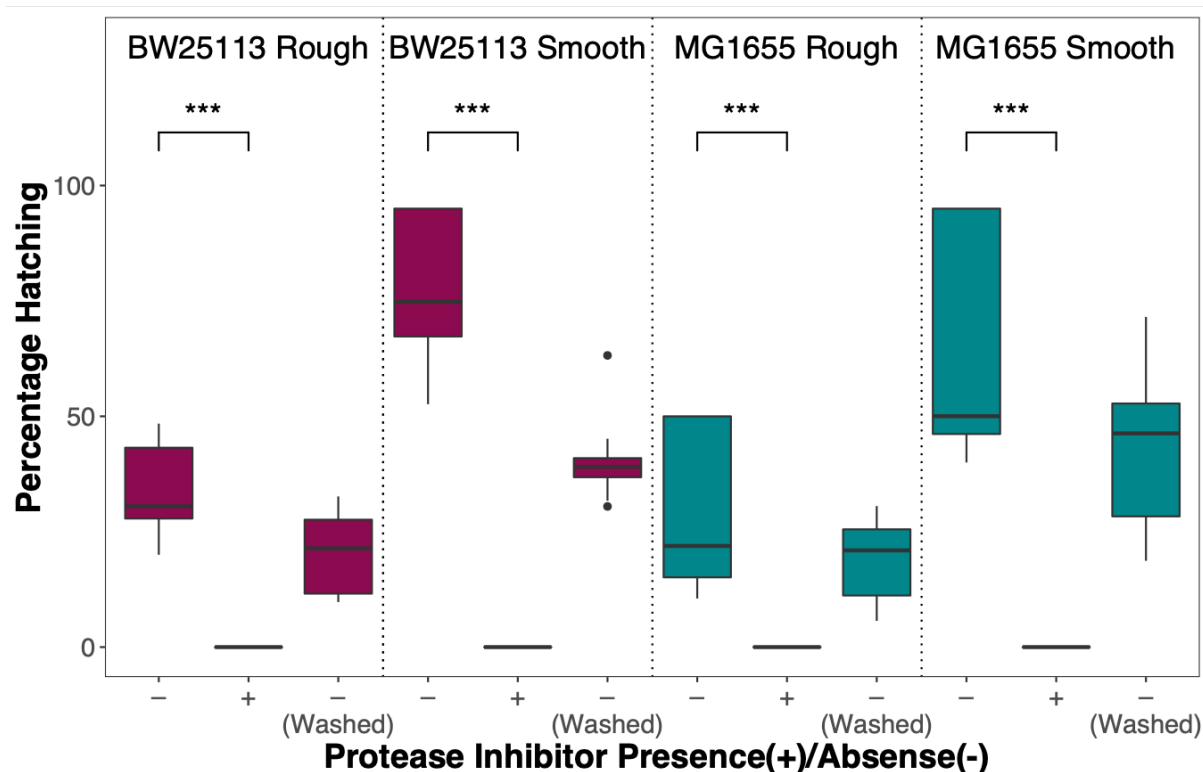
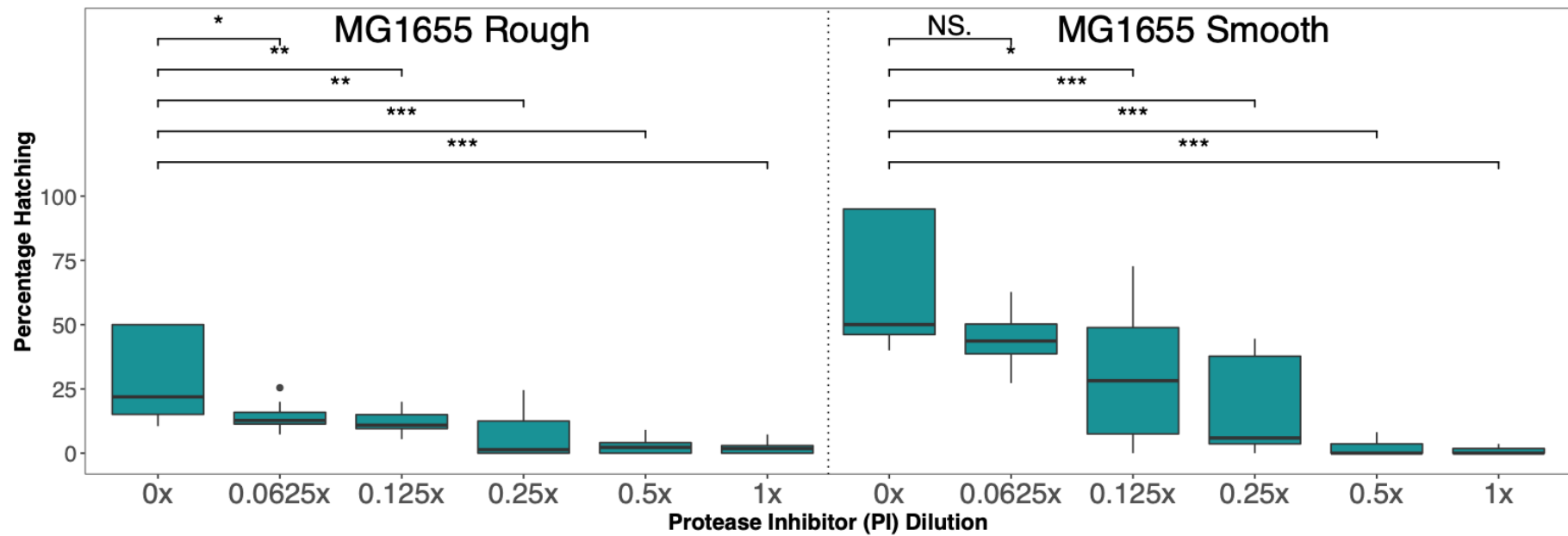


Figure 3.8. Protease inhibitors mediate a reversible interruption of *E. coli* induced hatching of *T. muris* eggs. Hatching of *T. muris* eggs was induced using rough and smooth colonies of *E. coli* BW25113 and K12 MG1655S. Percentage hatching was recorded after 24 h of co-culture with bacteria (–) or with bacteria in the presence of the protease inhibitor (+) (1x cComplete™, Mini, EDTA-free Protease Inhibitor Cocktail- Roche). After co-culture in the presence of the inhibitor the *T. muris* eggs were washed to remove the inhibitor, and re-exposed to bacterial cultures; percentage hatching was recorded 24 h later (– Washed). Hatching was completed in triplicate, across 4 independent experiments (n=12), median and interquartile range are shown, and statistical analysis was performed using the paired samples Wilcoxon test (***) $p \leq 0.001$.

a



b

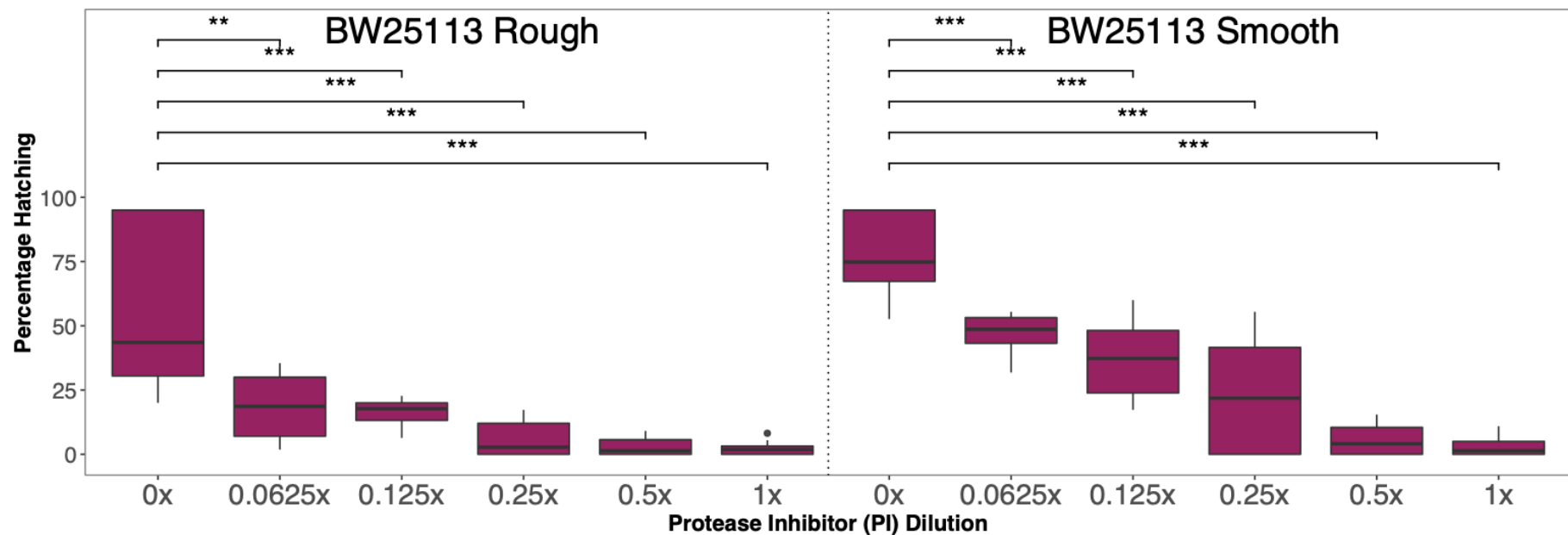


Figure 3.9. Protease inhibitors mediate a titratable interruption of *E. coli*

induced hatching of *T. muris* eggs. Hatching of *T. muris* eggs was induced using rough and smooth colonies of *E. coli* K12 MG1655S (a) and BW25113 (b).

Percentage hatching was recorded after 24 h of co-culture with bacteria or with bacteria in the presence of the dilution series of the protease inhibitor (1x, 0.5x, 0.25x, 0.125x, 0.0625x cOmplete™, Mini, EDTA-free Protease Inhibitor Cocktail-Roche). Hatching was completed in quadruplicate, across 2 independent experiments (n=8), median and interquartile range are shown, and statistical analysis was performed using the paired samples Wilcoxon test (** $p \leq 0.001$, * $p \leq 0.01$, * $p \leq 0.05$).

The progression of the hatching cascade and degradation of the polar plugs is likely driven by both bacterial and larval proteases. It is not currently possible to generate mutant worms to investigate larval proteases, so to further characterise the class of proteases responsible for hatching I used a panel of serine and cysteine inhibitors, and single gene knockouts for *E. coli* K12 serine and cysteine proteases. The protease inhibitor cocktail contains a proprietary mix of enzymes with broad activity across the majority of serine and cysteine proteases. Therefore, to determine the relative importance of serine or cysteine proteases for hatching, I tested dual inhibitors with a narrower activity spectrum (antipain and leupeptin), and single inhibitors for both cysteine (E64) and serine (aprotinin, chymostatin, Pefabloc) proteases. I did not see a reduction with antipain or leupeptin, however this proved to still be informative. Antipain is an inhibitor specific to trypsin and papain; leupeptin targets trypsin, plasmin, porcine kallikrein, papain, cathepsin B, and endoproteinase Lys-C (ChEBI 2021) which suggests that these proteases are not implicated in hatching. I observed significant ($p < 0.05$) reduction with the cysteine inhibitor E64, and complete ablation with the protease inhibitor cocktail and the serine protease inhibitor Pefabloc (Figure 3.10). Pefabloc is the commercial name of 4-(2-Aminoethyl) benzenesulfonyl fluoride hydrochloride (AEBSF), a widely used broad spectrum serine protease inhibitor (Powers et al. 2002). It is challenging to confirm the substrate specificity of proteases but it is known that Pefabloc interacts at the active site of S1 family serine proteases (Powers et al. 2002). There are 704 S1 family serine proteases and Pefabloc has action against: trypsin, chymotrypsin, plasmin, thrombin, and kallikreins (Kim et al. 2014; Neil D. Rawlings 2010). The results show that hatching was not ablated by the inhibitors of chymotrypsin (Chymostatin), trypsin (Aprotonin), plasmin (Leupeptin), and porcine kallikrein (Leupeptin), suggesting that hatching

is likely not driven by any of those proteases but may be driven by proteases similar to thrombin or other types of kallikrein proteases.

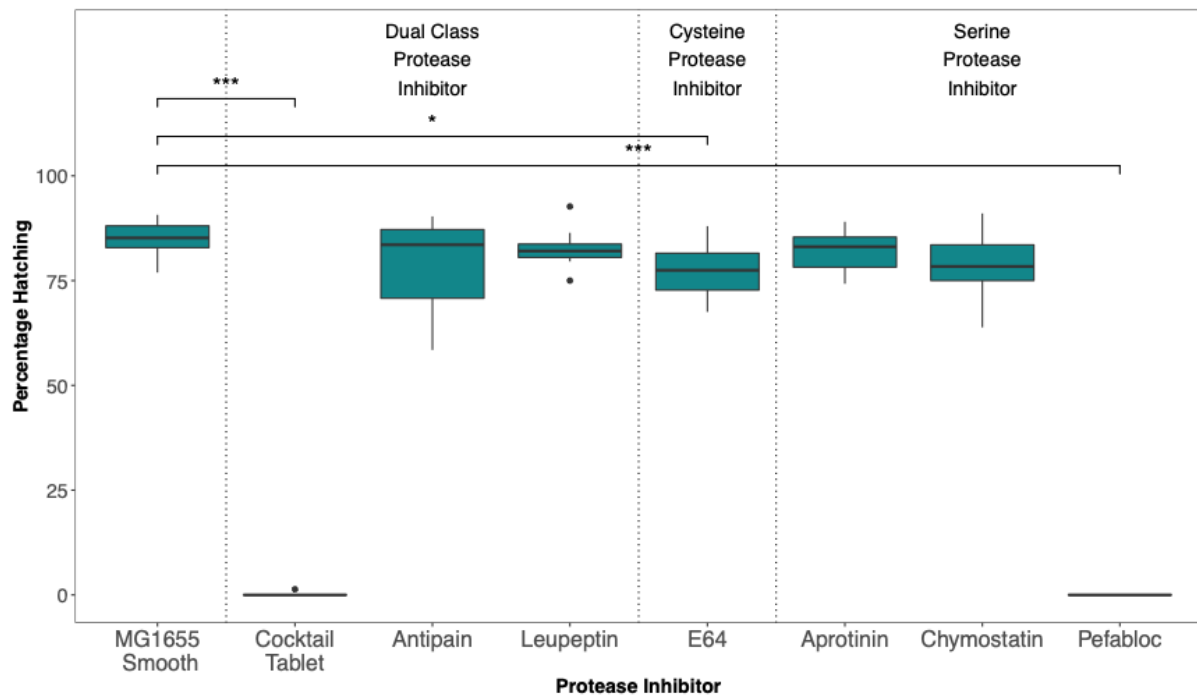


Figure 3.10. *E. coli* induced hatching of *T. muris* eggs is ablated by the addition of a protease inhibitor cocktail, or serine protease inhibitor Pefabloc™.

Hatching of *T. muris* eggs was induced using smooth colonies of *E. coli* K12 MG1655S. Percentage hatching was recorded after 24 h of co-culture with bacteria or with bacteria in the presence of a panel of serine and cysteine protease inhibitors (1x cComplete™, Mini, EDTA-free Protease Inhibitor Cocktail, Roche). Hatching was completed in triplicate, across 3 independent experiments (n=9), median and interquartile range are shown, and statistical analysis was performed using the paired samples Wilcoxon test (** $p \leq 0.001$, * $p \leq 0.05$).

The *E. coli* genome encodes at least 21 serine proteases. The genes comprising serine protease operons available as knockout clones in the Keio collection are *clpA*, *clpP*, *clpX*, *degP*, *degQ*, and *glpG*, and the other serine proteases are likely essential genes (“*E. Coli* Proteases” 2021; Yamamoto et al. 2009). I co-cultured *T. muris* eggs with these knockouts alongside BW25113, and observed a significant reduction in hatching (50%) with the *clpP* knockout (Figure 3.11), which suggests that this protease is important to the induction and progression of hatching. This gene encodes the proteolytic subunit of the *clpX-clpP* and *clpA-clpP* ATP-dependent serine proteases. (“*E. Coli* Proteases - Serine Proteases” 2021).

ClpP proteases are well characterised in several species including *E. coli*, they facilitate the proteolysis of damaged, misfolded, ribosome-stalled, and regulatory proteins, and there are 50 known substrates of *E. coli* ClpP protease (Bhandari et al. 2018; Flynn et al. 2003).

The *E. coli* genome encodes at least 6 cysteine proteases. The cysteine protease gene knockouts available in the Keio collection are *elaD*, *hchA*, *nlpC*, *yafL*, *ydhO*, and *yhbO* ("*E. Coli Proteases*" 2021; Yamamoto et al. 2009). I co-cultured *T. muris* with these knockouts alongside BW25113 smooth cultures, and observed a modest but significant reduction in hatching with the *hchA* and *ydhO* knockouts (Figure 3.12). The *hchA* gene encodes a molecular chaperone and aminopeptidase and removing this gene likely results in decreased fitness of these bacterial cells (Mujacic and Baneyx 2006). The *ydhO* gene encodes a member of the peptidoglycan hydrolysing C40 family of peptidases (Singh et al. 2012). The slight reduction in hatching suggests that these proteases are involved but necessary for hatching.

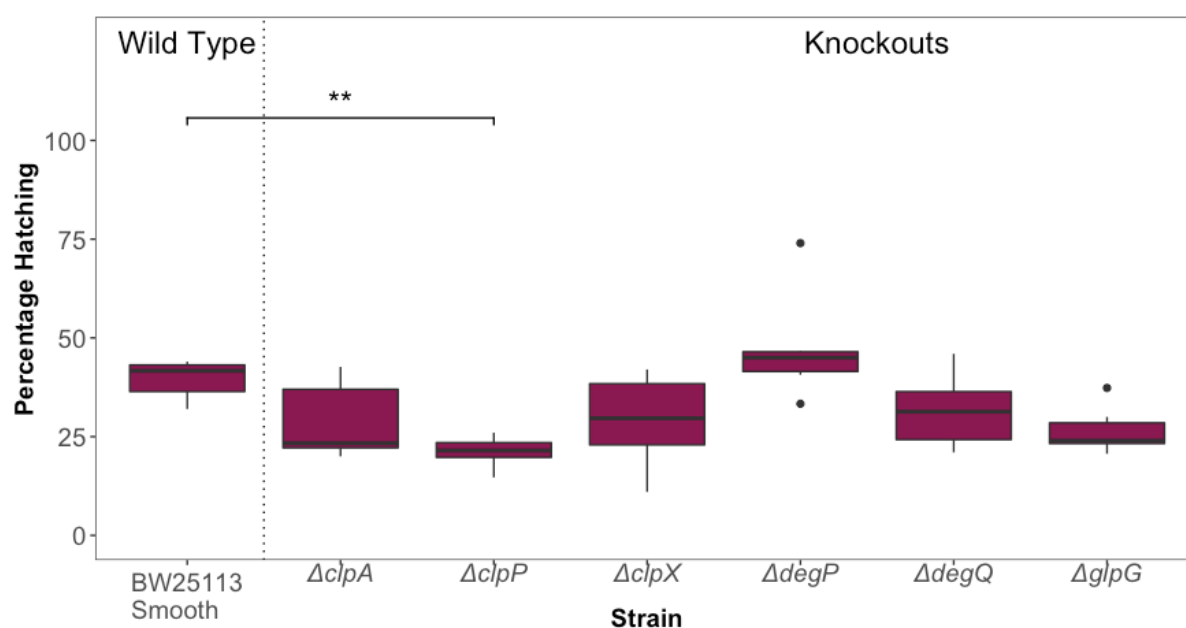


Figure 3.11. *E. coli* K12 serine protease gene knockout *clpP* displays reduced capability to induce hatching of *T. muris* eggs. Hatching of *T. muris* eggs was induced using *E. coli* K12 single gene knockouts of genes comprising serine protease operons from the Keio collection (*clpA*, *clpP*, *clpX*, *degP*, *degQ*, *glpG*). Smooth colonies of the parent strain of the Keio collection *E. coli* K12 BW25113 were used as a control for hatching. Percentage hatching was recorded after 24 h of co culture. Hatching was completed in triplicate across 2 independent experiments (n=6), median and interquartile range are shown, and statistical analysis was performed using paired samples Wilcoxon test (** $p \leq 0.01$).

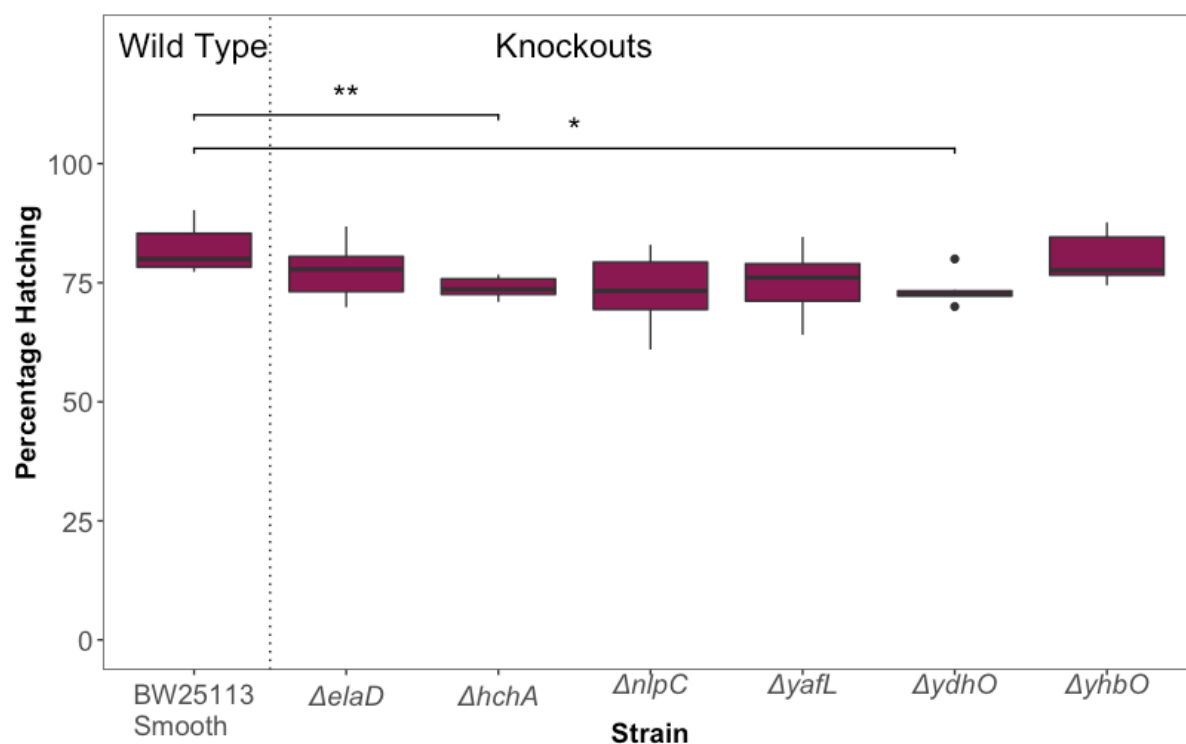


Figure 3.12. *E. coli* K12 cysteine protease gene knockouts *hchA* and *ydhO* display reduced capability to induce hatching of *T. muris* eggs. Hatching of *T. muris* eggs was induced using *E. coli* K12 cysteine protease single gene knockouts from the Keio collection (*elaD*, *hchA*, *nlpC*, *yafL*, *ydhO*, *yhbO*). Smooth colonies of the parent strain of the Keio collection *E. coli* K12 BW25113 were used as a control for hatching. Percentage hatching was recorded after 24 h of co culture. Hatching was completed in triplicate across 2 independent experiments (n=6), median and interquartile range are shown, and statistical analysis was performed using the paired samples Wilcoxon test (** $p \leq 0.01$, * $p \leq 0.05$).

In order to examine the role of proteases during *T. muris* hatching with bacterial species other than *E. coli* I evaluated the effects of a protease inhibitor cocktail targeting both serine and cysteine proteases on hatching induced by *P. aeruginosa*, *S. aureus*, and *S. typhimurium* over a 24 h period. As shown in Figure 3.13, I observed that irrespective of their expression of type 1 fimbriae, hatching is interrupted by inhibition of proteases.

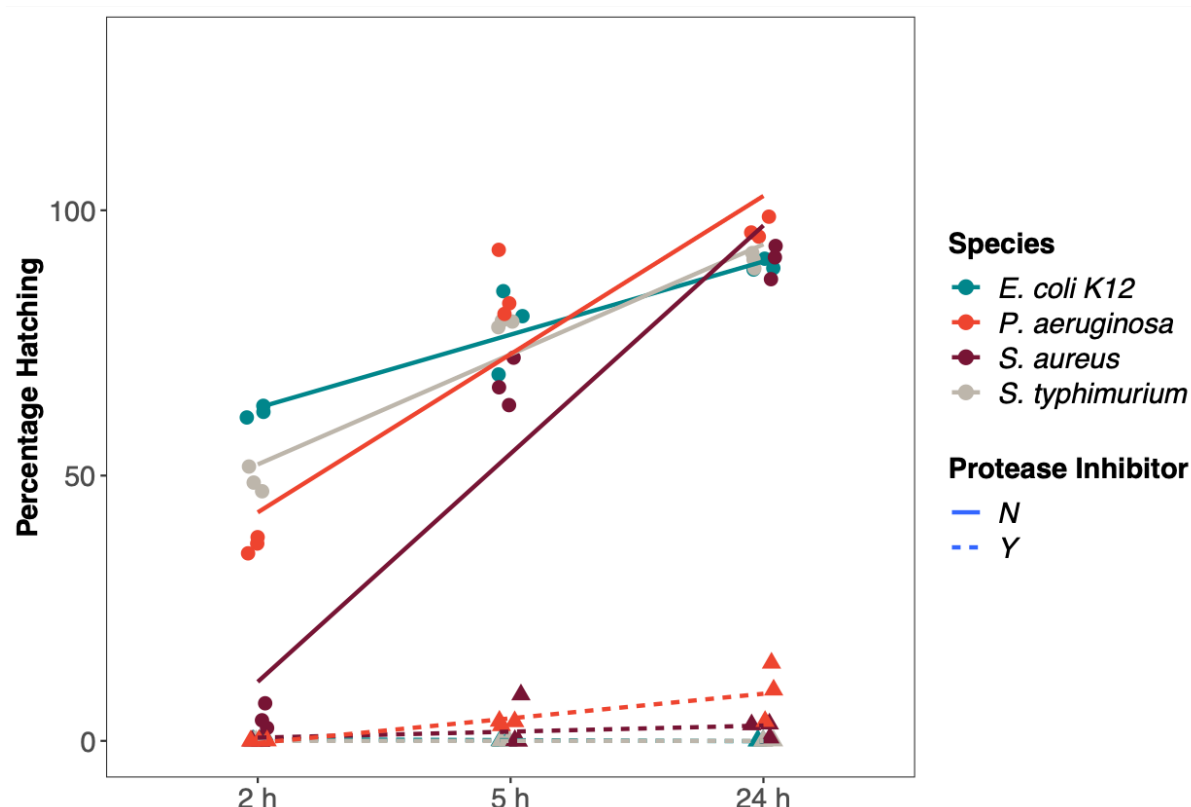


Figure 3.13. Protease inhibitors interrupt bacterial mediated hatching of *T. muris* eggs. Hatching of *T. muris* eggs was induced using *E. coli* K12 MG1655S, *P. aeruginosa*, *S. aureus*, and *S. typhimurium* in the presence or absence of the protease inhibitor (2x cComplete™, Mini, EDTA-free Protease Inhibitor Cocktail-Roche). Hatching was completed in triplicate (n=3), and percentage hatching was recorded after 2, 5, and 24 h.

Overall the data shows that the serine proteases are more important to hatching than the cysteine proteases. I observed a greater reduction in hatching with bacterial serine protease knockouts and complete ablation of hatching in the presence of Pefabloc™. Additionally, the proteases are likely secreted by both bacteria and the worm larvae, as the bacterial serine protease knockouts tested did not result in complete ablation of hatching. Furthermore, ablation is seen across bacterial species regardless of attachment style. Proteases are therefore crucial to the induction and progression of *T. muris* hatching.

3.5 The composition of the polar plug

As shown in previous studies (Hayes et al. 2010) and above the polar plug is the site of bacterial binding and subsequent eclosion, therefore understanding the composition of the polar plug would enable us to identify bacterial or larval enzymes capable of degrading these components. Proteomics was used to examine the components of the polar plugs, and to evaluate the different components of the egg a subtractive approach was used. The polar plugs are tough to isolate and represent a very small region of the egg that is susceptible to degradation. I hypothesised that characterising large quantities of egg and larval proteins would allow me to perform a differential analysis. Peptides were characterised from: whole eggs, hatched larvae (bleach and bacteria), and empty egg shells, and analysed by LC-MS/MS (kindly provided by J Choudhary, L Yu, and J Wright, ICR). In comparing the peptide compositions of whole eggs, eggshells, and larvae, I aimed to identify peptides that were present in the whole egg, and not present in any of the other samples. I considered these peptides to be unique to the polar plug. Peptides identities were assigned using the Sequest HT search engine in Proteome Discoverer™ (PD) 2.4 to search translated *T. muris* transcriptomic data, and protein databases for *T. muris*, *T. suis*, and *T. trichiura* for hits. Once identified, WormBase ParaSite (Howe et al. 2017) and BLAST (Johnson et al. 2008) were used to annotate sequences, and iTasser (J. Yang et al. 2015) was used to predict structure and find structural homologues. Eleven of the high-quality peptides identified were unique to the polar plug, and most of these proteins contain chitin-binding molecules. The presence of the chitin-binding function supports previous observations that the polar plug is formed of a chitin matrix supporting other molecules (D. A. Wharton and Jenkins 1978). In addition, the structure of three of the chitin binding peptides resembled factor H, a glycoprotein present in human plasma (Table 3.2) (Józsi 2017). Interestingly, a protein containing a bactericidal permeability-increasing protein (BPI) domain was observed in the polar plug, proteins containing this domain can neutralise bacteria (Table 3.2) (Canny and Levy 2008; Balakrishnan et al. 2013). Further proteomic and RNAseq studies on eggs and larvae will be crucial to clarify the role these proteins play as intrinsic hatching factors of *T. muris*.

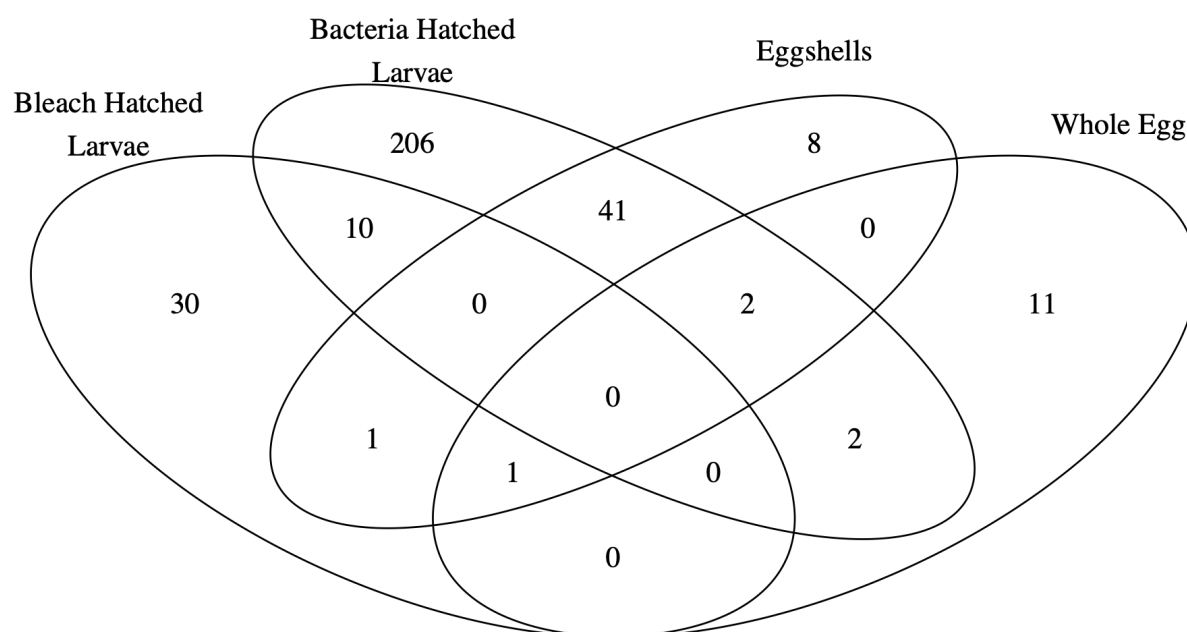


Figure 3.14. Unique peptides of the polar plug inferred by subtractive proteomic analysis. Proteins were extracted from mature *T. muris* eggs, bleach-hatched larvae, *E. coli*-hatched larvae, and empty eggshells. Proteins underwent tryptic digestion, alkylation, deglycosylation, and desalination; and peptides were analysed using LC-MS/MS. Peptide identities were assigned using the Sequest HT search engine in Proteome Discoverer TM (PD) 2.4 (L Yu, and J Wright, ICR). High quality peptide hits unique to each sample are shown.

Table 3.2 Putative components of the polar plugs of *T. muris* eggs

Gene/Transcript	WormBase/ BLAST Annotated Domains	iTasser Prediction (TM Score >0.90)
TMUE_3000011828	Uncharacterized protein Chitin-Binding type 2 Carbohydrate-Binding Module Family 14	Human Complement Factor H
HS30_20402:8:2212:8792:65867_9	—	—
TMUE_3000012569	Uncharacterized protein Chitin-Binding type 2 Carbohydrate-Binding Module Family 14	—
TMUE_1000003367	Uncharacterized protein Bactericidal permeability-increasing protein, alpha/beta domain superfamily	—
HS30_20402:8:2115:18868:66551_5	—	—
TMUE_3000014619	Uncharacterized protein Carbohydrate-Binding Module Family 14 Thrombospondin type 1 repeats Chitin-Binding type 2	Human Complement Factor H
HS30_20402:8:1304:13832:66582_7	PREDICTED: Orbicella faveolata ubiquitin-60S ribosomal protein L40 (LOC110050203), mRNA	—
TTRE_0000054801_mRNA_1	Uncharacterized protein	Variant Surface Glycoprotein VSG^{sur}
D918_04857	—	—
HS30_20402:8:1216:19006:67976_6	PREDICTED: Drosophila ficusphila transcription factor grauzone (LOC108091102), mRNA	—
TTRE_0000321001_mRNA_1	Carbohydrate-Binding Module Family 14 chitin-binding lectins	Human Complement Factor H
<i>Trichuris</i> gene annotations from WormBase ParaSite (Howe et al. 2017) Transcript identity assigned in BLAST (Johnson et al. 2008) Structural and functional predictions made using iTasser (J. Yang et al. 2015)		

3.6 Bacteria induced hatching of *T. muris* occurs after a minimum amount of embryonation

The progression of hatching relies on interactions between bacteria and the eggs as well as the active participation of larvae. I hypothesise that a minimum amount of embryonation is required for larvae to respond to natural cues and initiate the hatching cascade. Through monitoring changes in gene expression during embryonation I investigated genes that may be essential for hatching. Embryonation in *Trichuris* eggs occurs in the absence of light and is driven by temperature; embryonation progresses at room temperature although this process can be sped up by incubating at 28°C (Nolf 1932; Forman et al. 2021; Vejzagić et al. 2016). To study embryonation I collected eggs laid over a 4 or 24 h period by adult worms isolated from six infected SCID mice and embryonated them for eight weeks in the dark and at room temperature. Aliquots of ~500 eggs were taken every 7 days for microscopy, hatching, and RNAseq. The microscopy images allowed me to track morphological development over the duration of embryonation. One day after being laid, eggs are unembryonated and internal contents unsegmented (Figure 3.15a). After 1 week of embryonation, cleavage has progressed to the four-cell stage (Figure 3.15b) At week 5, the larva visually appears morphologically mature, and at 8 weeks of embryonation the larva is considered mature (Figure 3.15c and d). The eggs collected to test hatching were co-cultured with *E. coli* for 24 h and for the stages prior to larval development I looked for degradation of the polar plugs as a read-out for hatching. After larvae had formed, eclosed larvae were counted and the percentage of hatched larvae calculated. I did not observe any hatching before six weeks, and observed the highest levels of hatching at seven weeks. At eight weeks the levels of hatching reduced slightly but remained constant when these mature eggs were tested again a month later (Figure 4.2 e). At each time point one aliquot of ~500 eggs were flash frozen at -80°C for RNA extraction and subsequent sequencing.

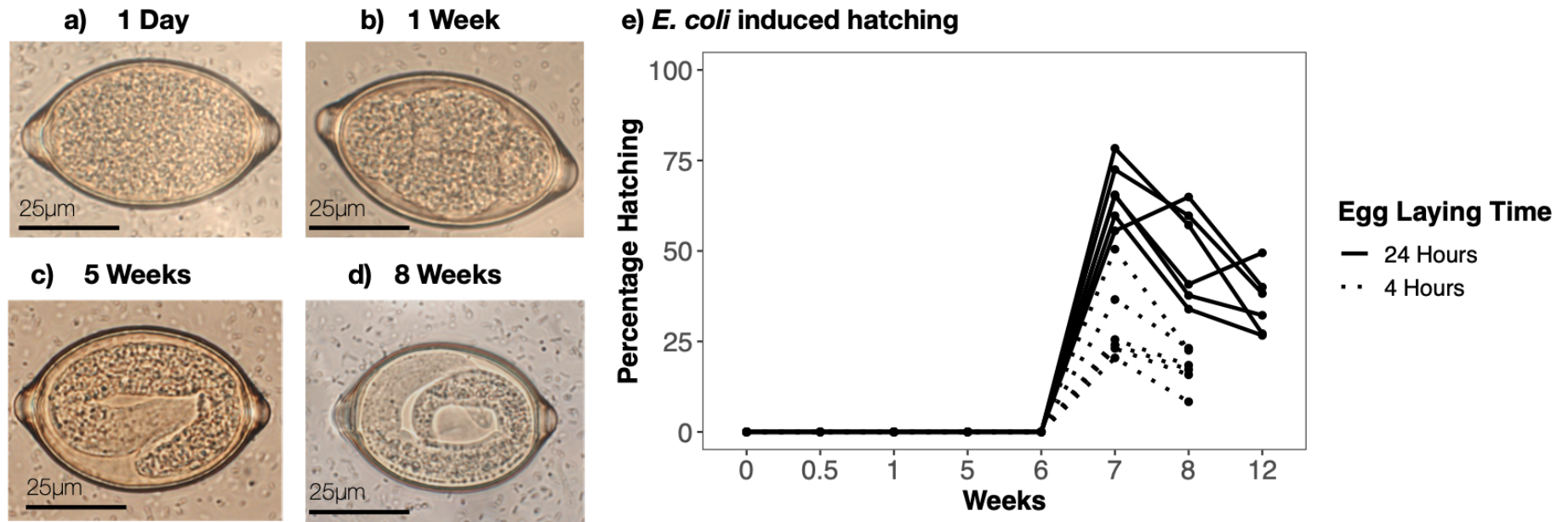


Figure 3.15. A minimum of 7 weeks of embryonation is required to observe *E. coli* induction of *T. muris* egg hatching. Six SCID mice were infected with a high dose of *T. muris* eggs and adult worms collected at 35 days post infection. Worms were cultured in medium and their eggs collected at 4 h (dotted lines) and 24 h (solid lines). The eggs were embryonated and samples collected weekly. a)–d) Light microscopy images taken at one day, one week, five weeks, and eight weeks. e) Percentage hatching was recorded weekly after 24 h of incubation with *E. coli* (n=6).

3.7 Changes in gene expression of *T. muris* occurring during embryonation

In this chapter I considered hatching primarily looking at bacterial components and the role they play in hatching. However, as shown above, intrinsic factors such as embryonation impact hatching (Figure 3.15) I used RNAseq to evaluate changes in gene expression during embryonation that explained the development of hatching in response to bacterial induction at seven weeks (Figure 3.15). Differential gene expression analysis between eggs after 8 and 6 weeks of embryonation showed many transcriptional differences between eggs collected at each time point and yielded 6,408 significantly differentially expressed genes. Genes were filtered by adjusted p value (Benjamini and Hochberg method, p value < 0.05) and then sorted by effect size (fold change >2), and this analysis inspects 40 of these highly significant genes in mature or immature eggs (Table 4.1). The genes that appear on the left hand side of the plot are more abundant in mature eggs, and genes that appear on the right hand side are more abundant in immature eggs (Figure 3.16). Interestingly, the expression of several major classes of enzymes, including serine, cysteine, and metalloproteases, are differentially expressed before and after eggs are able to hatch. Of particular interest are the S1 family serine proteases that are highly expressed in mature eggs (TMUE_2000008704, TMUE_3000011680, TMUE_2000006651) (Table 4.1). These proteases may be the target of the inhibitor Pefabloc which causes the complete ablation of hatching (Figure 3.12). Mature eggs are also expressing an inhibitor (TMUE_2000008020) with action against S1 proteases (Table 4.1). Further work would be needed to determine how this inhibitor is activated and regulated, especially in the context of hatching progression.

Genes of interest expressed in the immature eggs include two genes encoding proteins with patched and sterol sensing domains (SSD), and one gene encoding a putative bactericidal permeability-increasing protein (BPI). In *C. elegans* patched proteins contain the transmembrane SSD and are signal transducers during life cycle transitions, like moulting, and population expansion (Entchev and Kurzchalia 2005; N. C. Lu, Newton, and Stokstad 1977; Soloviev et al. 2011). BPI is a multifaceted signalling protein with several roles, including the neutralisation of predominantly gram-negative bacteria, but also gram positive bacteria and apicomplexans (Canny and Levy 2008; Balakrishnan et al. 2013).

Week 6 Vs Mature

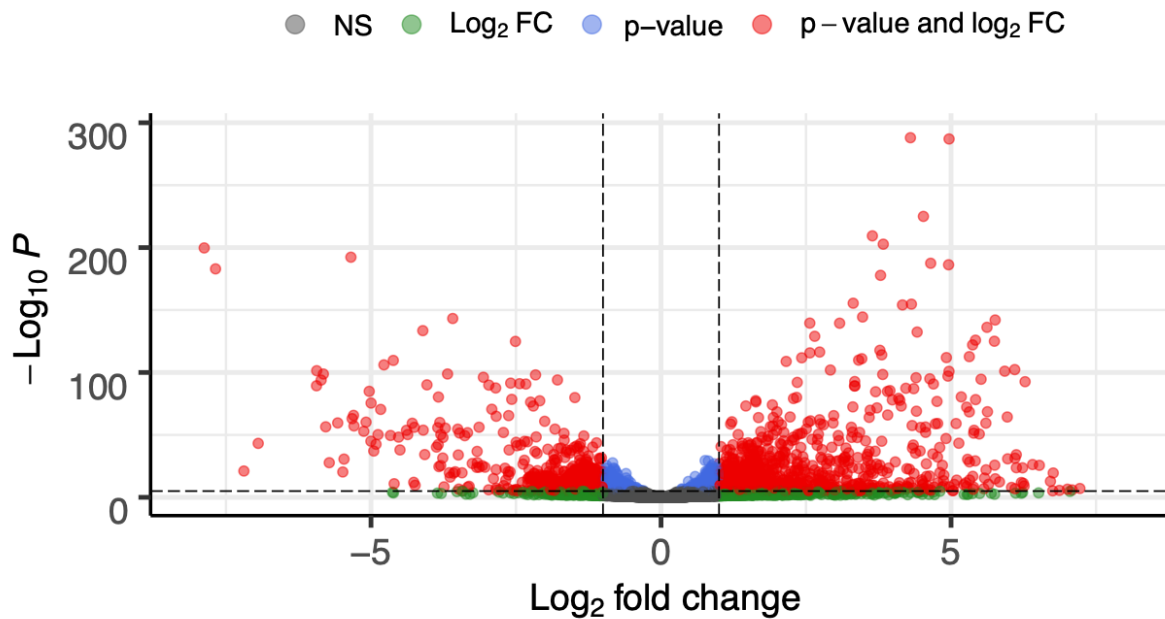


Figure 3.16. Immature and fully mature *T. muris* eggs have distinct RNA expression profiles. *T. muris* eggs were collected after 6 (n=5) and 8 weeks (n=6) of embryonation for RNA extraction and sequencing. Read counts were collected after mapping to the *T. muris* genome (WormBase ParaSite 11-Apr-2019). Differential expression analysis was conducted using Deseq2 (Anders and Huber 2012). Log transformed P values (y axis) and log transformed fold change (x axis) were plotted to identify genes with significant fold changes (Log_2 fold change $>|1|$ or $\text{Log}_{10} P > 1.3$) at each time point yielding 6,408 significantly differentially expressed genes out of a total 13,848. Genes more abundant in mature eggs appear on the left, and genes more abundant in immature eggs appear on the right.

Table 3.3 Top 20 genes expressed in immature and fully mature eggs

Gene Identifier	Description	Egg Age	Associated GO terms	Predicted Domains, Structures, or Function	Fold Change
TMUE_3000014195	NULL	Mature	Anhydride Hydrolase	Folate-sensitive fragile site protein Fra10Ac1 Enzyme catalysing the hydrolysis of any acid anhydride	-7.88
TMUE_2000008704	Apple Domain Protein	Mature		Plasma kallikrein and coagulation factor XI like serine protease (McMullen, Fujikawa, and Davie 1991; Ho et al. 1998)	-7.68
TMUE_1000005399	NULL	Mature	Ester Hydrolase, DNA Enzyme	Deoxyribonuclease II; YacP-like NYN domain. An enzyme catalysing the hydrolysis of phosphodiester linkages of deoxyribonucleotides in DNA	-5.35
TMUE_3000011512	Inhibitor-I29 domain protein	Mature	Cysteine peptidase	Salarin like cysteine peptidase inhibitors (Olonen, Kalkkinen, and Paulin 2003)	-6.94
TMUE_1000003203	NULL	Mature	none	EB module; Dickkopf N-terminal cysteine-rich region; Carboxypeptidase A inhibitor	-7.19
TMUE_3000013381	NULL	Mature	none	Repeat protein with two Protein A-DHR14 repeat modules	-4.62
TMUE_3000011680	Peptidase S1 Domain	Mature		MEROPS peptidase family S1 (PA clan) cysteine or serine proteases (Bazan and Fletterick 1988)	-4.78
TMUE_3000011251	NULL	Mature	none	Ion binding protein; interacting selectively and non-covalently with ions, charged atoms or groups of atoms.	-5.94
TMUE_3000011159	NULL	Mature	none	Ion binding protein; interacting selectively and non-covalently with ions, charged atoms or groups of atoms.	-5.82
TMUE_2000009348	TIL domain protein	Mature		Cysteine rich trypsin inhibitors. (Grasberger, Clore, and Gronenborn 1994)	-5.86
TMUE_2000010508	NULL	Mature	Ester Hydrolase, DNA Enzyme	Deoxyribonuclease II An enzyme catalysing the hydrolysis of phosphodiester linkages of deoxyribonucleotides in DNA	-5.94
TMUE_3000011401	Purine Nucleoside Phosphorylase	Mature		Enzyme catalyzing the chemical reaction of purine nucleoside and phosphate, to purine and alpha-D-ribose 1-phosphate.	-3.59
TMUE_2000007058	NULL	Mature	Glycosyl Transferase	UDP-glucuronosyl and UDP-glucosyl transferase; ComR tetratricopeptide Enzyme catalyzing the addition of the glycosyl group from a UTP-sugar to a small hydrophobic molecule	-4.11

TMUE_2000008020	NULL	Mature	Enzyme Inhibitor	Kunitz/Bovine pancreatic trypsin inhibitor domain; SAD/SRA domain, Unkempt Zinc finger domain 1 (Znf1) MEROPS inhibitor family I2, clan IB; inhibiting proteases of the S1 family (Neil D. Rawlings, Tolle, and Barrett 2004)	-4.04
TMUE_3000014577	Reverse Transcriptase domain protein	Mature		Transposable Element	-3.68
TMUE_2000010053	NULL	Mature	none	Glycosyl hydrolase family 1 Enzymes that hydrolyse the glycosidic bond between two or more carbohydrates, or between a carbohydrate and a non-carbohydrate moiety.	-5.03
TMUE_3000012561	NULL	Mature	Anhydride Hydrolase	Enzyme catalysing the hydrolysis of any acid anhydride	-3.06
TMUE_2000006651	NULL	Mature	Serine Protease	Trypsin; Domain of unknown function (DUF5122) beta-propeller Serine peptidase (N. D. Rawlings and Barrett 1994)	-2.16
TMUE_2000008732	NULL	6 Wks	Serine Hydrolase/ Peptidase	Homocysteine S-methyltransferase; Trypsin Enzyme catalyzing the chemical reaction of S-methylmethionine and L-homocysteine, to 2 molecules of L-methionine.	4.30
TMUE_3000012389	NULL	6 Wks	Peptidase Inhibitor/ Regulator	WAP-type (Whey Acidic Protein) 'four-disulfide core', Trypsin Inhibitor like cysteine rich domain The WAP domain comprises eight cysteine residues involved in disulfide bonds in a conserved arrangement. This domain has been shown to exhibit antiproteinase function (Bingle, Singleton, and Bingle 2002)	4.97
TMUE_3000013087	NULL	6 Wks	none	Dickkopf N-terminal cysteine-rich region; EB Module; Carboxypeptidase A inhibitor; Magi 5 toxic peptide family	4.52
TMUE_2000008408	Zinc metalloproteinase	6 Wks		An enzyme requiring zinc for its catalytic activity	3.64
TMUE_2000008856	Carrier domain-containing protein	6 Wks		The Carrier Protein domain comprises a 3- or 4-helix bundle; CP domains are involved in the transfer of thiol ester-bound intermediates during metabolite biosynthesis	3.83
TMUE_3000012555	Metalloendopeptidase	6 Wks		An enzyme requiring a metal for its catalytic activity	4.65
TMUE_3000011631	BPTI/Kunitz inhibitor domain-containing protein	6 Wks		MEROPS inhibitor family I2, clan IB; inhibiting proteases of the S1 family (Neil D. Rawlings, Tolle, and Barrett 2004)	4.96

TMUE_3000013206	NULL	6 Wks	none	The EB domain comprises eight cysteine residues that may be involved in disulfide bonds. This domain has no known function	3.78
TMUE_2000008478	Reverse transcriptase Ty1/copia-type domain-containing protein	6 Wks		Transposable element	3.31
TMUE_0000001260	SSD domain-containing protein	6 Wks		The sterol-sensing domain (SSD) comprises ~180 residues arranged in five membrane-spanning segments; and confers sensitivity to regulation by sterol (Kuwabara and Labouesse 2002)	4.32
TMUE_2000007793	MAM domain-containing protein	6 Wks		The MAM (meprin, A-5 protein, and receptor protein-tyrosine phosphatase mu) domain comprises of approximately 170 amino acids and occurs in several cell surface proteins; it is likely to have an adhesive function. (Beckmann and Bork 1993)	4.16
TMUE_3000012260	NULL	6 Wks	membrane component	Short chain dehydrogenase; Phthiocerol/phthiodiolone dimycocerosyl transferase C-terminus Enzymes often comprising of 250 to 300 amino acid residues and at least 2 domains: coenzyme and substrate binding. (Jörnvall et al. 1995)	3.47
TMUE_1000004728	Peptidase_M14 domain-containing protein	6 Wks		MEROPS metallopeptidase family M14 (N. D. Rawlings and Barrett 1995)	5.76
TMUE_3000013218	NULL	6 Wks	membrane component, catalytic activity	AMP-binding enzyme, AMP-binding enzyme C-terminal domain An enzyme utilising ATP-dependent covalent binding of AMP to their substrate (Schröder 1989)	2.57
TMUE_1000003391	ShKT domain-containing protein	6 Wks		Proteins that contain domains resembling the toxins BgK and ShK, giving rise to potent ion channel blockers and enzymes with potential channel-modulatory activity. (Möhrlen, Hutter, and Zwilling 2003)	3.08
TMUE_0000001749	BPI2 domain-containing protein	6 Wks		Bactericidal permeability-increasing protein (BPI) a potent antimicrobial protein of 456 residues that binds to and neutralises lipopolysaccharides from the outer membrane of Gram-negative bacteria (Beamer, Carroll, and Eisenberg 1997)	5.62
TMUE_1000005295	SSD domain-containing protein	6 Wks		The sterol-sensing domain (SSD) comprises ~180 residues arranged in five membrane-spanning segments; and confers sensitivity to regulation by sterol (Kuwabara and Labouesse 2002)	4.42
TMUE_2000008088	PNP_UDP_1 domain-containing protein	6 Wks		Purine nucleoside phosphorylase (PNP)/ Uridine phosphorylase (UdRPase) like phosphorylase (Takehara et al. 1995)	2.65

3.8 Discussion and Conclusions

I hypothesised that hatching in *Trichuris* species is driven by bacteria aggregating around the polar plugs, using physical interactions to adhere to one another and the eggs. As hatching progresses, the polar plugs are degraded through enzymatic activity and disappear facilitating larval eclosion. I investigated this hypothesis using the interactions between *T. muris* and *E. coli* and other bacterial strains as an *in vitro* model to provide key insights into the molecular determinants of the natural *Trichuris* egg hatching cascade. In doing so, this chapter expanded on previous work that had identified two types of bacterial induced hatching of *T. muris*: fimbriae independent and type 1 fimbriae dependent (Hayes et al. 2010) and provided visualisations of these interactions by SEM (Goulding 2021).

Physical interactions formed the basis for the first half of my hypothesis regarding the minimum requirements for the hatching of *Trichuris*, and through the work in this chapter I was able to examine this. My first observation was that the levels of hatching were highly variable across experiments; as discussed earlier this variation may be experimental due to batch effects in egg viability that occur during routine parasite maintenance. However, despite this variability, there were consistent differences in the levels of hatching induced by rough and smooth colony forms of *E. coli* (Figure 3.3). Colony morphology has previously been linked to fimbriae expression, with smooth colonies expressing fimbriae and rough colonies being afimbriate (Hasman, Schembri, and Klemm 2000). The *fim* operon uses an invertible promoter to allow highly flexible regulation of expression of fimbriae proteins, assembling fimbriae at the surface of the bacterium as required (Chen et al. 2014). Differences in expression of fimbriae are often considered in the context of infectivity or virulence as fimbriae are utilised to attach to epithelial cells (Lim et al. 1998). However, independently of infection, culture conditions can cause the switching of the promoter either triggering expression of fimbriae or silencing the operon (Chen et al. 2014). Indeed, culturing on agar plates favours *fimOFF* (rough colonies), and culturing in static broth favours *fimON* (smooth colonies) (Chen et al. 2014).

FimA was previously identified as a component of the *fim* operon in *E. coli* Nissle required to mediate hatching of *T. muris* (Hayes et al. 2010). I used single gene knockouts from the Keio collection, as well as a knockout of the whole *fim* operon (Yamamoto et al. 2009; Hamrick et al. 2000) in order to investigate the role of fimbriae components in *E. coli* K12 mediated hatching. Based on the observations in this chapter and previous studies (Hayes et al. 2010; Duque- Correa and Goulding 2017), I propose that type 1 fimbriae expression drives the difference in colony morphologies, and the levels of hatching induced rough and smooth *E.*

coli K12 MG1655 colonies. Additionally, the mechanism of action of the *fim* operon, with its flexible promoter, may also explain the variability observed in hatching levels. Even though a single colony of one morphology was collected and used to inoculate the liquid cultures, some colony switching may have occurred during overnight liquid culture generations. This would in turn affect the ratio of rough to smooth bacteria in the cultures, an increase in the amounts of fimbriae expressing bacteria will increase the ability of the cultures to induce hatching. In previous observations (Hayes et al. 2010), the removal of *fimA* did cause the greatest reduction in hatching; this gene encodes the pillin structures that comprise the main body of the fimbrial projection and dictates fimbrial length (Schwan 2011). However, I also discovered that type 1 fimbriae are not solely responsible for the induction of hatching, removing components of the operon or indeed the whole operon does not result in ablation, only a non-significant reduction in hatching (Figure 3.7). There are several possible explanations for this discrepancy with previous observations (Hayes et al. 2010). First, the effect of removing fimbriae on hatching may be temporal, causing a delayed hatching phenotype. The experiments by Hayes et al were conducted over 2 h whereas I conducted mine over 24 h. Second, while removing the *fimA* gene has the greatest effect on hatching, this gene dictates fimbrial length but is not responsible for mediating adhesion of fimbriae—a function of *fimH*. Shortened fimbriae may impede but not ablate bacterial attachment, and perhaps delay the formation of aggregates around the polar plug and the induction of hatching. Last, *E. coli* K12 expresses another kind of fimbriae, curli fimbriae, that facilitate both adhesion and biofilm formation that may be involved in the induction *T. muris* egg hatching (Ogasawara et al. 2020; Beloin, Roux, and Ghigo 2008). Expression of these curli fimbriae in lab strains has typically been regarded as cryptic—silent under typical laboratory conditions, but activated by mutations and alternative nutrients (Ochi, Tanaka, and Tojo 2014; Tamburini and Mastromei 2000). Recent studies in *E. coli* K12 BW25113 have uncovered transcription factors that regulate curli expression through the stress mediated control of the biofilm formation master regulator gene *csgD* (Ogasawara et al. 2020; Beloin, Roux, and Ghigo 2008). Curli fimbriae may provide redundancy as an alternative mode of physical attachment that is not routinely expressed, and is less efficient at inducing hatching, resulting in delayed and reduced levels of hatching. *T. muris* can be induced to hatch by a variety of bacterial surface proteins beyond type 1 fimbriae. I hypothesise that this allows eggs to detect the intestinal niche and induce hatching even if a host contains bacteria with mutated adhesin genes or is lacking a bacterial strain that expresses specific adhesins.

Hayes et al reported the range of bacteria that can induce hatching of *T. muris* and, in the present chapter, the interactions between these bacteria and the eggs were visualised (Hayes et al. 2010; Goulding 2021). SEM data on *T. muris* and *E. coli* or *S. typhimurium* co-

cultures showed that proximity to the polar plug resulted in increased fimbrial expression on the bacteria around the polar plug (Figure 3.5, 3.6). I propose that contact with the egg, specifically the glycolipid components of the polar plug mediates fimbrial expression which can be triggered to facilitate adhesion under specific conditions i.e. infection or invasion (Lim et al. 1998). In the case of *P. aeruginosa*, some fimbriae/pili like physical projections were observed on the surface of the cells (Figure 3.7), demonstrating that *P. aeruginosa* also expresses a structural molecule to facilitate adherence to the polar plug (Goulding 2021). Previous investigations in *P. aeruginosa* have demonstrated that the bacteria have a distinct proteome upon attachment to a surface that is expressed as rapidly as 20 minutes post attachment (Crouzet et al. 2017). While *P. aeruginosa* typically uses type IV pili to attach to surfaces, the authors found it difficult to conclusively state the role of type IV pili within the 20-minute time frame. However, they did find an over-expression of outer membrane and biofilm formation proteins during early attachment (Crouzet et al. 2017). It is possible that *P. aeruginosa* experiences chemotaxis to the components of the polar plug and expresses a specific repertoire of proteins in order to bind to them. While we have not yet visualised physical interactions between *S. aureus* and *T. muris*, one feature of *S. aureus* pathogenicity is the ability to form biofilms during adhesion to surfaces. Studies have identified many cell wall anchored proteins in *S. aureus* that contribute to adhesion and biofilm formation (Foster et al. 2014). For several of these proteins including those encoded by the genes *sasG*, *sasX*, *sasC*, the ligands and binding mechanisms are yet to be fully characterised (Foster et al. 2014). In particular, *sasC* has been implicated in the primary attachment and accumulation phases of biofilm formation (Schroeder et al. 2009) making it a particularly attractive starting target for further study as hatching interactions primarily occur during the first few hours of co-culture as shown in Figure 3.12. The expression of this biofilm generation gene could be responsible for hatching induction.

Having visually examined the interactions between bacteria and eggs at the polar plug, I characterised the composition of the plugs. The proteomics results supported the hypothesis that the plugs are composed of a chitin fibre matrix supporting chitin bound molecules, and provided some clues as to the identity of these components. 11 peptides were found to be unique to the polar plug including: glycoproteins with chitin binding domains and structures similar to human Factor H and a trypanosome VSG, and the BPI protein that had also been detected by RNAseq (Table 3.2). Together these hits indicate that the polar plugs contain chitin binding glycoproteins (Factor H and VSG), and lipopolysaccharide binding activity (BPI) (InterPro 2021). To investigate the composition of the polar plugs and the role these molecules play, further targeted analysis of the polar plugs is needed. One strategy that could be particularly useful is laser microdissection that would allow the polar plugs to be

directly isolated for analysis by mass spectrometry or chromatography. This would give a more definitive answer as to their composition. The main consideration is the time cost of this strategy, microdissecting enough polar plug material is labour intensive. In my attempts to undertake laser microdissection, I found that the easiest way to isolate the plug was to slice and collect one third of the egg; and that the dissection of an individual polar plug could take several minutes to complete. MS requires at least 40 micrograms of protein which can be isolated from ~ 500 whole eggs, therefore in order to isolate enough protein from the polar plugs for one complete sample, at least 1500 eggs would need to be dissected. Assuming a dissection rate of 2.5 minutes per plug working 8 hours a day it would take an operator just over a week (7.8 days) to dissect 1500 eggs, and almost a month (23.4 days) to create 3 replicate samples

The second half of my hypothesis concerns enzymatic activity, and its role in degradation of the polar plugs that results in eclosion. In chapter one (section 1.6) the role of enzymes in the hatching of various nematodes was discussed. Briefly, enzymes have been detected in hatching fluid of many nematodes and contribute to the weakening of the eggshell to facilitate eclosion (Perry 2002; Rogers 1958). Additionally, previous investigations in the lab visualising *T. muris* eclosion showed degradation of the polar plugs (Figure 3.1c) (Duque-Correa and Goulding 2017). As shown in Figure 3.13, I found that inhibition of protease activity using a cocktail containing both serine and cysteine protease inhibitors ablated hatching triggered by *E. coli*, *P. aeruginosa*, *S. aureus*, and *S. typhimurium* bacteria. These results demonstrate that regardless of the type of physical interaction with the polar plug hatching progresses using proteases.

To understand the effects of the protease inhibitor cocktail, I tested the dose dependency and recoverability. I observed that as the dose of the inhibitor was decreased, more hatching was observed; suggesting that the inhibition could be maximised by considering the enzyme kinetics and stoichiometry. The variability hatching reduction due to enzyme dose will become more evident in chapter 4 during *in vitro* hatching experiments with gastrointestinal tract samples where the quantities of bacteria cannot be controlled using OD values as they are in the above experiments. I also investigated the recoverability, and discovered that removing the inhibitor and co-culturing parasite eggs with fresh bacteria recovered hatching to levels comparable with those observed in the controls without protease inhibitors (Figure 3.8). These results indicate that while disturbing the proteases prevents hatching, it does not affect viability of the larvae inside the eggs. It would be interesting to see if the protease inhibitor can cross the eggshell and be internalised, or if it is merely acting on secreted proteases external to the egg. Controlling the expression of proteases may be one strategy

utilised by the parasite to prevent premature hatching, and this idea is explored further in chapter 4.

Next, I aimed to identify the class of proteases that contributed to hatching, and determine if the proteases were from bacterial or larval origin as in the co-cultures, the protease inhibitor may be acting on both bacterial and larval proteases. The effect seen with the serine protease inhibitor Pefabloc™ was greater than seen with the cysteine protease inhibitor E64. Inhibiting using Pefabloc™ resulted in complete ablation, whereas inhibition with E64 resulted in a 10% decrease suggesting that serine proteases are more crucial to hatching (Figure 3.10). As mentioned earlier, redundancy allows multiple proteins to contribute to a biological phenomenon (Nowak et al. 1997). Perhaps cysteine proteases provide an alternative mechanism of progressing hatching, however there is only a small effect on hatching as a result of inhibiting them. Hatching largely progresses as normal, likely driven by serine proteases. This highlights the unique hatching requirements in nematodes, as in *in vitro* hatching of *H. contortus* using E64 resulted in an ~30% reduction in hatching (Ribeiro et al. 2021) suggesting that cysteine proteases are more crucial for hatching in that species.

To further investigate the role of proteases I used the Keio Collection knockout bacteria to obtain *E. coli* strains lacking individual serine and cysteine proteases. Co-cultures of *T. muris* with these strains revealed a significant reduction in hatching for one serine protease knockout *clpP* and two cysteine protease knockouts *hchA*, and *yhdO* (Figure 3.11, 3.12). However, the effect was greater with *clpP*, where I observed a two-fold reduction in hatching compared to a 20% reduction seen with *hchA*, and *yhdO*, suggesting that the bacterial serine protease *clpP* is therefore more crucial for hatching than the two bacterial cysteine proteases. However, while the reduction was strong, hatching was not completely shut down. Incomplete ablation with a single gene knockout further illustrates the redundancy in the hatching system and the wide mix of both larval and bacterial proteases that can facilitate hatching. As the addition of a protease inhibitor prevented hatching and caused complete ablation it is likely that it is perturbing both larval and bacterial proteases; I observed that knocking out bacterial proteases only accounted for a 50% reduction in hatching. Testing multiple gene knockouts and silencing the bacterial serine proteases gene that are lethal when knocked out would complete the investigation into bacterial serine proteases.

In addition to characterising extrinsic bacterial factors it is important to characterise intrinsic hatching factors to understand the molecular processes that govern hatching. Intrinsic factors can govern the commencement of hatching, for example the level of embryonation

has been shown to be important for nematode hatching; forced eclosion of larvae results in non viable larvae (Geenen et al. 1999; Vejzagić, Adelfio, et al. 2015). Intrinsic factors also govern the progression of hatching, upon induction of hatching, viable larvae have been shown to release enzymes into the perivitelline or hatching fluid (Rogers 1958; Abriola et al. 2019; Perry 2002), and in *C. elegans* the absence of the protease encoded by *hch-1* prevents eclosion (Hishida et al. 1996). I hypothesised that the level of embryonation affects the response of *T. muris* to bacterial hatching cues, and I reasoned that tracking temporal gene expression of larvae during embryonation would reveal a genetic explanation for the change in response.

My results confirmed that a minimum level of embryonation is required to observe a response to bacteria in *T. muris*. The larva appears morphologically developed at 5 weeks, but hatching in response to *E. coli* does not commence until week 7 (Figure 3.15 c and e). These results suggest that additional maturation occurs between weeks 5 and 7 allowing the egg to respond to bacterial stimulation. These results also confirm observations previously made in *T. muris*, *T. suis* and *A. suum*, that showed the presence of a visually morphologically complete larva does not indicate viability or the ability to hatch (Vejzagić, Thamsborg, et al. 2015; Panesar and Croll 1981; Geenen et al. 1999). Furthermore, the hatching results show the variation in batches of eggs and their ability to hatch; this may arise from being cultivated in different hosts and individual variations in the microbiota. Indeed similar observations have been reported in mice colonised with various *E. coli* mutants; adult worms isolated from these mice displayed variations in egg laying and egg viability (Venzon et al. 2021).

Bacterial stimulation of *T. muris* hatching did not commence before six weeks of embryonation, despite the presence of a fully formed larva from week 5 (Figure 3.15c), and many of the significantly differentially expressed genes encode enzymes (Table 3.3). I utilised the transcriptome data to examine eggs on either side of this developmental threshold, to explain the development of hatching in response to bacteria. First, I discovered that at six weeks of embryonation there is expression of genes encoding proteins with patched and sterol sensing domains (SSD) (TMUE_1000005295, TMUE_0000001260) (Table 3.3). The expression of these genes typically relates to life cycle transitions in particular growth and moulting (Entchev and Kurzchalia 2005; Zugasti, Rajan, and Kuwabara 2005; Shivakumara et al. 2019). Interestingly deletion of *patched-3* in *C. elegans* causes embryonic lethality during hatching, and embryos die with a fluid filled appearance suggesting that this gene aids with osmoregulation (Soloviev et al. 2011). As discussed in chapter 1, osmotic changes are key to initiating hatching, and identifying genes that regulate

them will provide further insight into the molecular regulation of hatching. Second, at six weeks of embryonation the eggs are also expressing a protein containing a BPI domain; an antimicrobial that acts against bacteria, and apicomplexans (Canny and Levy 2008; Balakrishnan et al. 2013). It will be interesting to study its role in parasite hatching and the interactions between BPI and the microbiota in the niche, perhaps BPI plays a protective role by neutralising bacteria that bind to the polar plug to prevent exogenous degradation of the plugs.

In the mature eggs I found increased expression of genes encoding for enzymes that may be involved in hatching, in particular an S1 family protease. The S1 family of proteases includes: kallikrein, plasmin, thrombin, chymotrypsin and trypsin. The protease inhibitor panel experiment highlighted which of the members of the S1 family of proteases may be involved in hatching in *T. muris* (Chapter 3, Figure 3.10). I concluded that kallikrein, plasmin, or thrombin like proteases are more likely to be crucial than chymotrypsin or trypsin like S1 proteases. Indeed, one of the proteases highly expressed in mature eggs was identified as a kallikrein like serine protease. Changes in the expression of proteases implicated in hatching during embryonation, have also been observed in *Ascaris*, and proteases detected in the hatching fluid of *A. ceylanicum* (Justus and Ivey 1969; K. A. Ward and Fairbairn 1972; Abriola et al. 2019). More investigations are needed to confirm that targeted expression of proteases is a general mechanism of hatching for the STH. Altogether these three changes in gene expression I identified provide candidates for future studies on genes implicated in hatching. Patched and SSD proteins may be implicated in regulating the hatching transition, BPI in binding to bacteria, and serine proteases in facilitating eclosion via degradation of the polar plug. In the future silencing or knocking out larval protease genes will isolate the larval hatching enzymes. Significant work has recently been done in sequencing and annotating the *Trichuris* genomes (Foth et al. 2014; Jex et al. 2014). Developing knockdown RNAi or knockout CRISPR techniques for use in *Trichuris* would allow these larval protease genes to be studied and will greatly accelerate investigation into the specific genes that regulate hatching.

In summary, in this chapter I can conclude that both physical projections and enzymatic activity facilitate bacterial mediated hatching of *T. muris*. I provided further evidence for the role of type 1 fimbriae in *T. muris* egg hatching and visualised the alternative methods of adhesion utilised by afimbriate gram positive strains. I also identified serine proteases as a class of proteases that play a crucial role in hatching in the *T. muris* model. I examined the changes in expression in the larvae as they became viable. The data from these studies suggests that the level of embryonation affects *T. muris* hatching and changes in the

expression of genes including S1 proteases may facilitate this. I also identified some peptides in the polar plug confirming its composition as a chitin fibril matrix suspending other molecules including glycoproteins. In chapter 4 I continue to use this knowledge of the role of proteases in hatching to study *in vitro* hatching in *T. suis* and identify suitable *in vitro* and *in vivo* hatching conditions for *T. trichiura*. Lastly in chapter 5, I will continue my study of the microbiota, searching for relevant genes in the microbiota of humans, humanised mice, and pigs.

Chapter 4- Identification of extrinsic host microbiota factors for hatching *Trichuris* spp

Declaration of contributions

M. Duque Correa and M. Berriman supervised this work. A. Kirch Dige performed the colonoscopies, A. Fick Thomsen provided access to porcine gastrointestinal tract material. A. Toftegaard Boysen, and P. Nejsum assisted in performing and troubleshooting the hatching experiments with the human colonic biopsies and porcine gastrointestinal tract samples. C. Brandt and S. Clare performed mouse infections, as well as tissue collection and sectioning. S. Thompson and R. K. Grencis performed immunological analysis on mouse sera samples. I performed all inoculum preparations, hatching experiments, and analyses.

Publication.

4.1 Introduction

The *in vitro* model of *T. muris*–*E. coli* hatching provides a useful tool to study the molecular details of the hatching process. However, the Edinburgh strain of *T. muris* that I used is highly lab-adapted having been passaged in laboratory mice for many years (Wakelin 1967). Findings in this strain do not always translate to other strains of *T. muris* (Koyama 2013, 2016) or other whipworm species (Vejzagić, Adelfio, et al. 2015). In chapter three I studied the interactions between *T. muris* and bacteria. In the present chapter I investigated whether my findings regarding proteases apply to *T. suis* and *T. trichiura*, identified extrinsic host factors capable of inducing hatching of these species. Previous studies in *T. suis* have shown that eggs do not hatch in response to bacterial mono cultures in the same way as *T. muris* eggs, hatching of *T. suis* can be induced at high levels by gastrointestinal contents, or at low levels by a combination of methods to simulate the gut environment (Vejzagić, Thamsborg, et al. 2015; Vejzagić, Adelfio, et al. 2015). These include exposure to acids to mimic gastric pH, and stirring with glass beads to mimic peristalsis (Vejzagić, Thamsborg, et al. 2015; Vejzagić, Adelfio, et al. 2015). Interestingly, despite the gut being considered a largely anaerobic environment, utilising anaerobic conditions has not increased the levels of hatching (Vejzagić, Thamsborg, et al. 2015; Vejzagić, Adelfio, et al. 2015). The key finding

from these investigations is that the defined populations of bacteria from along the gastrointestinal tract induce different levels of hatching. Hatching in *T. suis* is primarily driven by gastrointestinal contents isolated from the mucosa of the caecum (Vejzagić, Thamsborg, et al. 2015).

The gastrointestinal tract can be sectioned longitudinally into regions i.e. the stomach, duodenum, ileum, caecum, colon, and rectum. The conditions and availability of resources, like nutrients and oxygen, varies in each region creating niches in which distinct microbial communities reside (Figure 4.1) (Donaldson, Lee, and Mazmanian 2016). Given that the species composition of the gastrointestinal tract is region-specific and this specificity can have an effect on parasite hatching, it is important to understand how the composition changes. Additionally, the gastrointestinal tract can be further stratified transversely from the lumen to the epithelium, once again each layer exhibits distinct properties capable of supporting specific organisms (Figure 4.1) (Albenberg et al. 2014; Zheng, Kelly, and Colgan 2015).

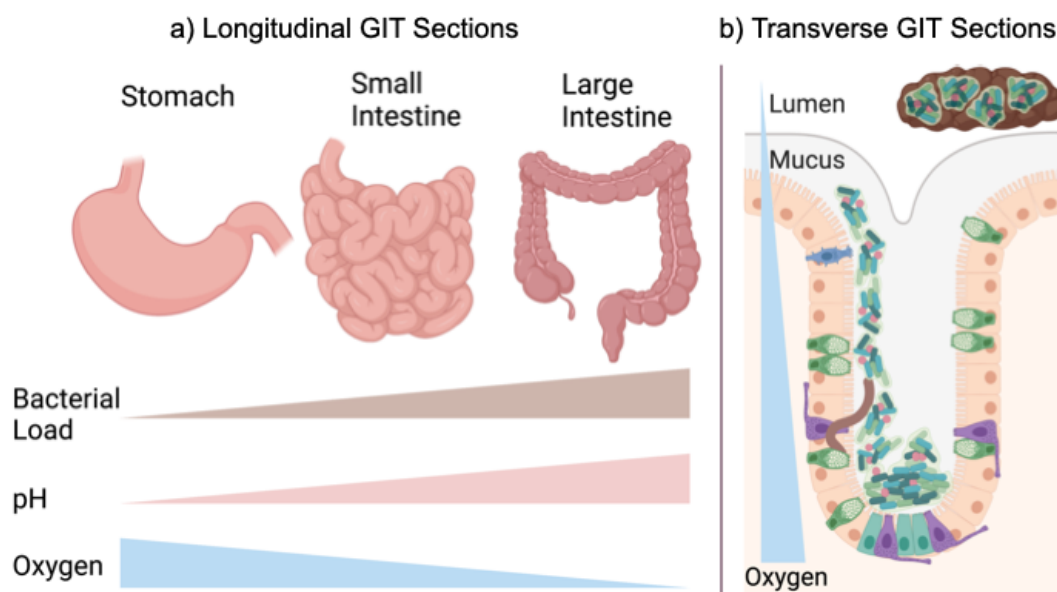


Figure 4.1. The distribution of bacteria and resources along the longitudinal and transverse axes of the gastrointestinal tract. a) Longitudinally the gastrointestinal tract is partitioned into regions by organ. The stomach has low pH and a higher oxygen concentration; as a result, fewer but more-extremophile bacteria reside there. At the end of the gastrointestinal tract, in the large intestine, the pH is closer to neutral and the predominantly anaerobic environment is able to support a more diverse collection of bacteria including anaerobes and facultative anaerobes. b) Transversely the gastrointestinal tract can be sectioned from the lumen through to the epithelium. The lumen is largely anaerobic and is densely packed with digestive

contents and bacteria. Moving away from the lumen through the mucus to the highly vascularised mucosa the concentration of oxygen increases.

Caecal mucosal scrapings are the fraction of the gastrointestinal tract that most accurately represents the parasite niche (Vejzagić, Thamsborg, et al. 2015). As all *Trichuris* species eventually make a home in the intestinal mucosa, *T. trichiura* may also respond preferentially to the bacteria associated with the mucosa of the human ascending colon. Unlike in mice or pigs the human caecum does not form a defined bag like structure, and *T. trichiura* infections occur along the length of the ascending colon in addition to the caecum (Else et al. 2020). Studying the human gastrointestinal tract mucosal microbiota is a challenge. The bulk of studies investigating the composition of the microbiota in humans utilise stool samples, as collecting mucosal samples from the length of the gastrointestinal tract from otherwise healthy individuals by colonoscopy is invasive, and the other option is to collect samples post mortem (James et al. 2020; Tang et al. 2020). However, sampling faeces alone does not provide a complete picture of the gastrointestinal microbiota (Tang et al. 2020; Kastl et al. 2020). In the present chapter I tested my hypothesis that *Trichuris* species preferentially respond to microbiota from the host site of infection. I performed a range of *in vitro* hatching experiments to determine the host gastrointestinal samples capable of inducing hatching of *T. muris*, *T. suis*, and *T. trichiura*; and a range of *in vivo* experiments to examine the role of the murine and humanised microbiota during *T. muris* and *T. trichiura* infections. In addition to testing gastrointestinal tract samples from the various hosts I also investigated the role of proteases and aerobic Vs anaerobic culturing conditions. One additional benefit of my study is that all of the collected samples were sequenced and analysed in chapter 5 to understand the bacterial composition of samples that induce hatching in *Trichuris* species.

4.2 Inhibition of proteases impacts *in vitro* hatching of *T. muris* eggs with murine microbiota and humanised microbiota mice gastrointestinal tract samples

Previous studies on extrinsic host factors utilised caecal contents to hatch *T. muris* (Panesar and Croll 1980), however the mucosa is the parasite niche and I hypothesised that bacteria from the mucosa preferentially induce hatching. In order to evaluate the ability of samples isolated from different transverse fractions of the caecum to induce hatching of *T. muris*, caecal mucosal scrapings and caecal contents were collected from murine microbiota mice. In addition to investigating specificity for the region of the gastrointestinal tract, I investigated host specificity of *T. muris*, performing hatching experiments with caecal mucosal scrapings and caecal contents from two humanised microbiota mouse strains, and *E. coli* hatching was utilised as a control (Figure 4.2).

Under aerobic conditions hatching was observed with both caecal scrapings and caecal contents, and caecal scrapings induced higher levels of hatching. Across the mouse strains the highest levels of *T. muris* hatching were observed when using caecal scrapings from the donor A humanised mice (median 90.4% hatching) (Figure 4.2 c). Surprisingly this surpassed hatching with murine microbiota control mice (median 59.3% hatching) or *E. coli* (median 65.6%, 73.5%, 76.5% hatching) (Figure 4.2 a). The lowest levels of hatching were induced with donor B samples (median 33.5% hatching). For all tested conditions, treatment with a protease inhibitor reduced hatching. In donor A mice, the addition of a protease inhibitor generally caused a small reduction in hatching, with complete ablation rarely observed (median 82.4% hatching) (Figure 4.2 c), in donor B mice the addition of a protease inhibitor resulted in a larger reduction in hatching (median 4% hatching) (Figure 4.2 e). However, once again, unlike with *E. coli* the level of inhibition was not complete. I believe this is due to the protease inhibition occurring in a dose-dependent manner (Chapter 3, Figure 3.9). Unlike the experiments with bacterial monocultures, the bacterial load in the gastrointestinal tract slurry could not be controlled by measuring optical density. Despite this, these results suggest that the composition of the microbiota at various sampling sites affects the levels of hatching. Cysteine and serine proteases in the caecal mucosal scrapings and caecal contents from murine and humanised microbiota mice mediate *T. muris* egg hatching.

Under anaerobic conditions, there were lower levels of hatching with the gastrointestinal tract samples compared to the aerobic conditions. Interestingly, I observed “spontaneous” hatching of *T. muris*, in the wells containing only RPMI and there was no visible contamination in these wells (Figure 4.5 b, d, f). This spontaneous hatching appeared in some cases (Figure 4.2 d) to respond to the presence of a protease inhibitor, further

suggesting that the proteases involved in hatching are not solely bacterial in origin and likely larval in origin. Bacterial-independent hatching of *T. muris* has previously been reported, but the mechanism is not fully characterised or understood (Koyama 2013, 2016).

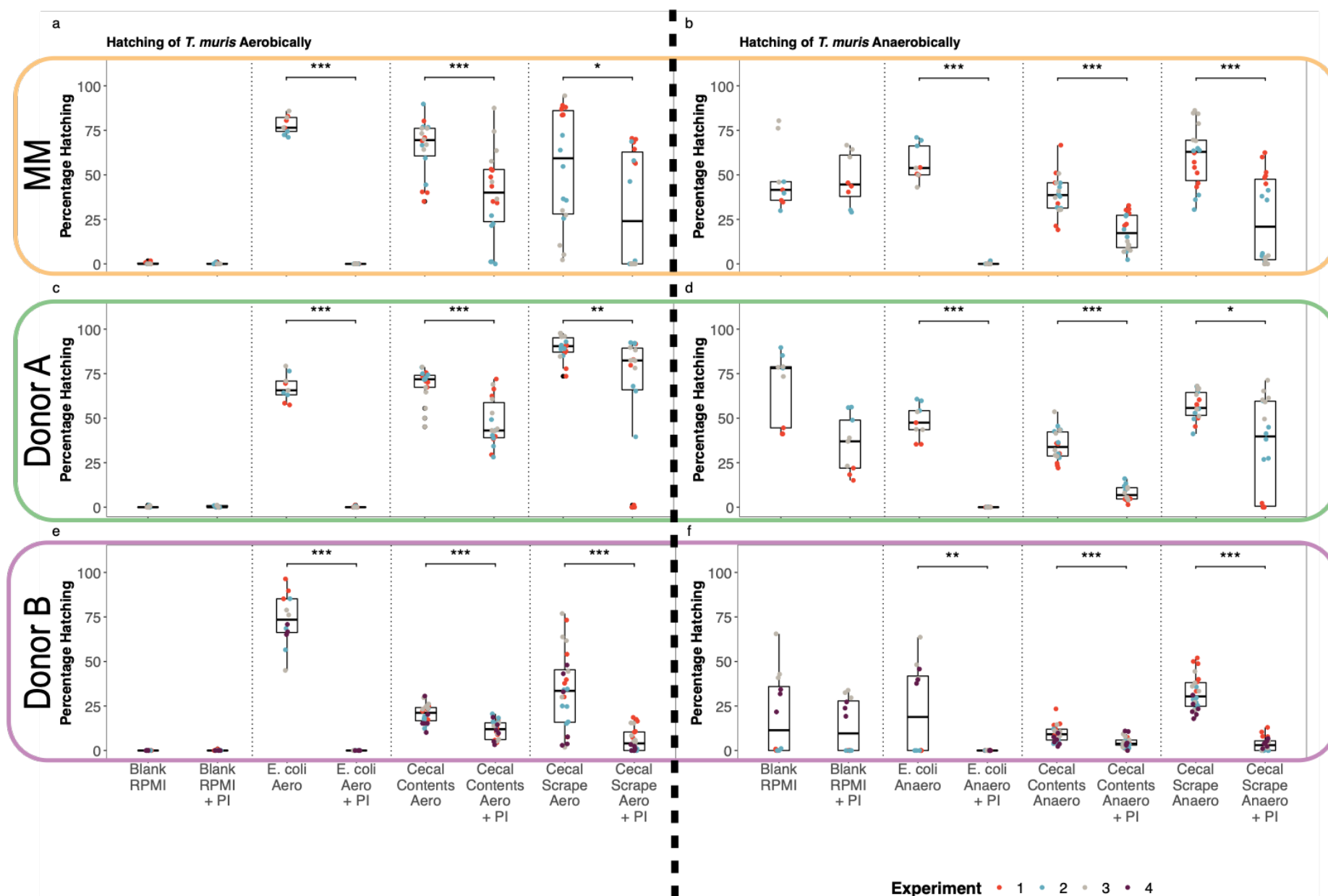


Figure 4.2. Hatching of *T. muris* with gastrointestinal tract samples from murine microbiota mice or mice with humanised microbiota is mediated by protease inhibitors. Hatching of *T. muris* eggs was induced using caecal contents and caecal scrapings collected from adult uninfected C57BL/6 murine microbiota (MM) (a and b) and humanised microbiota mice Donor A (c and d) and B (e and f). Percentage hatching was recorded after 24 h of co-culture with gastrointestinal tract samples alone or with gastrointestinal tract samples in the presence of a protease inhibitor cocktail (PI), under aerobic and anaerobic conditions. Data was collected from four independent experiments. Median and IQR are shown and statistical analysis was performed using the paired samples Wilcoxon test (** $p \leq 0.001$, ** $p \leq 0.01$, * $p \leq 0.05$) test. Donor B, $n = 12$ males. Donor A, $n = 3$ females + 6 males. MM, $n = 9$ males.

4.3 Gastrointestinal tract samples from pigs display differing capabilities to induce hatching of *T. suis* and *T. muris* in vitro.

In order to investigate if the microbiota isolated from the different transverse fractions of the porcine gastrointestinal tract, have an effect on hatching of *T. suis* and *T. muris*. I collected samples from the caecum, ileum, and duodenum of adult uninfected pigs and determined whether they preferentially induced hatching. Hatching was only observed with caecal samples but not ileal and duodenal samples and these results are not included. Interestingly, during these *in vitro* hatching experiments *T. muris* displayed low host specificity responding to porcine caecal contents and scrapings, albeit at lower levels than in hatchings with *E. coli*. As seen in previous studies (Vejzagić, Thamsborg, et al. 2015), the highest levels of hatching in *T. suis* were observed using caecal mucosal scrapings, and reduced hatching was observed with the caecal contents (Figure 4.3). With the caecal scrapings and contents there was high variability in the level of hatching; four pigs were sampled but hatching was only observed with gastrointestinal tract samples from two pigs (Figure 4.3). Additionally, co-culturing in the presence of a protease inhibitor caused a slight but non-significant decrease in the levels of hatching observed with caecal mucosal scrapings (Figure 4.3), indicating that proteases may play a role in the hatching of *T. suis* in the porcine gastrointestinal tract context, however more sampling is required. Through this work I was able to confirm the findings by Vejzagić (Vejzagić, Thamsborg, et al. 2015); test my hypothesis regarding the role of proteases in hatching; as well as collect samples for metagenomic analysis in Chapter 5 (Section 5.4).

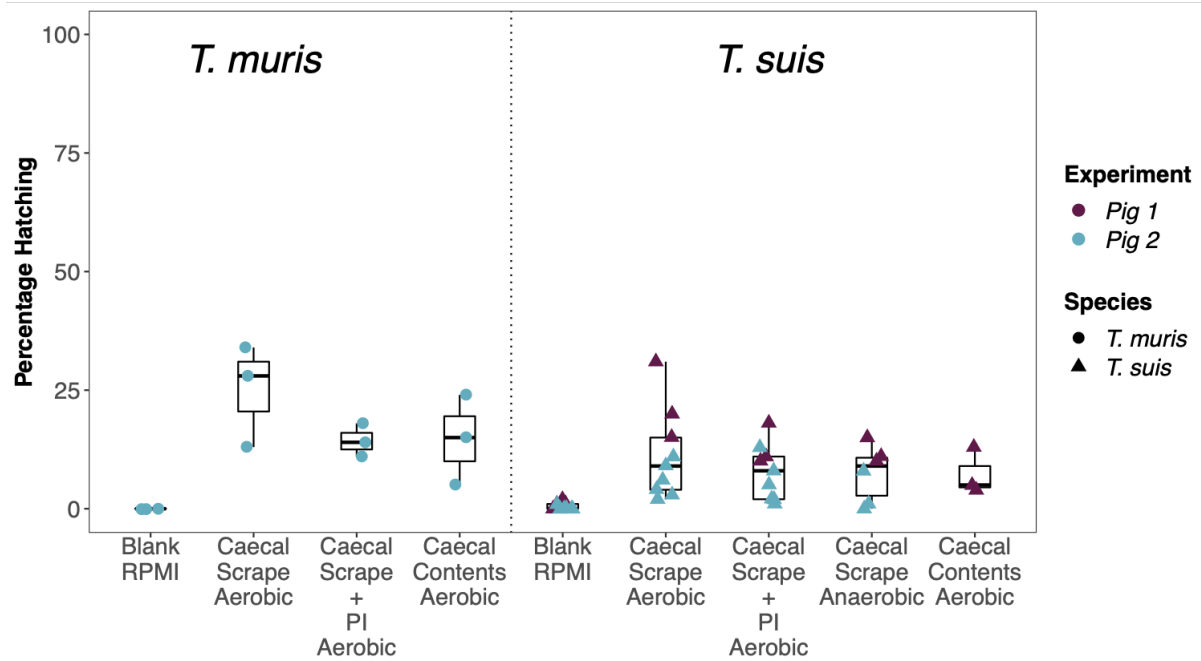


Figure 4.3 Greater levels of *T. muris* and *T. suis* egg hatching observed with porcine caecal mucosal scrapings. Hatching of *T. muris* eggs was induced using caecal contents and caecal scrapings collected from adult uninfected pigs.

Percentage hatching was recorded after 24 h of co-culture with gastrointestinal tract samples alone or with gastrointestinal tract samples in the presence of a protease inhibitor cocktail (PI), under aerobic and anaerobic conditions. Data was collected from 1 (*T. muris*) or 2 (*T. suis*) independent experiments, median and interquartile range are shown.

4.4 *In vitro* hatching of *T. trichiura* eggs with Human Colon Biopsies

T. muris and *T. suis* both displayed increased hatching in the presence of mucosal scrapings compared to intestinal contents. I hypothesised that *T. trichiura* would hatch in response to human gastrointestinal mucosa. To test this hypothesis, intestinal biopsies were collected from a range of regions of the gastrointestinal tracts of patients undergoing a colonoscopy at Aarhus University Hospital, Denmark to investigate hatching of *T. trichiura* using biologically relevant samples. The majority of the patients (76.4%) did not have visible inflammation of the gastrointestinal tract at the time of sampling and were considered healthy. Several patients had slight inflammation of the gastrointestinal tract (19.7%), and one patient had their whole gastrointestinal tract removed. *T. trichiura* exhibited specificity for the different intestinal regions, and the highest levels of hatching were observed using samples from the ascending colon (Figure 4.4). These results suggest that the composition of the ascending colon is more suitable for inducing hatching of *T. trichiura* than the composition of the descending colon. Samples from the transverse colon and the rectum did not induce hatching suggesting that they too do not contain the appropriate microbiota composition. Interestingly, there was no hatching observed with the stool samples collected from the same individual that produced the *T. trichiura* eggs for this study (Figure 4.4) (Dige et al. 2017). The addition of a serine and cysteine protease inhibitor cocktail reduced the levels of hatching observed in the samples capable of inducing hatching, demonstrating that proteases are required for the hatching of *T. trichiura* (Figure 4.4). Therefore, *T. trichiura* hatches in response to samples collected from the site of infection and cysteine or serine proteases contribute to hatching in the human gastrointestinal tract context.

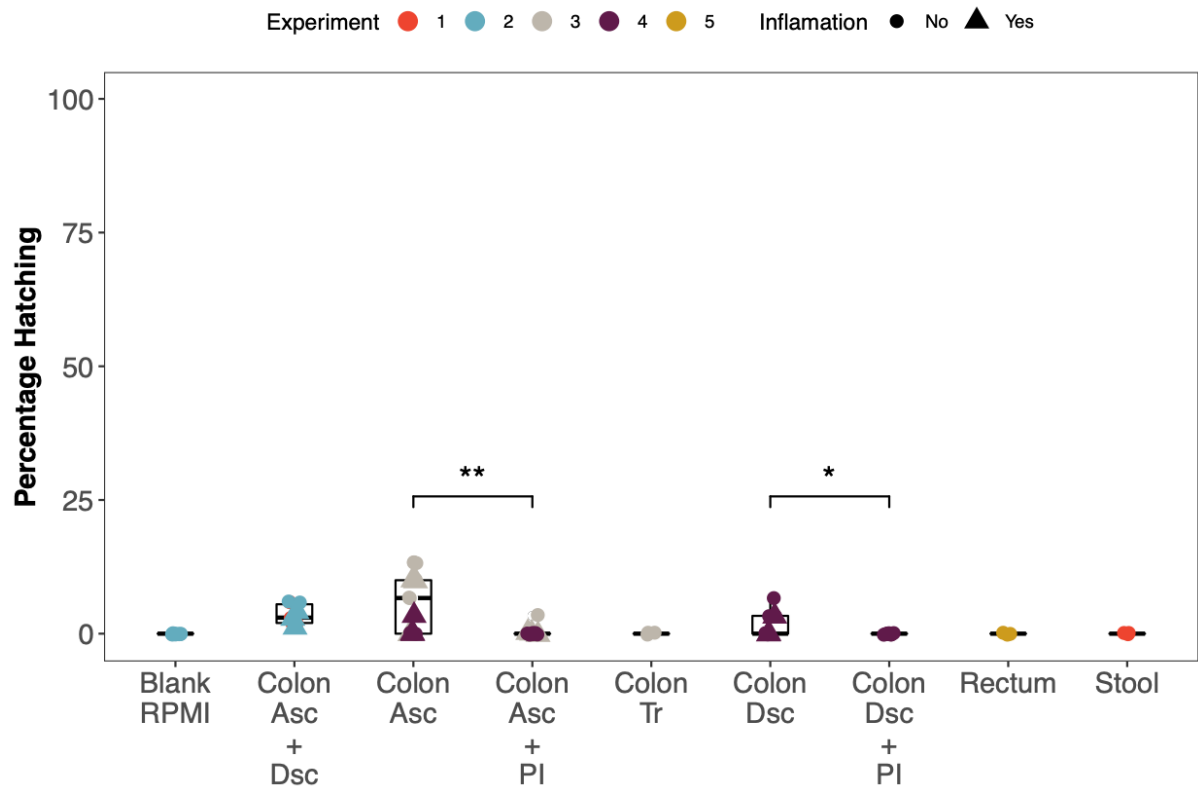


Figure 4.4. Hatching of *T. trichiura* eggs induced by human mucosal gastrointestinal tract contents is mediated by proteases. *T. trichiura* eggs were co-cultured with punch biopsies from the length of the gastrointestinal tract of uninfected colonoscopy patients in the presence or absence of a protease inhibitor (PI). Percentage hatching was recorded after 24 h. Hatching rates are reported for each gastrointestinal site. Data were collected in triplicate from five independent experiments, median and interquartile range are shown, and statistical analysis was performed using the paired samples Wilcoxon test (** $p \leq 0.01$, * $p \leq 0.05$). Asc- Ascending, Tr- Transverse, Dsc- Descending. Colon Asc + Dsc $n = 12$. Colon Asc $n = 15$. Colon Asc + PI $n = 15$. Colon Tr $n = 3$. Colon Dsc $n = 9$. Colon Dsc + PI $n = 9$. Rectum $n = 3$. Stool $n = 3$.

4.5 Gastrointestinal tract samples from humanised microbiota mice induce *in vitro* hatching of *T. trichiura* eggs.

After hatching *T. trichiura* with samples from the human large intestine, I utilised mouse strains containing a humanised microbiota to investigate their suitability as a model for *T. trichiura* hatching and infection. I previously unsuccessfully used various proxies for a reduced human microbiota including stool samples from children under 5, as well as monocultures and defined bacterial mixes of some of the most abundant strains in the human gastrointestinal tract microbiota, to attempt to induce hatching. I evaluated the hatching of *T. trichiura* in the presence of caecal scrapings and caecal contents from humanised and murine microbiota mice *in vitro*, with a protease inhibitor, and under aerobic and anaerobic conditions. These results represent the first report of *in vitro* hatching of *T. trichiura* using a laboratory model of the human host microbiota (Figure 4.5). No hatching was observed under any conditions with gastrointestinal samples from mice with a murine microbiota. Under aerobic conditions samples from the donor B mouse line were much better at inducing hatching than those of the donor A. Donor B caecal scrapings induced a median of 53.3% hatching, while those of Donor A, a median of 37.2% (Figure 4.5 c and e). The protease inhibitor decreased the levels of hatching and I observed variability in the levels of reduction of hatching, once again likely due to variations in bacterial load. Under anaerobic conditions, I observed lower levels of hatching with the gastrointestinal tract samples (Figure 4.5 b,d,f) and unlike with *T. muris* there was no spontaneous hatching when using an anaerobic chamber (Figure 4.2 b,d,f). Whenever hatching was observed in the blank RPMI wells (Figure 4.5f), there was visible contamination in the well and this media was collected, the DNA extracted and sent for whole genome sequencing to identify the contaminant. The sequences were taxonomically classified and the results indicated that the most abundant species in the contaminant were *Escherichia coli* D with 55% of the reads and *Citrobacter freundii* with 15% of the reads.

Altogether these results also show the increased host or niche specificity in *T. trichiura*, there was no hatching with a murine microbiota and are clear differences in the levels of hatching induced by the two humanised mouse models reflecting the *in vivo* results; additionally, hatching was rarely observed with caecal contents.

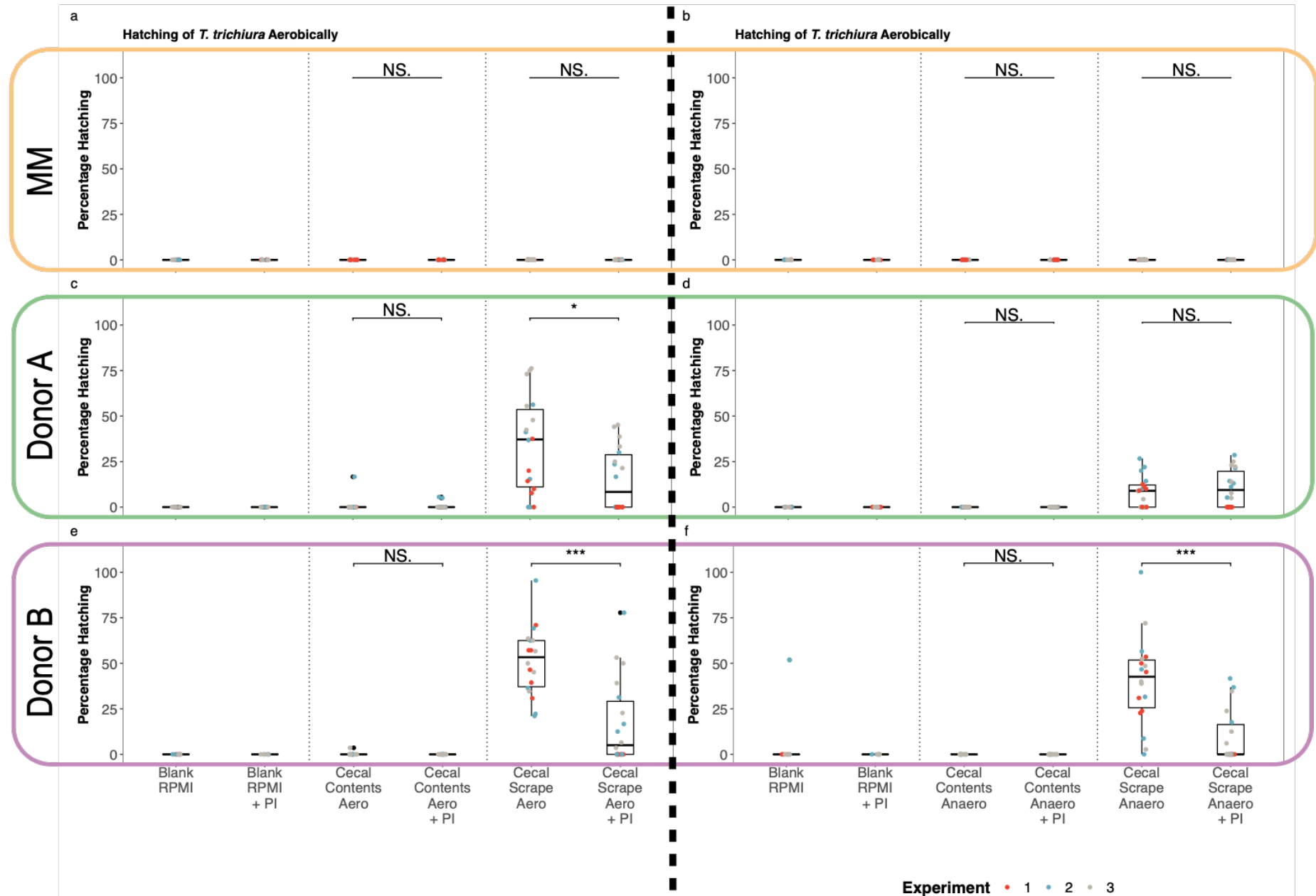


Figure 4.5. gastrointestinal tract samples collected from two humanised mice models display differing capability to induce hatching of *T. trichiura* *in vitro*. Hatching of *T. trichiura* eggs was induced using caecal contents and caecal scrapings collected from adult uninfected C57BL/6 murine microbiota (a and b) and humanised microbiota mice Donor A (c and d) and B (e and f). Percentage hatching was recorded after 24 h of co-culture with gastrointestinal tract samples alone or with gastrointestinal tract samples in the presence of a protease inhibitor cocktail (PI), under aerobic and anaerobic conditions. Data was collected from three independent experiments. Median and IQR are shown and statistical analysis was performed using the paired samples Wilcoxon test (** $p \leq 0.001$, * $p \leq 0.05$) test. Donor B, $n = 9$ males. Donor A, $n = 3$ females + 6 males. WT, $n = 9$ males.

4.6 *In vivo* study of *T. trichiura* and *T. muris* infections in murine microbiota and humanised microbiota mice

Humanised microbiota mouse models are an interesting prospect as a model to study *T. trichiura*. In *Trichuris* species there is evidence of cross host infections, with *T. suis* able to hatch in humans and cause an immune response before ultimately being expelled. Therefore, initiating hatching rather than invasion of the tissue, is likely to be a barrier to studying *T. trichiura* *in vivo* in laboratory animals as it does not respond to gastrointestinal tract samples from murine microbiota mice. I hypothesise that populating the gastrointestinal tract of a mouse with the members of the microbiota that induce *T. trichiura* hatching will lead to the establishment of a chronic infection. To test the hypothesis that the humanised-microbiota mice contain the relevant gut flora to induce hatching of *T. trichiura*, I performed low dose (20 eggs) infections over 35 and 90 days in control murine microbiota mice and both humanised microbiota mouse strains. I evaluated the worm burdens, antibody ODs, as well as changes to the composition of the microbiota.

T. trichiura was only able to infect donor B mice (6/6 mice infected), no adult worms were recovered from donor A or murine microbiota mice at 35 days post infection (Figure 4.6). The infections were allowed to persist for 90 days in murine microbiota and donor A mice to allow *T. trichiura* to reach maturity; however, no *T. trichiura* were recovered and these data are not shown. During infections with *T. muris*, worms were recovered from all strains at 35 days post infection, 12/12 murine microbiota infected, 2/6 donor A mice, and 1/6 donor B mice. In addition, few *T. muris* were recovered from control mice at 90 days (2/6 murine microbiota mice infected), likely because 90 days is much longer than the traditional infection duration for this species that reaches maturity by 35 days (Else et al. 2020).

Parasite specific antibodies (IgG1 and IgG2a) were measured in the serum of infected mice as an indicator of the development of type 2 or 1 immune responses leading to worm expulsion or

chronicity, respectively (Bancroft, Else, and Grencis 1994). The antibody OD results largely reflect the worm burden results. As expected, on day 35 p.i. chronically *T. muris*-infected WT mice presented both IgG1 and IgG2a ODs, indicative of a mixed type 1 and 2 response. Similar results were observed chronically *T. muris*-infected Donor A mice (Figure 4.7). A single adult *T. muris* was recovered from a donor B mouse, which showed low ODs of IgG1 (Figure 4.7). In contrast, several donor B mice were chronically infected with *T. trichiura* (Figure 4.6), and presented high ODs of IgG1 in serum (Figure 4.9), indicating a type 2 immune response developed in these mice. This result is unexpected because worm expulsion was incomplete (Figures 4.6). Adult *T. trichiura* worms were not found in donor A or WT mice (Figure 4.6). However, some of these mice showed low IgG1 (5/15 mice) and IgG2a (7/15 mice) ODs (Figure 4.7) suggesting that they had been infected with *T. trichiura* but had expelled the worms by day 35 post infection.

Together these results indicate that the different humanised mice lines have differing ability to sustain an infection of either *T. trichiura* or *T. muris*, and these differences likely arise from the difference in microbiota composition. The data shown in this chapter supports the hypothesis that the successful induction of hatching and not invasion of the host epithelium is the limiting factor to chronically infecting mice with *T. trichiura* and humanised microbiota models can be used to study *T. trichiura* infection.

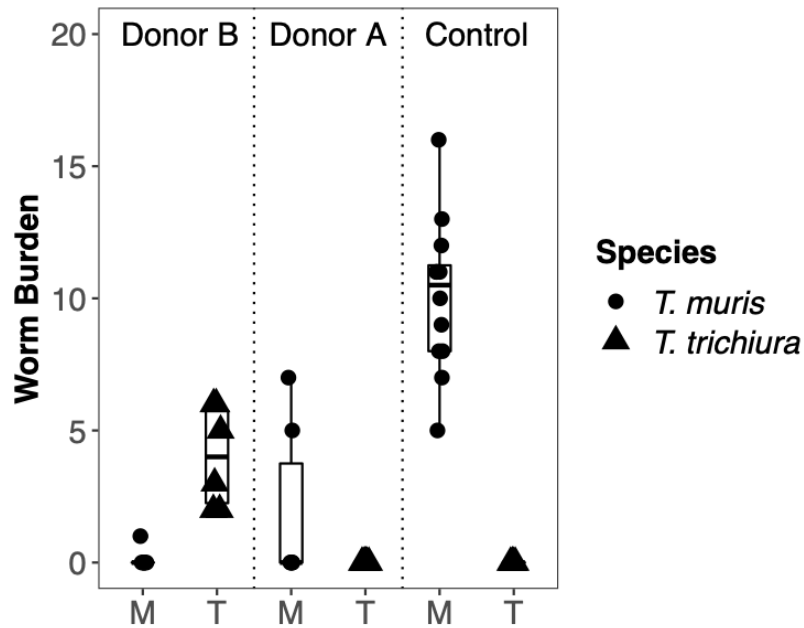


Figure 4.6. *T. trichiura* can establish an infection in humanised-microbiota mouse models. C57BL/6 humanised-microbiota mice as well as C57BL/6 murine microbiota mice were infected with a low dose (20 eggs) of *T. trichiura* or *T. muris*. Mice were culled at 35 days post infection, and caecal worm burdens were evaluated. Data was collected from four independent experiments; median and interquartile range are shown. donor B, n = 6 males (M) + 6 males (T); donor A, n = 4 females (T) + 3 females (M) + 5 males (T) + 3 males (M) ; murine microbiota, 4 females (T) + 3 females (M) + 5 males (T) + 3 males (M).

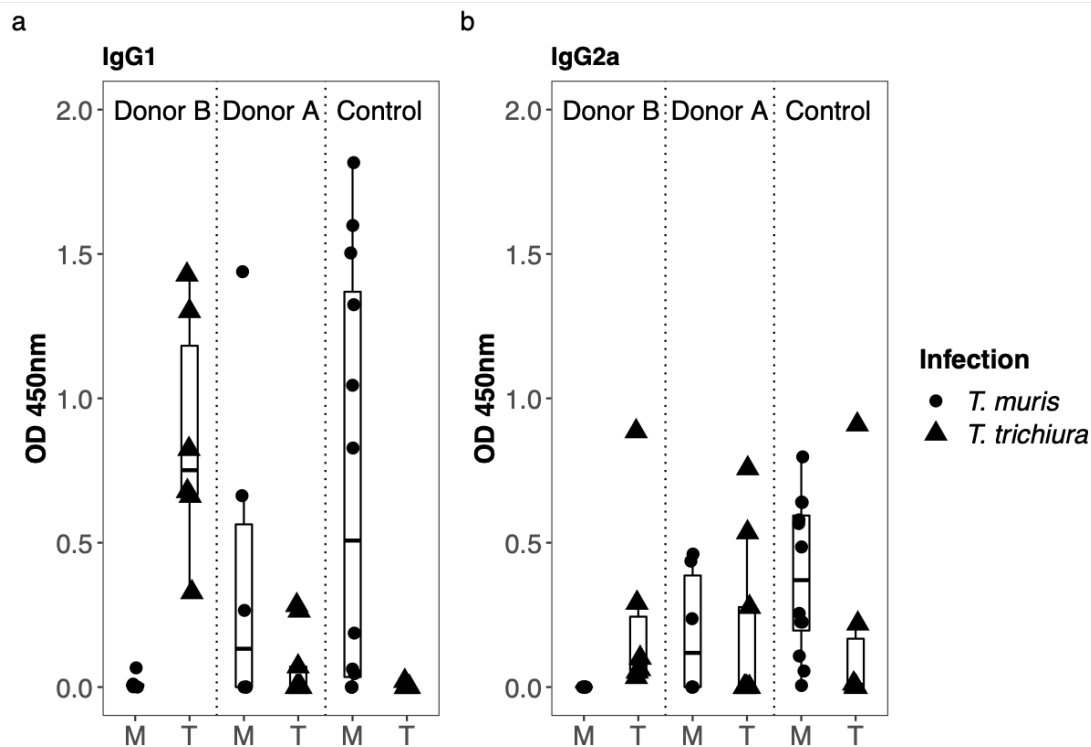


Figure 4.7. Two humanised microbiota mice models display differing antibody responses to infections with *T. muris* and *T. trichiura*. Antibody (IgG1 and IgG2a) ODs of *T. muris* or *T. trichiura* infected C57BL/6 humanised microbiota mice and C57BL/6 murine microbiota mice after 35 days of low dose infection (20 eggs). A 1 in 40 dilution of serum was tested against *T. muris* excretory secretory antigen. Data was collected from 4 independent experiments, median and interquartile range are shown, donor B, n = 6 males (M) + 6 males (T); donor A, n = 4 females (T) + 3 females (M) + 5 males (T) + 3 males (M); murine microbiota, 4 females (T) + 3 females (M) + 5 males (T) + 3 males (M).

4.7 Discussion and Conclusions

In the previous chapter my investigations into hatching focussed on *T. muris* and its interactions with *E. coli*; however, different *Trichuris* species respond differently to bacterial stimuli and findings in one species do not necessarily translate to the others (Vejzagić, Adelfio, et al. 2015). Thus, in order to expand our understanding of egg hatching in *T. suis* and *T. trichiura*, whipworms infecting pigs and humans respectively, I investigated the role of the microbiota isolated from different gastrointestinal samples from along the gastrointestinal tract in *in vitro* hatching experiments. I studied hatching of *T. suis* in response to porcine gastrointestinal tract samples confirming the observations by Vejzagić that demonstrated caecal mucosal scrapings can induce hatching in *T. suis* (Vejzagić, Thamsborg, et al. 2015). Additionally, the different levels of hatching induced by caecal scrapings and caecal contents indicate the specificity with which *T. suis* responds to samples from the site of infection i.e. the appropriate niche. However, hatching was very variable and only observed with two of the four pigs sampled. One explanation is that the bacterial strains required for hatching are sensitive to the collection process and the changes in temperature and oxygen after the organs were collected meant they did not survive transport from the operating theatre or processing in the lab. I expanded on this study by looking at the role of proteases in hatching induced by gastrointestinal mucosa microbiota and slight but non-significant reduction suggests that proteases are also important in *T. suis* hatching, however more sampling is needed to confirm this (Figure 4.3). Additionally, the lack of complete ablation is likely due to the high bacterial load of the samples that cannot be experimentally controlled. Once specific strains of microbiota that induce hatching of *T. suis* have been isolated, it will be easier to optimise the level of inhibition needed.

I then sought to conduct my investigations into the role of the microbiota in a biologically relevant setting this time using *T. trichiura* to see if the human parasite hatches in response to mucosal microbiota. I reported the *in vitro* hatching of *T. trichiura* using human microbiota samples for the first time (Figure 4.4). It was the ascending colon that induced the most hatching in *T. trichiura*; a reduced level of hatching was also seen with samples from the descending colon. Interestingly stool samples from an infected individual did not induce hatching; the eggs being unresponsive to the bacteria in their faeces may indicate that the luminal contents of the gastrointestinal tract do not contain the required members of the microbiota for *T. trichiura* hatching. While samples from the ascending colon were regularly able to induce hatching, the levels of hatching induced did not exceed 25% (Figure 4.4). This was likely due to the small sample size; each sample tube contained six 3mm x 3mm tissue sections representing a very low bacterial load. Indeed, sub-culturing one of these

homogenised samples yielded only 10 bacterial colonies. Additionally, when the same batch of *T. trichiura* eggs was co-cultured with samples from the humanised microbiota mice, hatching routinely exceeded 25% (median 53.3%, 37.2% hatching) (Figure 4.5), demonstrating that the problem did not lie with the viability of the eggs but likely with bacterial load.

Understanding hatching will be key to inform the development of *in vivo* models of *T. trichiura* infections, allowing researchers to study host parasite interactions as well as the passage of human whipworms in the lab environment. Hatching of *Trichuris* species appears to be host microbiota dependent, and I hypothesised that utilising humanised microbiota models may provide an environment that recapitulates the host well enough to induce hatching of *T. trichiura*. I was able to study the feasibility of this using two humanised microbiota mice strains for *in vitro* and *in vivo* studies of hatching and infection with *T. muris* and *T. trichiura*.

The *in vivo* infections revealed that the host origin of the microbiota is key in the establishment of an infection of *T. trichiura* (Figure 4.6). This is the first time a mouse model has been infected with *T. trichiura*. While encouraging, these results indicate that there are several factors that need to be optimised when creating a mouse line that can sustain a chronic *T. trichiura* infection. The observed worm burden was variable, murine microbiota and Donor A mice did not sustain a chronic infection, adult worms were only found in Donor B mice (Figure 4.6). As expected it is likely that the parasite eggs did not even hatch in the gastrointestinal tract of the murine microbiota mice, the lack of an antibody response in 4/6 mice that indicates an infection was not established (Figure 4.7). In the case of the donor A mice the composition of the microbiota may have prevented the establishment of a chronic infection, no adult worms were recovered (Figure 4.6) and an antibody response was only recorded in 4/9 mice (Figure 4.7). The donor A mice also induced less hatching *in vitro* (Figure 4.5c and d), further suggesting the composition of their microbiota does not adequately support *T. trichiura* hatching. In addition to the composition of the microbiota the mixed antibody responses observed indicate that alterations to the immune system may need to be tailored to the proposed application. To study host parasite interactions, we may need to develop a mouse model with both the gastrointestinal tract microbiota and immune system humanised. However for parasite production immunocompromised mice are typically used (Duque-Correa et al. 2019; Duque-Correa, Schreiber, et al. 2020), as the laboratory mice strains that are frequently used (C57BL/6, B10.BR, CBA and C57BL/10) display differing susceptibility to high dose infections of *T. muris* (Bancroft, Else, and Grencis 1994; Klementowicz, Travis, and Grencis 2012). Therefore, in the case of parasite maintenance

and production it may be beneficial to create an immunocompromised mouse with a humanised or defined microbiota of several bacterial strains capable of inducing hatching and supporting parasite development. This mouse strain could then be infected with a high dose of *T. trichiura* and the adult worms used to lay eggs, allowing us to have easy access to all life cycle stages in the lab for the first time. The results of the *in vitro* hatching assays partially explain the observations seen with the *in vivo* experiments. *T. trichiura* was only able to infect the donor B mice and caecal mucosal scrapings from these mice induced the highest levels of hatching *in vitro* (Figure 4.5 e and f). Donor B mice did not establish a chronic infection with *T. muris* and mice did not exhibit an antibody response (Figure 4.6, 4.7); this correlates with the observation that the levels of *in vitro* hatching observed were also lower with donor B mice than observed with murine microbiota control mice or *E. coli* (Figure 4.2 a and e). This data suggests that the microbiota of donor B mice promotes hatching of and colonisation with *T. trichiura* but not *T. muris*.

As mentioned earlier the humanised microbiota mice model allowed me to address some the challenges of studying the microbiota during parasite infections experiments, in particular, providing greater control over variability. Mice were from the same genetic background, age and sex matched, handled identically, additionally all caecal collections were conducted in the same time window to account for the circadian rhythmicity of the gastrointestinal microbiota. Considering these controls, the differences observed when utilising multiple humanised microbiota models highlight the role of the microbiota in infections and demonstrate that there is some degree of host specificity during a sustained or chronic infection. Interestingly *T. muris* hatches *in vitro* pretty indiscriminately, responding to porcine samples, and during *in vitro* hatching experiments, greater hatching was observed with donor A mice compared to murine microbiota mice. Together these results demonstrate that the composition of the microbiota affects the ability of mice to sustain an infection of either *T. trichiura* or *T. muris*. Understanding the taxonomic composition of these samples, and in particular identifying differences between the two strains of humanised microbiota mice, will help to identify the bacterial species that contribute to hatching of each whipworm species. However, as there are some differences between the response observed *in vitro* and *in vivo* in *T. muris*, there are likely other factors involved in maintaining a chronic infection such as the immune response.

The *in vitro* hatching experiments also allowed me to investigate the role of proteases in hatching induced by these gastrointestinal tract samples. The hatching induced by the ascending and descending colon biopsies was ablated by the addition of a protease inhibitor demonstrating that proteases play a role in the hatching of *T. trichiura* mediated by samples

from the human gastrointestinal tract. Additionally, the levels of *T. trichiura* hatching induced by caecal scrapings or caecal contents from humanised microbiota mice were significantly reduced by the addition of a protease inhibitor. The only exception to this was the hatching of *T. trichiura* anaerobically with caecal scrapings from donor A, it is likely that the starting levels of hatching were not high enough to observe a significant reduction in hatching without complete ablation in this case (Figure 4.5 d). This means that the inhibition of serine and cysteine proteases has consistently reduced the levels of hatching in all three whipworm species using a variety of bacterial samples, and I can conclude that serine and cysteine proteases are essential to hatching in *Trichuris* species.

One unexpected result was the spontaneous hatching of *T. muris* under anaerobic conditions. Vejzagić had previously reported that despite the bulk of the gastrointestinal tract being anaerobic, the use of anaerobic conditions did not improve the levels of hatching observed in *T. suis in vitro* (Vejzagić, Thamsborg, et al. 2015). In my results I largely observed this to be true, the use of anaerobic conditions reduced the overall amount of hatching seen when using humanised mice samples (Figure 4.2 & Figure 4.5). Spontaneous hatching was only observed when using an anaerobic chamber not when utilising anaerobic gas jars (Figure 4.2 e). The AnaeroGen anaerobic jar system is generally reported to perform as well as anaerobic chambers, however it can be easier to cultivate more bacterial strains using an anaerobic chamber (Miller, Wiggs, and Miller 1995; Bennett, Hickford, and Zhou 2006; Don Whitely Scientific 2020). In *T. muris* spontaneous hatching was observed with no visible contamination in the wells. To investigate if this hatching was truly spontaneous I collected the media from the wells with spontaneous hatched larvae, extracted the DNA and sequenced it. For this test, I placed *T. muris* eggs in RMPI, LB, and water in the anaerobic chamber; spontaneous hatching was observed in RMPI and LB but not in water. I extracted and sequenced DNA from the media from one of the wells where the spontaneous hatching was observed. After classifying these sequences, the dominant species observed in LB was *Alistipes onderdonkii*, the dominant species observed in RPMI was *Citrobacter freundii*. The presence of bacteria in these samples suggests that the hatching was not truly spontaneous but driven by contaminants not visible to the eye. Therefore, more investigation and testing of this phenomenon is needed to elucidate if *T. muris* truly hatches spontaneously in anaerobic conditions, however it is not entirely unfeasible. Similar observations under anaerobic conditions have been observed by other labs (Cadwell 2020), as well as bacterial independent hatching of certain strains of *T. muris* (Koyama 2013, 2016).

I was also able to get the first indication of specific species that induce hatching of *T. trichiura* by sequencing contaminated media, and *E. coli D* was found to be the most abundant bacterial species in these wells. Previous attempts to induce hatching of *T. trichiura* using *E. coli K12* have been unsuccessful; however, utilising a strain of *E. coli D* may yield positive results. The second most abundant bacteria was *C. freundii* a facultative anaerobe gram negative commensal and opportunistic pathogen that like *E. coli* utilises various virulence genes to facilitate infection (J. T. Wang et al. 2000; Schloissnig et al. 2013; Schierack et al. 2007; Jansson et al. 2010). *C. freundii* is a known member of human and animal microbiomes, and has been isolated from the lumen and the mucosa of humans and pigs (Schierack et al. 2007; Marsh et al. 2020); and the virulence genes it can express facilitate adhesion to the gastrointestinal mucosa (Bai et al. 2012; Mirelman, Altmann, and Eshdat 1980; Jansson et al. 2010). Interestingly, *C. freundii* expresses both type 1 fimbriae and the *ClpP* serine protease complex (Jones et al. 1995; Uniprot 2021). It will be interesting to test *C. freundii* alongside other strains of *E. coli* for the ability to induce hatching of *T. trichiura* as monocultures.

In summary, in this chapter after conducting *in vitro* hatching experiments with *T. muris*, *T. suis*, and *T. trichiura* experiments using gastrointestinal samples from pigs, humans, and a humanised microbiota mouse model, I can conclude that the composition of the microbiota affects both *in vitro* hatching and *in vivo* infections. Additionally, I was able to begin identifying species of interest in *T. trichiura* hatching by examining an instance of contamination. In chapter 5, I continue my study of the microbiota, searching for relevant species in the microbiota of humans, humanised microbiota mice, and pigs.

Chapter 5- Metagenomic analysis to identify bacterial species involved in hatching across *Trichuris* species.

Declaration of contributions

M. Duque Correa and M. Berriman supervised this work. K. Ambridge, performed DNA extractions. K. Ambridge, and Sanger Sequencing Pipelines performed genomic library prep and sequencing. Sanger Pathogen Informatics Pipelines and A. Almeida provided informatics support. I performed DNA extractions, and all analyses.

Publication

5.1 Introduction

The role of the microbiota in hatching has been studied in *T. muris* and *T. suis* (Panesar and Croll 1980; Vejzagić, Thamsborg, et al. 2015; Koyama 2013). These studies observed hatching in the presence of gastrointestinal samples, and showed that the addition of antibiotics to these samples ablated hatching. Studies *in vivo* showed reduced infection when utilising germ-free mice or mice with a depleted microbiota via antibiotic treatment, but mono-colonising or re-colonising mice with bacteria restored infection (White et al. 2018). These results indicate that the bacteria in these samples are responsible for hatching and establishing an infection.

However, the relationship between host bacteria and parasite is more complex, in fact the nematodes themselves have also been shown to acquire their microbiota from and adapt to the microbiota of the host (White et al. 2018), additionally whipworm infection alters the composition of the host microbiota. Studying the effects of nematode infection on the microbiota has been difficult, often yielding conflicting results. Infection with nematodes can show no effects but some studies have managed to observe changes in the abundance of phyla, as well as bacterial diversity and species richness (Cooper et al. 2013; Cantacessi et al. 2014; Rapin and Harris 2018). In C57BL/6 mice a chronic infection with *T. muris* causes significant changes to the host microbiota (Houlden et al. 2015; Holm et al. 2015). Including

an overall reduction in the diversity and abundance of the members of the Bacteroidetes phylum and species from the *Prevotella* and *Parabacteroides* genera, as well as an increase in the abundance of *Lactobacillaceae* (Houlden et al. 2015; Holm et al. 2015). These changes to the microbiota result in reduced host susceptibility to the parasite, suggesting that the presence of the parasite causes a decrease in the abundance of bacterial species required for those initial stages of colonisation, which includes hatching (White et al. 2018).

In pigs, infection with *T. suis* results in generalised gastrointestinal tract dysbiosis; and the disruption of the mucosa during parasite invasion may be the driving factor behind the observed increase in the abundance of mucin-feeding and epithelium-invading bacterial species (R. W. Li et al. 2012). The dysbiosis causes further disruption of the intestinal epithelium and results in dysentery (Rutter and Beer 1975; Li et al. 2012). In humans the effects of *T. trichiura* on the microbiota have been harder to study and often produce conflicting results (Lawson, Roberts, and Grencis 2021). Some studies have shown alterations in the abundance of several phyla including Bacteroidetes, Proteobacteria, and Actinobacteria in infected people compared to healthy controls (H. Chen et al. 2021). While others have not found any significant associations between infection and species-abundance or richness (Cooper et al. 2013). The difficulty in studying the interactions of *T. trichiura* with the human host microbiota likely arises from two factors. Firstly, in endemic regions individuals are rarely infected with one gastrointestinal parasite let alone one nematode species, making it a challenge to dissect specific effects. Secondly, individuals are rarely observed before and after their primary parasite exposure, many patients have suffered several recurring infections before they are sampled. Studies have tried to address this by comparing the composition of the microbiota in individuals, pre and post anthelmintic treatment, however this approach did not reveal any significant taxa (Cooper et al. 2013). Studying infections in a humanised microbiota mouse model presents a unique opportunity to address some of these challenges and study the effects of *T. trichiura* on the host microbiome during a primary infection.

In chapter three I identified bacterial genes that are implicated in *T. muris*–*E. coli* hatching interactions. Additionally, in chapter four, I demonstrated that hatching in *Trichuris* species (*T. muris*, *T. suis*, and *T. trichiura*) is host microbiota dependent, with microbiota from the site of infection, the caecal mucosa, inducing the highest levels of hatching. In similar previous studies, the composition of the microbiota was not analysed creating a gap in the knowledge of hatching factors (Panesar and Croll 1980; Vejzagić, Thamsborg, et al. 2015). In the present chapter, I sought to address this, and I searched the human microbiota for fimbrial and serine protease genes. Additionally, I collected and analysed crude caecal

contents and scrapings from naive humans, pigs and mice, leading to the identification of the members of the microbiota responsible for inducing hatching *in vitro*. Furthermore, for the porcine and humanised microbiota mouse samples, I used advancements in culturing to capture the bacteria that are able to grow in 24 h alongside the *in vitro* hatching experiments in the form of metascrapes. These samples were then sequenced and analysed in the same way as the crude samples. I also examined the changes in host microbiota during infection of humanised microbiota mice with *T. muris* or *T. trichiura*, by collecting and analysing caecal contents from infected mice. In summary, I aimed to gain a detailed understanding of hatching factors using metagenomics to investigate the composition of the microbiota. In doing so I gained a greater understanding of the interactions between host, parasite, and microbiota and shed more light on the interactions between eggs and bacteria that highlight the mechanisms behind hatching in *Trichuris*.

Metagenomic approaches aim to isolate individual species from mixed samples to understand their functional contributions. The tools available today were primarily developed to study the composition of commensal organisms isolated from various body sites, in particular the gastrointestinal tract. There have been many advances in the field of metagenomics and analysis has expanded from 16S metagenomics to include whole genome shotgun metagenomics. As well as the multi pronged approach termed ‘culturomics’— that utilises 16S sequencing, mass spectrometry, and advanced culturing to study metagenomic samples. However, there are still challenges with metagenomic analysis; the two primary strategies— reference based and de novo assemblies, each come with caveats.

Reference based strategies utilise a curated set of genomes to identify members of the microbiota in a given sample. Reference based approaches can also be used to quantitatively analyse the composition of the microbiota and provide a differential analysis of bacterial abundance. However, reference-based approaches are only as good as the reference catalogue. While this catalogue has been dramatically expanded with recent additions of the genomes of previously “unculturable” species and large-scale curation efforts; many members of the human gastrointestinal tract remain uncharacterised and unidentified (Zou et al. 2019; Forster et al. 2019; Almeida et al. 2021; Browne et al. 2016). I classified the un-assembled reads using Kraken2 (Wood, Lu, and Langmead 2019) with a curated human gut metagenome database: the Unified Human Gastrointestinal Genome (UHGG) (Almeida et al. 2021). Kraken 2 utilises databases to provide classification of all the organisms in a sample at each taxonomic level from kingdom through to species. The UHGG also contains putative clade information from the Genome Taxonomy Database but

as the collection contains many unculturable microbiota, these clades are often not validated (Chaumeil et al. 2019). This approach with Kraken 2 (Wood, Lu, and Langmead 2019) and the UHGG (Almeida et al. 2021) performed well on average, classifying nearly 70% of the reads (mean percentage unclassified = 30.7%). The relative abundances reported by Kraken 2 were used to visualise the beta diversity (differences in taxonomic composition between the different samples) and for differential analysis of the presence of different taxa. MaAsLin 2 (Mallick et al. 2021) was used to evaluate if the observed differences were statistically significant in each of the various categories of metadata. A q value threshold of 0.05 was used and effect size reported as beta coefficients, a general measure of magnitude of effect (i.e. with a coeff of 0.75 a 1-unit increase in the predictor variable results in a 0.75 unit increase in the outcome variable).

In contrast to reference-based approaches, *de novo* assembly pipelines seek to assemble bacterial genomes from metagenomic reads. In practice, metagenome-assembled genomes (MAGs) are generated through a binning process, whereby reads or contigs are sorted into taxonomically similar pools in order to reconstitute individual genomes that can then be used for qualitative analysis, including functional annotation and phylogenetics (Saheb Kashaf et al. 2021). The primary caveat of the binning process is that it removes the ability to study the composition of bacterial species quantitatively because the assembly and binning processes preferentially assemble species with greater sequencing coverage i.e. more abundant species. Despite this, assembly can capture species that have been previously unidentified especially due to culturing difficulties, and allows for qualitative analysis of the genomes. There are two thresholds to consider when creating MAGs: completeness and contamination, which refer to how much of the complete genome is acceptable and how many misassigned reads are acceptable, respectively. Altering both of these thresholds alters what is detected in the samples. Acceptable thresholds for completeness begin at 50% for undefined samples, and can be set as high as 95% for well characterised samples (Uritskiy, DiRuggiero, and Taylor 2018; Saheb Kashaf et al. 2021). As many of my samples are low abundance samples in the form of the very small human biopsies, I used 65% completeness, and 5% contamination to balance these stringencies and aim for shorter but less-contaminated genomes. I completed these assemblies using the MetaWRAP pipeline which offers two tools for assembly, metaSPAdes and MEGAHIT (Uritskiy, DiRuggiero, and Taylor 2018; Bankevich et al. 2012; D. Li et al. 2015). I used both tools on all samples and then re-classified the MAGs using Kraken 2 after assembly, to compare the assembler performance. Overall MEGAHIT out-performed metaSPAdes. The majority of samples that failed assembly, failed when using the metaSPAdes tool but were successfully assembled by MEGAHIT; therefore, MEGAHIT assemblies were used going forwards. After MAGs were

assembled I once again tried to classify the reads using Kraken 2. Generally, assembly did improve the rates of classification and the new mean percentage of reads unclassified was 24.2%. Detailed in Figure 5.1 is the workflow undertaken and tools used in the present chapter to compare the various analysis approaches on the gastrointestinal tract samples collected in chapter four.

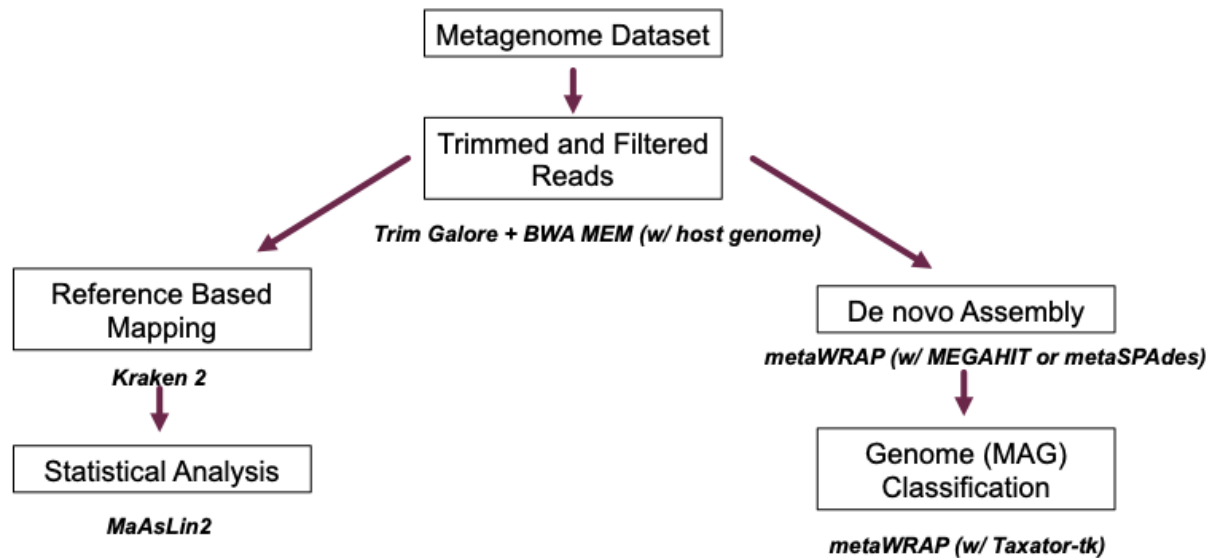


Figure 5.1 Metagenomic analysis, workflow and tools. There are two approaches to metagenomic analysis: reference-based analysis and *de novo* assembly. Reads are first trimmed and filtered, and then for the reference based approach, reads were mapped to the Unified Human Gastrointestinal Genome (UHGG) (Almeida et al. 2021) using Kraken 2 (Chaumeil et al. 2019), statistical analysis of differences in abundance was performed using MaAsLin2. For the *de novo* approach MAGs were assembled using the metaWRAP pipeline (Uritskiy, DiRuggiero, and Taylor 2018; Bankevich et al. 2012; D. Li et al. 2015).

5.2 Candidate genes important to hatching of whipworm eggs are found in human gut bacteria

The HBC, is a collection of 737 whole-genome-sequenced bacterial isolates including 105 novel species, isolated from the faecal samples of healthy donors (Forster et al. 2019). I used these genomes as a representation of the healthy human gut to predict the abundance of genes integral to hatching in the primary intestinal bacterial phyla. I primarily focussed on fimbrial and serine protease genes, given their likely involvement in hatching. Type 1 fimbriae are primarily expressed in gram negative species (Telford et al. 2006), however the gastrointestinal microbiota is primarily composed of gram positive species like *S. aureus* and *P. aeruginosa* which can induce hatching in *T. muris* independent of fimbriae (Hayes et al. 2010)(Chapter 3). Thus, I expanded my search to look for pili expressed in gram positive bacteria (Telford et al. 2006).

The Sanger Pathogen Informatics Pipeline annotation tool searches several databases to provide an initial annotation on the draft genomes of all the species in the HBC (Chapter 2) (Page et al. 2016; Seemann 2014). Using custom search terms, I identified 152 fimbrial or pili genes, the majority of these are uncharacterised (Table 5.1), the known genes most frequently counted in these annotated genomes are the type 1 fimbrial proteins (*fimA-G*), fimbrial chaperones (*focC*, *htrE*, *matC*) and the T6 pili antigen (*tee6*) (Table 5.1). *E. coli* express type 1 fimbriae encoded by the *fim* operon containing the genes *fimA-fimI*, *S. typhimurium* expresses type 1 fimbriae encoded by the genes *fimW,Y,& Z*, *P. aeruginosa* expresses type IV pili, and the genes *fimT-fimV* encode minor pilins. Lastly *S. aureus* only expresses short surface adhesins; however, the *tee6* gene encodes T6 pilin one of the major pilus subunits in other gram-positive cocci– the *Streptococcus* spp (Telford et al. 2006; Schneewind, Jones, and Fischetti 1990). The distribution of these abundant genes was plotted against the HBC maximum likelihood phylogram to observe which phyla are enriched for them, revealing that the majority of *fim* genes were annotated in Proteobacteria, and *tee6* genes in Actinobacteria and Firmicutes (Figure 5.2). However, while many Actinobacteria and Firmicutes isolates do not possess the full *fim* operon they do possess *fimA* genes. As the most frequently annotated genes type 1 fimbriae genes and T6 pili genes likely mediate adhesion in Proteobacteria, Actinobacteria, and Firmicutes; characterising the large quantity of unknown genes will help to confirm this. In order to refine my observations and characterise the unknown genes, I performed *de novo* functional annotation on the final assembled versions of these genomes, using a higher quality assembly to improve the annotation. Annotation was performed using prodigal and eggNOG (Hyatt et al. 2010; Huerta-Cepas et al. 2019) and once the genomes were annotated I used custom search

terms to pull out isolates with *fim* genes. Once again, this methodology easily confirmed the presence of these genes in Proteobacteria; however, this search did reveal more Firmicute isolates with several predicted fimbrial genes (Figure 5.3). This suggests that gram positive species do express *fim* genes, but as many of these species have only recently been isolated and sequenced the genes are under characterised.

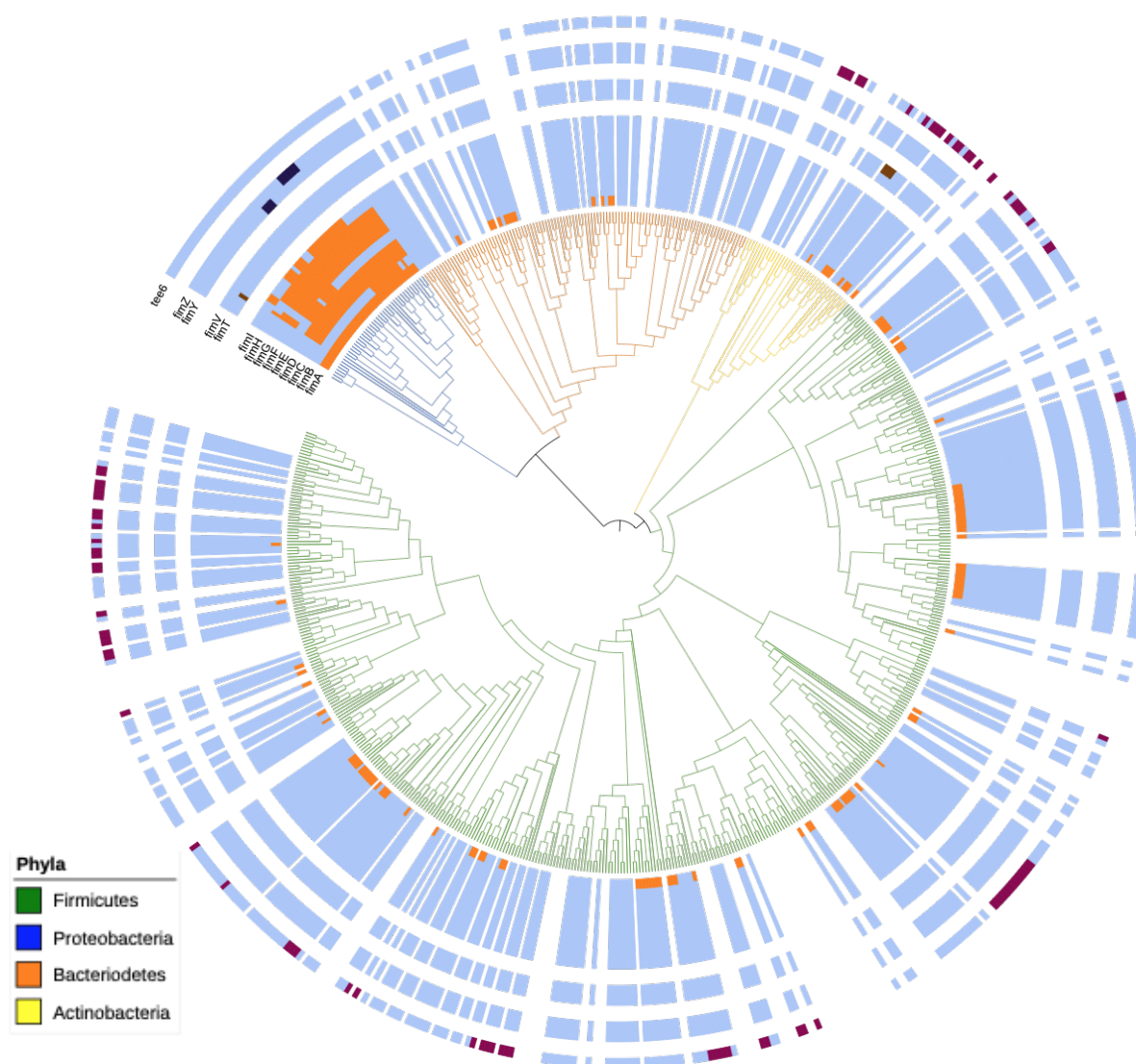


Figure 5.2. The diversity of fimbrial and pili genes annotated in the HBC phylogram. Maximum-likelihood tree generated using 40 universal core marker genes from each genome. Branch colours distinguish phyla, and outer tracks display the presence or absence of genes encoding fimbriae and pili, each plotted as a concentric track outside the tree. The majority of *fim* genes were annotated in phylum proteobacteria, and *tee6* genes were primarily annotated in gram positive phyla, actinobacteria and firmicutes. Track labels, from inner to outer ring: (1) Orange- *fimA*, *fimB*, *fimC*, *fimD*, *fimE*, *fimF*, *fimG*, *fimH*, *fimI*; (2) Brown- *fimT*, *fimV*; (3) Black- *fimY*, *fimZ*; and (4) Purple- *tee6*

Table 5.1 Fimbrial and pili genes annotated in the HBC

Gene	Number of Annotations	Gene	Number of Annotations
ab initio prediction	1592	<i>aufD</i>	7
<i>fimA</i>	370	<i>eafC</i>	7
<i>fimD</i>	245	<i>epsF</i>	7
<i>fimC</i>	211	<i>fms20</i>	7
<i>fimF</i>	123	<i>sfmD</i>	7
<i>tee6</i>	118	<i>stbB</i>	7
<i>htrE</i>	99	<i>stbE</i>	7
<i>matC</i>	96	<i>yadM</i>	7
<i>focC</i>	81	<i>yfcO</i>	7
<i>fimG</i>	79	<i>yfcR</i>	7
<i>fimH</i>	68	<i>lpfD</i>	6
<i>papD</i>	64	<i>yfcV</i>	6
<i>papC</i>	59	<i>faeE</i>	5
<i>smfA</i>	51	<i>fimZ</i>	5
<i>matB</i>	46	<i>focD</i>	5
<i>mrpA</i>	40	<i>sfaD</i>	5
<i>fim</i>	39	<i>sfmA</i>	5
<i>papH</i>	37	<i>sfmC</i>	5
<i>sfaG</i>	35	<i>sfmF</i>	5
<i>sfaA</i>	28	<i>sfmH</i>	5
<i>yadK</i>	25	<i>ycbQ</i>	5
<i>epsE</i>	23	<i>ycbR</i>	5
<i>csgC</i>	22	<i>ycbS</i>	5
<i>xerD</i>	21	<i>ycbT</i>	5
<i>fimI</i>	20	<i>ycbU</i>	5
<i>caf1A</i>	19	<i>yhcD</i>	5
<i>elfA</i>	18	<i>papI</i>	4
<i>ycgG</i>	18	<i>yadC</i>	4
<i>stbA</i>	17	<i>ybgP</i>	4
<i>papB</i>	16	<i>ybgQ</i>	4
<i>yehC</i>	15	<i>fimV</i>	3
<i>lpfB</i>	14	<i>fimY</i>	3
<i>sfaS</i>	14	<i>lpfE</i>	3
<i>stbC</i>	13	<i>papA1</i>	3
<i>stbD</i>	13	<i>papF</i>	3
<i>fimB</i>	12	<i>spaF</i>	3
<i>hifA</i>	12	<i>srtA</i>	3
<i>matA</i>	12	<i>yadL</i>	3
<i>pilC</i>	12	<i>atfC</i>	2
<i>pmfA</i>	12	<i>csoA</i>	2
<i>yehD</i>	12	<i>fszA</i>	2
<i>cfaE</i>	11	<i>fszB1</i>	2
<i>fimE</i>	11	<i>hofM</i>	2
<i>prsF</i>	11	<i>hofN</i>	2
<i>xerC</i>	11	<i>hofO</i>	2
<i>lpfC</i>	10	<i>mrfB</i>	2
<i>yadN</i>	10	<i>mrkA</i>	2
<i>yfcS</i>	10	<i>mrpD</i>	2
<i>cfaB</i>	9	<i>papE</i>	2
<i>papA</i>	9	<i>sdrD</i>	2
<i>papK</i>	9	<i>sfaC</i>	2
<i>caf1M</i>	8	<i>yehA</i>	2
<i>lpfA</i>	8	<i>yehB</i>	2

<i>yfcU</i>	8	<i>ygiL</i>	2
<i>yqiG</i>	2		
<i>yraH</i>	2		
<i>yral</i>	2		
<i>yraK</i>	2		
3.2.1.8	1		
<i>aafB</i>	1		
<i>aafC</i>	1		
<i>afaE3</i>	1		
<i>atfA</i>	1		
<i>atfB</i>	1		
<i>aufF</i>	1		
<i>cfaD</i>	1		
<i>cna</i>	1		
<i>cph2</i>	1		
<i>epsG</i>	1		
<i>fimT</i>	1		
<i>mrfE</i>	1		
<i>mrfF</i>	1		
<i>mrpB</i>	1		
<i>mrpC</i>	1		
<i>mrpE</i>	1		
<i>mrpF</i>	1		
<i>mrpG</i>	1		
<i>mrpH</i>	1		
<i>mrpI</i>	1		
<i>mrpJ</i>	1		
<i>pac</i>	1		
<i>pezA</i>	1		
<i>pilA</i>	1		
<i>pilE</i>	1		
<i>pilE1</i>	1		
<i>pilF</i>	1		
<i>pmfC</i>	1		
<i>pmfD</i>	1		
<i>pmfE</i>	1		
<i>pmfF</i>	1		
<i>pmpA</i>	1		
<i>prsK</i>	1		
<i>sfaH</i>	1		
<i>spaA</i>	1		
<i>spaC</i>	1		
<i>srtB</i>	1		
<i>uca</i>	1		
<i>xpsE</i>	1		
<i>yjcC</i>	1		
<i>zraR</i>	1		

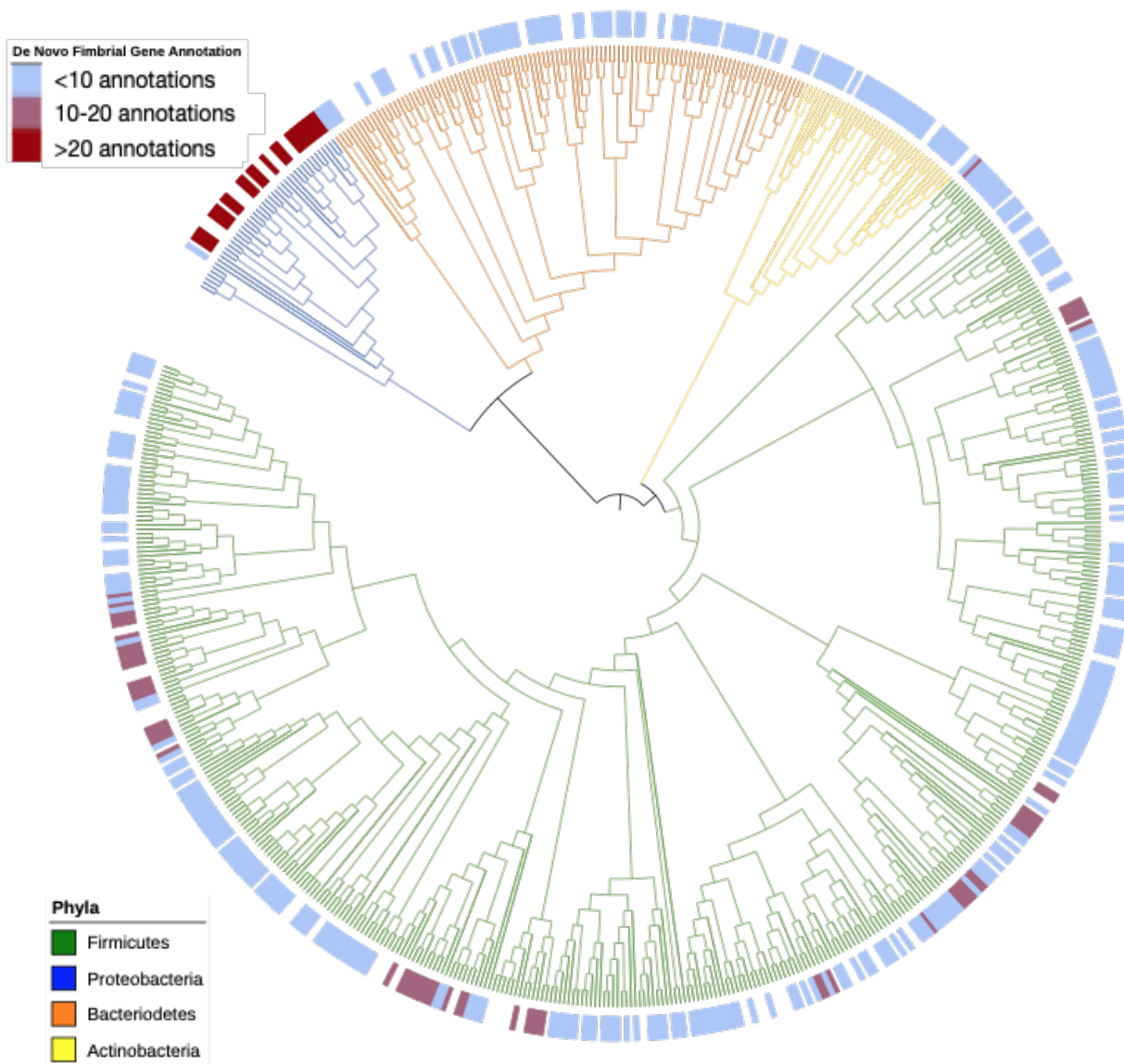


Figure 5.3. de novo annotation increases the prediction of fimbrial genes in Firmicutes the HBC. Maximum-likelihood tree generated using 40 universal core marker genes from each genome. Branch colours distinguish phyla, and outer tracks display the number of predicted *fim* genes per isolate. Isolates were grouped according to the number of predicted genes low (<10), medium (10-20), and high (>20). This confirmed the presence of multiple *fim* genes in many Proteobacteria isolates, and more Firmicute isolates.

In chapter 3 I also tested the effect of knocking out *clpA*, *clpP*, *clpX*, *degP*, *degQ*, and *glpG* on hatching, and found the greatest reduction in hatching of *T. muris* with a *clpP* knockout (Figure 3.11). I used the sequences of six genes to search for these serine proteases in the genomes of HBC using Blastx (Figure 5.4). The genes *clpA*, and *clpX* (inner two tracks) were most abundant across the gut phyla with an average of 10 and 11 genes identified per

isolate. The gene with the greatest effect, *clpP* (middle track), was less abundant with an average of 3 genes identified per isolate. However, *clpP* was still found in all phyla indicating that serine protease activity relevant to the hatching of a *Trichuris* species is ubiquitous in the human microbiota. In order to expand these observations and identify more serine protease genes, I performed *de novo* functional annotation on the final assembled versions of the HBC genomes. Once the genomes were annotated I used custom search terms to pull out isolates with serine protease genes in the same gene ontology family as *clpP* (EMBL-EBI 2021). This confirmed the abundance of serine proteases in the HBC, multiple serine protease genes were predicted in many isolates across all phyla (Figure 5.4).

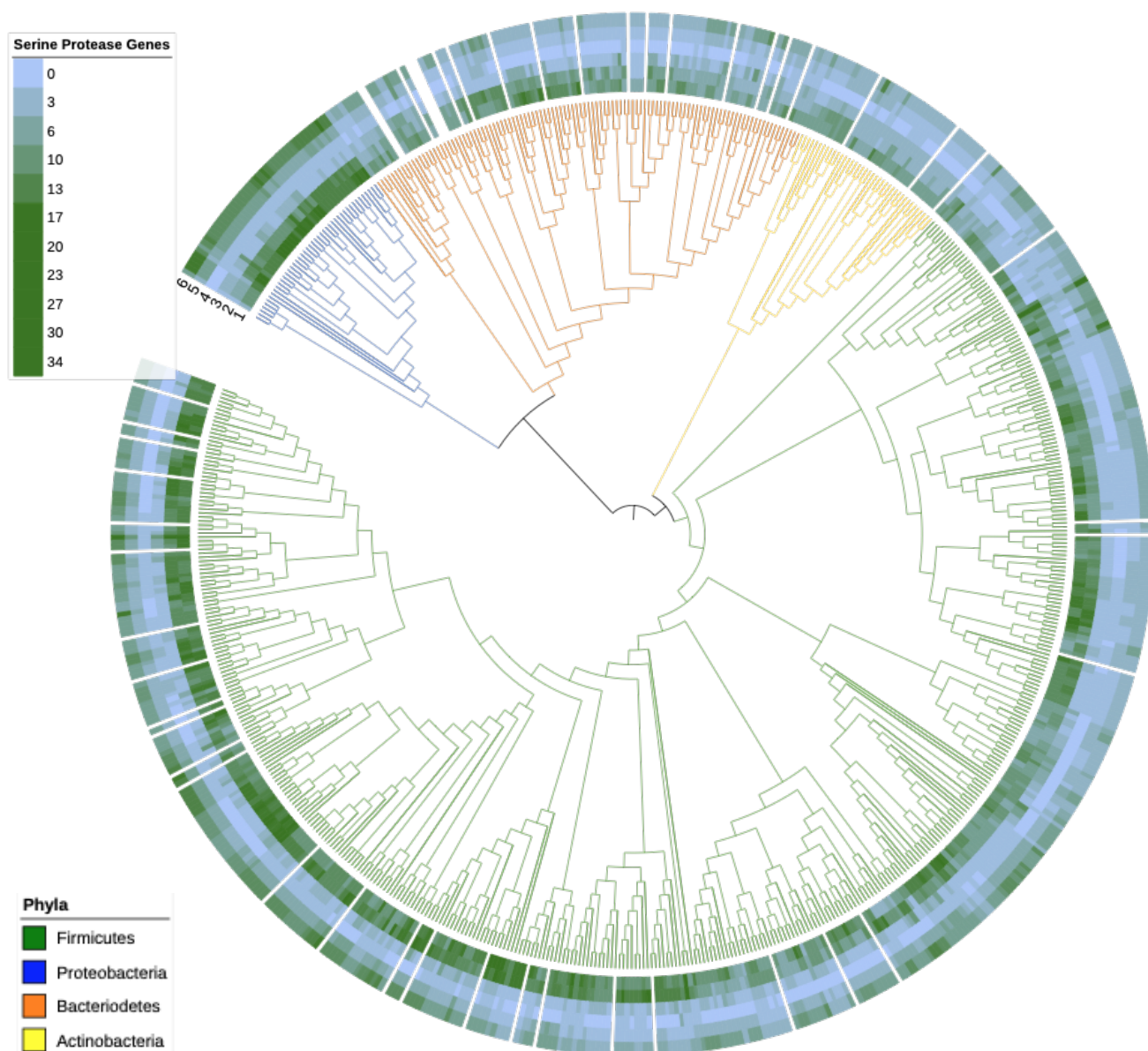


Figure 5.4. The distribution of serine protease genes involved in *T. muris* hatching in the HBC. Maximum-likelihood tree generated using 40 universal core marker genes from each genome. Branch colours distinguish phyla, and outer tracks display the number of Blastx hits to *clpA*, *clpP*, *clpX*, *degP*, *degQ*, and *glpG* genes. The genes *degP*, *degQ*, *clpA*, and *clpX* are found in abundance across all phyla; fewer hits to *clpP* and *glpG* were observed however they were still identified in all phyla. Track labels from inner to outer ring: 1) *clpA*- ATPase and specificity subunit of ClpA-ClpP ATP-dependent serine protease, chaperone activity. 2) *clpX*- ATPase and specificity subunit of ClpX-ClpP ATP-dependent serine protease. 3) *clpP*- proteolytic subunit of ClpA-ClpP and ClpX-ClpP ATP-dependent serine proteases. 4) *glpG*- rhomboid intramembrane serine protease. 5) *degP*- serine endoprotease (protease Do), membrane-associated. 6) *degQ*- serine endoprotease, periplasmic)

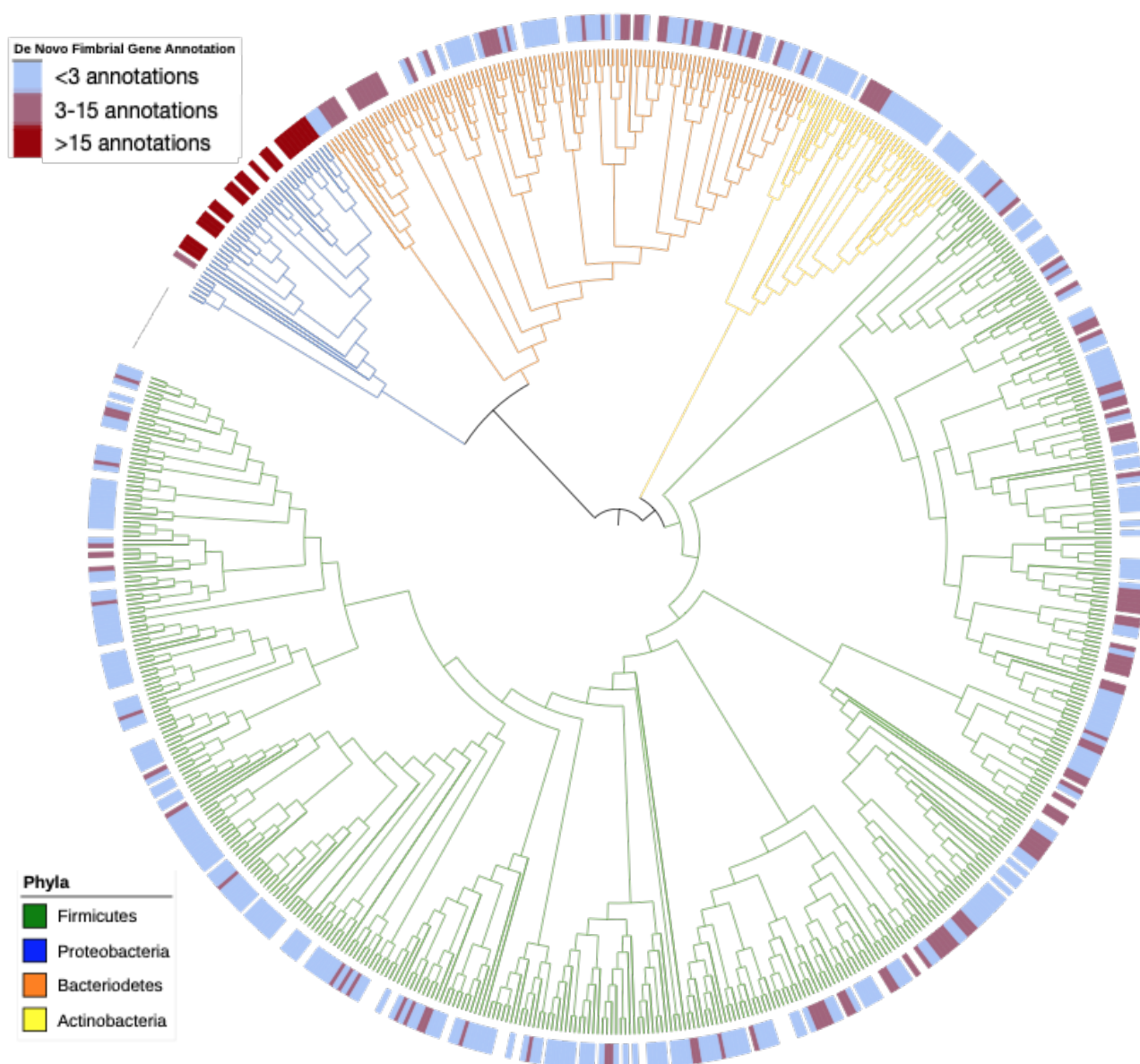


Figure 5.5. *de novo* annotation increases the prediction of serine protease genes in the HBC. Maximum-likelihood tree generated using 40 universal core marker genes from each genome. Branch colours distinguish phyla, and outer tracks display the number of predicted *fim* genes per isolate. Isolates were grouped according to the number of predicted genes low (<3), medium (3-15), and high (>15). This confirmed the presence of multiple serine protease genes in many isolates across all phyla.

5.3 A differential analysis of relative taxonomic abundances in human biopsies capable of inducing hatching in *T. trichiura*

Having confirmed the genes important for hatching are present in the human gut microbiota generally I sought to characterise the taxonomic composition of samples with demonstrated capability to induce hatching (Chapter 4). In the human biopsies I was interested in identifying taxa relevant to hatching through looking for associations between taxonomic groups and either the region of the gastrointestinal tract collected or the level of hatching observed *in vitro* (Chapter 4). I began by classifying the samples using Kraken 2 and the UHGG database before and after MAG assembly. For the unassembled reads, the rate of classification was very variable, however many samples were well classified (median percentage unclassified = 30.7%) and only one sample remained completely unclassified (Figure 5.6). The unclassified reads in the unassembled samples can potentially be attributed to the gastrointestinal tract virome and mycobiome. Classification did not improve after MAG assembly and the new median percentage of reads unclassified was 52.1%, additionally 16 samples were now reported as 100% unclassified (Figure 5.6). The shift in the levels of classification further supports the idea that the human biopsy samples contain large proportions of non-bacterial components that were preferentially assembled and could not be identified by the UHGG database.

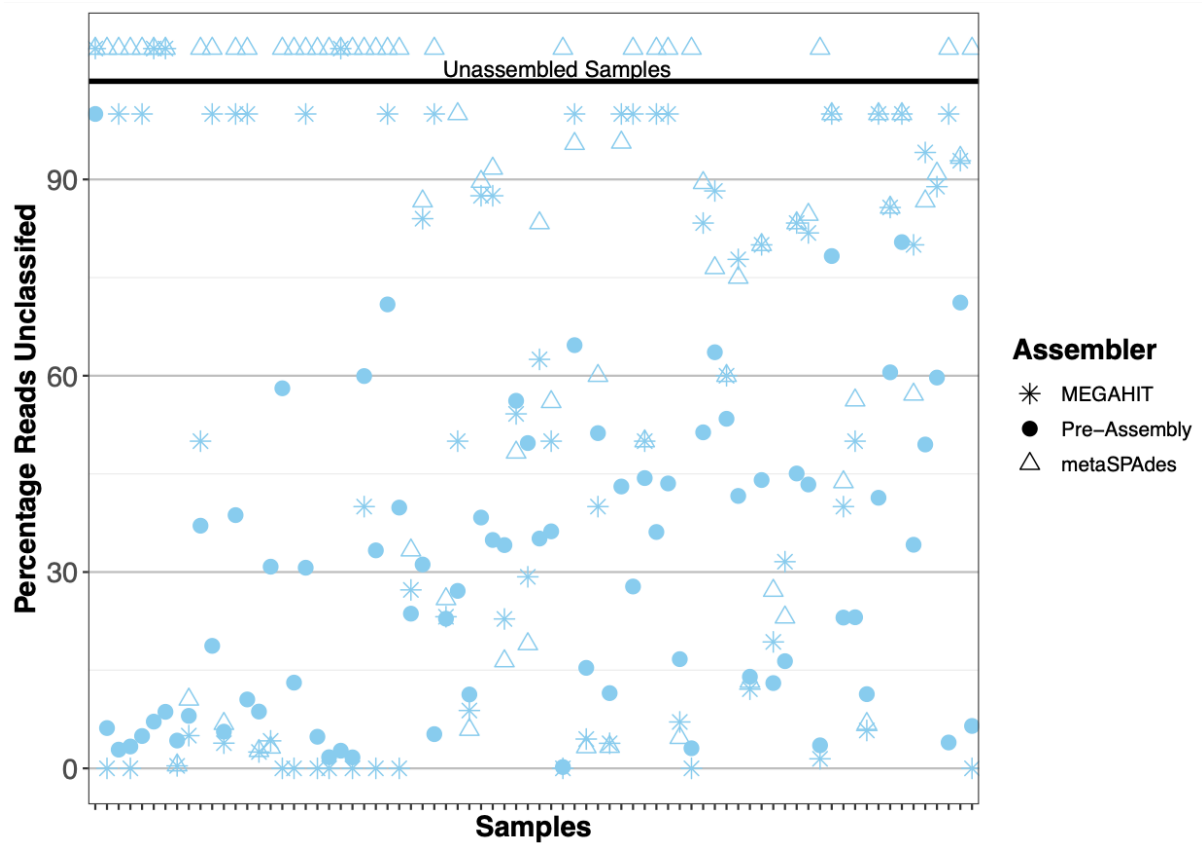


Figure 5.6 Genome assembly using MEGAHIT does not improve classification of gastrointestinal tract samples from humans. Metagenomic assembled genomes (MAGs) were created using the metawrap pipeline and the assembly tools MEGAHIT and metaSPAdes. MEGAHIT out performed metaSPAdes, successfully assembling MAGs from more samples. Samples were classified with Kraken 2 before and after assembly and fewer samples were successfully classified after assembly.

I annotated the samples by gastrointestinal tract collection site and the hatching readouts from chapter four to identify samples with similar taxonomic composition within the clusters dictated by the metadata (Figure 5.7). The most diverse samples were the mixed colon biopsies which is to be expected because these contained a combination of bacteria from both ascending and descending colon. The majority of the samples from the ascending and descending colon clustered together however there were several diverse samples (Figure 5.7). Hatching was observed with mixed, ascending, and descending colon samples (Figure 4.4), and the spread observed in the beta diversity of these biopsies suggests that the factors that can induce hatching are present in a diverse range of samples (Figure 5.7)

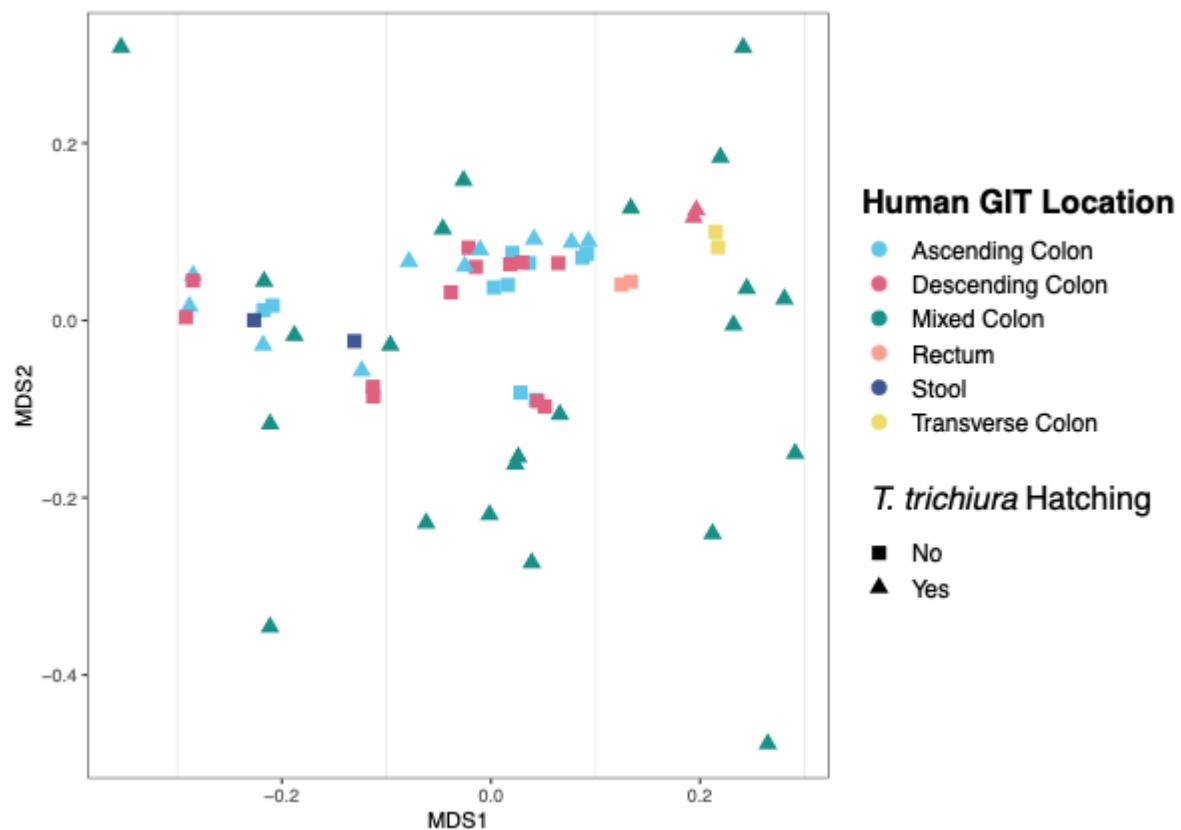


Figure 5.7 Beta diversity of gastrointestinal tract samples from human biopsies reveals that a diverse collection of samples can induce hatching of *T. trichiura*.

Using a Bray–Curtis distance matrix generated from the relative taxa abundances reported by Kraken 2, a Principal Coordinates Analysis (PCoA) revealed the human biopsy samples do not cluster by gastrointestinal tract sampling site or hatching readouts

The human biopsy samples were primarily composed of the four phyla most commonly reported in the gut: Firmicutes, Proteobacteria, Bacteroides, and Actinobacteria (Figure 5.8). The abundances of eight phyla (~31% of all phyla in the database) were significantly different ($q < 0.05$) when comparing gastrointestinal tract sites sampled (Table 5.2). The significant differences identified were primarily increases in phyla abundance in the transverse colon samples (Table 5.2), which suggests that bacteria from these phyla are relatively more abundant in this fraction of the gastrointestinal tract. While interesting, it does not explain hatching as the transverse colon is not the parasite niche, additionally the transverse colon samples did not induce hatching (Figure 4.4). The site that is relevant to hatching is the ascending colon where an infection establishes. In chapter four hatching of *T. trichiura* was observed with both ascending and descending colon samples, however the level of hatching was greater with ascending colon samples (Figure 4.4). To observe the difference between these samples that demonstrated a clear impact on *T. trichiura* hatching, I performed a pairwise comparison between ascending and descending colon biopsies. There were some associations but with q -values between 0.25 and 0.05 they did not meet my threshold for significance. The beta diversity plot indicated that the ascending and descending colon samples did not form distinct clusters (Figure 5.7) so it was unsurprising that isolating differences was a challenge; the difference in abundance of the species relevant to hatching is likely very slight. Indeed, other studies have shown that there is little variation along the colonic segments, and the biggest difference exists between the caecum and rectum (Jiao et al. 2021).

Given the challenges in identifying significant differences in composition by comparing gastrointestinal tract biopsy sites I compared the biopsies that were able to induce hatching with those that were not. I identified three phyla that were significantly more abundant in samples capable of inducing hatching; these were Desulfobacterota A, Firmicutes B, and Verrucomicrobiota (Table 5.3). Desulfobacterota is a relatively new phylum redefined out of the Deltaproteobacteria that primarily comprises sulfate reducing bacteria found in the environment and gastrointestinal microbiota (Murphy et al. 2021; Jiao et al. 2021). Firmicutes are the most abundant in the gastrointestinal tract, and are largely health associated (Marchesi et al. 2016). The Verrucomicrobiota phylum comprises primarily environmental species, as well as several gastrointestinal bacteria, including *Akkermansia muciniphila*, a mucin degrading bacteria and well known component of the intestinal mucosa (Wagner and Horn 2006; Derrien et al. 2008; Karlsson et al. 2012; Johansson and Larsson 2011).

Looking below the phyla level I identified which species are contributing to *T. trichiura* hatching by comparing biopsies that can and can't induce hatching and looking for differently abundant species. I found 144 species with a significant change in relative abundance; 98 of these were more abundant in samples capable of inducing hatching (Table 5.3). The strongest association was found with *Bilophila wadsworthia*, a gram negative, sulfite reducing, anaerobe. *B. wadsworthia* has been found in low abundance the microbiota of healthy people and in increased abundance in people with conditions pertaining to gastrointestinal inflammation, like appendicitis (Baron et al. 1989; Feng et al. 2017; McOrist et al. 2001). The next association is *ER4 sp900317525* an uncultured member of the *Oscillospiraceae* family. Completing the top three associations is *Faecalibacterium prausnitzii*, and several strains of this species are reported throughout the list of significant results (Table 5.3). *F. prausnitzii* is a gram positive, extremely oxygen sensitive (EOS) species and a well-known member of the microbiota. It is found ubiquitously in healthy individuals and changes in its abundance are a good biomarker for dysbiosis (Miquel et al. 2013; Fitzgerald et al. 2018; Lopez-Siles et al. 2017; Leylabadlo et al. 2020; Sun and Dudeja 2018; Zhang et al. 2021).

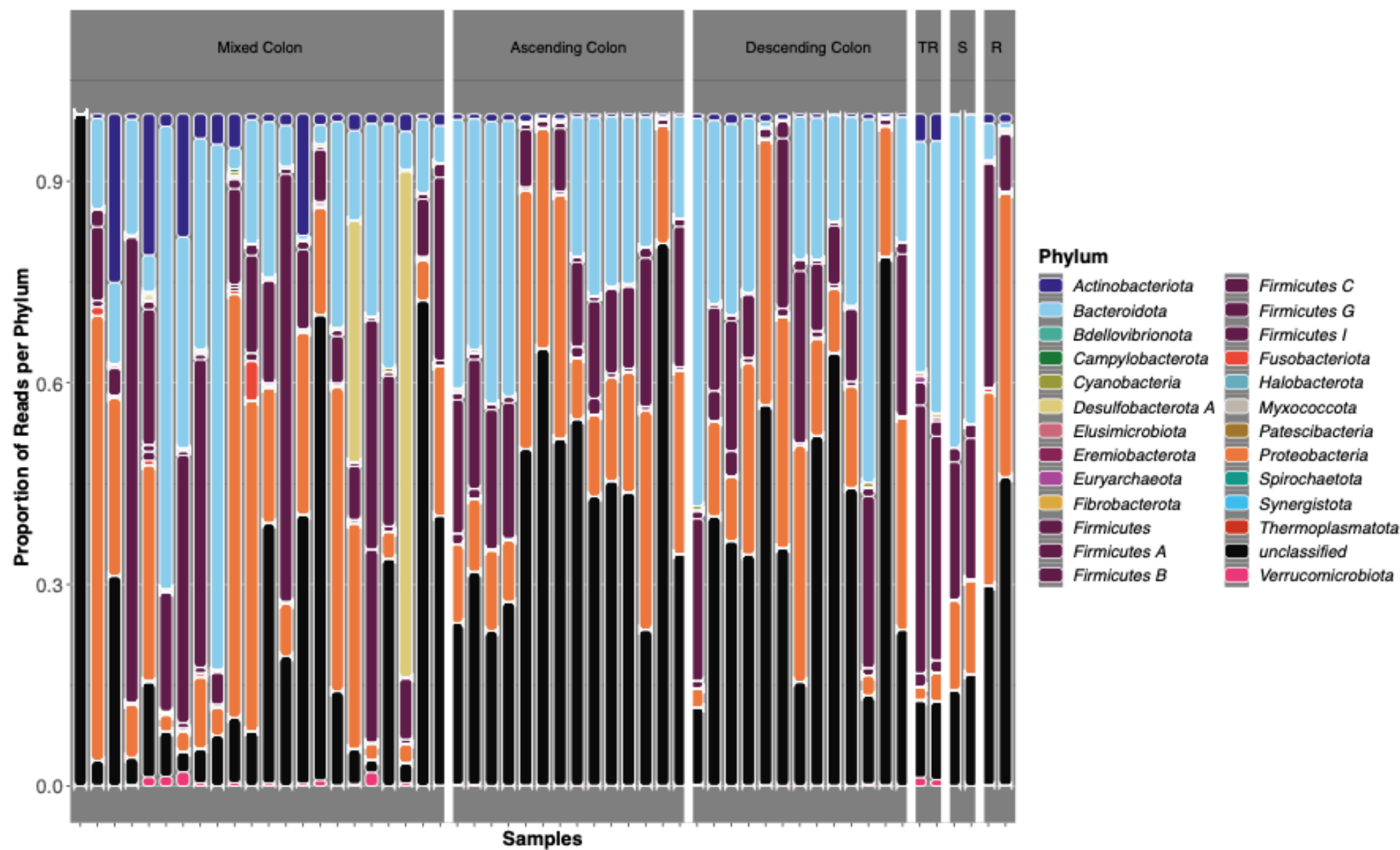


Figure 5.8 The relative abundances of bacterial phyla in human gastrointestinal tract biopsies. Human biopsy samples were primarily composed of the 4 phyla most commonly reported in the gut: Firmicutes, Proteobacteria, Bacteroides, and Actinobacteria.

Tr- Transverse, S- Stool, R- Rectum

Table 5.2 Differentially abundant phyla in human biopsies isolated from the length of the lower gastrointestinal tract. (positive effect/negative effect)

Phylum	Location	coef	stderr	pval	qval
Euryarchaeota	Colon Transverse	1.83	0.24	7.80E-09	7.80E-07
Verrucomicrobiota	Colon Transverse	1.54	0.22	5.53E-08	2.76E-06
Actinobacteriota	Colon Transverse	0.82	0.14	7.50E-07	2.50E-05
Synergistota	Colon Transverse	1.07	0.19	2.24E-06	5.60E-05
Desulfobacterota A	Colon Transverse	1.61	0.31	1.04E-05	2.07E-04
Actinobacteriota	Rectum	-0.64	0.14	4.70E-05	7.84E-04
Proteobacteria	Colon Transverse	-0.91	0.20	5.75E-05	8.22E-04
unclassified	Colon Transverse	-0.60	0.15	4.63E-04	0.01
Desulfobacterota A	Stool	1.03	0.31	2.23E-03	0.02
unclassified	Rectum	-0.47	0.15	4.25E-03	0.03
Fusobacteriota	Stool	0.82	0.27	4.51E-03	0.03
Firmicutes B	Colon Descending	0.28	0.10	0.01	0.05

Table 5.3 Differentially abundant phyla and species in human biopsies capable of inducing *T. trichiura* hatching. (positive effect/negative effect)

Phylum	<i>T. trichiura</i> Hatching	coef	stderr	pval	qval
Desulfobacterota A	Yes	0.62	0.16	3.33E-04	4.17E-03
Verrucomicrobiota	Yes	0.39	0.11	1.52E-03	0.02
Firmicutes B	Yes	0.31	0.10	4.62E-03	0.03
Species	<i>T. trichiura</i> Hatching	coef	stderr	pval	qval
<i>Bilophila wadsworthia</i>	Yes	0.987	0.151	1.80E-07	9.90E-06
<i>ER4 sp900317525</i>	Yes	0.408	0.075	4.38E-06	1.94E-04
<i>Faecalibacterium prausnitzii D</i>	Yes	0.838	0.162	1.02E-05	4.17E-04
<i>Faecalibacterium prausnitzii H</i>	Yes	1.074	0.216	1.83E-05	0.001
<i>Faecalibacterium prausnitzii I</i>	Yes	1.104	0.224	2.08E-05	0.001
<i>Prevotella stercorea</i>	Yes	0.694	0.141	2.12E-05	0.001
<i>Faecalibacterium prausnitzii G</i>	Yes	1.085	0.237	5.90E-05	0.002
<i>MGYG HGUT 03166</i>	Yes	0.783	0.171	6.16E-05	0.002
<i>MGYG HGUT 00512</i>	Yes	0.617	0.138	8.40E-05	0.003
<i>MGYG HGUT 02712</i>	Yes	0.331	0.075	9.78E-05	0.003
<i>MGYG HGUT 00414</i>	Yes	0.290	0.066	1.11E-04	0.004
<i>MGYG HGUT 01157</i>	Yes	0.297	0.068	1.13E-04	0.004
<i>MGYG HGUT 01927</i>	Yes	0.369	0.085	1.20E-04	0.004
<i>Zag111 sp002102825</i>	Yes	0.658	0.153	1.30E-04	0.004
<i>MGYG HGUT 03335</i>	Yes	0.490	0.114	1.33E-04	0.004

<i>Prevotella copri</i>	Yes	1.148	0.267	1.35E-04	0.004
MGYG HGUT 01178	Yes	0.516	0.120	1.39E-04	0.004
<i>Bacteroides A sp00066455</i>	Yes	0.560	0.131	1.48E-04	0.004
<i>Prevotella sp002265625</i>	Yes	1.177	0.276	1.52E-04	0.004
ER4 sp000765235	Yes	0.384	0.091	1.68E-04	0.005
MGYG HGUT 01627	Yes	0.529	0.125	1.70E-04	0.005
MGYG HGUT 04456	Yes	0.656	0.156	1.85E-04	0.005
MGYG HGUT 03675	Yes	0.398	0.095	1.97E-04	0.006
<i>Prevotella lascolaii</i>	Yes	0.565	0.138	2.40E-04	0.007
<i>Prevotella timonensis</i>	Yes	0.221	0.054	2.51E-04	0.007
<i>Bacillus A sp001884105</i>	Yes	0.205	0.050	2.56E-04	0.007
MGYG HGUT 03480	Yes	0.406	0.100	2.63E-04	0.007
MGYG HGUT 00701	Yes	0.312	0.077	2.63E-04	0.007
MGYG HGUT 00534	Yes	0.410	0.101	2.66E-04	0.007
MGYG HGUT 02960	Yes	0.556	0.137	2.81E-04	0.007
<i>Prevotella copri A</i>	Yes	0.630	0.156	2.86E-04	0.007
<i>Prevotella sp000436035</i>	Yes	0.370	0.091	2.85E-04	0.007
<i>Gordonibacter pamelaee</i>	Yes	0.327	0.082	3.28E-04	0.008
<i>Butyrivibrio virosa</i>	Yes	0.238	0.060	3.41E-04	0.009
<i>Odoribacter laneus</i>	Yes	0.218	0.055	3.43E-04	0.009
MGYG HGUT 02704	Yes	0.426	0.107	3.52E-04	0.009
<i>Prevotella sp002299635</i>	Yes	0.274	0.069	3.73E-04	0.009
MGYG HGUT 00090	Yes	0.656	0.167	3.95E-04	0.010
<i>Prevotella sp000436915</i>	Yes	0.297	0.076	3.99E-04	0.010
MGYG HGUT 02603	Yes	0.641	0.164	4.08E-04	0.010
MGYG HGUT 00553	Yes	0.324	0.083	4.34E-04	0.011
MGYG HGUT 03903	Yes	0.367	0.094	4.46E-04	0.011
<i>Prevotella sp000434515</i>	Yes	0.850	0.219	4.61E-04	0.011
MGYG HGUT 02080	Yes	0.426	0.110	4.64E-04	0.011
MGYG HGUT 00589	Yes	0.372	0.096	4.76E-04	0.012
MGYG HGUT 01921	Yes	0.212	0.055	4.81E-04	0.012
<i>Acetatifactor sp003447295</i>	Yes	0.715	0.186	0.001	0.012
MGYG HGUT 01056	Yes	0.598	0.156	0.001	0.012
MGYG HGUT 04571	Yes	0.268	0.070	0.001	0.012
MGYG HGUT 00574	Yes	0.320	0.084	0.001	0.013
<i>Akkermansia muciniphila</i>	Yes	0.519	0.136	0.001	0.013
MGYG HGUT 03291	Yes	0.462	0.122	0.001	0.013
MGYG HGUT 03665	Yes	0.204	0.054	0.001	0.013
CAG 170 sp000432135	Yes	0.243	0.064	0.001	0.013
MGYG HGUT 00500	Yes	0.182	0.048	0.001	0.013
MGYG HGUT 01882	Yes	0.173	0.046	0.001	0.014
<i>Erysipelatoclostridium saccharogumia</i>	Yes	0.559	0.149	0.001	0.014
MGYG HGUT 00644	Yes	0.661	0.176	0.001	0.014
MGYG HGUT 01975	Yes	0.265	0.070	0.001	0.014
CAG 279 sp000437795	Yes	0.579	0.154	0.001	0.014
<i>Prevotella sp003447235</i>	Yes	0.227	0.061	0.001	0.014
MGYG HGUT 04262	Yes	0.147	0.039	0.001	0.015
MGYG HGUT 01051	Yes	0.384	0.103	0.001	0.015
MGYG HGUT 02834	Yes	0.436	0.117	0.001	0.016
MGYG HGUT 01225	Yes	0.256	0.069	0.001	0.016
<i>Bacteroides A plebeius A</i>	Yes	1.220	0.330	0.001	0.016

<i>Faecalibacterium prausnitzii E</i>	Yes	0.730	0.198	0.001	0.017
<i>Prevotella sp900313215</i>	Yes	0.497	0.135	0.001	0.017
<i>Prevotella disiens</i>	Yes	0.137	0.037	0.001	0.017
MGYG HGUT 01171	Yes	0.236	0.064	0.001	0.017
<i>Ruminococcus E bromii</i>	Yes	0.137	0.038	0.001	0.018
MGYG HGUT 01024	Yes	0.209	0.057	0.001	0.019
<i>Eubacterium R sp000436835</i>	Yes	0.440	0.122	0.001	0.019
MGYG HGUT 04336	Yes	0.567	0.157	0.001	0.020
MGYG HGUT 03899	Yes	0.656	0.182	0.001	0.020
<i>Barnesiella intestinihominis</i>	Yes	0.663	0.186	0.001	0.021
MGYG HGUT 03163	Yes	0.441	0.124	0.001	0.022
CAG 56 sp900066615	Yes	0.808	0.227	0.001	0.022
MGYG HGUT 00707	Yes	0.273	0.077	0.001	0.022
MGYG HGUT 03543	Yes	0.444	0.125	0.001	0.022
<i>Prevotellamassilia timonensis</i>	Yes	0.403	0.114	0.001	0.022
MGYG HGUT 00983	Yes	0.301	0.086	0.001	0.024
MGYG HGUT 02075	Yes	0.360	0.105	0.002	0.029
MGYG HGUT 00834	Yes	0.148	0.043	0.002	0.030
<i>Ruminococcus C sp000433635</i>	Yes	0.145	0.043	0.002	0.030
MGYG HGUT 01783	Yes	0.314	0.092	0.002	0.030
MGYG HGUT 03460	Yes	0.137	0.040	0.002	0.031
<i>Sutterella wadsworthensis B</i>	Yes	1.012	0.302	0.002	0.034
MGYG HGUT 00559	Yes	0.234	0.070	0.002	0.034
CAG 103 sp000432375	Yes	0.203	0.061	0.002	0.037
<i>Akkermansia muciniphila A</i>	Yes	0.253	0.077	0.002	0.038
<i>Prevotella sp000431975</i>	Yes	0.204	0.062	0.002	0.040
RC9 sp000432515	Yes	0.106	0.032	0.002	0.041
<i>Paraprevotella clara</i>	Yes	0.554	0.170	0.003	0.041
<i>Prevotella sp002299275</i>	Yes	0.144	0.044	0.003	0.042
<i>Coproccoccus sp000154245</i>	Yes	0.240	0.074	0.003	0.045
MGYG HGUT 01964	Yes	0.159	0.050	0.003	0.047
MGYG HGUT 03921	Yes	0.460	0.145	0.003	0.049

5.4 A differential analysis of relative taxonomic abundances in porcine gastrointestinal tract samples identifying hatching determinants in porcine caecal scrapings

In the porcine samples to identify taxonomic groups relevant to hatching I looked for associations between caecal scrapings and caecal contents (Figure 4.3), classifying the samples using Kraken 2 and the UHGG before and after MAG assembly. Interestingly, despite using a database curated for human metagenomic studies, using this approach to classify porcine samples was effective and the median percentage of reads unclassified in crude samples was 32.5% (Figure 5.9). The crude caecal scrapings and caecal contents were also cultured as metascrapes. The classification of the metascrapes was much higher and the median percentage of unclassified reads was 7.76% (Figure 5.9). This highlights the relative ease of classifying culturable members of the microbiome. Classification of the crude and cultured samples improved after MAG assembly. For the porcine crude samples the new median percentage of reads unclassified was 15.8%, and in cultured samples it was 4.0% (Figure 5.9). While using Kraken 2 and the UHGG worked well, it would be interesting to see how these results change in light of recent large-scale porcine gastrointestinal tract microbiome curation efforts (C. Chen et al. 2021). Beta diversity analysis in porcine samples revealed that they were grouped into two distinct clusters, one containing crude samples and another one, those cultured by metascrape (Figure 5.10). Samples cultured aerobically were more uniform in composition, forming a distinct cluster, and those cultured anaerobically were more diverse (Figure 5.10)

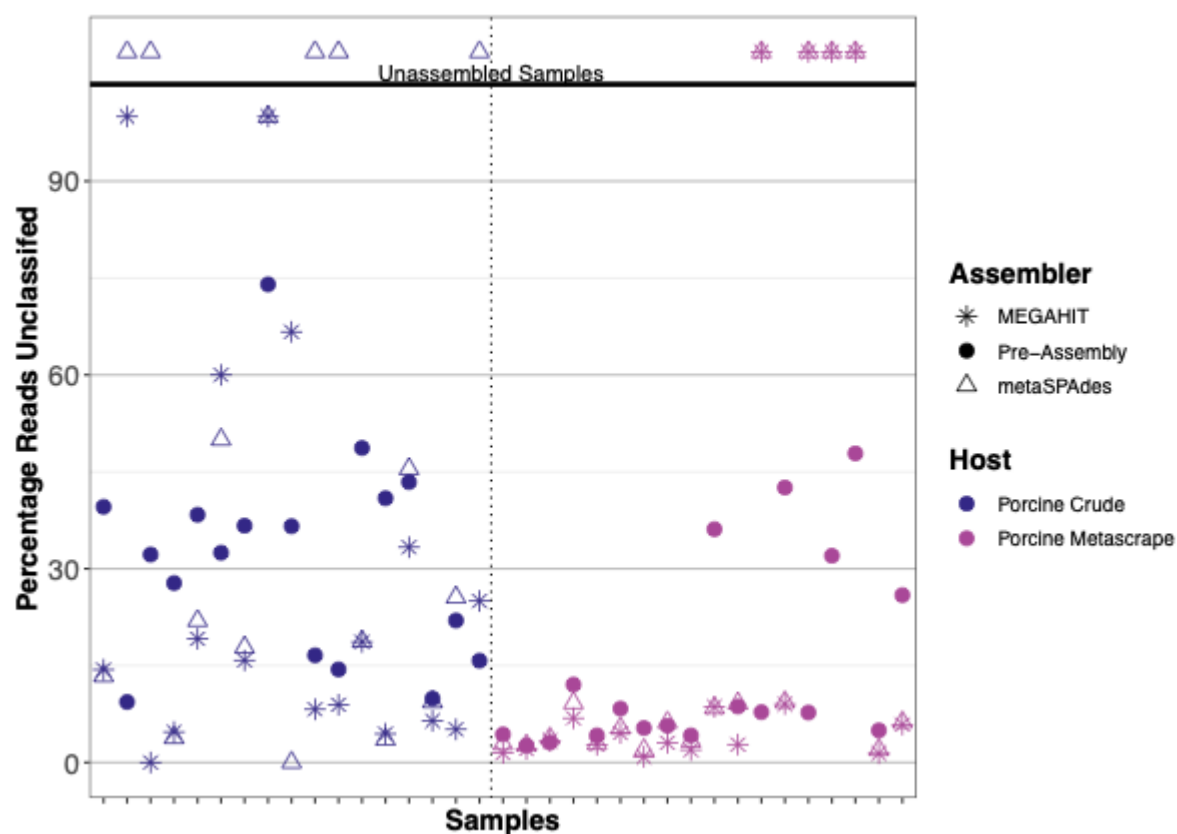


Figure 5.9 Genome assembly using MEGAHIT improves classification of crude and cultured gastrointestinal tract samples from porcine caeca Metagenomic assembled genomes (MAGs) were created using the metawrap pipeline and the assembly tools MEGAHIT and metaSPAdes. MEGAHIT out-performed metaSPAdes, successfully assembling MAGs from more samples. Samples were classified with Kraken 2 before and after assembly and the level of classification increased after assembly for both crude and cultured.

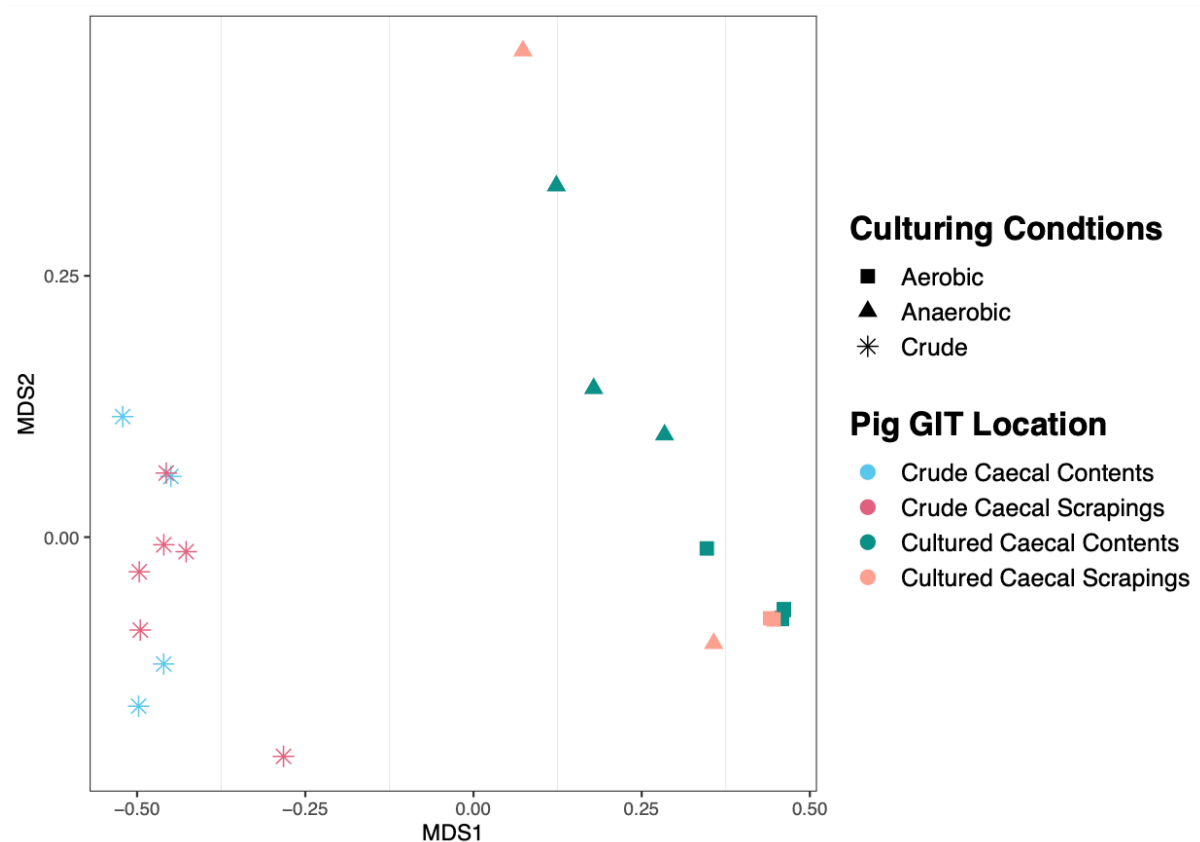


Figure 5.10 Beta diversity of gastrointestinal tract samples from pigs reveals that culturing is the greatest source of variation. Using a Bray–Curtis distance matrix generated from the relative taxa abundances reported by Kraken 2, a Principal Coordinates Analysis (PCoA) reveals distinct clusters of crude samples and cultured metascrapes; additionally, aerobic samples appear more uniform.

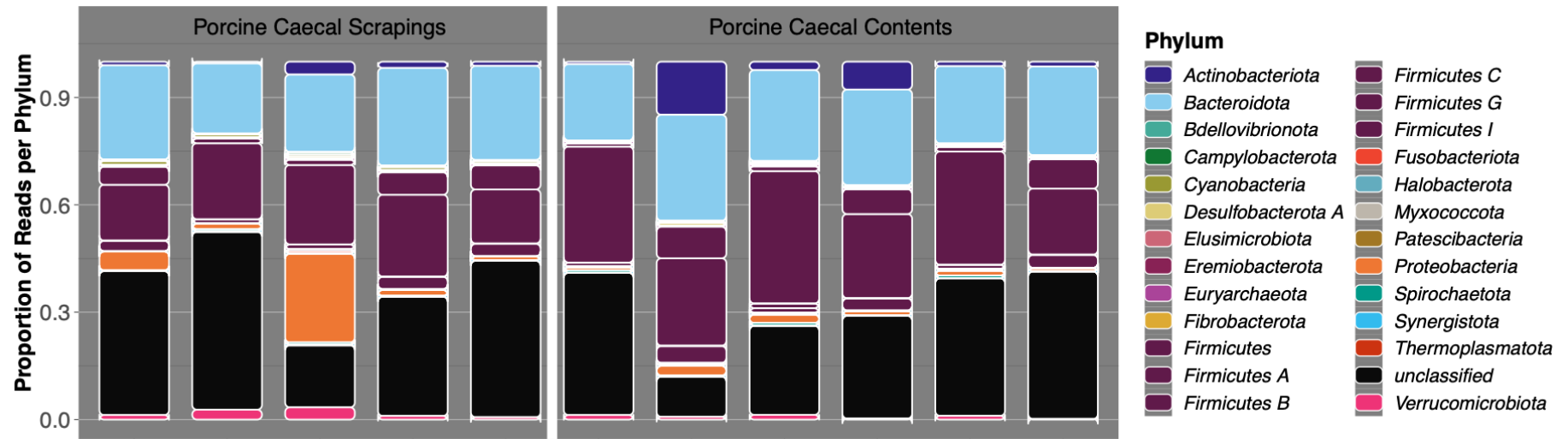
In the porcine gastrointestinal samples once again, the bacteria reported were primarily Firmicutes, Proteobacteria, Bacteroides, and Actinobacteria (Figure 5.11). Using MaAsLin 2, I looked for statistically significant differences ($q_{val} < 0.05$) in the distribution of phyla by: comparing caecal scrapings to contents to identify phyla and species enriched in the site of infection. Comparing cultured metascrapes to crude samples to identify phyla enriched in *in vitro* cultures. As well as comparing aerobic to anaerobic culturing conditions to examine the aerotolerance of phyla.

My analysis comparing caecal contents and caecal scrapings revealed that two phyla were more abundant in caecal scrapings: Cyanobacteria and Campylobacterota. Cyanobacteria have been previously identified in the gastrointestinal tract of pigs and humans and many are likely the product of ingesting groundwater. However, there are some non-photosynthetic Cyanobacteria and their function in the gastrointestinal tract is as yet uncharacterised (Crespo-Piazuelo et al. 2018; Kubickova et al. 2019; Soo 2015). The porcine gastrointestinal tract is a well known reservoir of Campylobacterota, gram negative bacteria that cause diarrheal disease in humans but no clinical disease in pigs (Kempf et al. 2017; Quintana-Hayashi and Thakur 2012; de Vries et al. 2017). The increased abundance of this phyla of gram-negative bacteria in the caecal scrapings suggests they are implicated in hatching. A change in the abundance of 15 phyla was observed when comparing the crude and cultured samples (Table 5.5). Overall, culturing resulted in a decreased abundance of the majority of these phyla except for Proteobacteria, highlighting the challenge that remains in capturing gastrointestinal tract commensal bacteria in the lab through culturing. When comparing aerobic and anaerobic culturing (Table 5.6) the only significant results demonstrated that culturing in anaerobic conditions increased the abundance of Firmicutes B & C, and Desulfobacterota A, confirming the visual increase in the abundance of Firmicutes shown in figure 5.11. It will be interesting to see what role the members of these phyla play in hatching as anaerobic conditions do not increase hatching in *T. suis* (Vejzagić, Thamsborg, et al. 2015), and result in decreased hatching in *T. muris* and in *T. trichiura* (Figure 4.2, 4.5).

At the species level, when comparing caecal contents and caecal scrapings I found 41 species with a significant change in abundance; 32 of these were more highly abundant in caecal scrapings (Table 5.4). The top association found was *Sutterella parvirubra*; *S. parvirubra* is one of three *Sutterella* species found ubiquitously in the human and porcine gut flora (Sakon et al. 2008; Guevarra et al. 2019; Hiippala et al. 2016). The top ten associations are dominated by uncultured and thereby uncharacterised strains. Four of these species are cyanobacteria and belong to the family *Gastranaerophilaceae*, while relatively understudied these bacteria represent non photosynthetic cyanobacteria and have been identified in the

microbiota are beginning to be implicated in dysbiosis (Soo 2015; Bowerman et al. 2020). Two belong to the class Kiritimatiellae, one the class Lentisphaeria, and one the family *Elusimicrobiaceae* (Spring et al. 2016; Cho, Derrien, and Hedlund 2015; Brune 2014). *Campylobacter hyointestinalis* is also high on the list of associations. It resides in the porcine caecal mucus and as discussed previously, like other members of its phylum, it is a zoonotic pathogen transferred from pigs to humans (Wilkinson et al. 2018).

a



b

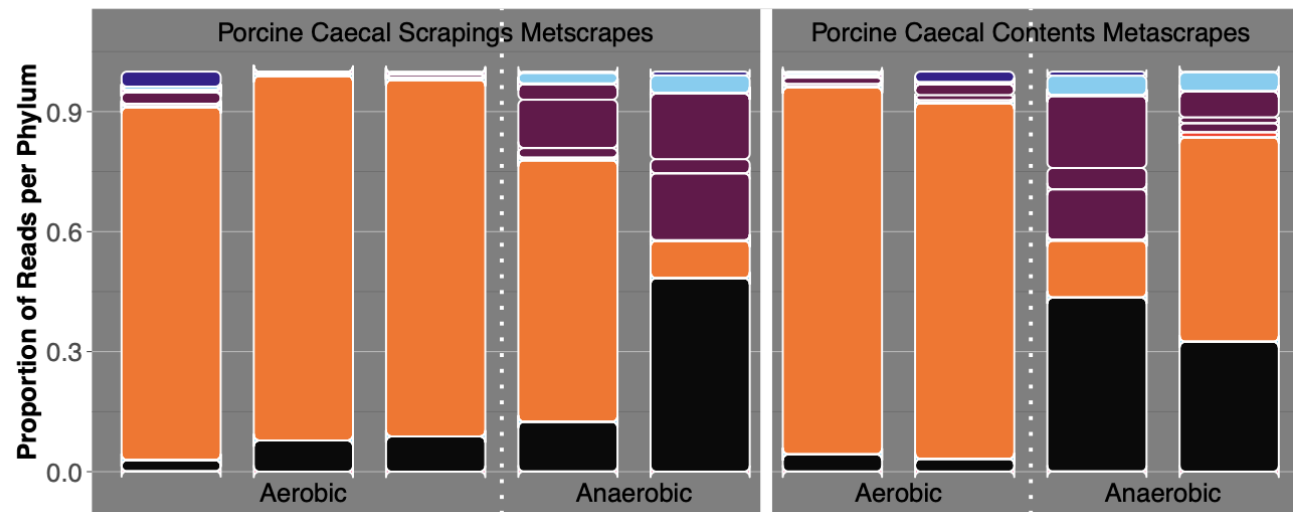


Figure 5.11 The relative abundance of bacterial phyla in porcine crude and cultured caecal samples. Porcine samples were primarily composed of the four phyla most commonly reported in the gut: Firmicutes, Proteobacteria, Bacteroides, and Actinobacteria. In the crude samples, caecal scrapings visually appear to have more Verrucomicrobiota. In the cultured samples, anaerobic metascrapes visually appear to have more Firmicutes.

Table 5.4 Differentially abundant phyla and species in porcine scrapings and contents isolated from the caecum. (*positive effect/negative effect*)

Phylum	Location	coef	stderr	pval	qval
Cyanobacteria	caecal Scrapings	0.53	0.10	2.59E-04	3.11E-03
Campylobacterota	caecal Scrapings	0.32	0.09	0.01	0.03
Species	Location	coef	stderr	pval	qval
<i>Sutterella parvirubra</i>	caecal Scrapings	0.37	0.02	6.05E-09	1.05E-06
MGYG HGUT 03483	caecal Scrapings	0.64	0.08	5.02E-06	1.45E-04
MGYG HGUT 00629	caecal Scrapings	0.72	0.09	9.76E-06	2.59E-04
MGYG HGUT 02803	caecal Scrapings	0.80	0.11	2.00E-05	4.75E-04
MGYG HGUT 03528	caecal Scrapings	0.97	0.14	2.78E-05	6.19E-04
MGYG HGUT 00618	caecal Scrapings	0.76	0.11	3.48E-05	7.51E-04
MGYG HGUT 02219	caecal Scrapings	0.74	0.12	5.80E-05	1.14E-03
MGYG HGUT 04492	caecal Scrapings	0.31	0.06	3.17E-04	4.42E-03
<i>Campylobacter hyointestinalis</i>	caecal Scrapings	0.57	0.12	4.20E-04	0.01
MGYG HGUT 02235	caecal Scrapings	0.57	0.12	4.32E-04	0.01
MGYG HGUT 00507	caecal Scrapings	0.85	0.18	5.39E-04	0.01
MGYG HGUT 03617	caecal Scrapings	0.42	0.09	5.77E-04	0.01
CAG 306 sp000980375	caecal Scrapings	0.30	0.07	8.76E-04	0.01
CAG 484 sp000431315	caecal Scrapings	0.30	0.07	8.76E-04	0.01
Zag111 sp002102825	caecal Scrapings	0.30	0.07	8.76E-04	0.01
MGYG HGUT 02077	caecal Scrapings	0.30	0.07	8.76E-04	0.01
MGYG HGUT 04187	caecal Scrapings	0.30	0.07	8.76E-04	0.01
<i>Campylobacter B hominis</i>	caecal Scrapings	0.30	0.07	1.04E-03	0.01
CAG 196 sp002102975	caecal Scrapings	0.42	0.10	1.80E-03	0.02
<i>Escherichia sp000208585</i>	caecal Scrapings	0.58	0.14	2.14E-03	0.02
<i>Escherichia coli D</i>	caecal Scrapings	0.63	0.16	2.37E-03	0.02
MGYG HGUT 00755	caecal Scrapings	0.68	0.18	3.02E-03	0.02
MGYG HGUT 03506	caecal Scrapings	0.50	0.13	3.07E-03	0.02
MGYG HGUT 04053	caecal Scrapings	0.35	0.10	3.84E-03	0.03
<i>Methanomethylophilus alvus</i>	caecal Scrapings	0.45	0.13	0.01	0.03
<i>Escherichia fergusonii</i>	caecal Scrapings	0.51	0.15	0.01	0.03
<i>Campylobacter lanienae</i>	caecal Scrapings	0.60	0.18	0.01	0.04
UBA2883 sp002103075	caecal Scrapings	0.76	0.23	0.01	0.04
MGYG HGUT 03294	caecal Scrapings	0.31	0.09	0.01	0.04
<i>Prevotella copri</i>	caecal Scrapings	0.37	0.11	0.01	0.04
MGYG HGUT 00542	caecal Scrapings	0.54	0.17	0.01	0.04
MGYG HGUT 04456	caecal Scrapings	0.24	0.08	0.01	0.05

Table 5.5 Differentially abundant phyla in crude porcine scrapings and contents and cultured metascrapes isolated from the caecum. (positive effect/negative effect)

Phylum	Location	coef	stderr	pval	qval
<i>Proteobacteria</i>	caecal Contents Metascape	1.57	0.22	1.26E-07	2.41E-05
<i>Proteobacteria</i>	caecal Scrapings Metascape	1.59	0.24	4.82E-07	2.53E-05
<i>Elusimicrobiota</i>	caecal Contents Metascape	-0.74	0.11	2.95E-07	2.53E-05
<i>Fibrobacterota</i>	caecal Contents Metascape	-0.83	0.13	1.24E-06	4.76E-05
<i>Cyanobacteria</i>	caecal Contents Metascape	-0.85	0.14	1.58E-06	5.07E-05
<i>Elusimicrobiota</i>	caecal Scrapings Metascape	-0.71	0.12	2.08E-06	5.72E-05
<i>Cyanobacteria</i>	caecal Scrapings Metascape	-0.91	0.15	2.48E-06	5.96E-05
<i>Fibrobacterota</i>	caecal Scrapings Metascape	-0.83	0.14	4.97E-06	7.95E-05
<i>Firmicutes B</i>	caecal Scrapings Metascape	-0.99	0.17	5.66E-06	8.24E-05
<i>Verrucomicrobiota</i>	caecal Scrapings Metascape	-1.52	0.27	6.86E-06	8.79E-05
<i>Firmicutes B</i>	caecal Contents Metascape	-0.88	0.16	7.74E-06	9.29E-05
<i>Spirochaetota</i>	caecal Scrapings Metascape	-1.31	0.24	8.52E-06	9.62E-05
<i>Bacteroidota</i>	caecal Scrapings Metascape	-1.58	0.30	2.23E-05	1.82E-04
<i>Verrucomicrobiota</i>	caecal Contents Metascape	-1.26	0.25	2.55E-05	1.82E-04
<i>Spirochaetota</i>	caecal Contents Metascape	-1.11	0.22	2.54E-05	1.82E-04
<i>Firmicutes A</i>	caecal Scrapings Metascape	-1.11	0.22	3.20E-05	2.05E-04
<i>Firmicutes A</i>	caecal Contents Metascape	-1.00	0.20	3.80E-05	2.28E-04
<i>Campylobacterota</i>	caecal Scrapings Metascape	-1.02	0.20	3.77E-05	2.28E-04
<i>Bacteroidota</i>	caecal Contents Metascape	-1.21	0.28	1.96E-04	8.97E-04
<i>Campylobacterota</i>	caecal Contents Metascape	-0.77	0.19	3.58E-04	1.53E-03
<i>Patescibacteria</i>	caecal Contents Metascape	-0.95	0.24	4.52E-04	1.89E-03
<i>Patescibacteria</i>	caecal Scrapings Metascape	-0.97	0.26	9.39E-04	3.76E-03
<i>Desulfobacterota A</i>	caecal Scrapings Metascape	-1.21	0.35	2.05E-03	0.01
<i>Synergistota</i>	caecal Contents Metascape	-0.57	0.17	3.03E-03	0.01
<i>Myxococcota</i>	caecal Contents Metascape	-0.24	0.08	0.01	0.02
<i>Thermoplasmatota</i>	Crude caecal Scrapings	0.44	0.15	0.01	0.02
<i>Cyanobacteria</i>	Crude caecal Scrapings	0.42	0.14	0.01	0.02
<i>Desulfobacterota A</i>	caecal Contents Metascape	-0.90	0.32	0.01	0.03
<i>Myxococcota</i>	caecal Scrapings Metascape	-0.24	0.09	0.01	0.03
<i>Synergistota</i>	caecal Scrapings Metascape	-0.51	0.19	0.01	0.04

Table 5.6 Differentially abundant phyla in aerobically and anaerobically cultured metascrapes isolated from the porcine caecum. (positive effect/negative effect)

Phylum	Location	coef	stderr	pval	qval
<i>Firmicutes B</i>	Anaerobic caecal Contents	0.60	0.08	5.04E-06	5.30E-04
<i>Firmicutes C</i>	Anaerobic caecal Contents	1.26	0.19	2.99E-05	1.57E-03
<i>Desulfobacterota A</i>	Anaerobic caecal Contents	0.97	0.21	6.75E-04	0.02
<i>Firmicutes C</i>	Anaerobic caecal Scrapings	1.00	0.22	7.37E-04	0.02
<i>Firmicutes B</i>	Anaerobic caecal Scrapings	0.39	0.09	0.00	0.02

5.5 A differential analysis of relative taxonomic abundances in naive humanised microbiota mice

In the naive humanised microbiota mice taxonomic groups relevant to hatching were identified through associations between caecal scrapings and caecal contents within each strain, and observing differences between the murine and humanised microbiota strains. Samples were classified using Kraken 2 and the UHGG before and after MAG assembly. Performing this method of classification on caecal scrapings and contents from naive and infected humanised microbiota mice resulted in average classification of the samples. The median percentages of unclassified reads were 40.0% in caecal scrapings and 50.3% in caecal contents (Figure 5.12). Kraken 2 and the UHGG did however classify the majority of species in the humanised microbiota mice metascrapes (median percentage of reads unclassified = 8.84%) (Figure 5.12). Kraken 2 utilised with the UHGG performed poorly on the naive murine microbiota mice samples (median percentage reads unclassified = 64.3%)(Figure 5.12) and these results highlight how different the murine microbiota is compared to the humanised microbiota. Once again culturing was able to improve this classification rate with the median percentage of unclassified reads in murine microbiota mice metascrapes sitting at 23.0% (Figure 5.12). In both the humanised microbiota mice, and murine microbiota mice assembly improved the rate of classification, and the new median percentages of reads unclassified in cultured naive samples were 34.1% and 38.8% respectively (Figure 5.12).

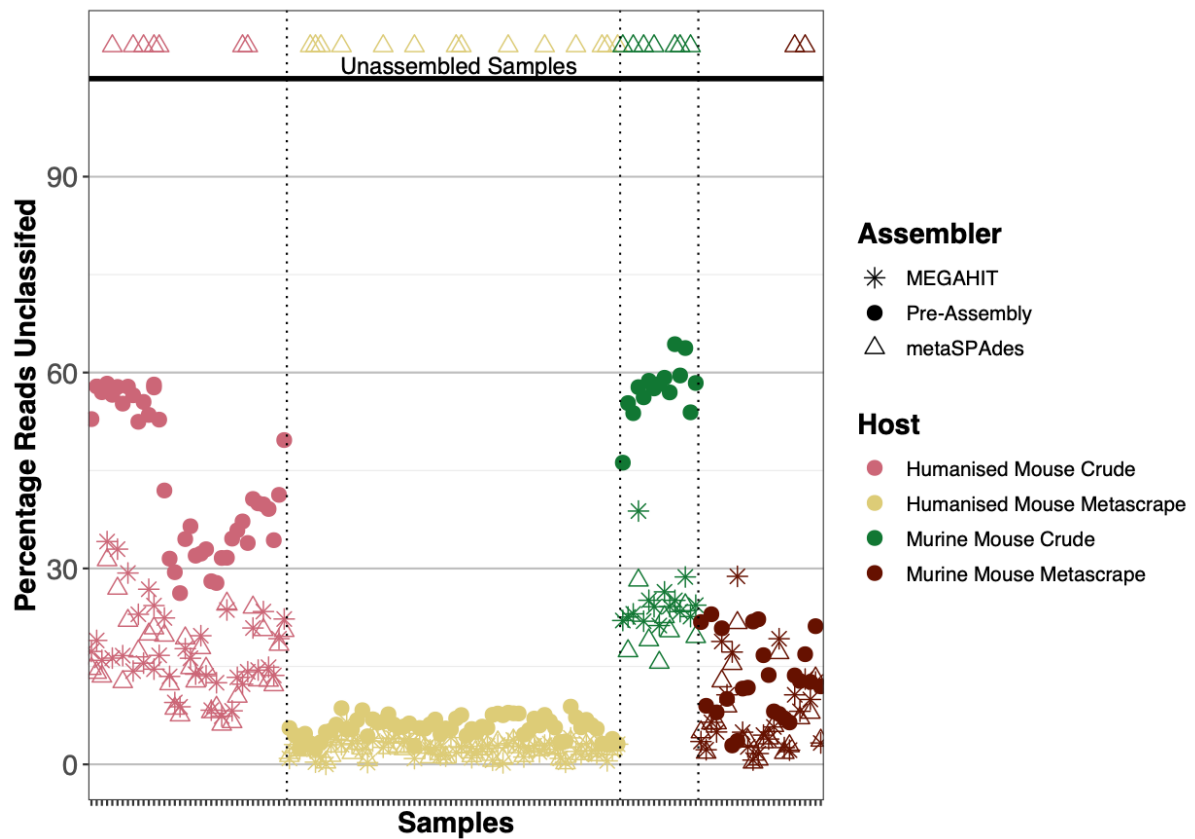


Figure 5.12 Genome assembly using MEGAHIT improves classification of crude and cultured gastrointestinal tract samples from naive humanised microbiota mice and murine microbiota caeca Metagenomic assembled genomes (MAGs) were created using the metaWRAP pipeline and the assembly tools MEGAHIT and metaSPAdes. MEGAHIT out-performed metaSPAdes successfully assembling MAGs from more samples. Samples were classified with Kraken 2 before and after assembly and the level of classification increased after assembly for both crude and cultured samples.

In chapter four there were very clear differences in the ability of the three mouse lines to induce parasite hatching *in vitro* (Figure 4.2, 4.5). Examining the crude caecal samples taken from each mouse strain for *in vitro* hatching revealed that the samples from the population of donor A mice displayed very uniform composition clustering together in the centre (Figure 5.13). The variation between donor B mice was greater; however, the samples capable of inducing hatching in *T. trichiura* cluster at the top of the graph (Figure 5.13). The murine microbiota mice form their own cluster at the bottom of the graph demonstrating the differences between hosts. All the samples in the plot from all three mouse strains were able to induce hatching of *T. muris*, highlighting the range of microbiota *T. muris* responds to (Figure 5.13).

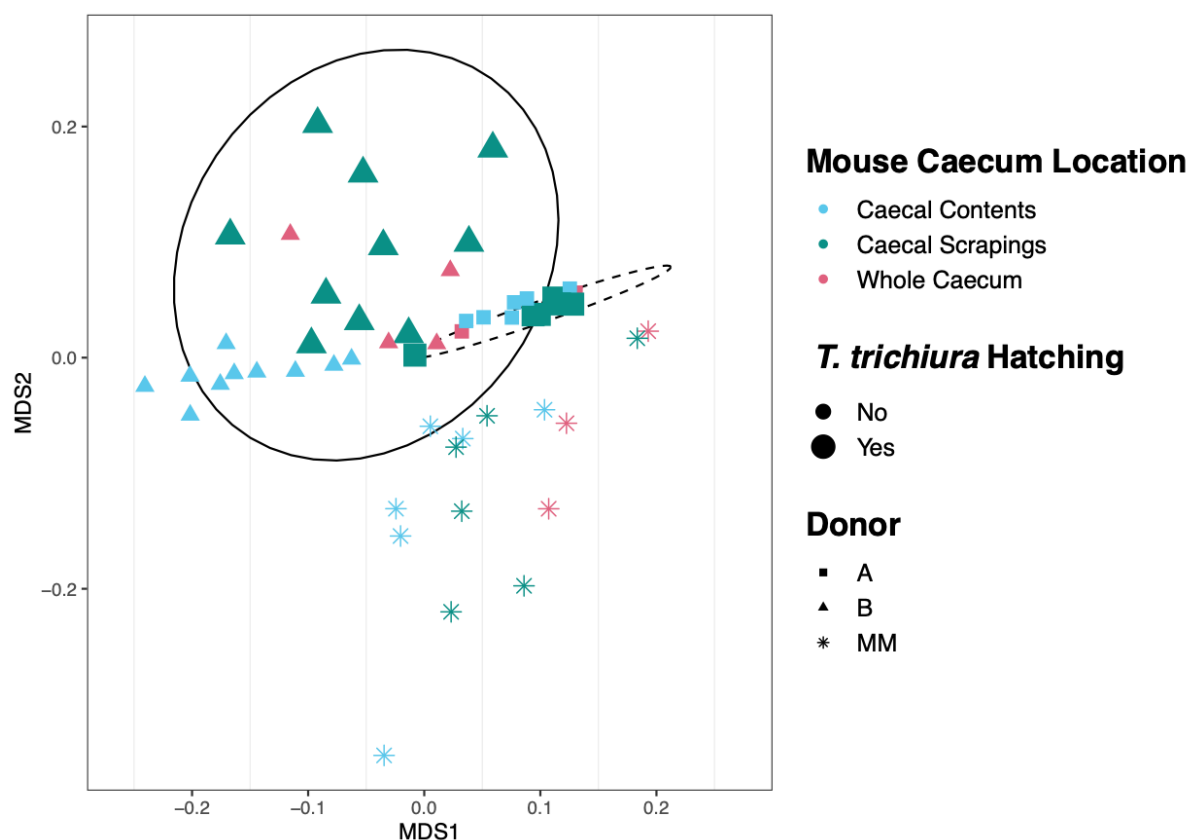


Figure 5.13 Beta diversity of gastrointestinal tract samples from naive murine microbiota and humanised microbiota mice reveals samples capable of inducing hatching of *T. trichiura* form a distinct cluster. Using a Bray–Curtis distance matrix generated from the relative taxa abundances reported by Kraken 2 a Principal Coordinates Analysis (PCoA) reveals distinct clusters of humanised microbiota and murine microbiota (MM) mice. Donor B samples capable of inducing hatching of *T. trichiura* form a cluster (solid line).

In addition to looking at the composition of the crude caecal scrapings and contents I cultured bacterial metascrapes of the caecal samples in aerobic and anaerobic conditions to identify bacteria capable of growing *in vitro* during the same time scale (24 h) as the *in vitro* hatching experiments (Figure 4.2, 4.5). Culturing resulted in a large amount of variation, of at least 50% dissimilarity (Figure 5.14), upon further inspection oxygen conditions provide the greatest source of variation with samples clustering into aerobic and anaerobic clusters, regardless of caecal site or even host microbiota (Figure 5.14).

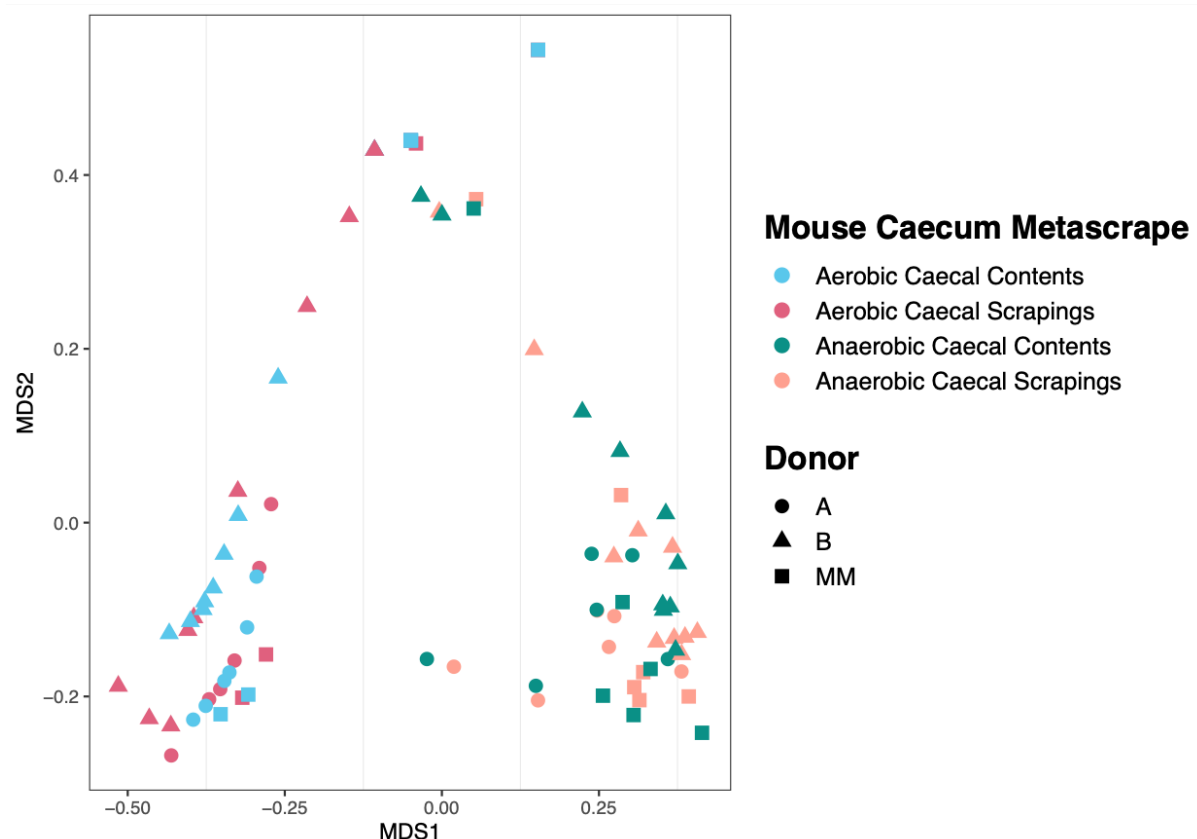


Figure 5.14 Beta diversity of cultured gastrointestinal tract metascrapes from naive murine microbiota and humanised microbiota mice reveals that oxygen culturing conditions are the greatest source of variation. Using a Bray–Curtis distance matrix generated from the relative taxa abundances reported by Kraken 2, a Principal Coordinates Analysis (PCoA) reveals distinct clusters of aerobic and anaerobic cultured metascrapes, indicating that the origin of the microbiota is not a primary source of variation.

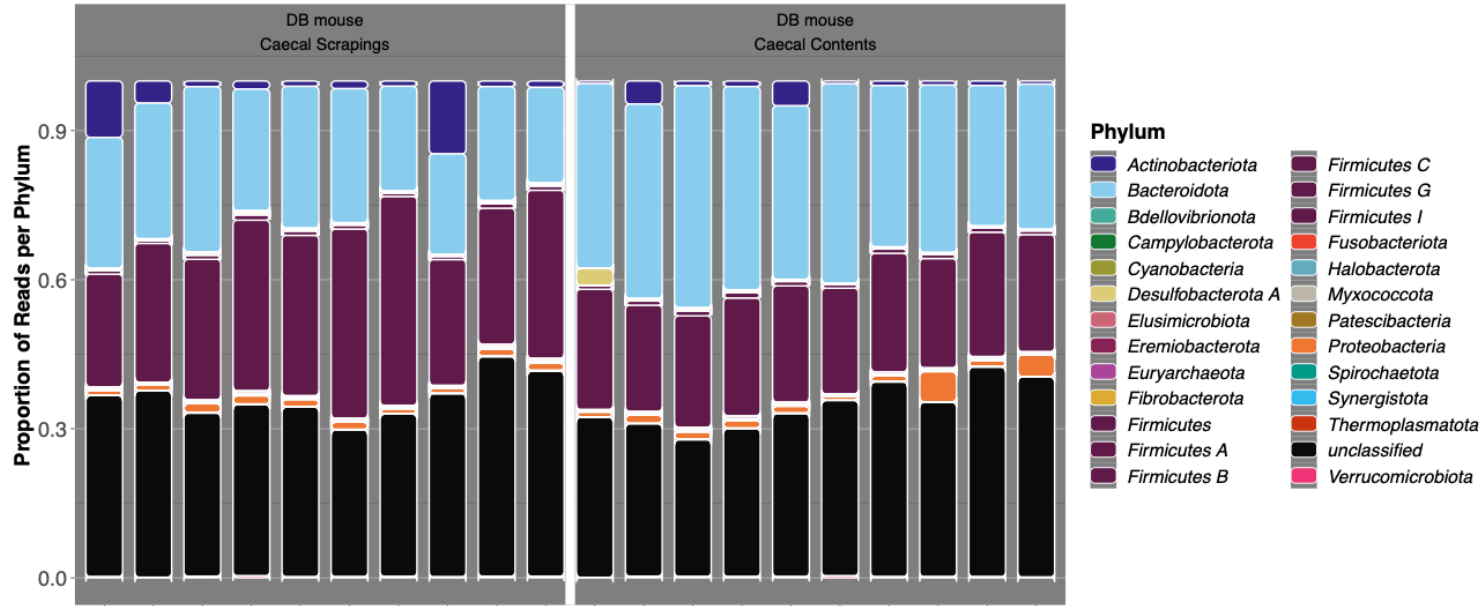
In the crude naive donor B humanised microbiota mice gastrointestinal samples there was a consistent proportion of reads unclassified ~30% (Figure 5.12), and once again the bacteria reported were primarily Firmicutes, Proteobacteria, Bacteroides, and Actinobacteria (Figure 5.15). Using MaAsLin 2 I looked for any statistically significant differences ($qval < 0.05$) in the distribution of phyla by: comparing caecal scrapings to contents to identify phyla and species enriched in the site of infection; comparing cultured metascrapes to crude samples to identify phyla enriched in *in vitro* cultures, as well as comparing aerobic to anaerobic culturing conditions to examine the aerotolerance of phyla.

My analysis comparing caecal scrapings and contents revealed that in caecal scrapings there were significant differences in the abundances of two phyla: Bacteroidetes, which was less abundant, and Firmicutes A, which was more abundant (Table 5.7). When comparing crude and cultured samples, 21 phyla were differentially present in these samples. Overall, culturing reduced the presence of these 21 phyla in caecal contents and caecal scrapings (Table 5.8). Only one phylum was found to have an increased presence after culturing; the abundance of Firmicutes increased in both cultured caecal contents and caecal scrapings (Table 5.8). An increased abundance of this phylum in the metascrapes suggests that these populations are living and expanding throughout the duration of the *in vitro* experiments, and thereby able to contribute to inducing hatching of *T. muris* and *T. trichiura*. Members of one phylum of archaea, Thermoplasmatota, were found in increased abundance in caecal scrapings, suggesting they are more closely associated with the mucosa and caecal scrapings rather than the lumen and the caecal contents (Table 5.8). Digging into the differences between aerobic and anaerobic culturing revealed that aerobic culturing resulted in an decreased abundance of Desulfobacterota, and anaerobic culturing resulted in an decreased abundance of Proteobacteria (Table 5.9).

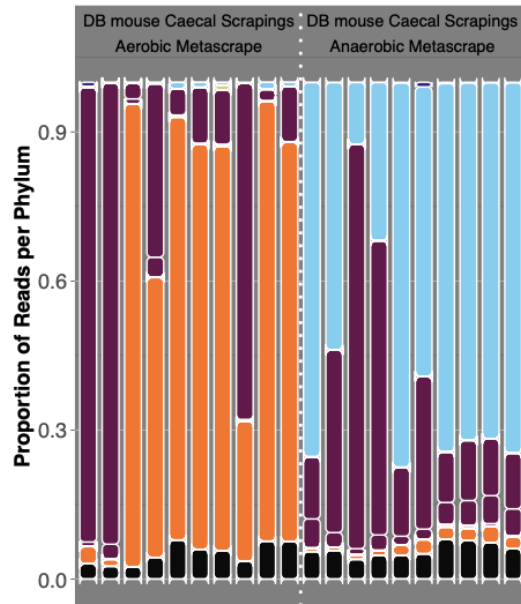
At the species level, comparisons between the caecal scrapings and caecal contents revealed 50 species with a significant change in abundance. The majority of these were bacteroides species that had decreased abundance; however, four species were found in increased abundance in caecal scrapings *Ureaplasma parvum*, *Lactobacillus acidophilus*, and two uncultured species (Table 5.7). It is interesting that *U. parvum* was found to be present in the caecal scrapings; while it is a human commensal, it is typically associated with the urogenital mucosa rather than the intestinal mucosa (Paralanov et al. 2012; Yarbrough, Winkle, and Herbst-Kralovetz 2015). *L. acidophilus* is a well known member of the gut microbiota and known for its interactions with the mucosa including binding to mucin producing cells (Xiong et al. 2018; Ortega-Anaya, Marciniak, and Jiménez-Flores 2021; Juge

2019; Carmo et al. 2018). The last two species are both uncultured and the lowest level of classification for each is genus *Stomatobaculum* and family *Ruminococcaceae* (Sizova et al. 2013).

a



b



c

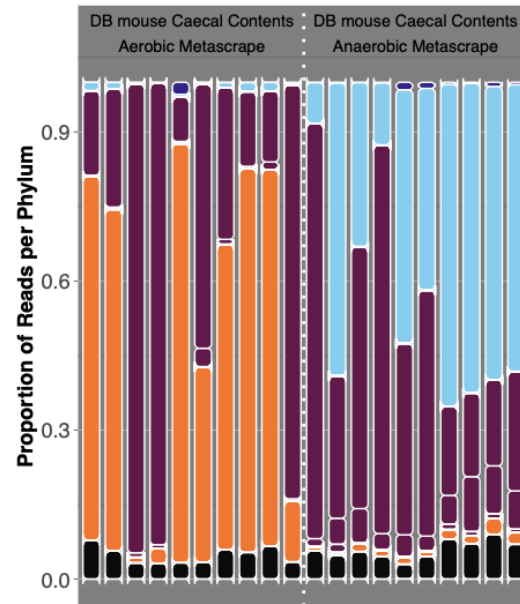


Figure 5.15 The relative abundances of bacterial phyla in donor B humanised microbiota mice crude and cultured caecal samples. Samples were primarily composed of the four phyla most commonly reported in the gut: Firmicutes, Proteobacteria, Bacteroides, and Actinobacteria. In the crude samples caecal scrapings appeared to have more Firmicutes and fewer Bacteroides. In the cultured samples there is a clear difference between aerobic and anaerobic culturing; aerobic metascrapes have more Proteobacteria and anaerobic metascrapes have more Bacteroides

Table 5.7 Differentially abundant phyla and species in donor B scrapings and contents isolated from the caecum. (positive effect/negative effect)

Phylum	Location	coef	stderr	pval	qval
Bacteroidota	caecal Scrapings	-0.16	0.03	7.05E-05	1.48E-03
Firmicutes A	caecal Scrapings	0.12	0.03	2.38E-04	2.50E-03
Species	Location	coef	stderr	pval	qval
<i>Ureaplasma parvum</i>	caecal Scrapings	0.43	0.09	0.00	0.01
<i>Lactobacillus acidophilus</i>	caecal Scrapings	0.25	0.06	0.00	0.01
MGYG HGUT 02052	caecal Scrapings	0.25	0.07	0.00	0.03
MGYG HGUT 03104	caecal Scrapings	0.22	0.06	0.00	0.05

Table 5.8 Differentially abundant phyla in crude donor B scrapings and contents and cultured metascrapes isolated from the caecum. (positive effect/negative effect)

Phylum	Location	coef	stderr	pval	qval
Firmicutes B	Cultured caecal Scrapings	-1.10	0.03	7.91E-39	4.99E-37
Firmicutes B	Cultured caecal Contents	-1.05	0.03	2.76E-38	8.68E-37
unclassified	Cultured caecal Contents	-0.83	0.05	6.74E-23	1.42E-21
unclassified	Cultured caecal Scrapings	-0.83	0.05	1.75E-22	2.75E-21
Firmicutes I	Cultured caecal Scrapings	-0.91	0.07	4.42E-18	5.57E-17
Firmicutes G	Cultured caecal Contents	-0.90	0.07	1.31E-17	1.37E-16
Firmicutes I	Cultured caecal Contents	-0.86	0.07	2.28E-17	2.05E-16
Firmicutes G	Cultured caecal Scrapings	-0.90	0.07	2.60E-17	2.05E-16
Firmicutes	Cultured caecal Contents	1.54	0.13	1.22E-16	8.51E-16
Verrucomicrobiota	Cultured caecal Scrapings	-1.21	0.10	1.62E-16	1.02E-15
Verrucomicrobiota	Cultured caecal Contents	-1.18	0.10	2.36E-16	1.35E-15
Bdellovibrionota	Cultured caecal Contents	-0.53	0.05	3.75E-16	1.97E-15
Bdellovibrionota	Cultured caecal Scrapings	-0.53	0.05	7.22E-16	3.50E-15
Synergistota	Cultured caecal Contents	-0.37	0.04	1.08E-14	4.87E-14
Synergistota	Cultured caecal Scrapings	-0.37	0.04	2.01E-14	8.43E-14
Firmicutes	Cultured caecal Scrapings	1.35	0.13	3.61E-14	1.42E-13
Desulfobacterota A	Cultured caecal Scrapings	-1.40	0.14	5.41E-14	2.01E-13
Desulfobacterota A	Cultured caecal Contents	-1.27	0.14	1.01E-12	3.54E-12
Campylobacterota	Cultured caecal Scrapings	-0.80	0.09	3.93E-12	1.24E-11
Spirochaetota	Cultured caecal Scrapings	-0.78	0.09	3.87E-12	1.24E-11

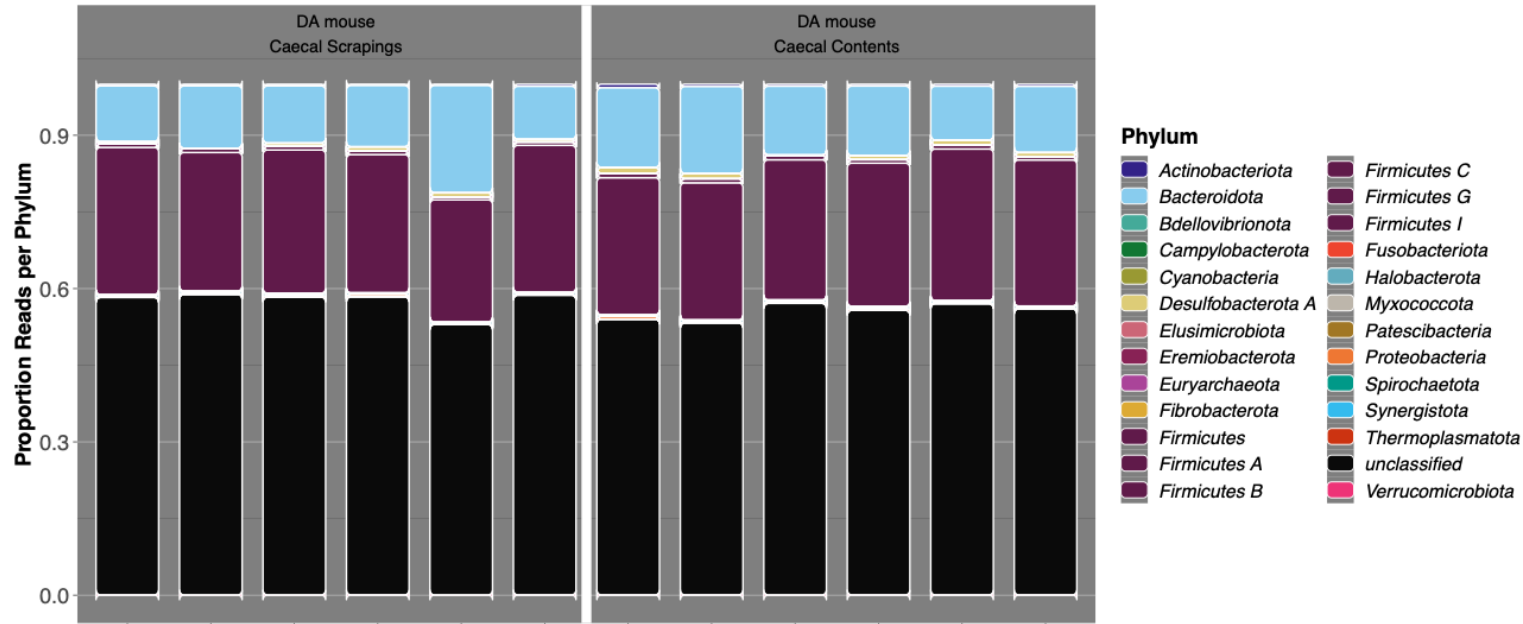
Campylobacterota	Cultured caecal Contents	-0.78	0.09	5.70E-12	1.71E-11
Eremiobacterota	Cultured caecal Scrapings	-0.70	0.08	1.48E-11	4.25E-11
Spirochaetota	Cultured caecal Contents	-0.70	0.09	5.43E-11	1.49E-10
Eremiobacterota	Cultured caecal Contents	-0.65	0.08	9.16E-11	2.40E-10
Cyanobacteria	Cultured caecal Scrapings	-0.78	0.11	1.35E-09	3.39E-09
Cyanobacteria	Cultured caecal Contents	-0.76	0.11	2.07E-09	5.02E-09
Firmicutes A	Cultured caecal Scrapings	-1.23	0.19	1.80E-08	4.20E-08
Firmicutes A	Cultured caecal Contents	-1.13	0.18	9.03E-08	2.03E-07
Fusobacteriota	Cultured caecal Scrapings	-0.71	0.13	1.48E-06	3.21E-06
Actinobacteriota	Cultured caecal Scrapings	-1.07	0.20	1.76E-06	3.70E-06
Fusobacteriota	Cultured caecal Contents	-0.64	0.13	7.55E-06	1.54E-05
Thermoplasmatota	Crude caecal Scrapings	0.15	0.03	2.70E-05	5.32E-05
Actinobacteriota	Cultured caecal Contents	-0.85	0.20	6.42E-05	1.23E-04
Euryarchaeota	Cultured caecal Contents	-0.21	0.05	7.63E-05	1.41E-04
Firmicutes C	Cultured caecal Scrapings	-0.85	0.20	8.84E-05	1.59E-04
Euryarchaeota	Cultured caecal Scrapings	-0.19	0.05	3.74E-04	6.54E-04
Firmicutes C	Cultured caecal Contents	-0.63	0.20	2.14E-03	3.65E-03
Bacteroidota	Cultured caecal Contents	-0.89	0.34	0.01	0.02
Bacteroidota	Cultured caecal Scrapings	-0.85	0.34	0.02	0.03
Proteobacteria	Cultured caecal Contents	0.63	0.27	0.02	0.04

Table 5.9 Differentially abundant phyla in aerobically and anaerobically cultured metascrapes isolated from the caecum in donor B mice. (positive effect/negative effect)

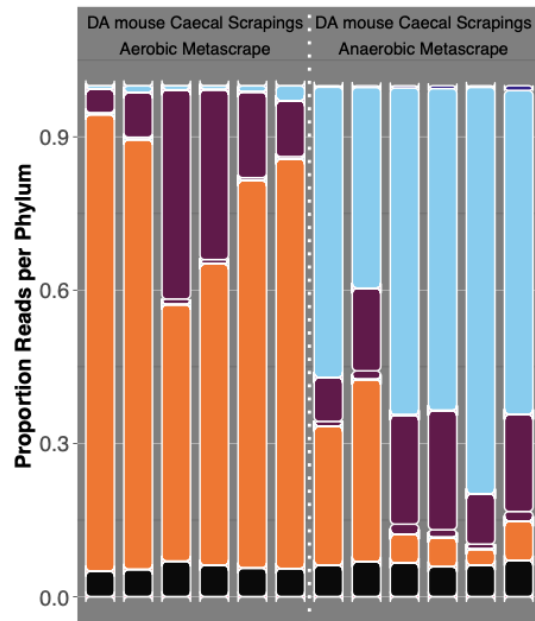
Phylum	Location	coef	stderr	pval	qval
Bacteroidota	Anaerobic caecal Contents	1.74	0.15	4.72E-13	3.78E-11
Bacteroidota	Anaerobic caecal Scrapings	1.89	0.18	4.96E-12	1.98E-10
Cyanobacteria	Anaerobic caecal Contents	0.47	0.07	1.73E-07	4.61E-06
Proteobacteria	Anaerobic caecal Contents	-1.38	0.23	9.85E-07	1.97E-05
Firmicutes C	Anaerobic caecal Contents	1.07	0.19	2.01E-06	3.22E-05
Proteobacteria	Anaerobic caecal Scrapings	-1.49	0.27	4.91E-06	6.55E-05
Cyanobacteria	Anaerobic caecal Scrapings	0.45	0.09	8.71E-06	9.95E-05
Firmicutes A	Anaerobic caecal Contents	0.86	0.17	1.25E-05	1.25E-04
Fusobacteriota	Anaerobic caecal Contents	0.52	0.12	1.48E-04	1.32E-03
Firmicutes A	Anaerobic caecal Scrapings	0.72	0.20	1.04E-03	0.01
Fusobacteriota	Anaerobic caecal Scrapings	0.49	0.14	1.56E-03	0.01
Actinobacteriota	Anaerobic caecal Contents	0.60	0.20	4.98E-03	0.03
Desulfobacterota A	Aerobic caecal Scrapings	-0.53	0.18	0.01	0.04

Kraken 2 classification of the donor A humanised microbiota mice gastrointestinal samples was poor compared to the donor B samples, with a consistent proportion of reads unclassified of ~60% (Figure 5.8). However, once again the bacteria reported were primarily Firmicutes, Proteobacteria, Bacteroides, and Actinobacteria (Figure 5.12). As before I used MaAsLin 2, to look for statistically significant differences ($q_{val} < 0.05$) in the distribution of phyla. My analysis did not reveal any statistically different phyla abundances when comparing caecal contents and caecal scrapings; at the species level there were some associations but with a q value between 0.25 and 0.05 they did not meet my threshold for significance. This mirrored what I saw in the PCoA (Figure 5.13), the distances between samples were small indicating that the samples were uniform in composition, sharing many of the same species. Poor classification of these samples likely also contributed to the lack of statistical differences. Indeed, the level of classification was greatly improved using the cultured metascape samples and I was able to identify clear associations. Once again culturing primarily resulted in the reduced representation of phyla except Firmicutes and Proteobacteria. Comparing crude and cultured samples also revealed that crude caecal scrapings contained more members of the phyla Spirochaetota and Thermoplasmatota. There was a clear visual difference in composition between aerobically and anaerobically cultured samples, particularly in the relative abundance of Proteobacteria and Bacteroides (Figure 5.16). This was confirmed statistically with Proteobacteria displaying an increased abundance in cultured samples generally, and a decreased abundance in anaerobic cultures. While Bacteroides were not enriched in cultured samples generally, there was an increased abundance of this phylum in the anaerobic cultures of both caecal scrapings and caecal contents. Overall culturing reduced the abundance of 11 phyla.

a



b



c

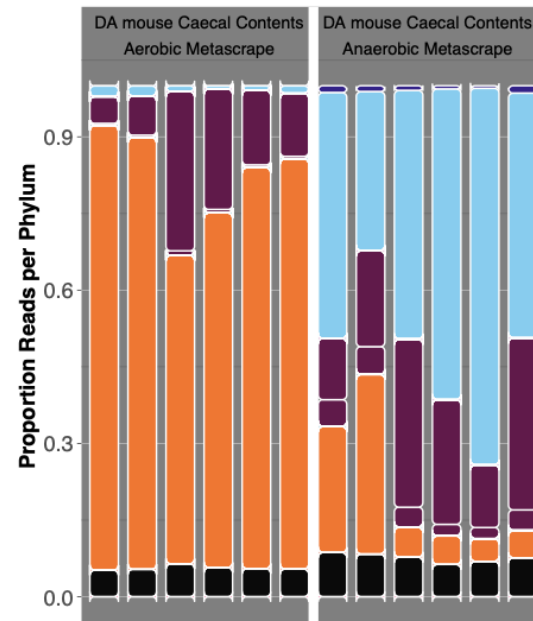


Figure 5.16 The relative abundances of bacterial phyla in donor A humanised microbiota mice crude and cultured caecal samples. Samples were primarily composed of the four phyla most commonly reported in the gut: Firmicutes, Proteobacteria, Bacteroides, and Actinobacteria. There were no obvious difference in the crude samples, however, in the cultured samples there was a clear difference between aerobic and anaerobic culturing; aerobic metascrapes have more Proteobacteria and anaerobic metascrapes have more Bacteroides

Table 5.10 Differentially abundant phyla in crude donor A scrapings and contents and cultured metascrapes isolated from the caecum. (positive effect/negative effect)

Phylum	Location	coef	stderr	pval	qval
Spirochaetota	Cultured caecal Contents	-0.30	2.73E-05	7.29E-107	1.97E-105
Spirochaetota	Cultured caecal Scrapings	-0.30	2.73E-05	7.29E-107	1.97E-105
unclassified	Cultured caecal Scrapings	-0.96	0.03	5.59E-27	1.01E-25
unclassified	Cultured caecal Contents	-0.93	0.03	1.51E-26	2.04E-25
Verrucomicrobiota	Cultured caecal Contents	-0.41	0.02	4.77E-22	4.29E-21
Verrucomicrobiota	Cultured caecal Scrapings	-0.41	0.02	4.77E-22	4.29E-21
Firmicutes B	Cultured caecal Contents	-0.32	0.01	3.13E-21	2.11E-20
Firmicutes B	Cultured caecal Scrapings	-0.32	0.01	3.13E-21	2.11E-20
Firmicutes	Cultured caecal Contents	1.33	0.11	2.00E-13	1.20E-12
Campylobacterota	Cultured caecal Contents	-0.30	0.03	2.86E-13	1.55E-12
Firmicutes	Cultured caecal Scrapings	1.29	0.11	4.50E-13	2.11E-12
Firmicutes I	Cultured caecal Scrapings	-0.88	0.08	4.68E-13	2.11E-12
Firmicutes I	Cultured caecal Contents	-0.83	0.08	2.15E-12	8.95E-12
Campylobacterota	Cultured caecal Scrapings	-0.28	0.03	2.68E-12	1.03E-11
Cyanobacteria	Cultured caecal Contents	-0.67	0.07	1.81E-11	6.53E-11
Firmicutes A	Cultured caecal Scrapings	-1.49	0.15	3.64E-11	1.23E-10
Cyanobacteria	Cultured caecal Scrapings	-0.64	0.07	4.59E-11	1.46E-10
Firmicutes A	Cultured caecal Contents	-1.30	0.15	8.59E-10	2.58E-09
Proteobacteria	Cultured caecal Contents	1.86	0.23	2.74E-09	7.78E-09
Proteobacteria	Cultured caecal Scrapings	1.85	0.23	3.02E-09	8.17E-09
Firmicutes C	Cultured caecal Scrapings	-1.20	0.15	3.56E-09	9.16E-09
Euryarchaeota	Cultured caecal Contents	-0.25	0.03	2.67E-08	6.27E-08
Euryarchaeota	Cultured caecal Scrapings	-0.25	0.03	2.67E-08	6.27E-08
Firmicutes C	Cultured caecal Contents	-1.08	0.15	3.19E-08	7.18E-08
Desulfobacterota A	Cultured caecal Scrapings	-1.60	0.28	2.82E-06	6.08E-06
Desulfobacterota A	Cultured caecal Contents	-1.48	0.28	1.04E-05	2.16E-05
Spirochaetota	Crude caecal Scrapings	0.00	0.00	7.91E-04	1.58E-03
Thermoplasmatota	Crude caecal Scrapings	0.15	0.05	2.20E-03	4.24E-03

Table 5.11 Differentially abundant phyla in aerobically and anaerobically cultured metascrapes isolated from the caecum in donor A mice. (positive effect/negative effect)

Phylum	Location	coef	stderr	pval	qval
Actinobacteriota	Anaerobic caecal Contents	1.33	0.08	4.06E-13	8.58E-12
Bacteroidota	Anaerobic caecal Scrapings	1.69	0.10	4.77E-13	8.58E-12
Bacteroidota	Anaerobic caecal Contents	1.61	0.10	1.14E-12	1.37E-11
Actinobacteriota	Anaerobic caecal Scrapings	1.01	0.08	6.28E-11	5.00E-10
Firmicutes C	Anaerobic caecal Contents	0.77	0.06	6.95E-11	5.00E-10
Firmicutes A	Anaerobic caecal Contents	0.81	0.09	1.96E-08	1.18E-07
Firmicutes C	Anaerobic caecal Scrapings	0.53	0.06	3.76E-08	1.93E-07
Synergistota	Anaerobic caecal Contents	-0.50	0.08	2.77E-06	1.11E-05
Synergistota	Anaerobic caecal Scrapings	-0.50	0.08	2.76E-06	1.11E-05
Desulfobacterota A	Anaerobic caecal Contents	1.04	0.17	7.08E-06	2.55E-05
Fusobacteriota	Anaerobic caecal Contents	0.46	0.08	1.49E-05	4.87E-05
unclassified	Anaerobic caecal Contents	0.13	0.02	2.99E-05	8.26E-05
Proteobacteria	Anaerobic caecal Contents	-0.91	0.17	2.85E-05	8.26E-05
Proteobacteria	Anaerobic caecal Scrapings	-0.90	0.17	3.21E-05	8.26E-05
Fusobacteriota	Anaerobic caecal Scrapings	0.39	0.08	1.09E-04	2.63E-04
Firmicutes A	Anaerobic caecal Scrapings	0.41	0.09	1.91E-04	4.12E-04
Desulfobacterota A	Anaerobic caecal Scrapings	0.79	0.17	1.95E-04	4.12E-04
Cyanobacteria	Anaerobic caecal Contents	0.25	0.06	2.71E-04	5.22E-04
Cyanobacteria	Anaerobic caecal Scrapings	0.25	0.06	2.75E-04	5.22E-04
Firmicutes I	Anaerobic caecal Contents	0.25	0.09	0.01	0.02
unclassified	Anaerobic caecal Scrapings	0.06	0.02	0.02	0.04

5.6 A differential analysis of relative taxonomic abundances in infected humanised microbiota mice

In the infected humanised microbiota mice I was interested in identifying taxa relevant to hatching through looking for associations between taxonomic groups and infection with *T. trichiura* (Figure 4.6). I classified the samples using Kraken 2 and the UHGG before and after MAG assembly. Performing this method of classification on caecal contents from infected murine and humanised microbiota mice yielded average results. In infected humanised microbiota mice the median percentage of reads unclassified was 50.3%, and in the infected murine microbiota mice samples the median percentage of reads unclassified was 68.6% (Figure 5.17). MAG assembly improved the rate of classification. For infected humanised microbiota mice, the new median percentage of unclassified reads was 19.8% and in the infected murine microbiota mice samples the new median percentage of unclassified reads was 27.9% (Figure 5.17).

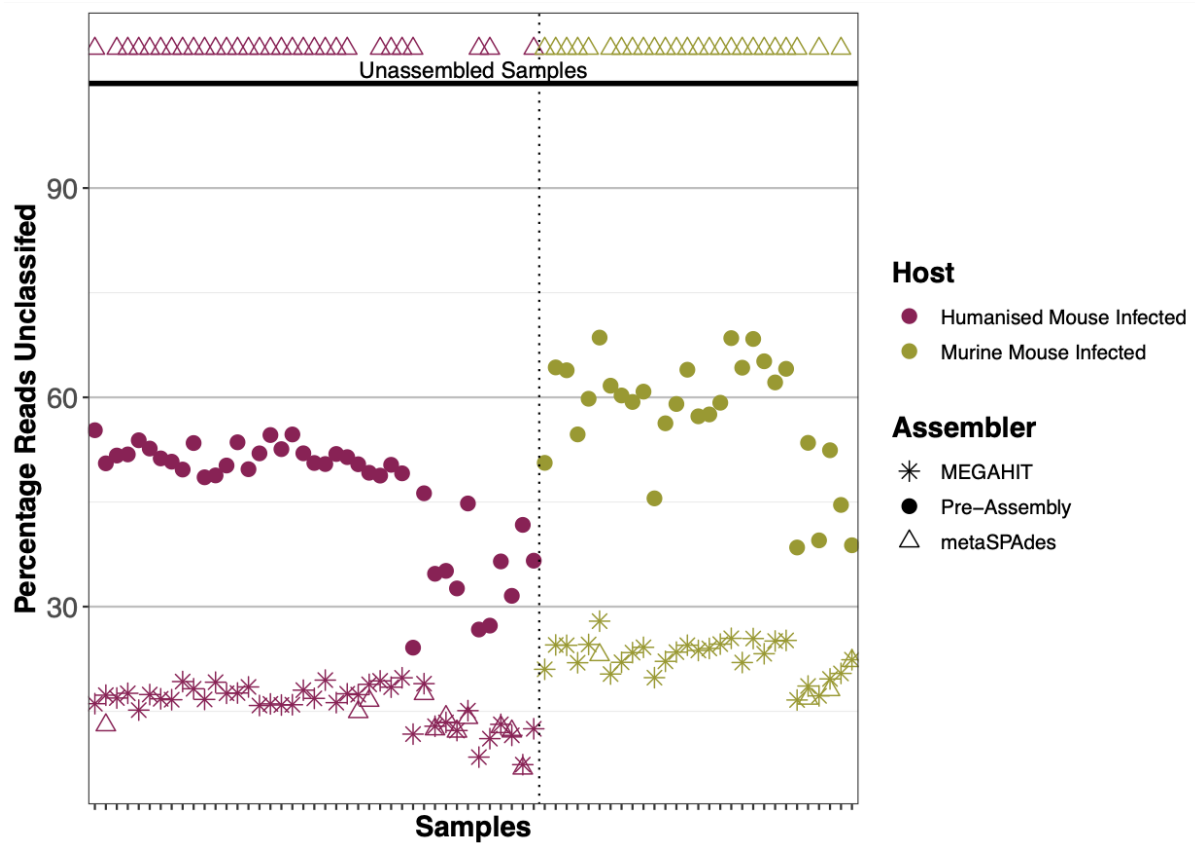


Figure 5.17 Genome assembly using MEGAHIT improves classification of crude gastrointestinal tract samples from infected humanised microbiota mice and murine microbiota mice caeca Metagenomic assembled genomes (MAGs) were created using the metawrap pipeline and the assembly tools MEGAHIT and metaSPAdes. MEGAHIT out-performed metaSPAdes successfully assembling MAGs from more samples. Samples were classified with Kraken 2 before and after assembly and the level of classification increased after assembly for samples from both hosts.

Whipworm infection has previously been shown to alter the microbiota (Holm et al. 2015; Houlden et al. 2015), I sought to observe variations in the composition of caecal contents from naive and infected mice in order to understand the effects of infection with *T. muris* or *T. trichiura* on composition. Samples were annotated by infection and donor microbiota, and the samples primarily clustered by donor. The donor A mice were the least diverse forming a tight central cluster and the donor B mice were the most diverse with the least tightly arranged cluster. Additionally, in donor A and murine microbiota mice there is no clear separation between infected and uninfected mice; in donor B the uninfected mice separate out from the infected mice.

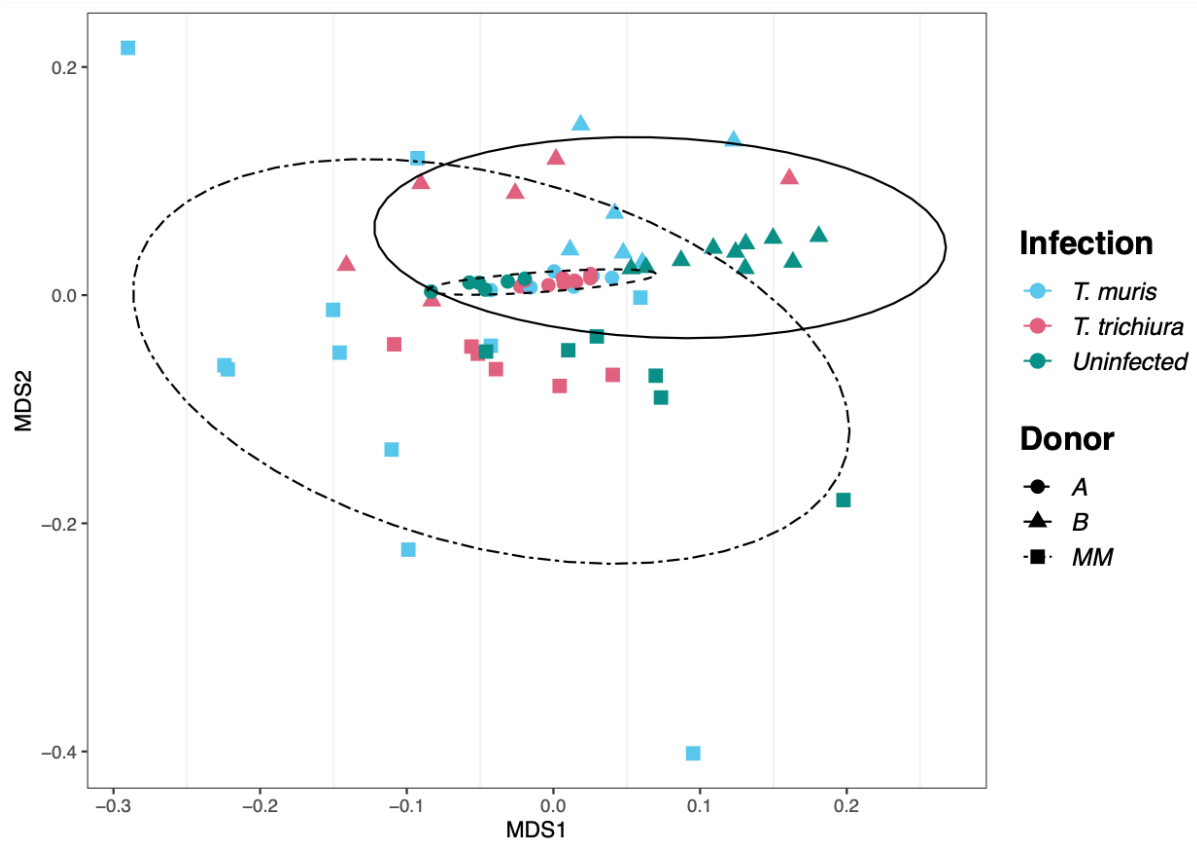


Figure 5.18 Beta diversity of gastrointestinal tract samples from naive infected murine microbiota and humanised microbiota mice reveals that donor microbiota is the greatest source of variation. Using a Bray–Curtis distance matrix generated from the relative taxa abundances reported by Kraken 2 a Principal Coordinates Analysis (PCoA) reveals clusters of samples by origin of the microbiota, with donor B represented by the solid line cluster, donor A by the dashed line cluster, and murine microbiota mice by the dash-dotted line cluster. Infection with either *T. muris* or *T. trichiura* was a source of variation in donor B mice.

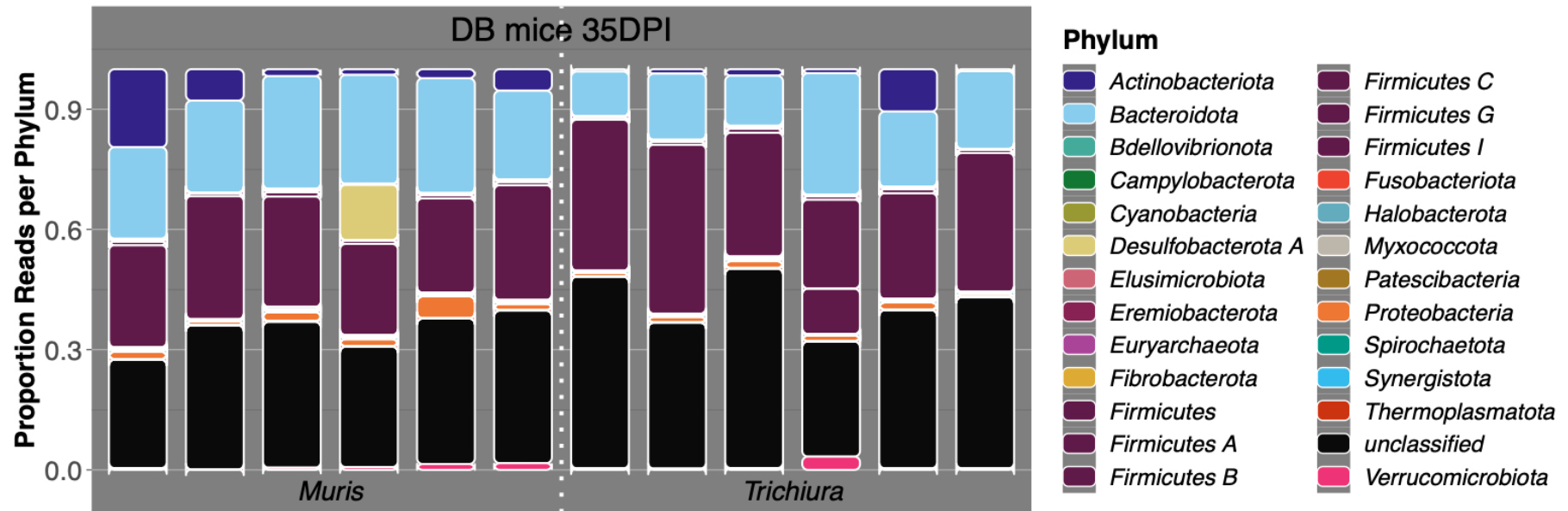
In chapter four I present the first time humanised microbiota mice models have been used to study *Trichuris* infections, the caecal contents of these infected donor A and donor B mice were sequenced and studied. The level of classification of these samples was once again lower in the donor A mice compared to the donor B mice; and the bacteria reported were primarily Firmicutes, Proteobacteria, Bacteroides, and Actinobacteria (Figure 5.19). Using MaAsLin 2 I looked for any statistically significant differences ($q_{val} < 0.05$) in the distribution of phyla comparing: naive and infected mice, and infection with *T. muris* or *T. trichiura*.

When comparing naive and infected mice my analysis revealed that in the donor A mice there were only statistical differences at the phyla level between naive and infected donor A mice that were infected with *T. muris*, but not *T. trichiura* at 35 days post infection. This is consistent with the worm burdens reported in chapter four; only adult *T. muris* were recovered from these mice, and the antibody ODs suggested that *T. trichiura* had been expelled (Figure 4.6, 4.7). Parasite modulation of the microbiota in mice has been shown to be transient and only occurs when worms are present; once the parasite has been expelled the microbiota returns to normal (Houlden et al. 2015). Naive donor A mice presented an increase in the abundance of Verrucomicrobiota and Firmicutes A, and a decrease in the abundance of Bacteroides, Campylobacterota, and Spirochaetota (Table 5.12). Surprisingly, despite the lack of adult *T. trichiura* there were clear differences in the composition of the microbiota of donor A mice infected with *T. muris* and those infected with *T. trichiura*. Mice that were given a low dose of *T. trichiura* had a decreased abundance of Proteobacteria (coeff= -0.40, q_{val} = 0.04).

In the donor B mice, associations were found between naive mice, and mice with either infection. When compared to *T. muris* infected mice, naive donor B mice displayed a decrease in the abundance of: Patescibacteria, Firmicutes A and C, Actinobacteriota, Campylobacterota, and Verrucomicrobiota, as well as an increase in Firmicutes G and Bacteroides (Table 5.12, Figure 5.19). This increase in abundance of Firmicutes G and Bacteroides was also observed when comparing naive donor B mice and *T. trichiura* infected mice. In the *T. trichiura* infected mice, a decrease in abundance was seen in three phyla: Firmicutes A, Patescibacteria, and Thermoplasmatota (Table 5.12). There were no significant associations reported when comparing infections. These results indicate that the composition of the microbiota is altered by infection, and while there is a lot of overlap between infection related alterations with the two *Trichuris* species, they can also alter the microbiota in different ways. Differences can also be seen when comparing the responses by host, the abundances of Verrucomicrobiota and Bacteroides moved in opposite directions during infection with *T. muris* in each humanised microbiota mouse line (Table 5.12).

To identify potential phyla that may contribute to supporting chronic infection of *T. trichiura* I compared the relative abundances of bacteria in the caecal contents of mice with and without adult worms. Infection of mice with *T. muris* has been shown to remodel the composition of the murine microbiota in a way that prevents subsequent parasite infection (Houlden et al. 2015; White et al. 2018). I hypothesised that *T. trichiura* may behave similarly modulating the human microbiota and depleting bacterial species that lead to successful establishment of an infection. As hatching is the first step in infection, depletion of these bacteria may have an effect on hatching. Recovery of adult worms was not associated with a decrease in the abundance of any phyla, and was associated with an increase in the abundance of Firmicutes A, B, and C, as well as Verrucomicrobiota (Table 5.13). However, at the species level several examples of decreased abundance were seen in the mice where adult *T. trichiura* were recovered (Table 5.13). The top result in this list of associations was an uncultured species (*MGYG HGUT 02992*) assigned to the genus *Dorea*; this genus has previously been isolated from human colon mucosa (Shen et al. 2010). The next species (*Alistipes sp002161445*) belonged to the *Alistipes* genus, which is relatively novel and still being characterised; however, it is a known member of the microbiota and has been implicated in dysbiosis related to several conditions (Parker et al. 2020). Several *Alistipes* species are enriched in the caecum compared to other regions of the gastrointestinal tract (Parker et al. 2020). Completing the top three associations is an uncultured member of the family *Lachnospiraceae* (*MGYG HGUT 01797*). Members of this family are routinely found in the human gut microbiota and while they are normally health associated, changes to the population can be biomarkers of dysbiosis (Vacca et al. 2020).

a



b

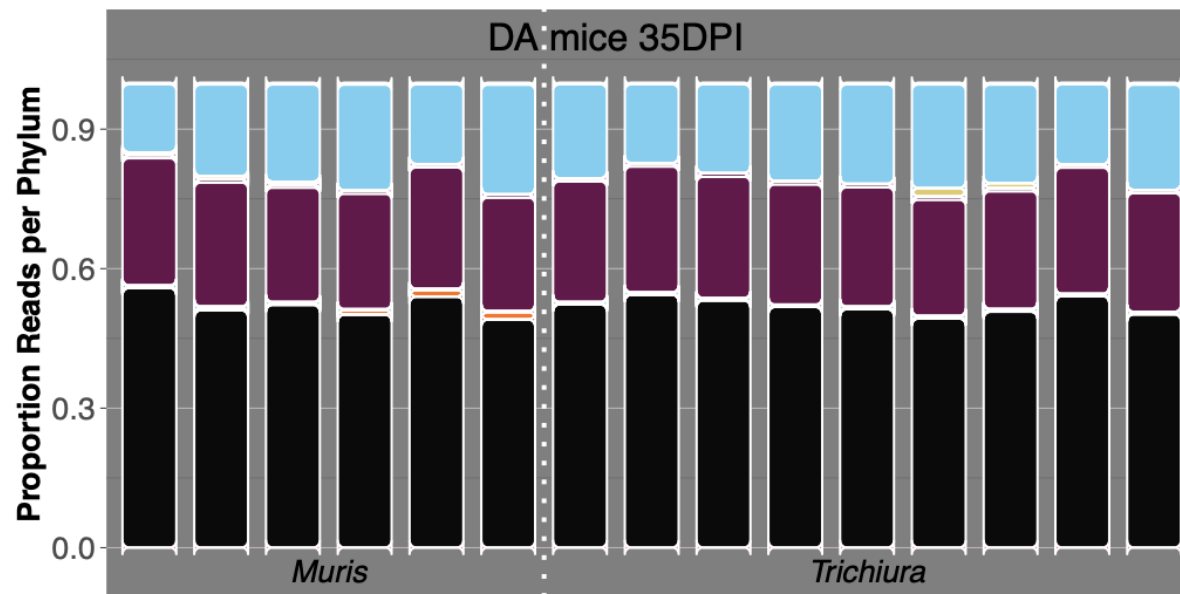


Figure 5.19 The relative abundances of bacterial phyla in donor B and donor A humanised microbiota mice infected with *T. muris* and *T. trichiura*. Samples were primarily composed of the 4 phyla most commonly reported in the gut: Firmicutes, Proteobacteria, Bacteroides, and Actinobacteria. There are no obvious differences between the donor A mice, however in the donor B mice mice infected with *T. trichiura* appear to have a reduced abundance of Actinobacteria and increased abundance of Firmicutes.

Table 5.12 Differentially abundant phyla and in naive humanised microbiota mice caecal contents and the caecal contents of mice infected with *T. muris* or *T. trichiura*.
(positive effect/negative effect)

Phylum	Donor	Infection	Infection Status	coef	stderr	pval	qval
Verrucomicrobiota	A	<i>T. muris</i>	Naive	0.10	0.02	5.49E-04	0.01
Firmicutes A	A	<i>T. muris</i>	Naive	0.04	0.01	0.01	0.03
Bacteroidota	A	<i>T. muris</i>	Naive	-0.15	0.04	0.01	0.03
Campylobacterota	A	<i>T. muris</i>	Naive	0.00	0.00	0.01	0.03
Spirochaetota	A	<i>T. muris</i>	Naive	0.00	0.00	0.01	0.03
unclassified	A	<i>T. muris</i>	Naive	0.03	0.01	0.02	0.05
Bacteroidota	B	<i>T. trichiura</i>	Naive	0.32	0.05	4.44E-05	4.88E-04
Firmicutes G	B	<i>T. trichiura</i>	Naive	0.84	0.14	2.60E-05	4.88E-04
Firmicutes A	B	<i>T. trichiura</i>	Naive	-0.14	0.03	1.08E-03	0.01
Patescibacteria	B	<i>T. trichiura</i>	Naive	-0.21	0.05	9.33E-04	0.01
Thermoplasmatota	B	<i>T. trichiura</i>	Naive	-0.23	0.06	1.16E-03	0.01
Bacteroidota	B	<i>T. muris</i>	Naive	0.15	0.03	2.41E-04	0.01
Patescibacteria	B	<i>T. muris</i>	Naive	-0.22	0.05	9.38E-04	0.01
Firmicutes A	B	<i>T. muris</i>	Naive	-0.06	0.02	0.01	0.04
Actinobacteriota	B	<i>T. muris</i>	Naive	-0.56	0.20	0.01	0.04
Firmicutes C	B	<i>T. muris</i>	Naive	-0.11	0.04	0.01	0.04
Campylobacterota	B	<i>T. muris</i>	Naive	-0.28	0.10	0.02	0.04
Verrucomicrobiota	B	<i>T. muris</i>	Naive	-0.45	0.15	0.01	0.04
Firmicutes G	B	<i>T. muris</i>	Naive	0.42	0.15	0.02	0.04
Thermoplasmatota	B	<i>T. muris</i>	Naive	-0.18	0.07	0.01	0.04

Table 5.13 Differentially abundant phyla species in the caecal contents of mice capable of supporting a chronic *T. trichiura* infection. (positive effect/negative effect)

Phylum	Adult <i>T. trichiura</i>	coef	stderr	pval	qval
Proteobacteria	No	-0.61	0.10	6.15E-07	2.71E-05
Campylobacterota	No	-0.62	0.13	3.62E-05	7.96E-04
Cyanobacteria	No	-0.25	0.06	2.20E-04	2.51E-03
Verrucomicrobiota	No	-0.60	0.15	3.23E-04	2.51E-03
Fusobacteriota	No	-0.46	0.12	3.09E-04	2.51E-03
Euryarchaeota	No	-0.13	0.03	3.43E-04	2.51E-03
Spirochaetota	No	-0.36	0.10	5.15E-04	3.24E-03
Firmicutes I	No	-0.34	0.09	7.47E-04	3.65E-03
Eremiobacterota	No	-0.42	0.12	7.02E-04	3.65E-03
Firmicutes C	Yes	0.45	0.13	9.27E-04	4.08E-03
Bdellovibrionota	No	-0.37	0.11	1.08E-03	4.31E-03
Thermoplasmata	No	-0.14	0.04	2.08E-03	0.01
Firmicutes A	Yes	0.10	0.03	2.98E-03	0.01
Firmicutes B	No	-0.10	0.03	3.07E-03	0.01
Firmicutes B	Yes	0.13	0.04	3.33E-03	0.01
Actinobacteriota	No	-0.44	0.14	4.27E-03	0.01
Verrucomicrobiota	Yes	0.61	0.21	0.01	0.01
Desulfobacterota A	No	-0.59	0.22	0.01	0.02
unclassified	No	0.08	0.03	0.01	0.03
Synergistota	No	-0.16	0.06	0.01	0.03
Firmicutes C	No	-0.22	0.09	0.02	0.04
Species	Adult <i>T. trichiura</i>	coef	stderr	pval	qval
MGYG HGUT 02992	Yes	-0.27	0.04	3.45E-07	3.60E-04
Alistipes sp002161445	Yes	-0.58	0.11	4.55E-06	1.55E-03
MGYG HGUT 01797	Yes	-0.31	0.07	8.96E-05	0.01
Lachnoclostridium A edouardi	Yes	-0.31	0.07	1.57E-04	0.02
An181 sp002160325	Yes	-0.14	0.04	6.65E-04	0.02
Hungatella sp000526575	Yes	-0.30	0.07	2.24E-04	0.02
Eubacterium G sp000432355	Yes	-0.14	0.04	6.65E-04	0.02
MGYG HGUT 01566	Yes	-0.14	0.04	6.65E-04	0.02
MGYG HGUT 04132	Yes	-0.30	0.08	5.68E-04	0.02
MGYG HGUT 04381	Yes	-0.27	0.07	5.64E-04	0.02
MGYG HGUT 01998	Yes	-0.14	0.04	6.65E-04	0.02
MGYG HGUT 00145	Yes	-0.28	0.08	6.73E-04	0.02
MGYG HGUT 00194	Yes	-0.27	0.07	6.76E-04	0.02
Bacteroides sp002491635	Yes	-1.13	0.31	7.94E-04	0.02
MGYG HGUT 02280	Yes	-0.27	0.08	8.54E-04	0.02
Clostridium M sp000155435	Yes	-0.17	0.05	8.65E-04	0.02
Paraprevotella xylaniphila	Yes	-0.28	0.08	1.03E-03	0.02
MGYG HGUT 00152	Yes	-0.24	0.07	1.08E-03	0.02
Dorea sp000765215	Yes	-0.26	0.07	1.14E-03	0.02

MGYG HGUT 01748	Yes	-0.24	0.07	1.28E-03	0.02
MGYG HGUT 03573	Yes	-0.24	0.07	1.32E-03	0.02
<i>Faecalicatena gnavus</i>	Yes	-0.23	0.07	1.64E-03	0.02
MGYG HGUT 00623	Yes	-0.23	0.07	1.84E-03	0.03
MGYG HGUT 01250	Yes	-0.25	0.08	1.86E-03	0.03
MGYG HGUT 01247	Yes	-0.36	0.11	1.89E-03	0.03
MGYG HGUT 00127	Yes	-0.20	0.06	1.94E-03	0.03
MGYG HGUT 01087	Yes	-0.24	0.07	2.05E-03	0.03
MGYG HGUT 03903	Yes	-0.32	0.10	2.20E-03	0.03
MGYG HGUT 01224	Yes	-0.23	0.07	2.18E-03	0.03
<i>Dorea sp900240315</i>	Yes	-0.21	0.06	2.38E-03	0.03
<i>Alistipes A ihumii</i>	Yes	-0.47	0.15	2.48E-03	0.03
<i>Lachnospira sp000437735</i>	Yes	-0.23	0.07	2.43E-03	0.03
MGYG HGUT 02711	Yes	-0.27	0.08	2.42E-03	0.03
MGYG HGUT 01645	Yes	-0.24	0.07	2.75E-03	0.03
MGYG HGUT 00650	Yes	-0.25	0.08	2.82E-03	0.03
<i>Alistipes shahii</i>	Yes	-0.42	0.13	2.85E-03	0.03
MGYG HGUT 00287	Yes	-0.30	0.10	3.00E-03	0.03
MGYG HGUT 01961	Yes	-0.24	0.08	3.08E-03	0.03
MGYG HGUT 04604	Yes	-0.22	0.07	3.10E-03	0.03
MGYG HGUT 03892	Yes	-0.18	0.06	3.53E-03	0.03
MGYG HGUT 03245	Yes	-0.19	0.06	3.85E-03	0.03
MGYG HGUT 00574	Yes	-0.20	0.07	3.91E-03	0.03
<i>Bacteroides F pectinophilus</i>	Yes	-0.24	0.08	4.00E-03	0.03
<i>Blautia A sp000436615</i>	Yes	-0.22	0.07	4.02E-03	0.03
MGYG HGUT 03316	Yes	-0.21	0.07	4.28E-03	0.04
<i>Bariatricus massiliensis</i>	Yes	-0.21	0.07	4.37E-03	0.04
<i>CAG 791 sp000431495</i>	Yes	-0.09	0.03	0.01	0.04
<i>Bittarella massiliensis</i>	Yes	-0.30	0.10	4.99E-03	0.04
<i>Butyrivibrio A crossotus</i>	Yes	-0.09	0.03	0.01	0.04
<i>Butyrivibrio A sp000431815</i>	Yes	-0.09	0.03	0.01	0.04
<i>Oribacterium sinus</i>	Yes	-0.09	0.03	0.01	0.04
<i>Anaerostipes caccae</i>	Yes	-0.09	0.03	0.01	0.04
<i>Ruminococcus A sp003011855</i>	Yes	-0.23	0.08	4.81E-03	0.04
<i>TF01 11 sp001916135</i>	Yes	-0.09	0.03	0.01	0.04
<i>Blautia A obeum</i>	Yes	-0.09	0.03	0.01	0.04
<i>Coproccoccus B comes</i>	Yes	-0.09	0.03	0.01	0.04
MGYG HGUT 03151	Yes	-0.09	0.03	0.01	0.04
MGYG HGUT 01024	Yes	-0.09	0.03	0.01	0.04
MGYG HGUT 02676	Yes	-0.32	0.11	0.01	0.04
<i>Faecalicatena sp900066545</i>	Yes	-0.25	0.09	0.01	0.04
<i>Ruminococcus G gauvreauii</i>	Yes	-0.18	0.06	0.01	0.04
MGYG HGUT 03970	Yes	-0.20	0.07	0.01	0.04

<i>MGYG HGUT 01603</i>	Yes	-0.31	0.11	0.01	0.04
<i>MGYG HGUT 02685</i>	Yes	-0.27	0.09	0.01	0.05
<i>Clostridium Q sp003024715</i>	Yes	-0.24	0.08	0.01	0.05
<i>Anaerotignum sp001304995</i>	Yes	-0.27	0.09	0.01	0.05
<i>MGYG HGUT 01637</i>	Yes	-0.22	0.08	0.01	0.05
<i>MGYG HGUT 00181</i>	Yes	-0.22	0.08	0.01	0.05
<i>Dorea faecis</i>	Yes	-0.16	0.06	0.01	0.05
<i>MGYG HGUT 01144</i>	Yes	-0.23	0.08	0.01	0.05

5.7 Discussion and Conclusions

In the present chapter I set out to characterise the differences in the composition of the microbiota that were demonstrated to have an effect on the hatching of *Trichuris* species in chapters three and four. In order to identify members of the microbiota responsible for variation in hatching observed I carried out analysis of the gastrointestinal tract samples. In addition to allowing me to study hatching requirements, this collection of sequences forms a valuable dataset contributing to the understanding of the mucosal microbiota of mice, pigs and humans. Before beginning my analysis, I evaluated the efficacy of various approaches available to me. Reference based approaches classified the majority of microbial species in samples collected due to the extensiveness of the reference database (Almeida et al. 2021). A matrix of relative abundances was utilised for differential analysis of the presence of different taxa. Identification of species using one human database (UHGG) across the various hosts was possible, but for future studies it would be interesting to use a variety of host databases (Beresford-Jones et al. 2021; C. Chen et al. 2021) and ideally build and curate a new combined database to achieve maximum classification.

In addition to reference-based approaches, I performed *de novo* assembly (Saheb Kashaf et al. 2021). Assembly increases the rate of classification but this is biased towards more abundant species. Additionally, it removes the ability to study samples quantitatively, and possibly results in missed rare events. I generated MAGs for future quantitative studies, these sequences can be searched for the candidates identified in my taxonomic study, and genomes of interest further analysed. It would be ideal to generate high quality reference genomes and frozen isolates for all the species in these samples. However, in the humanised microbiota mice it is estimated that ~30,000 bacterial colonies would need to be picked from repeated metascrapes to recover single purified isolates of all the OTUs present in these two humanised microbiota mice lines making this a large undertaking (Pike 2020).

Using the *T. muris* *E. coli* model, I identified several bacterial proteins crucial for whipworm egg hatching (Chapter 3). In order to begin extrapolating this information to other *Trichuris* species, in particular the relationship between *T. trichiura* and the human microbiota, I examined the abundance of genes encoding fimbrial and serine proteases across the primary phyla comprising the gut microbiome. Perturbing these genes was shown to have the greatest effects on hatching and I was particularly interested to see if I could identify these genes in the Firmicutes, one of the dominant phyla of the human gastrointestinal tract microbiota (Ley, Peterson, and Gordon 2006; Marchesi et al. 2016; Rinninella et al. 2019). Together Bacteroides and Firmicutes can comprise up to 90% of the gut microbiome and it

is these predominantly gram positive bacteria that perform many functions in the gut related to health, disease, and dysbiosis. However despite their abundance in the gastrointestinal tract, many Firmicutes in particular have only recently been isolated, so the full scope of their contribution to intestinal health is not yet understood (Rinninella et al. 2019). Given their abundant representation in the gastrointestinal tract of healthy individuals across the world and the vast functions they perform in the gut, the Firmicutes are likely involved in hatching of *T. trichiura* in humans. I was able to detect the presence of genes comprising fimbrial and serine protease operons across the phylogenetic tree using *de novo* predictions, annotations and BlastX searches of the genomes of these isolates. The results of these investigations (Figure 5.2-5.4) demonstrated a preference for calling the presence of these genes in Proteobacteria. This is to be expected given that Proteobacteria is one of the most studied bacterial phyla, and that I am using observations in *E. coli* to extrapolate predictions. However, sequence similarity searches revealed that the genes of the fimbriae and serine protease operons are readily found across the gut phyla that make up the majority of the human microbiota- Bacteroides and Firmicutes. Future studies can utilise the *E. coli* gene sequences to search the MAGs generated in this chapter to confirm the presence of fimbriae and protease operons in gastrointestinal samples with demonstrated capability to induce hatching in *Trichuris* species and be mediated by protease inhibitors. Further these MAGs can be used to perform comparative genomic analyses to examine genes for conservation of structure and function, as well as study evolutionary relationships.

The response of *Trichuris* species to a wide variety of bacteria is demonstrated by the beta diversity and the plethora of associations at phylum and at species level between hatching or infection. In the human biopsies, samples that can induce hatching are found across the distance matrix (Figure 5.7). In investigating associations at phylum level, associations were primarily found relating to the transverse colon. A pairwise comparison of the ascending and descending colon did not reveal any significant differences in the abundances of phyla. This mirrors the challenges previously seen in studies of this nature, utilising biopsies and post mortem samples revealed that the regions of the colon are very similar (Jiao et al. 2021; James et al. 2020). Differences are primarily seen when comparing more distant regions e.g. comparing the caecum to either the sigmoid colon or rectum (Jiao et al. 2021; James et al. 2020). Grouping samples by their ability to induce hatching proved to be more informative than grouping by colon sampling site in order to identify which species in the human biopsies are likely contributing to *T. trichiura* hatching. I looked for differently abundant species and found 98 species more abundant in samples capable of inducing hatching (Table 5.3). Focussing on just the top three associations reported provides more insight into the factors involved in human whipworm hatching. The species topping the list of associations with *T.*

trichiura hatching is *B. wadsworthia*; this bacterium is a known member of the human gut microbiota. However, it is a slow growing bacterium and also low in abundance in faeces. This has made it challenging to isolate *B. wadsworthia*, and it has remained relatively under characterised since it was first described (Feng et al. 2017; Baron et al. 1989). While its low abundance makes it difficult to isolate from the microbiota of healthy individuals, *B. wadsworthia* is often abundant in patients with conditions pertaining to gastrointestinal inflammation like appendicitis (Baron et al. 1989; Feng et al. 2017; McOrist et al. 2001), which perhaps explains why hatching of *T. trichiura* has not been observed using healthy stool samples but was observed with these human biopsies. Several of the patients undergoing colonoscopy had inflammation and possibly an inflated population of *B. wadsworthia*. I hypothesise that these bacteria are strong candidates for further study of its effects in *T. trichiura* hatching as it displays some of the necessary molecular components required for hatching. For instance, strains of *B. wadsworthia* have been shown to adhere to intestinal epithelial cells in culture. To facilitate adhesion, different outer membrane proteins including fimbriae are expressed (Gerardo et al. 1998). One potential confounder is that this species of bacteria is an obligate anaerobe, however aerotolerance in obligate anaerobes varies (Lu and Imlay 2021).

The next association highlighted the challenges associated with this type of study; it is an uncultured species, known as *ER4 sp900317525*. This genome was isolated and reassembled from a rumen gut microbiota study ("GTDB - GCA_900317525.1" 2021), it's only characterisation tells us that it belongs to the *Oscillospiraceae* family. *Oscillospiraceae* species are known for being mucin degraders in the human gastrointestinal tract (Raimondi et al. 2021), and therefore associated with the mucosa. The next challenge would be to isolate and culture this species from the gastrointestinal tract to generate a high-quality reference genome and culture stocks for *in vitro* assays.

Associations 3 through 5 on the list (Table 5.3) are strains of *F. prausnitzii* which is a gram positive extremely oxygen sensitive (EOS) species and a well-known member of the microbiota. It is found ubiquitously in healthy individuals and is also a good biomarker for dysbiosis associated with diseases such as ulcerative colitis and Crohn's (Miquel et al. 2013; Fitzgerald et al. 2018; Lopez-Siles et al. 2017; Leylabadlo et al. 2020; Sun and Dudeja 2018; Zhang et al. 2021). *F. prausnitzii* resides in both the faecal and mucosal layers of the gastrointestinal tract forming a transversal gradient, and it is known for its immunomodulatory effects through the production of butyrate and other anti-inflammatory molecules (Lopez-Siles et al. 2018). *F. prausnitzii* warrants further study of its role in hatching of *T. trichiura*; my previous attempts at inducing hatching of *T. trichiura in vitro*

using *F. prausnitzii* were unsuccessful. One possible explanation for this is the culturing approach, the previous attempts were carried out in anaerobic gas jars, and as shown in chapter four, gas jars and anaerobic chambers produce different results. Additionally, hatching of *T. trichiura* may require more of the host environment to be recapitulated *in vitro* to see hatching; bacterial mono cultures may not be suitable for inducing hatching for this particular whipworm. Studying the relationship between *F. prausnitzii* and *T. trichiura* will be helped by the development of novel culturing methods that more accurately recapitulate the gut. The method developed by Zhang, allows continuous culture of *F. prausnitzii* against an intestinal epithelium culture; the system is capable of maintaining the bacteria anaerobically and the cells aerobically (Zhang et al. 2021). Through methods like this we may be able to recreate the gut environment and begin to truly unpick the relationship between bacterial aerotolerance and parasite hatching.

Through my analysis of porcine caecal samples I was able to identify which species may be contributing to *T. suis* hatching. I looked for differently abundant species and found 32 that were more abundant in caecal scrapings (Table 5.4). At the top of the list of associations is *S. pavorubra*. *Sutterella* species are gram negative gastrointestinal tract commensals that have been isolated from pigs and humans (Guevarra et al. 2019; Sakon et al. 2008). They grow in microaerophilic or anaerobic conditions and are mildly pro-inflammatory in humans (Hiippala et al. 2016). The modes of their adherence to the mucosa have been studied and demonstrate that different species display different affinities for the components of the gastrointestinal tract (Hiippala et al. 2016). *S. pavorubra* preferentially adheres to differentiated intestinal epithelial cells, and can even displace *Sutterella wadsworthensis* which preferentially binds to porcine and human mucus (Hiippala et al. 2016). Members of the *Sutterella* genus are clearly intimately associated with the mucosa and it will be interesting to see how the species specific affinities for binding the cells, extracellular matrix (ECM), and mucus of the gastrointestinal tract affect their interactions with *T. suis* eggs and induction of hatching.

The rest of the top 10 associations in the list (Table 5.4) are predominantly uncultured species highlighting the lack of knowledge in the field of porcine gastrointestinal tract commensals. Large scale culturing efforts will need to be matched with the advances in *in silico* analyses (Chen et al. 2021) to ensure that we can isolate these bacteria. Four of these uncultured species are Cyanobacteria and belong to the family Gastranaerophilaceae, two belong to the class Kiritimatiellae, one the class Lentisphaerae, and one the family *Elusimicrobiaceae* (Spring et al. 2016; Cho, Derrien, and Hedlund 2015; Brune 2014; Soo 2015; Bowerman et al. 2020).

The other known association high up on the list is *C. hyointestinalis*, a member of the porcine microbiota (Wilkinson et al. 2018; On et al. 1995). One feature of members of the *Campylobacter* genus and one potential mode for their enrichment in the gastrointestinal tract mucosa is their use of lectin - glycan based adhesion (Rubinchik, Seddon, and Karlyshev 2012; Corbel and Gill 1987). Through their affinity for protein and carbohydrate lectins (Corbel and Gill 1987) *Campylobacter* species adhere to the mucosa and may also adhere to the polar plug, it will be interesting to study how this relates to *T. suis* hatching.

In examining the beta diversity of the humanised microbiota mice, the samples that can induce hatching appear uniform in composition (Figure 5.13). In chapter 1, I reasoned that the factors that can induce hatching should be ubiquitous in the human gut microbiota of individuals globally. Despite *Trichuris* infections being localised to the tropics and subtropics, historically the parasite did and can still infect individuals outside of these regions (Else et al. 2020; Søre et al. 2015; Gildner and Casana 2021; Dige et al. 2017). Additionally, hatching inducing factors are not likely to be derived from one member of the microbiota as redundancy builds a biological safety net (Nowak et al. 1997). The levels of variation displayed in my samples supported this, suggesting that samples with differing compositions can still induce hatching provided they contain suitable factors. In fact, the donor B samples, which were more diverse, induced more hatching of *T. trichiura* than the donor A samples, which were more uniform (Figure 4.5) (Figure 5.13)

I was able to get an understanding of the species present in the humanised microbiota mice that may be involved in hatching by looking at bacterial species that are enriched in caecal scrapings (Table 5.8), and by looking at the species modulated during infections (Table 5.12, 5.13). I did not find any associations when comparing samples that can and cannot induce hatching in either mouse strain. Additionally, in the donor A mice, there were no significant differences between caecal contents and scrapings. In the donor B mice however, 4 species were more abundant in the caecal scrapings: *U. parvum*, *L. acidophilus* and two uncultured strains. *U. parvum* is typically associated with the urogenital mucosa rather than the intestinal mucosa (Paralanov et al. 2012; Yarbrough, Winkle, and Herbst-Kralovetz 2015). *Ureaplasma* spp have been shown to adhere to a variety of human cell types including epithelial cells, this adhesion would facilitate adherence to the gastrointestinal tract and possibly to the polar plug (Torres-Morquecho et al. 2010). Also associated with the caecal scrapings was *L. acidophilus*, a microaerophilic gram positive species that binds to the mucosa through a variety of S-layer proteins (*Slp*) capable of interacting with epithelial and mucus producing cells, components of the ECM, and the intestinal mucus (Xiong et al. 2018; Ortega-Anaya, Marciniak, and Jiménez-Flores 2021; Celebioglu and Svensson 2018; Carmo

et al. 2018). As a well characterised member of the microbiota, found ubiquitously in the gastrointestinal tracts of humans and routinely used as a probiotic supplement, it is an attractive candidate to study for the hatching of *T. trichiura*. If *L. acidophilus* can induce hatching in monocultures *in vitro*, there would also be the opportunity to study the role of various bacterial genes in hatching through the use of *Slp* gene knockouts. The last two species associated with the caecal mucosa were both uncultured species, one a member of the genus *Stomatobaculum* and the other a member of the family *Ruminococcaceae* (Sizova et al. 2013). *Stomatobaculum* is a recently discovered genus with one known species that was isolated from the oral microbiota (Sizova et al. 2013). Members of the *Ruminococcaceae* family are obligate anaerobes, and several have been isolated from the human gastrointestinal tract; the most notable member of the family is perhaps *F. prausnitzii* (Rajilić-Stojanović and de Vos 2014). Together with the results in the human biopsies this suggests that *F. prausnitzii* or *Ruminococcaceae* species generally play a role in the hatching of *T. trichiura*.

Previous studies have demonstrated that infection with *T. muris* alters the composition of the microbiota; this alteration is transient and the microbiota returns to its previous state once the parasite has been expelled (Houlden et al. 2015; Holm et al. 2015). It has been suggested that this alteration to the composition of the microbiota is to prevent further parasite infection as part of the parasite's host evasion mechanisms (White et al. 2018). Based on this information I reasoned that looking at species whose abundance is reduced during infection provides another way to identify bacteria that could be involved in hatching of *T. trichiura*. Several members of the family *Lachnospiraceae* had decreased abundance in mice with adult *T. trichiura* including: an uncultured species assigned to the genus *Dorea* (Shen et al. 2010). One uncultured species classified to the family level (*Lachnospiraceae*), and *Lachnoclostridium edouardi* (Traore et al. 2017). The *Lachnospiraceae* are routinely found in the human gastrointestinal tract and are one of the primary producers of short chain fatty acids; changes in abundance of members of this family have been observed in several inflammatory conditions (Vacca et al. 2020). Better classification of the uncultured species will allow us to select candidates from this family to test for their ability to induce hatching of *T. trichiura*. Another species high on the list is an *Alistipes* species that was recently assigned the name *Alistipes cottocaccae* sp. nov. (Parker et al. 2020; Gilroy et al. 2021). A decrease in *A. cottocaccae* during a *T. trichiura* infection aligns with previous observations in *T. muris* infections and demonstrates that infection with either of the two parasites results in similar alterations to the microbiota. Mice infected with *T. muris* were reported to have a decrease in the abundance of *Bacteroides* species, in particular members of the family *Rikenellaceae* (White et al. 2018; Houlden et al. 2015), of which *A. cottocaccae* is a

member. In addition to being identified *in silico*, *A. cottocaccae* has now been cultured, making it an attractive candidate for further characterisation of its role in *Trichuris* hatching (Gilroy et al. 2021).

Through this analysis, I have been able to demonstrate that as I hypothesised the factors that can induce hatching are ubiquitous in the human gut microbiota. Indeed, bacteria associated with hatching of *T. trichiura* have been identified in one of the biggest families of the human gastrointestinal tract: *Lachnospiraceae*. While this study has been informative it also highlights the challenges of studying the microbiota. Gram positive commensal bacteria dominate the gastrointestinal tract; however, many of these species are novel, and have previously been hard to isolate, culture, and therefore study (Browne et al. 2016). Continued advances in methods of culturing as well as metagenomic analysis, will help us isolate these species and the functions they perform in the gastrointestinal tract (Browne et al. 2016; Parks et al. 2017; Forster et al. 2019; Almeida et al. 2021; Gilroy et al. 2021; C. Chen et al. 2021; Beresford-Jones et al. 2021). In conclusion, the differential abundance analysis in the present chapter has highlighted several bacterial species that would make good candidates for further *in vitro* study for their role in hatching of *T. muris*, *T. suis*, or *T. trichiura*. These species should be cultured and isolated to perform *in vitro* or *in vivo* hatching experiments that utilise single strains or tailored mixes (Browne et al. 2016; Forster et al. 2019; Hayes et al. 2010; White et al. 2018; Vejzagić, Adelfio, et al. 2015).

S. pavirubra is an interesting candidate for the study of hatching in *T. suis*. *A. cottocaccae* and its taxonomic family (Houlden et al. 2015; White et al. 2018) have been implicated in both *T. trichiura* and *T. muris* infections, and it will be interesting to isolate and study *A. cottocaccae* *in vitro* with both these parasites. *F. prauznitzii* has been implicated directly in hatching in analysis of the human biopsies, and the family it resides in has been implicated in infections making it a very interesting candidate. It is well known and characterised as a member of the human gut, and the invention of novel culture methods (Zhang et al. 2021) make *F. prauznitzii* a really fascinating candidate for the development of next generation techniques to study host parasite microbiota relationships in a detailed way. In addition to the aforementioned species, other candidates reported in this chapter will be of particular interest if there are significant associations with parasite hatching and they are reasonably studied and characterised. As discussed, knowledge of aspects of bacterial biology such as the expression of surface proteins and proteases, is complemented by the availability of tools to study and manipulate these bacteria, and will facilitate further studies into the molecular mechanisms surrounding whipworm hatching.

Chapter 6- Discussion and Future Directions

6.1 Key messages and future work

In this thesis I explored my hypotheses regarding hatching in *Trichuris*, which states that First, hatching in *Trichuris*, which is centred around the polar plugs of the eggshell, occurs as a result of physical interaction between the bacteria of the parasite niche and the egg. Second, in addition to physical interaction, hatching also requires enzymatic activity. Last, the parasite niche is defined by the respective host microbiota, in particular the bacterial species residing in the caecal mucosa, and whipworm species preferentially respond to bacteria from their host that express the necessary adhesins and enzymes. I aimed firstly to identify *E. coli* molecule(s) responsible for inducing hatching in *T. muris*. Secondly, to identify intrinsic parasite based and extrinsic host-based factors responsible for hatching. Thirdly, to identify members of the human gut microbiome responsible for *T. trichiura* hatching. We evaluated the physical interactions between bacteria and *T. muris* eggs that can be facilitated by a variety of bacterial surface proteins including fimbriae. I also determined that the degradation around the plugs is primarily driven by serine proteases. These proteases can be either bacterial or larval in origin; through knockout studies I was able to identify bacterial proteases, and through RNAseq I was able to identify proteases of larval origin. Hatching is a process that occurs in the gastrointestinal tract, and through isolating samples from the gastrointestinal tract of pigs, humans, mice and humanised microbiota mice, I was able to demonstrate that the factors required for hatching of *T. muris*, *T. suis*, and *T. trichiura* are preferentially found in the mucosal layers of the site of infection. To my knowledge, this is the first time that *in vitro* hatching of *T. trichiura* in the presence of biologically relevant samples and mouse model samples has been reported. Additionally, I was able to infect a humanised microbiota mouse model with *T. trichiura* for the first time. My metagenomic analysis of the gastrointestinal tract samples I collected revealed the range of bacteria in the host microbiota that can contribute to the hatching of *T. trichiura* induced by the gastrointestinal tract samples. Overall this thesis highlights the power of a multi omic approach in understanding the biology of such a fundamental nematode life cycle process.

T. muris provides a useful model system for studying hatching and has been the driving system allowing us to make the majority of discoveries thus far (Fahmy 1954; Wakelin 1969; Panesar and Croll 1981; Hayes et al. 2010). The ability to study the parasite *in vitro* and *in vivo* has revealed much about its biology. In *in vitro* hatching studies we can examine how

the *T. muris* eggs interact with monocultures (Hayes et al. 2010) (Chapter 3) and through these studies some commonalities and differences have been observed. Bacterial induced hatching of *T. muris* is driven by attachment of bacterial cells to the polar plugs of the egg through various surface projections. Bacterial surface projections vary greatly between species and there are several modes of hatching induction. This was seen in the study by Hayes where they examined hatching dependent on type 1 fimbriae and also fimbriae independent hatching using *E. coli*, *S. typhimurium*, *S. aureus*, and *P. aeruginosa* (Hayes et al. 2010). Additionally, through the electron microscopy conducted by Goulding on co-cultures of these 4 bacteria with *T. muris* eggs displayed differences in their modes of attachment (Goulding 2021) (Chapter 3). It will be interesting to do further studies using higher resolution microscopy and also knockout studies in *S. typhimurium*, *S. aureus*, and *P. aeruginosa* to isolate the genes responsible for the attachment. In particular in *P. aeruginosa*, it will be crucial to identify the attachment structure and confirm if it is type IV pili (Goulding 2021) (Chapter 3). In addition to identifying bacterial adhesion molecules, gaining a greater understanding of the composition of the polar plug will help identify what egg molecules the bacteria are acting upon. Other advanced microscopy techniques such as laser microdissection can help in the study of the polar plugs. Dissected plugs can be analysed using mass spectrometry and hopefully provide more detailed answers on the composition of the plug. As with many strategies the primary considerations are time and labour intensity, and this is an intensive strategy (Chapter 3).

Despite the differences in the surface adhesion molecules of *E. coli*, *S. typhimurium*, *S. aureus*, and *P. aeruginosa*, hatching with these 4 strains of bacteria shares some commonalities. They require proteases to induce hatching of *T. muris*. I observed that inhibition of proteases with an inhibitor cocktail prevents hatching without affecting viability of either bacteria or eggs in a dose dependent manner (Chapter 3). Through my bacterial knockout studies, I identified that *ClpP* in *E. coli* is important for hatching. Similar knockout studies in *S. typhimurium*, *S. aureus*, and *P. aeruginosa* can help to identify other bacterial serine proteases involved in hatching. My findings in *T. muris* regarding bacterial attachment and proteases informed my investigations into the role of extrinsic host factors in hatching of *T. suis* and *T. trichiura*. I investigated if hatching in a system that more closely mimics the gastrointestinal tract environment than bacterial monocultures could also be regulated by protease inhibitors. While the protease inhibitors do modulate hatching, complete ablation was rarely seen in these experiments (Chapter 4). As the response to the protease inhibitor is dose dependent requiring a balance between inhibitor and bacterial load it is not surprising that complete ablation in hatching with crude gastrointestinal tract samples is harder to achieve. We can be encouraged that as we move towards mono cultures for hatching of *T.*

suis and *T. trichiura* we will be able to control bacterial load and get consistent ablation of hatching.

Knowing that hatching in *T. suis* is induced by caecal mucosal scrapings (Vejzagić, Thamsborg, et al. 2015), I reasoned that microbiota collected from each respective host intestinal mucosa, particularly the mucosa of the parasite niche- caecum and ascending colon would induce hatching. This was correct, and I observed varying levels of host specificity, with *T. trichiura* having the greatest specificity (Chapter 4). *T. muris* was shown to exhibit less specificity and in fact, had a greater response to the samples from the donor A mice (Chapter 4, Figure 4.2). One potential reasoning for the increased host specificity between *T. muris* and *T. trichiura* is the relative size of the host and its gastrointestinal tract. *Trichuris* L1 larvae are ~200µm in length (Beer 1973a), however the radial distance in the gastrointestinal tract increases dramatically with the size of the host. In rats the caecum has a radius of ~5mm (Kararli 1995), and in humans it is ~3.5cm (Kararli 1995). In a larger host it benefits the parasite to have increased affinity for the niche; making the difference between successfully establishing an infection, or facing a perilous migration and the risk of expulsion.

The varied specificity of *T. muris* in the *in vitro* studies, as well as evidence of cross host infections where *T. suis* infects humans (Bager et al. 2011), suggest that the limiting factor in making an chronic infection is not the host tissues but the microbiota. I hypothesised that using a mouse with a humanised microbiota that has been demonstrated to induce hatching *in vitro* could be used to generate a sustained infection. The *in vivo* infections of humanised microbiota mice were a useful trial and highlight some important considerations for future trials and refinement of the models. Firstly, it further emphasises that not all microbiota are equal, the donor A mice in addition to decreased *in vitro* hatching of *T. trichiura* also expelled the worms (Chapter 4). Not all humanised mice lines will be capable of supporting an infection, perhaps the ideal situation once we have a finalised list of hatching inducing microbiota, would be to create a mouse with a defined custom microbiota (Steimle et al. 2021). Secondly, in addition to the composition of the microbiota the role of the immune system cannot be ignored; and depending on the application of the mouse model a humanised or depleted immune system may also be required (Chapter 4). Further than the immune system, metabolically, humans and rodents are very different and the gut microbiota is inextricably linked to diet and metabolism. Perhaps these investigations would be more informative in a model that is better matched metabolically. Porcine models have been used for human studies and in the future may even be used for xenographic transplants due to their similarities to humans (Hong and Kim 2019; Sykes and Sachs 2019). There are

humanised immune and microbiota porcine models (Wang and Donovan 2015; Aluthge et al. 2020), and developing porcine gene knockout models has become more feasible with the development of CRISPR based techniques (Ratner et al. 2020). Perhaps developing models for *T. trichiura* hatching and infection in pigs may also yield good results; the primary caveat is that pigs are a less accessible model as they require larger facilities and more resources.

In addition to being utilised to study host parasite interactions *in vivo* infections in mice can be used to generate parasite material (Wakelin 1967; Panesar and Croll 1980; Panesar 1981; Houlden et al. 2015; White et al. 2018). Passaging *T. muris* allows generation of synchronous batches of eggs which I used to study changes in gene expression during embryonation. The changes in gene expression pre and post developing the ability to respond to bacteria for hatching, once again highlighted the role of proteases, this time as intrinsic factors. Identification of these genes is an important step in addressing some of the gaps in our knowledge; for example for several nematode species we know that hatching progresses due to larval participation but we do not know which genes are implicated (Mkandawire et al. 2021). Having generated this list of genes it will be interesting to investigate them using advances in genetic modification of parasites. The development of CRISPR systems to modify parasitic nematodes will allow researchers to develop parasite knockouts and to begin to truly understand the genes that govern the hatching processes (Ward 2015; O'Halloran 2021; Lok 2019). Developing mouse models to passage *T. trichiura* will be an important step in facilitating these kinds of studies in the human whipworm as it will allow us to have a reliable source of synchronous parasite material at all life cycle stages.

The *in vitro* and *in vivo* studies presented thus far have been incredibly informative, and one additional power of my study comes from combining all my observations in hatching and infection with strain level resolution analysis of the microbiota. To my knowledge this is the first study that has examined the bacterial composition of samples with a known capability to induce hatching of *Trichiuris* species. My range of hatching metadata associated with the samples provided several routes to tease out meaningful information and associations from the microbiota. Through examining differences between: regions of the gastrointestinal tract sampled, samples that can and can't induce hatching, as well as naive and infected mice (Chapter 5). This proved to be fortuitous as, in my analysis and the analysis of others, it can be hard to tease apart differences by looking at the sections of the colon alone (Jiao et al. 2021; James et al. 2020). Through my multiple layers of analysis, I was able to identify differences and this approach even allowed me to observe patterns, with certain taxa being

flagged multiple times increasing my confidence in these hits (Chapter 5). Through my analysis I was able to curate a diverse list of candidates for further study, and this diversity increases the chances of a successful screen.

In chapter 5 I presented the candidates I believe warrant further examination and study in the first instance. Screening these candidates and more is an exciting future challenge. Some results not shown in this thesis include the trial work carried out to develop a pipeline for high throughput bacterial screening. I developed and tested a high throughput screening platform that optimises bacterial growth monitoring and quantification of hatching. Many gut commensal species are novel with unknown growth kinetics. Generation times vary between species and may affect the efficiency of assays. The *Trichuris* hatching assay utilises bacteria at stationary phase, therefore monitoring bacterial growth is essential to normalise this across the microbiota. I ran a small pilot study recording OD for several microbiota species, and using GrowthCurver I applied the population equation to my data (Sprouffske and Wagner 2016). GrowthCurver finds the best values of K, r, and N_0 (N_0 = starting population size; K = carrying capacity; r = intrinsic growth rate), allowing researchers to work out the generation times for different bacterial strains. This is an important step for timing the mixing of bacterial and egg co cultures for optimal hatching and will also be important for maximising protease inhibition.

In addition to normalising the set up it will also be good to normalise and automate the counting. I also trialled automated counting using the IncuCyte® ZOOM platform, a cell imaging system that can be used to monitor hatching by taking a time course of images. I trained the machine to count fluorescently labelled *T. muris* larvae during hatching experiments with *E. coli* to get faster and more accurate readouts of percentage hatching. The IncuCyte® is an image-based system so one could apply other machine learning approaches to the raw images such as this method developed to count soybean cyst nematode eggs in soil samples (Akintayo et al. 2018). Taken together, assays like this will enable us to efficiently investigate gut microbiota candidates.

While a high throughput screen of individual members of the host microbiota would be ideal; given that previous monoculture experiments in *T. trichiura* and *T. suis* (Vežagić, Adelfio, et al. 2015) have failed it is prudent to consider that for the parasites with greater host specificity they may require further recapitulation of the host niche to see an effect. This can be achieved by using other novel *in vitro* methods that seek to recreate the gut micro environments including organoids (Puschhof et al. 2021; Duque-Correa, Maizels, et al. 2020; Smith et al. 2021; Duque-Correa et al. 2021). Other possible methods include microfluidics

gut on a chip devices (Xiang et al. 2020), and advanced culturing devices like the GuMI physiome platform (Zhang et al. 2021). The GuMI platform allows for long term culting of highly oxygen sensitive species like *F. prausnitzii* against primary colon cells. The author's study was on 2D cells but the platform is equipped to handle 3D cultures in the form of transwells. A system like this would be an excellent way to study the parasite in the presence of selected bacteria and cell lines or primary tissue cultures.

As demonstrated in chapter 5 metagenomic analysis can provide a strain level resolution of the composition of the microbiota and this led to the identification of some suitable candidates for testing (Chapter 5). However, there is one primary caveat and that is the fact that many strains banked in reference databases have only been isolated *in silico* and there is no physical isolate of the bacteria to study. In order to address this, one consideration for future iterations of this type of study of hatching in *Trichuris* with gastrointestinal tract samples would be to build in a culturomics aspect. Culturomics is the practice of picking colonies for multiple streams of analysis, and this method does result in the generation of live culture isolates for characterisation and functional studies (Chang et al. 2019). Colonies can be identified through mass spec and 16S sequencing. If combined with metagenomic sequencing of the samples, culturomics could offer an easier way to follow up on interesting hits identified through metagenomic analysis. One would simply need to scan the bank of picked colonies for a closest match. While a combined approach does expand the range of this kind of study it is a very labour and time intensive process, and the required number of colonies increases exponentially. Over 30,000 colonies would need to be picked to capture all the 427 OTUs represented in the two humanised microbiota mice lines (Pike 2020). This number is likely to be several orders of magnitude greater for the porcine or human caecum given that over 4000 OTUs have been identified in the human gastrointestinal tract (Nayfach et al. 2019).

In addition to looking for associations and doing taxonomic analysis, I generated MAGs that can be used for *in silico* genomic and functional analysis. One idea would be to repeat the searches carried out on the HBC (Chapter 5) looking at the presence of genes that comprise fimbriae or protease operons. Further to identifying genes of interest, phylogenetic studies can be carried out to study the relationship between isolates from the different hosts. This would allow researchers to study the conservation of genes related to hatching between isolates of interest and identify key similarities e.g. active site composition in proteases. Researchers could ascertain if genes of interest are essential or auxiliary genes, and get an understanding of how they are controlled in individual isolates. Understanding the control of expression can help uncover more synergistic relationships between bacteria and parasites.

The flexible expression of the *fim* operon in *E. coli* likely contributes to the pattern of fimbriae expression seen in cells proximal and distal to the polar plug (Chapter 3). Perhaps the other bacteria involved in hatching control the expression of surface molecules and proteases in a similar manner.

In summary, the gut microbiota contains molecules essential for hatching. These molecules are likely to facilitate a physical interaction and enzymatic activity around the polar plugs; both are required to induce hatching and are presented on the bacteria in specific conformations. While infection is currently segregated to the tropics and subtropics, historically it was global, and individuals from non-endemic countries can still be infected with the worm. It is members of the microbiota found across demographics that are responsible for defining the hatching niche, which is the caecal mucosa. Bacteria isolated from the caecal mucosa of the host induce hatching of *Trichuris* species (*T. muris*, *T. suis*, and *T. trichiura*), and this hatching is facilitated by the expression of serine proteases.

6.2 Concluding remarks

Hatching in nematodes is a fascinating process at the start of the life cycle; that in parasitic nematodes has implications for subsequent infection of the host and thereby survival. Having highlighted the gaps in our knowledge I sought to address some of them. Through the work carried out in this thesis I identified members of the host microbiota that induce hatching, and investigated what features they express that facilitate this. Concluding that proteases in particular serine proteases are crucial to hatching. I investigated parasite intrinsic hatching factors through changes in larval gene expression further cementing a role for proteases in hatching. The knowledge detailed in this thesis opens the way for further investigations that will shed light on the host parasite microbiota interactions involved in the hatching of *Trichuris* species, and will allow us to begin to manipulate them. Assays of this nature will be facilitated by continuing advances in parasite functional genomics, allowing genetic modification of whipworms; and advances in culturing and metagenomics allowing us to isolate crucial members of the microbiota. Achieving this will allow us to further fill in the gaps surrounding hatching and build meaningful models to study *Trichuris* species.

Bibliography

- Abriola, Laura, Denton Hoyer, Conor R. Caffrey, David L. Williams, Timothy P. Yoshino, and Jon J. Vermeire. 2019. "Development and Optimization of a High-Throughput Screening Method Utilizing *Ancylostoma Ceylanicum* Egg Hatching to Identify Novel Anthelmintics." *PloS One* 14 (6): e0217019.
- Akintayo, Adedotun, Gregory L. Tylka, Asheesh K. Singh, Baskar Ganapathysubramanian, Arti Singh, and Soumik Sarkar. 2018. "A Deep Learning Framework to Discern and Count Microscopic Nematode Eggs." *Scientific Reports* 8 (1): 9145.
- Albenberg, Lindsey, Tatiana V. Esipova, Colleen P. Judge, Kyle Bittinger, Jun Chen, Alice Laughlin, Stephanie Grunberg, et al. 2014. "Correlation between Intraluminal Oxygen Gradient and Radial Partitioning of Intestinal Microbiota." *Gastroenterology* 147 (5): 1055–63.e8.
- Almeida, Alexandre, Stephen Nayfach, Miguel Boland, Francesco Strozzi, Martin Beracochea, Zhou Jason Shi, Katherine S. Pollard, et al. 2021. "A Unified Catalog of 204,938 Reference Genomes from the Human Gut Microbiome." *Nature Biotechnology* 39 (1): 105–14.
- Alneberg, Johannes, Brynjar Smari Bjarnason, Ino de Bruijn, Melanie Schirmer, Joshua Quick, Umer Z. Ijaz, Nicholas J. Loman, Anders F. Andersson, and Christopher Quince. 2013. "CONCOCT: Clustering cONTigs on COverage and ComposiTion." *arXiv [q-bio.GN]*. arXiv. <http://arxiv.org/abs/1312.4038>.
- Aluthge, Nirosh D., Wesley A. Tom, Alison C. Bartenslager, Thomas E. Burkey, Phillip S. Miller, Kelly D. Heath, Craig Kreikemeier-Bower, et al. 2020. "Differential Longitudinal Establishment of Human Fecal Bacterial Communities in Germ-Free Porcine and Murine Models." *Communications Biology* 3 (1): 760.
- Anders, Simon, and Wolfgang Huber. 2012. "Differential Expression of RNA-Seq Data at the Gene Level—the DESeq Package." *Heidelberg, Germany: European Molecular Biology Laboratory (EMBL)* 10: f1000research.
- Anders, Simon, Paul Theodor Pyl, and Wolfgang Huber. 2014. "HTSeq—a Python Framework to Work with High-Throughput Sequencing Data." *Bioinformatics* 31 (2): 166–69.
- Appleton, C. C., and B. J. White. 1989. "The Structure of the Shell and Polar Plugs of the Egg of the Whipworm, *Trichuris Trichiura* (Nematoda: Trichuridae) from the Samango Monkey (*Cercopithecus Albogularis*)." *The Onderstepoort Journal of Veterinary Research* 56 (4): 219–21.
- Bager, Peter, Christian Kapel, Allan Roepstorff, Stig Thamsborg, John Arnved, Steen Rønborg, Bjarne Kristensen, Lars K. Poulsen, Jan Wohlfahrt, and Mads Melbye. 2011. "Symptoms after Ingestion of Pig Whipworm *Trichuris Suis* Eggs in a Randomized Placebo-Controlled Double-Blind Clinical Trial." *PloS One* 6 (8): e22346.
- Bai, Li, Shengli Xia, Ruiting Lan, Liyun Liu, Changyun Ye, Yiting Wang, Dong Jin, et al. 2012. "Isolation and Characterization of Cytotoxic, Aggregative *Citrobacter Freundii*." *PloS One* 7 (3): e33054.
- Balakrishnan, Arjun, Sandhya A. Marathe, Madhura Joglekar, and Dipshikha Chakravorty. 2013. "Bactericidal/permeability Increasing Protein: A Multifaceted Protein with Functions beyond LPS Neutralization." *Innate Immunity* 19 (4): 339–47.
- Baldwin, J. G., and Z. A. Handoo. 2018. "General Morphology of Cyst Nematodes." In *Cyst Nematodes*, 337–64. Wallingford: CABI.
- Bancroft, A. J., K. J. Else, and R. K. Grencis. 1994. "Low-Level Infection with *Trichuris Muris* Significantly Affects the Polarization of the CD4 Response." *European Journal of Immunology* 24 (12): 3113–18.
- Bankevich, Anton, Sergey Nurk, Dmitry Antipov, Alexey A. Gurevich, Mikhail Dvorkin, Alexander S. Kulikov, Valery M. Lesin, et al. 2012. "SPAdes: A New Genome Assembly

- Algorithm and Its Applications to Single-Cell Sequencing." *Journal of Computational Biology: A Journal of Computational Molecular Cell Biology* 19 (5): 455–77.
- Baron, E. J., P. Summanen, J. Downes, M. C. Roberts, H. Wexler, and S. M. Finegold. 1989. "Bilophila Wadsworthia, Gen. Nov. and Sp. Nov., a Unique Gram-Negative Anaerobic Rod Recovered from Appendicitis Specimens and Human Faeces." *Journal of General Microbiology* 135 (12): 3405–11.
- Bazan, J. F., and R. J. Fletterick. 1988. "Viral Cysteine Proteases Are Homologous to the Trypsin-like Family of Serine Proteases: Structural and Functional Implications." *Proceedings of the National Academy of Sciences of the United States of America* 85 (21): 7872–76.
- Beamer, L. J., S. F. Carroll, and D. Eisenberg. 1997. "Crystal Structure of Human BPI and Two Bound Phospholipids at 2.4 Angstrom Resolution." *Science* 276 (5320): 1861–64.
- Beckmann, G., and P. Bork. 1993. "An Adhesive Domain Detected in Functionally Diverse Receptors." *Trends in Biochemical Sciences* 18 (2): 40–41.
- Beer, R. J. 1973a. "Morphological Descriptions of the Egg and Larval Stages of Trichuris Suis Schrank, 1788." *Parasitology* 67 (3): 263–78.
- . 1973b. "Studies on the Biology of the Life-Cycle of Trichuris Suis Schrank, 1788." *Parasitology* 67 (3): 253–62.
- Bellaby, T., K. Robinson, D. Wakelin, and J. M. Behnke. 1995. "Isolates of Trichuris Muris Vary in Their Ability to Elicit Protective Immune Responses to Infection in Mice." *Parasitology* 111 (Pt 3) (September): 353–57.
- Beloin, C., A. Roux, and J. M. Ghigo. 2008. "Escherichia Coli Biofilms." *Current Topics in Microbiology and Immunology* 322: 249–89.
- Bennett, G. N., J. G. H. Hickford, and H. Zhou. 2006. "Convenient Anaerobic Techniques, Science from the Supermarket Shelf." *Anaerobe* 12 (1): 49–51.
- Beresford-Jones, Benjamin S., Samuel C. Forster, Mark D. Stares, George Notley, Elisa Viciani, Hilary P. Browne, Nitin Kumar, et al. 2021. "Functional and Taxonomic Comparison of Mouse and Human Gut Microbiotas Using Extensive Culturing and Metagenomics." *bioRxiv*. <https://doi.org/10.1101/2021.02.11.430759>.
- Bhandari, Vaibhav, Keith S. Wong, Jin Lin Zhou, Mark F. Mabanglo, Robert A. Batey, and Walid A. Houry. 2018. "The Role of ClpP Protease in Bacterial Pathogenesis and Human Diseases." *ACS Chemical Biology* 13 (6): 1413–25.
- Bingle, Lynne, Vanessa Singleton, and Colin D. Bingle. 2002. "The Putative Ovarian Tumour Marker Gene HE4 (WFDC2), Is Expressed in Normal Tissues and Undergoes Complex Alternative Splicing to Yield Multiple Protein Isoforms." *Oncogene* 21 (17): 2768–73.
- Bird, Alan F. 1977. "Cuticle Formation and Moulting in the Egg of Meloidogyne Javanica (Nematoda)." *Parasitology* 74 (2): 149–52.
- Bird, Alan F., and M. A. McClure. 1976. "The Tylenchid (Nematoda) Egg Shell: Structure, Composition and Permeability." *Parasitology*. <https://doi.org/10.1017/s0031182000043158>.
- Blaxter, Mark, and Georgios Koutsovoulos. 2015. "The Evolution of Parasitism in Nematoda." *Parasitology* 142 Suppl 1 (February): S26–39.
- Blaxter, M. L., P. De Ley, J. R. Garey, L. X. Liu, P. Scheldeman, A. Vierstraete, J. R. Vanfleteren, et al. 1998. "A Molecular Evolutionary Framework for the Phylum Nematoda." *Nature* 392 (6671): 71–75.
- Blighe, Kevin, Sharmila Rana, and Myles Lewis. 2019. "EnhancedVolcano: Publication-Ready Volcano Plots with Enhanced Colouring and Labeling." *R Package Version 1* (0).
- Bowerman, Kate L., Saima Firdous Rehman, Annalicia Vaughan, Nancy Lachner, Kurtis F. Budden, Richard Y. Kim, David L. A. Wood, et al. 2020. "Disease-Associated Gut Microbiome and Metabolome Changes in Patients with Chronic Obstructive Pulmonary Disease." *Nature Communications* 11 (1): 5886.
- Bridge, J. 1974. "Hatching of Tylenchorhynchus Maximus and Merlinius Icarus." *Journal of Nematology* 6 (2): 101–2.
- Browne, Hilary P., Samuel C. Forster, Blessing O. Anonye, Nitin Kumar, B. Anne Neville, Mark D. Stares, David Goulding, and Trevor D. Lawley. 2016. "Culturing of

- 'Unculturable' Human Microbiota Reveals Novel Taxa and Extensive Sporulation." *Nature* 533 (7604): 543–46.
- Brundage, L., L. Avery, A. Katz, U. J. Kim, J. E. Mendel, P. W. Sternberg, and M. I. Simon. 1996. "Mutations in a *C. Elegans* Gqalpha Gene Disrupt Movement, Egg Laying, and Viability." *Neuron* 16 (5): 999–1009.
- Brune, Andreas. 2014. "The Family Elusimicrobiaceae." In *The Prokaryotes: Other Major Lineages of Bacteria and The Archaea*, edited by Eugene Rosenberg, Edward F. DeLong, Stephen Lory, Erko Stackebrandt, and Fabiano Thompson, 637–40. Berlin, Heidelberg: Springer Berlin Heidelberg.
- Burden, D. J., and N. C. Hammet. 1976. "A Comparison of the Infectivity of *Trichuris Suis* Ova Embryonated by Four Different Methods." *Veterinary Parasitology* 2 (3): 307–11.
- Burden, D. J., N. C. Hammet, and P. A. Brookes. 1987. "Field Observations on the Longevity of *Trichuris Suis* Ova." *The Veterinary Record* 121 (2): 43.
- Cadwell, Kenneth. 2020. "Spontaneous Hatching of *T. Muris*," June 30, 2020. (Personal Communication)
- Caldwell, Fred C., and Elfreda L. Caldwell. 1928. "Preliminary Report on Observations on the Development of Ova of Pig and Human *Ascaris* under Natural Conditions, and Studies of Factors Influencing Development." *The Journal of Parasitology* 14 (4): 254–60.
- Canny, Geraldine, and Ofer Levy. 2008. "Bactericidal/permeability-Increasing Protein (BPI) and BPI Homologs at Mucosal Sites." *Trends in Immunology* 29 (11): 541–47.
- Cantacessi, Cinzia, Paul Giacomini, John Croese, Martha Zakrzewski, Javier Sotillo, Leisa McCann, Matthew J. Nolan, Makedonka Mitreva, Lutz Krause, and Alex Loukas. 2014. "Impact of Experimental Hookworm Infection on the Human Gut Microbiota." *The Journal of Infectious Diseases* 210 (9): 1431–34.
- Carmo, Fillipe L. R. do, Fillipe L. R. do Carmo, Houem Rabah, Rodrigo D. De Oliveira Carvalho, Floriane Gaucher, Barbara F. Cordeiro, Sara H. da Silva, Yves Le Loir, Vasco Azevedo, and Gwénaél Jan. 2018. "Extractable Bacterial Surface Proteins in Probiotic–Host Interaction." *Frontiers in Microbiology*. <https://doi.org/10.3389/fmicb.2018.00645>.
- Castagnone-Sereno, P. 2006. "Genetic Variability and Adaptive Evolution in Parthenogenetic Root-Knot Nematodes." *Heredity* 96 (4): 282–89.
- "CDC, Parasites - Trichuriasis." 2019. April 25, 2019. <https://www.cdc.gov/parasites/whipworm/biology.html>.
- Celebioglu, Hasan Ufuk, and Birte Svensson. 2018. "Dietary Nutrients, Proteomes, and Adhesion of Probiotic Lactobacilli to Mucin and Host Epithelial Cells." *Microorganisms* 6 (3). <https://doi.org/10.3390/microorganisms6030090>.
- Chang, Yuxiao, Fengyi Hou, Zhiyuan Pan, Zongyu Huang, Ni Han, Lei Bin, Huimin Deng, et al. 2019. "Optimization of Culturomics Strategy in Human Fecal Samples." *Frontiers in Microbiology* 10 (December): 2891.
- Charlier, J., L. Rinaldi, V. Musella, H. W. Ploeger, C. Chartier, H. Rose Vineer, B. Hinney, et al. 2020. "Initial Assessment of the Economic Burden of Major Parasitic Helminth Infections to the Ruminant Livestock Industry in Europe." *Preventive Veterinary Medicine* 182 (105103): 105103.
- Chaumeil, Pierre-Alain, Aaron J. Mussig, Philip Hugenholtz, and Donovan H. Parks. 2019. "GTDB-Tk: A Toolkit to Classify Genomes with the Genome Taxonomy Database." *Bioinformatics*, November. <https://doi.org/10.1093/bioinformatics/btz848>.
- CHEBI. 2021. "Leupeptin (CHEBI:6426)." 2021. <https://www.ebi.ac.uk/chebi/searchId.do?chebiId=6426>.
- Chen, Congying, Yunyan Zhou, Hao Fu, Xinwei Xiong, Shaoming Fang, Hui Jiang, Jinyuan Wu, Hui Yang, Jun Gao, and Lusheng Huang. 2021. "Expanded Catalog of Microbial Genes and Metagenome-Assembled Genomes from the Pig Gut Microbiome." *Nature Communications* 12 (1): 1106.
- Chen, Hongliang, Matteo Mozzicafreddo, Elisa Pierella, Vanessa Carletti, Angela Piersanti, Said M. Ali, Shaali M. Ame, Chunfeng Wang, and Cristina Miceli. 2021. "Dissection of the Gut Microbiota in Mothers and Children with Chronic *Trichuris Trichiura* Infection in

- Pemba Island, Tanzania." *Parasites & Vectors* 14 (1): 62.
- Chen, Qi, Wei Chen, Ashutosh Kumar, Xi Jiang, Matej Janezic, Kam Y. J. Zhang, and Qing Yang. 2021. "Crystal Structure and Structure-Based Discovery of Inhibitors of the Nematode Chitinase CeCht1." *Journal of Agricultural and Food Chemistry* 69 (11): 3519–26.
- Chen, Yi-Wen, Ching-Hao Teng, Yu-Hsuan Ho, Tien Yu Jessica Ho, Wen-Chun Huang, Masayuki Hashimoto, I-Yuan Chiang, and Chien-Sheng Chen. 2014. "Identification of Bacterial Factors Involved in Type 1 Fimbria Expression Using an Escherichia Coli K12 Proteome Chip." *Molecular & Cellular Proteomics*.
<https://doi.org/10.1074/mcp.m113.035667>.
- Chiejina, S. N. 1982. "Evaluation of Modified Baermann Apparatus for the Recovery of Infective Trichostrongylid Larvae from Herbage Samples." *Journal of Helminthology* 56 (2): 105–9.
- Chitwood, D. J., and R. N. Perry. 2009. "Reproduction, Physiology and Biochemistry." In *Root-Knot Nematodes*, 182–200. Wallingford: CABI.
- Choi, Jun Ho, Sang Kyun Park, Mi Kyung Park, Shin Ae Kang, Dain Lee, So Myong Song, Hye Jin Kim, Sung Hee Park, Eun-Min Kim, and Hak Sun Yu. 2019. "An Advanced Protocol for the Purification of Whipworm Eggs from Feces for Use as Therapeutic Agents." *Parasitology International* 70 (June): 41–45.
- Cho, Jang-Cheon, Muriel Derrien, and Brian P. Hedlund. 2015. "Lentisphaeria Class. Nov." In *Bergey's Manual of Systematics of Archaea and Bacteria*, 1–1. Chichester, UK: John Wiley & Sons, Ltd. <https://doi.org/10.1002/9781118960608.cbm00038>.
- Ciccarelli, Francesca D., Tobias Doerks, Christian von Mering, Christopher J. Creevey, Berend Snel, and Peer Bork. 2006. "Toward Automatic Reconstruction of a Highly Resolved Tree of Life." *Science* 311 (5765): 1283–87.
- Clarke, A. J., P. M. Cox, and A. M. Shepherd. 1967. "The Chemical Composition of the Egg Shells of the Potato Cyst-Nematode, *Heterodera rostochiensis* Woll." *Biochemical Journal* 104 (3): 1056–60.
- Cooper, Philip, Alan W. Walker, Jorge Reyes, Martha Chico, Susannah J. Salter, Maritza Vaca, and Julian Parkhill. 2013. "Patent Human Infections with the Whipworm, *Trichuris Trichiura*, Are Not Associated with Alterations in the Faecal Microbiota." *PLoS ONE*.
<https://doi.org/10.1371/journal.pone.0076573>.
- Corbel, M. J., and K. P. Gill. 1987. "Lectin Agglutination of Thermophilic *Campylobacter* Species." *Veterinary Microbiology* 15 (1-2): 163–73.
- Cotton, James A., Catherine J. Lilley, Laura M. Jones, Taisei Kikuchi, Adam J. Reid, Peter Thorpe, Isheng J. Tsai, et al. 2014. "The Genome and Life-Stage Specific Transcriptomes of *Globodera pallida* Elucidate Key Aspects of Plant Parasitism by a Cyst Nematode." *Genome Biology* 15 (3): R43.
- Crespo-Piazuelo, Daniel, Jordi Estellé, Manuel Revilla, Lourdes Criado-Mesas, Yuliaxis Ramayo-Caldas, Cristina Óvilo, Ana I. Fernández, Maria Ballester, and Josep M. Folch. 2018. "Characterization of Bacterial Microbiota Compositions along the Intestinal Tract in Pigs and Their Interactions and Functions." *Scientific Reports* 8 (1): 12727.
- Croll, N. A. 1974. "*Necator americanus*: Activity Patterns in the Egg and the Mechanism of Hatching." *Experimental Parasitology* 35 (1): 80–85.
- Cronin, D., Y. Moenne-Loccoz, A. Fenton, C. Dunne, D. N. Dowling, and F. O'gara. 1997. "Role of 2,4-Diacetylphloroglucinol in the Interactions of the Biocontrol Pseudomonad Strain F113 with the Potato Cyst Nematode *Globodera rostochiensis*." *Applied and Environmental Microbiology* 63 (4): 1357–61.
- Crouzet, Marc, Stéphane Claverol, Anne-Marie Lomenech, Caroline Le Sénéchal, Patricia Costaglioli, Christophe Barthe, Bertrand Garbay, Marc Bonneau, and Sébastien Vilain. 2017. "Pseudomonas Aeruginosa Cells Attached to a Surface Display a Typical Proteome Early as 20 Minutes of Incubation." *PloS One* 12 (7): e0180341.
- Curtis, R. H. C., A. F. Robinson, and R. N. Perry. 2009. "Hatch and Host Location." In *Root-Knot Nematodes*, 139–62. Wallingford: CABI.
- Derrien, Muriel, M. Carmen Collado, Kaouther Ben-Amor, Seppo Salminen, and Willem M.

- de Vos. 2008. "The Mucin Degradator Akkermansia Muciniphila Is an Abundant Resident of the Human Intestinal Tract." *Applied and Environmental Microbiology* 74 (5): 1646–48.
- Dige, A., T. K. Rasmussen, P. Nejsum, R. Hagemann-Madsen, A. R. Williams, J. Agnholt, J. F. Dahlerup, and C. L. Hvas. 2017. "Mucosal and Systemic Immune Modulation by Trichuris Trichiura in a Self-Infected Individual." *Parasite Immunology* 39 (1). <https://doi.org/10.1111/pim.12394>.
- Ding, Mei, Alexandr Goncharov, Yishi Jin, and Andrew D. Chisholm. 2003. "C. Elegans Ankyrin Repeat Protein VAB-19 Is a Component of Epidermal Attachment Structures and Is Essential for Epidermal Morphogenesis." *Development (Cambridge, England)* 130 (23): 5791–5801.
- Dobson, A., K. D. Lafferty, A. M. Kuris, R. F. Hechinger, and W. Jetz. 2008. "Homage to Linnaeus: How Many Parasites? How Many Hosts?" *Proceedings of the National Academy of Sciences*. <https://doi.org/10.1073/pnas.0803232105>.
- Donaldson, Gregory P., S. Melanie Lee, and Sarkis K. Mazmanian. 2016. "Gut Biogeography of the Bacterial Microbiota." *Nature Reviews. Microbiology* 14 (1): 20–32.
- Doncaster, C. C., and Audrey M. Shepherd. 1967. "The Behaviour of Second-Stage Heterodera Rostochiensis Larvae Leading to Their Emergence from the Egg." *Nematologica* 13 (3): 476–78.
- Don Whitely Scientific. 2020. "Anaerobic Workstations vs Anaerobic Jars: What Are the Real Benefits?" 2020. <https://www.dwscientific.com/blog/anaerobic-workstations-vs-anaerobic-jars>.
- Duceppe, Marc-Olivier, Joël Lafond-Lapalme, Juan Emilio Palomares-Rius, Michaël Sabeh, Vivian Blok, Peter Moffett, and Benjamin Mimee. 2017. "Analysis of Survival and Hatching Transcriptomes from Potato Cyst Nematodes, Globodera Rostochiensis and G. Pallida." *Scientific Reports* 7 (1): 3882.
- Duncan, Sylvia H., Georgina L. Hold, Hermie J. M. Harmsen, Colin S. Stewart, and Harry J. Flint. 2002. "Growth Requirements and Fermentation Products of Fusobacterium Prausnitzii, and a Proposal to Reclassify It as Faecalibacterium Prausnitzii Gen. Nov., Comb. Nov." *International Journal of Systematic and Evolutionary Microbiology* 52 (Pt 6): 2141–46.
- Duque-Correa, M. A., D. Goulding, F. H. Rodgers, and C. Cormie. 2021. "Defining the Early Stages of Intestinal Colonisation by Whipworms." *bioRxiv*. <https://www.biorxiv.org/content/10.1101/2020.08.21.261586.abstract>.
- Duque-Correa, M. A., Natasha A. Karp, Catherine McCarthy, Simon Forman, David Goulding, Geetha Sankaranarayanan, Timothy P. Jenkins, et al. 2019. "Exclusive Dependence of IL-10Rα Signalling on Intestinal Microbiota Homeostasis and Control of Whipworm Infection." *PLoS Pathogens* 15 (1): e1007265.
- Duque-Correa, María A., Rick M. Maizels, Richard K. Grencis, and Matthew Berriman. 2020. "Organoids - New Models for Host-Helminth Interactions." *Trends in Parasitology* 36 (2): 170–81.
- Duque-Correa, María A., Fernanda Schreiber, Faye H. Rodgers, David Goulding, Sally Forrest, Ruby White, Amy Buck, Richard K. Grencis, and Matthew Berriman. 2020. "Development of Caecaloids to Study Host-pathogen Interactions: New Insights into Immunoregulatory Functions of Trichuris Muris Extracellular Vesicles in the Caecum." *International Journal for Parasitology* 50 (9): 707–18.
- Duque- Correa, Maria, and Dave Goulding. 2017. "SEM and TEM of the Interactions between E. coli MG1655 and T. muris." (Unpublished Data)
- Ebino, K. Y. 1993. "Studies on Coprophagy in Experimental Animals." *Jikken Dobutsu. Experimental Animals* 42 (1): 1–9.
- "E. Coli Proteases." 2021. 2021. <https://www.uni-due.de/zmb/microbiology/e-coli-proteases.php>.
- "E. Coli Proteases - Serine Proteases." 2021. 2021. <https://www.uni-due.de/zmb/microbiology/serine-proteases.php>.
- Eichenberger, Ramon M., Md Hasanuzzaman Talukder, Matthew A. Field, Phurpa

- Wangchuk, Paul Giacomini, Alex Loukas, and Javier Sotillo. 2018. "Characterization of Trichuris Muris Secreted Proteins and Extracellular Vesicles Provides New Insights into Host-parasite Communication." *Journal of Extracellular Vesicles* 7 (1): 1428004.
- Else, Kathryn J., Jennifer Keiser, Celia V. Holland, Richard K. Grencis, David B. Sattelle, Ricardo T. Fujiwara, Lilian L. Bueno, Samuel O. Asaolu, Oluyomi A. Sowemimo, and Philip J. Cooper. 2020. "Whipworm and Roundworm Infections." *Nature Reviews. Disease Primers* 6 (1): 44.
- EMBL-EBI. 2021. "GO:0004252." 2021. <https://www.ebi.ac.uk/QuickGO/term/GO:0004252>.
- Entchev, Eugeni V., and Teymuraz V. Kurzchalia. 2005. "Requirement of Sterols in the Life Cycle of the Nematode Caenorhabditis Elegans." *Seminars in Cell & Developmental Biology* 16 (2): 175–82.
- Eves-van den Akker, S., and J. T. Jones. 2018. "Genomics and Transcriptomics - a Revolution in the Study of Cyst Nematode Biology." In *Cyst Nematodes*, 27–43. Wallingford: CABI.
- Fahmy, M. A. 1954. "An Investigation on the Life Cycle of Trichuris Muris." *Parasitology* 44 (1-2): 50–57.
- Feng, Zhou, Wenmin Long, Binhan Hao, Ding Ding, Xiaoqing Ma, Liping Zhao, and Xiaoyan Pang. 2017. "A Human Stool-Derived Bilophila Wadsworthia Strain Caused Systemic Inflammation in Specific-Pathogen-Free Mice." *Gut Pathogens* 9 (October): 59.
- Fitzgerald, Cormac Brian, Andrey N. Shkoporov, Thomas D. S. Sutton, Andrei V. Chaplin, Vimalkumar Velayudhan, R. Paul Ross, and Colin Hill. 2018. "Comparative Analysis of Faecalibacterium Prausnitzii Genomes Shows a High Level of Genome Plasticity and Warrants Separation into New Species-Level Taxa." *BMC Genomics* 19 (1): 931.
- Flynn, Julia M., Saskia B. Neher, Yong In Kim, Robert T. Sauer, and Tania A. Baker. 2003. "Proteomic Discovery of Cellular Substrates of the ClpXP Protease Reveals Five Classes of ClpX-Recognition Signals." *Molecular Cell* 11 (3): 671–83.
- Forman, Ruth, Frederick A. Partridge, David B. Sattelle, and Kathryn J. Else. 2021. "Un-'Egg'-Plored: Characterisation of Embryonation in the Whipworm Model Organism Trichuris Muris." *Frontiers in Tropical Diseases*. <https://doi.org/10.3389/fitd.2021.790311>.
- Forster, Samuel C., Simon Clare, Benjamin S. Beresford-Jones, Katherine Harcourt, George Notley, Mark Stares, Nitin Kumar, et al. 2021. "Novel Gut Pathobionts Confound Results in a Widely Used Mouse Model of Human Inflammatory Disease." *bioRxiv*. <https://doi.org/10.1101/2021.02.09.430393>.
- Forster, Samuel C., Nitin Kumar, Blessing O. Anonye, Alexandre Almeida, Elisa Viciani, Mark D. Stares, Matthew Dunn, et al. 2019. "A Human Gut Bacterial Genome and Culture Collection for Improved Metagenomic Analyses." *Nature Biotechnology* 37 (2): 186–92.
- Foster, Timothy J., Joan A. Geoghegan, Vannakambadi K. Ganesh, and Magnus Höök. 2014. "Adhesion, Invasion and Evasion: The Many Functions of the Surface Proteins of Staphylococcus Aureus." *Nature Reviews. Microbiology* 12 (1): 49–62.
- Foth, Bernardo J., Isheng J. Tsai, Adam J. Reid, Allison J. Bancroft, Sarah Nichol, Alan Tracey, Nancy Holroyd, et al. 2014. "Whipworm Genome and Dual-Species Transcriptome Analyses Provide Molecular Insights into an Intimate Host-Parasite Interaction." *Nature Genetics*. <https://doi.org/10.1038/ng.3010>.
- Geenen, P. L., J. Bresciani, J. Boes, A. Pedersen, L. Eriksen, H. P. Fagerholm, and P. Nansen. 1999. "The Morphogenesis of Ascaris Suum to the Infective Third-Stage Larvae within the Egg." *The Journal of Parasitology* 85 (4): 616–22.
- Gerardo, S. H., M. M. Garcia, H. M. Wexler, and S. M. Finegold. 1998. "Adherence of Bilophila Wadsworthia to Cultured Human Embryonic Intestinal Cells." *Anaerobe* 4 (1): 19–27.
- Ghai, Ria R., Noah D. Simons, Colin A. Chapman, Patrick A. Omeja, T. Jonathan Davies, Nelson Ting, and Tony L. Goldberg. 2014. "Hidden Population Structure and Cross-Species Transmission of Whipworms (Trichuris Sp.) in Humans and Non-Human Primates in Uganda." *PLoS Neglected Tropical Diseases*.

- <https://doi.org/10.1371/journal.pntd.0003256>.
- Gildner, Theresa E., and Jesse Casana. 2021. "Intestinal Parasitic Infection within a Wealthy Nineteenth Century Household from Rural New England: Evidence from Dartmouth College, New Hampshire." *Journal of Archaeological Science: Reports* 37 (June): 102990.
- Gilroy, Rachel, Anuradha Ravi, Maria Getino, Isabella Pursley, Daniel L. Horton, Nabil-Fareed Alikhan, Dave Baker, et al. 2021. "Extensive Microbial Diversity within the Chicken Gut Microbiome Revealed by Metagenomics and Culture." *PeerJ*. <https://doi.org/10.7717/peerj.10941>.
- Goulding, David. 2021. "SEM of *T. muris* Eggs with *Escherichia coli*, *Pseudomonas Aeruginosa*, *Staphylococcus Aureus*, and *Salmonella Typhimurium*." (Unpublished Data)
- Grasberger, B. L., G. M. Clore, and A. M. Gronenborn. 1994. "High-Resolution Structure of Ascaris Trypsin Inhibitor in Solution: Direct Evidence for a pH-Induced Conformational Transition in the Reactive Site." *Structure* 2 (7): 669–78.
- "GTDB - GCA_900317525.1." 2021. 2021. https://gtdb.ecogenomic.org/genomes?gid=GCA_900317525.1.
- Guevarra, Robin B., Jun Hyung Lee, Sun Hee Lee, Min-Jae Seok, Doo Wan Kim, Bit Na Kang, Timothy J. Johnson, Richard E. Isaacson, and Hyeun Bum Kim. 2019. "Piglet Gut Microbial Shifts Early in Life: Causes and Effects." *Journal of Animal Science and Biotechnology* 10 (January): 1.
- Halbrendt, J. M., and D. J. Brown. 1992. "Morphometric Evidence for Three Juvenile Stages in Some Species of *Xiphinema Americanum* Sensu Lato." *Journal of Nematology* 24 (2): 305–9.
- Hall, David H., Laura A. Herndon, and Zeynep Altun. 2017a. "WormAtlas Embryo Handbook - Introduction to *C. Elegans* Embryo Anatomy, 6 Hatching." *WormAtlas*. <https://doi.org/10.3908/wormatlas.4.1>.
- . 2017b. "WormAtlas Embryo Handbook - Introduction to *C. Elegans* Embryo Anatomy, 6 Hatching." *WormAtlas*. <https://doi.org/10.3908/wormatlas.4.1>.
- Hamrick, T. S., S. L. Harris, P. A. Spears, E. A. Havell, J. R. Horton, P. W. Russell, and P. E. Orndorff. 2000. "Genetic Characterization of *Escherichia Coli* Type 1 Pilus Adhesin Mutants and Identification of a Novel Binding Phenotype." *Journal of Bacteriology* 182 (14): 4012–21.
- Han, Q., L. Eriksen, J. Boes, and P. Nansen. 2000. "Effects of Bile on the in Vitro Hatching, Exsheathment, and Migration of *Ascaris Suum* Larvae." *Parasitology Research* 86 (8): 630–33.
- Hasman, H., M. A. Schembri, and P. Klemm. 2000. "Antigen 43 and Type 1 Fimbriae Determine Colony Morphology of *Escherichia Coli* K-12." *Journal of Bacteriology*. <https://jlb.asm.org/content/182/4/1089.short>.
- Hayes, K. S., A. J. Bancroft, M. Goldrick, C. Portsmouth, I. S. Roberts, and R. K. Grencis. 2010. "Exploitation of the Intestinal Microflora by the Parasitic Nematode *Trichuris Muris*." *Science* 328 (5984): 1391–94.
- Hiippala, Kaisa, Veera Kainulainen, Marko Kalliomäki, Perttu Arkkila, and Reetta Satokari. 2016. "Mucosal Prevalence and Interactions with the Epithelium Indicate Commensalism of *Sutterella* Spp." *Frontiers in Microbiology* 7 (October): 1706.
- Hishida, R., T. Ishihara, K. Kondo, and I. Katsura. 1996. "Hch-1, a Gene Required for Normal Hatching and Normal Migration of a Neuroblast in *C. Elegans*, Encodes a Protein Related to TOLL and BMP-1." *The EMBO Journal* 15 (16): 4111–22.
- Ho, D. H., K. Badellino, F. A. Baglia, and P. N. Walsh. 1998. "A Binding Site for Heparin in the Apple 3 Domain of Factor XI." *The Journal of Biological Chemistry* 273 (26): 16382–90.
- Holm, Jacob Bak, Daniel Sorobetea, Pia Kiillerich, Yuliaxis Ramayo-Caldas, Jordi Estellé, Tao Ma, Lise Madsen, Karsten Kristiansen, and Marcus Svensson-Frej. 2015. "Chronic *Trichuris Muris* Infection Decreases Diversity of the Intestinal Microbiota and Concomitantly Increases the Abundance of Lactobacilli." *PloS One* 10 (5): e0125495.

- Hong, Kwonho, and Jin-Hoi Kim. 2019. "Humanized Pig Center." *Impact* 2019 (3): 12–14.
- Houlden, Ashley, Kelly S. Hayes, Allison J. Bancroft, John J. Worthington, Ping Wang, Richard K. Grencis, and Ian S. Roberts. 2015. "Chronic *Trichuris Muris* Infection in C57BL/6 Mice Causes Significant Changes in Host Microbiota and Metabolome: Effects Reversed by Pathogen Clearance." *PloS One* 10 (5): e0125945.
- Howe, Kevin L., Bruce J. Bolt, Myriam Shafie, Paul Kersey, and Matthew Berriman. 2017. "WormBase ParaSite - a Comprehensive Resource for Helminth Genomics." *Molecular and Biochemical Parasitology* 215 (July): 2–10.
- Huerta-Cepas, Jaime, Damian Szklarczyk, Davide Heller, Ana Hernández-Plaza, Sofia K. Forslund, Helen Cook, Daniel R. Mende, et al. 2019. "eggNOG 5.0: A Hierarchical, Functionally and Phylogenetically Annotated Orthology Resource Based on 5090 Organisms and 2502 Viruses." *Nucleic Acids Research* 47 (D1): D309–14.
- Hyatt, Doug, Gwo-Liang Chen, Philip F. Locascio, Miriam L. Land, Frank W. Larimer, and Loren J. Hauser. 2010. "Prodigal: Prokaryotic Gene Recognition and Translation Initiation Site Identification." *BMC Bioinformatics* 11 (March): 119.
- Inatomi, Seiiti. 1957. "A Study on the Structure of Egg Shell of *Enterobius Vermicularis* (Linnaeus, 1758) Leach, 1853, with the Electron Microscope." *Acta Medicinæ Okayama* 11 (1). <http://ousar.lib.okayama-u.ac.jp/en/31677>.
- InterPro. 2021. "IPR017943." 2021. <https://www.ebi.ac.uk/interpro/entry/InterPro/IPR017943/>.
- Jacobs, L., M. F. Jones, and Others. 1939. "Studies on Oxyuriasis. XXI. The Chemistry of the Membranes of the Pinworm Egg." *Proceedings of the Helminthological Society of Washington* 6 (2): 57–60.
- James, Kylie R., Tomas Gomes, Rasa Elmentaite, Nitin Kumar, Emily L. Gulliver, Hamish W. King, Mark D. Stares, et al. 2020. "Distinct Microbial and Immune Niches of the Human Colon." *Nature Immunology* 21 (3): 343–53.
- Jansson, Lena, Jonas Angström, Michael Lebens, Anne Imberty, Annabelle Varrot, and Susann Teneberg. 2010. "Carbohydrate Binding Specificities and Crystal Structure of the Cholera Toxin-like B-Subunit from *Citrobacter Freundii*." *Biochimie* 92 (5): 482–90.
- Jex, Aaron R., Peter Nejsum, Erich M. Schwarz, Li Hu, Neil D. Young, Ross S. Hall, Pasi K. Korhonen, et al. 2014. "Genome and Transcriptome of the Porcine Whipworm *Trichuris Suis*." *Nature Genetics* 46 (7): 701–6.
- Jiao, Li, Themistoklis Kourkoumpetis, Diane Hutchinson, Nadim J. Ajami, Kristi Hoffman, Donna L. White, David Y. Graham, et al. 2021. "Spatial Characteristics of Colonic Mucosa-Associated Gut Microbiota in Humans." *Microbial Ecology*, July. <https://doi.org/10.1007/s00248-021-01789-6>.
- Johansson, M. E. V., and J. M. H. Larsson. 2011. "The Two Mucus Layers of Colon Are Organized by the MUC2 Mucin, Whereas the Outer Layer Is a Legislator of Host–microbial Interactions." *Proceedings of the*. https://www.pnas.org/content/108/Supplement_1/4659.short.
- Johnson, Mark, Irena Zaretskaya, Yan Raytselis, Yuri Merezuk, Scott McGinnis, and Thomas L. Madden. 2008. "NCBI BLAST: A Better Web Interface." *Nucleic Acids Research* 36 (Web Server issue): W5–9.
- Johnston, C. E., J. E. Bradley, J. M. Behnke, K. R. Matthews, and K. J. Else. 2005. "Isolates of *Trichuris Muris* Elicit Different Adaptive Immune Responses in Their Murine Host." *Parasite Immunology*. <https://doi.org/10.1111/j.1365-3024.2005.00746.x>.
- Johnston, Wendy L., and James W. Dennis. 2012. "The Eggshell in the *C. Elegans* Oocyte-to-Embryo Transition." *Genesis* 50 (4): 333–49.
- Jones, C. H., J. S. Pinkner, R. Roth, J. Heuser, A. V. Nicholes, S. N. Abraham, and S. J. Hultgren. 1995. "FimH Adhesin of Type 1 Pili Is Assembled into a Fibrillar Tip Structure in the Enterobacteriaceae." *Proceedings of the National Academy of Sciences of the United States of America* 92 (6): 2081–85.
- Jörnvall, H., B. Persson, M. Krook, S. Atrian, R. González-Duarte, J. Jeffery, and D. Ghosh. 1995. "Short-Chain Dehydrogenases/reductases (SDR)." *Biochemistry* 34 (18): 6003–13.

- Jourdan, Peter Mark, Poppy H. L. Lamberton, Alan Fenwick, and David G. Addiss. 2018. "Soil-Transmitted Helminth Infections." *The Lancet* 391 (10117): 252–65.
- Józsi, Mihály. 2017. "Factor H Family Proteins in Complement Evasion of Microorganisms." *Frontiers in Immunology* 8 (May): 571.
- Juge, Nathalie. 2019. "Special Issue: Gut Bacteria-Mucus Interaction." *Microorganisms* 7 (1): 6.
- Justus, D. E., and M. H. Ivey. 1969. "Chitinase Activity in Developmental Stages of *Ascaris Suum* and Its Inhibition by Antibody." *The Journal of Parasitology* 55 (3): 472–76.
- Kang, Dongwan D., Feng Li, Edward Kirton, Ashleigh Thomas, Rob Egan, Hong An, and Zhong Wang. 2019. "MetaBAT 2: An Adaptive Binning Algorithm for Robust and Efficient Genome Reconstruction from Metagenome Assemblies." *PeerJ* 7 (July): e7359.
- Kararli, T. T. 1995. "Comparison of the Gastrointestinal Anatomy, Physiology, and Biochemistry of Humans and Commonly Used Laboratory Animals." *Biopharmaceutics & Drug Disposition* 16 (5): 351–80.
- Karlsson, Caroline L. J., Jenny Onnerfält, Jie Xu, Göran Molin, Siv Ahnér, and Kristina Thorngren-Jerneck. 2012. "The Microbiota of the Gut in Preschool Children with Normal and Excessive Body Weight." *Obesity* 20 (11): 2257–61.
- Kastl, Arthur J., Natalie A. Terry, Gary D. Wu, and Lindsey G. Albenberg. 2020. "The Structure and Function of the Human Small Intestinal Microbiota: Current Understanding and Future Directions." *Cellular and Molecular Gastroenterology and Hepatology*. <https://doi.org/10.1016/j.jcmgh.2019.07.006>.
- Katoh, Kazutaka, and Daron M. Standley. 2013. "MAFFT Multiple Sequence Alignment Software Version 7: Improvements in Performance and Usability." *Molecular Biology and Evolution* 30 (4): 772–80.
- Kempf, Isabelle, Annaelle Kerouanton, Stéphanie Bougeard, Bérengère Nagard, Valérie Rose, Gwénaëlle Mourand, Julia Osterberg, Martine Denis, and Björn O. Bengtsson. 2017. "Campylobacter Coli in Organic and Conventional Pig Production in France and Sweden: Prevalence and Antimicrobial Resistance." *Frontiers in Microbiology* 8 (May): 955.
- Kergunteuil, Alan, Raquel Campos-Herrera, Sara Sánchez-Moreno, Pascal Vittoz, and Sergio Rasmann. 2016. "The Abundance, Diversity, and Metabolic Footprint of Soil Nematodes Is Highest in High Elevation Alpine Grasslands." *Frontiers in Ecology and Evolution* 4: 84.
- Kerry, Brian R., and William M. Hominick. 2002. "Biological Control." In *The Biology of Nematodes*, edited by Donald L. Lee, 932–84. Taylor & Francis London.
- Kim, Boo-Young, Hyang Rim Park, Ji-Hyeon Shin, Sung Won Kim, Jin Hee Cho, Yong Jin Park, and Soo Whan Kim. 2014. "The Serine Protease Inhibitor, 4-(2-Aminoethyl) Benzene Sulfonyl Fluoride Hydrochloride, Reduces Allergic Inflammation in a House Dust Mite Allergic Rhinitis Mouse Model." *Allergy, Asthma & Immunology Research* 6 (6): 558–66.
- Klementowicz, Joanna E., Mark A. Travis, and Richard K. Grencis. 2012. "Trichuris Muris: A Model of Gastrointestinal Parasite Infection." *Seminars in Immunopathology* 34 (6): 815–28.
- Koyama, Koichi. 2013. "Evidence for Bacteria-Independent Hatching of *Trichuris Muris* Eggs." *Parasitology Research* 112 (4): 1537–42.
- . 2016. "Bacteria-Induced Hatching of *Trichuris Muris* Eggs Occurs without Direct Contact between Eggs and Bacteria." *Parasitology Research* 115 (1): 437–40.
- Kubickova, Barbara, Pavel Babica, Klára Hilscherová, and Lenka Šindlerová. 2019. "Effects of Cyanobacterial Toxins on the Human Gastrointestinal Tract and the Mucosal Innate Immune System." *Environmental Sciences Europe* 31 (1): 31.
- Kultima, Jens Roat, Shinichi Sunagawa, Junhua Li, Weineng Chen, Hua Chen, Daniel R. Mende, Manimozhiyan Arumugam, et al. 2012. "MOCAT: A Metagenomics Assembly and Gene Prediction Toolkit." *PloS One* 7 (10): e47656.
- Kuwabara, Patricia E., and Michel Labouesse. 2002. "The Sterol-Sensing Domain: Multiple

- Families, a Unique Role?" *Trends in Genetics: TIG* 18 (4): 193–201.
- Lambshhead, P. J. D. 1993. "Recent Developments in Marine Benthic Biodiversity Research." *Oceanis* 19: 5–24.
- Laughlin, C. W., J. A. Lugthart, and J. M. Vargas. 1974. "Observations on the Emergence of *Heterodera Iri* from the Egg." *Journal of Nematology* 6 (2): 100–101.
- Lawson, Melissa A. E., Ian S. Roberts, and Richard K. Grensis. 2021. "The Interplay between *Trichuris* and the Microbiota." *Parasitology*, June, 1–8.
- Lee, Donald L. 2002a. "Cuticle, Moulting and Exsheathment." In *The Biology of Nematodes*, edited by Donald L. Lee, 171–209. Taylor & Francis London.
- . 2002b. "Life Cycles." In *The Biology of Nematodes*, edited by Donald L. Lee, 61–72. CRC Press Boca Raton, FL, USA.
- Letunic, Ivica, and Peer Bork. 2021. "Interactive Tree Of Life (iTOL) v5: An Online Tool for Phylogenetic Tree Display and Annotation." *Nucleic Acids Research*. <https://doi.org/10.1093/nar/gkab301>.
- Leylabadlo, Hamed Ebrahimzadeh, Reza Ghotaslou, Mohammad Mehdi Feizabadi, Safar Farajnia, Seyed Yaghoob Moaddab, Khudaverdi Ganbarov, Ehsaneh Khodadadi, et al. 2020. "The Critical Role of *Faecalibacterium Prausnitzii* in Human Health: An Overview." *Microbial Pathogenesis* 149 (December): 104344.
- Ley, Ruth E., Daniel A. Peterson, and Jeffrey I. Gordon. 2006. "Ecological and Evolutionary Forces Shaping Microbial Diversity in the Human Intestine." *Cell* 124 (4): 837–48.
- Li, Dinghua, Chi-Man Liu, Ruibang Luo, Kunihiro Sadakane, and Tak-Wah Lam. 2015. "MEGAHIT: An Ultra-Fast Single-Node Solution for Large and Complex Metagenomics Assembly via Succinct de Bruijn Graph." *Bioinformatics* 31 (10): 1674–76.
- Li, Heng, and Richard Durbin. 2009. "Fast and Accurate Short Read Alignment with Burrows–Wheeler Transform." *Bioinformatics* 25 (14): 1754–60.
- Lim, J. K., N. W. Gunther 4th, H. Zhao, D. E. Johnson, S. K. Keay, and H. L. Mobley. 1998. "In Vivo Phase Variation of *Escherichia Coli* Type 1 Fimbrial Genes in Women with Urinary Tract Infection." *Infection and Immunity* 66 (7): 3303–10.
- Lindgren, Kristina, Stefan Gunnarsson, Johan Höglund, Cecilia Lindahl, and Allan Roepstorff. 2020. "Nematode Parasite Eggs in Pasture Soils and Pigs on Organic Farms in Sweden." *Organic Agriculture* 10 (3): 289–300.
- Li, Robert W., Sitao Wu, Weizhong Li, Karl Navarro, Robin D. Couch, Dolores Hill, and Joseph F. Urban Jr. 2012. "Alterations in the Porcine Colon Microbiota Induced by the Gastrointestinal Nematode *Trichuris Suis*." *Infection and Immunity* 80 (6): 2150–57.
- Lok, James B. 2019. "CRISPR/Cas9 Mutagenesis and Expression of Dominant Mutant Transgenes as Functional Genomic Approaches in Parasitic Nematodes." *Frontiers in Genetics* 10 (July): 656.
- Lopez-Siles, Mireia, Sylvia H. Duncan, L. Jesús Garcia-Gil, and Margarita Martinez-Medina. 2017. "*Faecalibacterium Prausnitzii*: From Microbiology to Diagnostics and Prognostics." *The ISME Journal* 11 (4): 841–52.
- Lopez-Siles, Mireia, Núria Enrich-Capó, Xavier Aldeguer, Miriam Sabat-Mir, Sylvia H. Duncan, L. Jesús Garcia-Gil, and Margarita Martinez-Medina. 2018. "Alterations in the Abundance and Co-Occurrence of *Akkermansia Muciniphila* and *Faecalibacterium Prausnitzii* in the Colonic Mucosa of Inflammatory Bowel Disease Subjects." *Frontiers in Cellular and Infection Microbiology* 8 (September): 281.
- Love, Michael, Simon Anders, and Wolfgang Huber. 2014. "Differential Analysis of Count Data--the DESeq2 Package." *Genome Biology* 15 (550): 10–1186.
- Lu, Nancy C., C. Newton, and E. L. R. Stokstad. 1977. "The Requirement of Sterol and Various Sterol Precursors in Free-Living Nematodes." *Nematologica* 23 (1): 57–61.
- Lu, Zheng, and James A. Imlay. 2021. "When Anaerobes Encounter Oxygen: Mechanisms of Oxygen Toxicity, Tolerance and Defence." *Nature Reviews. Microbiology*, June. <https://doi.org/10.1038/s41579-021-00583-y>.
- Malick, L. E., and R. B. Wilson. 1975. "Modified Thiocarbohydrazide Procedure for Scanning Electron Microscopy: Routine Use for Normal, Pathological, or Experimental Tissues." *Stain Technology* 50 (4): 265–69.

- Mallick, H., A. Rahnavard, L. J. McIver, S. Ma, and Y. Zhang. 2021. "Multivariable Association Discovery in Population-Scale Meta-Omics Studies." *Biorxiv*. <https://www.biorxiv.org/content/10.1101/2021.01.20.427420v1.abstract>.
- Marchesi, Julian R., David H. Adams, Francesca Fava, Gerben D. A. Hermes, Gideon M. Hirschfield, Georgina Hold, Mohammed Nabil Quraishi, et al. 2016. "The Gut Microbiota and Host Health: A New Clinical Frontier." *Gut* 65 (2): 330–39.
- Marsh, Alan J., Kshipra Chandrashekhar, Sandy Ng, Jeff Roach, Scott T. Magness, and M. Andrea Azcarate-Peril. 2020. "Genome Sequence of *Citrobacter Freundii* AMC0703, Isolated from the Intestinal Lumen of an 11-Year-Old Organ Donor." *Microbiology Resource Announcements* 9 (46). <https://doi.org/10.1128/MRA.00994-20>.
- Masler, E. P., and R. N. Perry. 2018. "Hatch, Survival and Sensory Perception." In *Cyst Nematodes*, 44–73. Wallingford: CABI.
- Matthews, Bernard E. 1985. "The Influence of Temperature and Osmotic Stress on the Development and Eclosion of Hookworm Eggs." *Journal of Helminthology* 59 (3): 217–24.
- Maung, M. 1978. "The Occurrence of the Second Moults of *Ascaris Lumbricoides* and *Ascaris Suum*." *International Journal for Parasitology* 8 (5): 371–78.
- McMullen, B. A., K. Fujikawa, and E. W. Davie. 1991. "Location of the Disulfide Bonds in Human Plasma Prekallikrein: The Presence of Four Novel Apple Domains in the Amino-Terminal Portion of the Molecule." *Biochemistry* 30 (8): 2050–56.
- McOrist, A. L., M. Warhurst, S. McOrist, and A. R. Bird. 2001. "Colonic Infection by *Bilophila Wadsworthia* in Pigs." *Journal of Clinical Microbiology* 39 (4): 1577–79.
- Meng, X. Q., S. S. Wang, B. X. Wang, G. H. Ying, X. Y. Li, and Y. Z. Zhao. 1981. "The Membranous Structure of Eggs of *Ascaris Lumbricoides* as Revealed by Scanning Electron Microscopy." *Scanning Electron Microscopy*, no. Pt 3: 187–90.
- Mercer, C. F., D. R. Greenwood, and J. L. Grant. 1992. "Effect of Plant and Microbial Chitinases On the Eggs and Juveniles of Meloidogyne Hapla Chitwood (Nematoda: Tylenchida)." *Nematologica*. <https://doi.org/10.1163/187529292x00199>.
- Miller, P. H., L. S. Wiggs, and J. M. Miller. 1995. "Evaluation of AnaeroGen System for Growth of Anaerobic Bacteria." *Journal of Clinical Microbiology* 33 (9): 2388–91.
- Miquel, S., R. Martín, O. Rossi, L. G. Bermúdez-Humarán, J. M. Chatel, H. Sokol, M. Thomas, J. M. Wells, and P. Langella. 2013. "*Faecalibacterium Prausnitzii* and Human Intestinal Health." *Current Opinion in Microbiology*. <https://doi.org/10.1016/j.mib.2013.06.003>.
- Mirelman, D., G. Altmann, and Y. Eshdat. 1980. "Screening of Bacterial Isolates for Mannose-Specific Lectin Activity by Agglutination of Yeasts." *Journal of Clinical Microbiology* 11 (4): 328–31.
- Mkandawire, Tapoka T., Richard K. Grencis, Matthew Berriman, and María A. Duque-Correa. 2021. "Hatching of Parasitic Nematode Eggs: A Crucial Step Determining Infection." *Trends in Parasitology* 0 (0). <https://doi.org/10.1016/j.pt.2021.08.008>.
- Möhrlen, Frank, Harald Hutter, and Robert Zwillig. 2003. "The Astacin Protein Family in *Caenorhabditis Elegans*." *European Journal of Biochemistry / FEBS* 270 (24): 4909–20.
- Mujacic, Mirna, and Francois Baneyx. 2006. "Regulation of *Escherichia Coli* hchA, a Stress-Inducible Gene Encoding Molecular Chaperone Hsp31." *Molecular Microbiology*. <https://doi.org/10.1111/j.1365-2958.2006.05207.x>.
- Muller, G. 1953. "Studies on the Life Span of *Ascaris* Eggs in Garden Soil." *Zentralblatt Für Bakteriologie, Parasitenkunde, Infektionskrankheiten Und Hygiene. 1. Abt. Medizinisch-Hygienische Bakteriologie, Virusforschung Und Parasitologie. Originale* 159 (5): 377–79.
- Murphy, Chelsea L., James Biggerstaff, Alexis Eichhorn, Essences Ewing, Ryan Shahan, Diana Soriano, Sydney Stewart, et al. 2021. "Genomic Characterization of Three Novel Desulfobacterota Classes Expand the Metabolic and Phylogenetic Diversity of the Phylum." *Environmental Microbiology* 23 (8): 4326–43.
- Navitsky, R. C., M. L. Dreyfuss, J. Shrestha, S. K. Khatry, R. J. Stoltzfus, and M. Albonico. 1998. "*Ancylostoma Duodenale* Is Responsible for Hookworm Infections among

- Pregnant Women in the Rural Plains of Nepal." *The Journal of Parasitology* 84 (3): 647–51.
- Nayfach, Stephen, Zhou Jason Shi, Rekha Seshadri, Katherine S. Pollard, and Nikos C. Kyrpides. 2019. "New Insights from Uncultivated Genomes of the Global Human Gut Microbiome." *Nature* 568 (7753): 505–10.
- Nicol, J. M., S. J. Turner, D. L. Coyne, L. D. Nijs, S. Hockland, and Z. T. Maafi. 2011. "Current Nematode Threats to World Agriculture. Jones J, Gheysen G, Fenoll C, Editor. Genomics & Molecular Genetics of Plant-Nematode Interactions." Springer London (UK).
- Nolf, L. O. 1932. "Experimental Studies on Certain Factors Influencing the Development and Viability of the Ova of the Human *Trichuris* as Compared with Those of the Human *Ascaris*." *American Journal of Epidemiology*.
<https://doi.org/10.1093/oxfordjournals.aje.a117862>.
- Nowak, M. A., M. C. Boerlijst, J. Cooke, and J. M. Smith. 1997. "Evolution of Genetic Redundancy." *Nature* 388 (6638): 167–71.
- Ochi, Kozo, Yukinori Tanaka, and Shigeo Tojo. 2014. "Activating the Expression of Bacterial Cryptic Genes by *rpoB* Mutations in RNA Polymerase or by Rare Earth Elements." *Journal of Industrial Microbiology & Biotechnology* 41 (2): 403–14.
- Ochola, Juliet, Laura Cortada, Margaret Ng'ang'a, Ahmed Hassanali, Danny Coyne, and Baldwyn Torto. 2020. "Mediation of Potato–Potato Cyst Nematode, *G. rostochiensis* Interaction by Specific Root Exudate Compounds." *Frontiers in Plant Science* 11: 649.
- O'Dempsey, Tim. 2010. "Helminthic Infections." In *Antibiotic and Chemotherapy*, 842–59. Elsevier.
- Ogasawara, Hiroshi, Toshiyuki Ishizuka, Shuhei Hotta, Michiko Aoki, Tomohiro Shimada, and Akira Ishihama. 2020. "Novel Regulators of the *csgD* Gene Encoding the Master Regulator of Biofilm Formation in *Escherichia Coli* K-12." *Microbiology* 166 (9): 880–90.
- O'Halloran, Damien M. 2021. "CRISPR-PN2: A Flexible and Genome-Aware Platform for Diverse CRISPR Experiments in Parasitic Nematodes." *BioTechniques* 71 (3): 495–98.
- Oksanen, Jari, Roeland Kindt, Pierre Legendre, Bob O'Hara, M. Henry H. Stevens, Maintainer Jari Oksanen, and Mass Suggests. 2007. "The Vegan Package." *Community Ecology Package* 10 (631-637): 719.
- Olonen, Anne, Nisse Kalkkinen, and Lars Paulin. 2003. "A New Type of Cysteine Proteinase Inhibitor--the Salarin Gene from Atlantic Salmon (*Salmo Salar* L.) and Arctic Charr (*Salvelinus Alpinus*)." *Biochimie* 85 (7): 677–81.
- On, S. L., B. Bloch, B. Holmes, B. Hoste, and P. Vandamme. 1995. "Campylobacter Hyointestinalis Subsp. Lawsonii Subsp. Nov., Isolated from the Porcine Stomach, and an Emended Description of Campylobacter Hyointestinalis." *International Journal of Systematic Bacteriology* 45 (4): 767–74.
- Ortega-Anaya, Joana, Alice Marciniak, and Rafael Jiménez-Flores. 2021. "Milk Fat Globule Membrane Phospholipids Modify Adhesion of Lactobacillus to Mucus-Producing Caco-2/Goblet Cells by Altering the Cell Envelope." *Food Research International* 146 (August): 110471.
- Page, Andrew J., Nishadi De Silva, Martin Hunt, Michael A. Quail, Julian Parkhill, Simon R. Harris, Thomas D. Otto, and Jacqueline A. Keane. 2016. "Robust High-Throughput Prokaryote de Novo Assembly and Improvement Pipeline for Illumina Data." *Microbial Genomics* 2 (8): e000083.
- Panesar, Tarlochan S. 1981. "The Early Phase of Tissue Invasion by *Trichuris Muris* (Nematoda: Trichuroidea)." *Zeitschrift Für Parasitenkunde* 66 (2): 163–66.
- Panesar, Tarlochan S., and Neil A. Croll. 1980. "The Location of Parasites within Their Hosts: Site Selection by *Trichuris Muris* in the Laboratory Mouse." *International Journal for Parasitology*. [https://doi.org/10.1016/0020-7519\(80\)90006-5](https://doi.org/10.1016/0020-7519(80)90006-5).
- . 1981. "The Hatching Process in *Trichuris Muris* (Nematoda: Trichuroidea)." *Canadian Journal of Zoology*. <https://doi.org/10.1139/z81-091>.
- Paralanov, Vanya, Jin Lu, Lynn B. Duffy, Donna M. Crabb, Susmita Shrivastava, Barbara A. Methé, Jason Inman, et al. 2012. "Comparative Genome Analysis of 19 *Ureaplasma*

- Urealyticum and Ureaplasma Parvum Strains." *BMC Microbiology* 12 (May): 88.
- Parker, Bianca J., Pamela A. Wearsch, Alida C. M. Veloo, and Alex Rodriguez-Palacios. 2020. "The Genus Alistipes: Gut Bacteria With Emerging Implications to Inflammation, Cancer, and Mental Health." *Frontiers in Immunology* 11 (June): 906.
- Parks, Donovan H., Michael Imelfort, Connor T. Skennerton, Philip Hugenholtz, and Gene W. Tyson. 2015. "CheckM: Assessing the Quality of Microbial Genomes Recovered from Isolates, Single Cells, and Metagenomes." *Genome Research* 25 (7): 1043–55.
- Parks, Donovan H., Christian Rinke, Maria Chuvochina, Pierre-Alain Chaumeil, Ben J. Woodcroft, Paul N. Evans, Philip Hugenholtz, and Gene W. Tyson. 2017. "Recovery of Nearly 8,000 Metagenome-Assembled Genomes Substantially Expands the Tree of Life." *Nature Microbiology* 2 (11): 1533–42.
- Perry, Roland. 2002. "Hatching." In *The Biology of Nematodes*, edited by Donald L. Lee, 147–70. Taylor & Francis London.
- Pike, Lindsay Jacqueline. 2020. "Characterising Antibiotic Susceptibility and Resistance in Human Commensal Gut Bacteria." Apollo - University of Cambridge Repository. <https://doi.org/10.17863/CAM.45970>.
- Powers, James C., Juliana L. Asgian, Ozlem Dogan Ekici, and Karen Ellis James. 2002. "Irreversible Inhibitors of Serine, Cysteine, and Threonine Proteases." *Chemical Reviews* 102 (12): 4639–4750.
- Price, Morgan N., Paramvir S. Dehal, and Adam P. Arkin. 2009. "FastTree: Computing Large Minimum Evolution Trees with Profiles instead of a Distance Matrix." *Molecular Biology and Evolution* 26 (7): 1641–50.
- Pullan, Rachel L., Jennifer L. Smith, Rashmi Jasrasaria, and Simon J. Brooker. 2014. "Global Numbers of Infection and Disease Burden of Soil Transmitted Helminth Infections in 2010." *Parasites & Vectors* 7 (January): 37.
- Puschhof, Jens, Cayetano Pleguezuelos-Manzano, Adriana Martinez-Silgado, Ninouk Akkerman, Aurelia Saftien, Charelle Boot, Amy de Waal, et al. 2021. "Intestinal Organoid Cocultures with Microbes." *Nature Protocols*, August. <https://doi.org/10.1038/s41596-021-00589-z>.
- Quilès, Fabienne, Jean-Yves Balandier, and Sandrine Capizzi-Banas. 2006. "In Situ Characterisation of a Microorganism Surface by Raman Microspectroscopy: The Shell of Ascaris Eggs." *Analytical and Bioanalytical Chemistry* 386 (2): 249–55.
- Quintana-Hayashi, Macarena P., and Siddhartha Thakur. 2012. "Longitudinal Study of the Persistence of Antimicrobial-Resistant Campylobacter Strains in Distinct Swine Production Systems on Farms, at Slaughter, and in the Environment." *Applied and Environmental Microbiology* 78 (8): 2698–2705.
- Raimondi, Stefano, Eliana Musmeci, Francesco Candelieri, Alberto Amaretti, and Maddalena Rossi. 2021. "Identification of Mucin Degradors of the Human Gut Microbiota." *Scientific Reports* 11 (1): 11094.
- Rajilić-Stojanović, Mirjana, and Willem M. de Vos. 2014. "The First 1000 Cultured Species of the Human Gastrointestinal Microbiota." *FEMS Microbiology Reviews* 38 (5): 996–1047.
- Rapin, Alexis, and Nicola L. Harris. 2018. "Helminth–Bacterial Interactions: Cause and Consequence." *Trends in Immunology* 39 (9): 724–33.
- Ratner, Laura Daniela, Gaston Emilio La Motta, Olinda Briski, Daniel Felipe Salamone, and Rafael Fernandez-Martin. 2020. "Practical Approaches for Knock-Out Gene Editing in Pigs." *Frontiers in Genetics* 11: 617850.
- Rawlings, N. D., and A. J. Barrett. 1994. "Families of Serine Peptidases." *Methods in Enzymology* 244: 19–61.
- . 1995. "Evolutionary Families of Metallopeptidases." *Methods in Enzymology* 248: 183–228.
- Rawlings, Neil D. 2010. "Peptidase Inhibitors in the MEROPS Database." *Biochimie* 92 (11): 1463–83.
- Rawlings, Neil D., Dominic P. Tolle, and Alan J. Barrett. 2004. "Evolutionary Families of Peptidase Inhibitors." *Biochemical Journal* 378 (Pt 3): 705–16.
- Reiss, Daniel, Michael Cappello, Lisa M. Harrison, and Richard Bungiro. 2007. "An Agar

- Plate Method for Culturing Hookworm Larvae: Analysis of Growth Kinetics and Infectivity Compared With Standard Coproculture Techniques." *The American Journal of Tropical Medicine and Hygiene*. <https://doi.org/10.4269/ajtmh.2007.77.1087>.
- Renahan, Tess, and Ray L. Hong. 2017. "A Species-Specific Nematocide That Results in Terminal Embryogenesis." *The Journal of Experimental Biology* 220 (Pt 18): 3238–47.
- Ribeiro, Helen Silva, Alexandra Martins Santos Soares, Daniella de Jesus Castro Brito, José Tadeu A. Oliveira, and Lívio Martins Costa-Junior. 2021. "Inhibition of Protease and Egg Hatching of *Haemonchus Contortus* by Soybean Seed Exudates." *The Journal of Parasitology* 107 (1): 23–28.
- Rinninella, Emanuele, Pauline Raoul, Marco Cintoni, Francesco Franceschi, Giacinto Miggiano, Antonio Gasbarrini, and Maria Mele. 2019. "What Is the Healthy Gut Microbiota Composition? A Changing Ecosystem across Age, Environment, Diet, and Diseases." *Microorganisms*. <https://doi.org/10.3390/microorganisms7010014>.
- Rivero, Julia, Cristina Cutillas, and Rocío Callejón. 2020. "Trichuris Trichiura (Linnaeus, 1771) from Human and Non-Human Primates: Morphology, Biometry, Host Specificity, Molecular Characterization, and Phylogeny." *Frontiers in Veterinary Science* 7: 626120.
- Rivero, Julia, Ángela María García-Sánchez, Antonio Zurita, Cristina Cutillas, and Rocío Callejón. 2021. "Correction to: Trichuris Trichiura Isolated from *Macaca Sylvanus*: Morphological, Biometrical, and Molecular Study." *BMC Veterinary Research* 17 (1): 160.
- Robbins, R. T., D. J. Brown, J. M. Halbrendt, and T. C. Vrain. 1996. "Compendium of Juvenile Stages of Xiphinema Species (Nematoda: Longidoridae)." *Russian Journal of Nematology* 4: 163–71.
- Rogers, W. P. 1958. "Physiology of the Hatching of Eggs of *Ascaris Lumbricoides*." *Nature* 181 (4620): 1410–11.
- Rogers, W. P., and F. Brooks. 1977. "The Mechanism of Hatching of Eggs of *Haemonchus Contortus*." *International Journal for Parasitology* 7 (1): 61–65.
- Rubinchik, S., A. Seddon, and A. V. Karlyshev. 2012. "Molecular Mechanisms and Biological Role of *Campylobacter Jejuni* Attachment to Host Cells." *European Journal of Microbiology & Immunology* 2 (1): 32–40.
- Rutter, J. M., and R. J. Beer. 1975. "Synergism between *Trichuris Suis* and the Microbial Flora of the Large Intestine Causing Dysentery in Pigs." *Infection and Immunity* 11 (2): 395–404.
- Saheb Kashaf, Sara, Alexandre Almeida, Julia A. Segre, and Robert D. Finn. 2021. "Recovering Prokaryotic Genomes from Host-Associated, Short-Read Shotgun Metagenomic Sequencing Data." *Nature Protocols* 16 (5): 2520–41.
- Saitoh, Yasuaki, Masumi Katane, Tetsuya Miyamoto, Masae Sekine, Taro Sakamoto, Hirotaka Imai, and Hiroshi Homma. 2019. "Secreted D-Aspartate Oxidase Functions in *C. Elegans* Reproduction and Development." *The FEBS Journal* 286 (1): 124–38.
- Sakaguchi, Ei. 2003. "Digestive Strategies of Small Hindgut Fermenters." *Animal Science Journal = Nihon Chikusan Gakkaiho* 74 (5): 327–37.
- Sakon, Hiroshi, Fumiko Nagai, Masami Morotomi, and Ryuichiro Tanaka. 2008. "*Sutterella Parvirubra* Sp. Nov. and *Megamonas Funiformis* Sp. Nov., Isolated from Human Faeces." *International Journal of Systematic and Evolutionary Microbiology* 58 (Pt 4): 970–75.
- Sapir, Amir. 2021. "Why Are Nematodes so Successful Extremophiles?" *Communicative & Integrative Biology* 14 (1): 24–26.
- Schierack, Peter, Nicole Walk, Katja Reiter, Karl D. Weyrauch, and Lothar H. Wieler. 2007. "Composition of Intestinal Enterobacteriaceae Populations of Healthy Domestic Pigs." *Microbiology* 153 (Pt 11): 3830–37.
- Schloissnig, Siegfried, Manimozhiyan Arumugam, Shinichi Sunagawa, Makedonka Mitreva, Julien Tap, Ana Zhu, Alison Waller, et al. 2013. "Genomic Variation Landscape of the Human Gut Microbiome." *Nature* 493 (7430): 45–50.
- Schneewind, O., K. F. Jones, and V. A. Fischetti. 1990. "Sequence and Structural Characteristics of the Trypsin-Resistant T6 Surface Protein of Group A Streptococci."

- Journal of Bacteriology* 172 (6): 3310–17.
- Schröder, J. 1989. "Protein Sequence Homology between Plant 4-coumarate:CoA Ligase and Firefly Luciferase." *Nucleic Acids Research* 17 (1): 460.
- Schroeder, Katrin, Mario Jularic, Samantha M. Horsburgh, Nina Hirschhausen, Claudia Neumann, Anne Bertling, Anja Schulte, et al. 2009. "Molecular Characterization of a Novel Staphylococcus Aureus Surface Protein (SasC) Involved in Cell Aggregation and Biofilm Accumulation." *PloS One* 4 (10): e7567.
- Schwan, William R. 2011. "Regulation of Fim Genes in Uropathogenic Escherichia Coli." *World Journal of Clinical Infectious Diseases* 1 (1): 17–25.
- Seemann, Torsten. 2014. "Prokka: Rapid Prokaryotic Genome Annotation." *Bioinformatics* 30 (14): 2068–69.
- Shatilovich, A. V., A. V. Tchesunov, T. V. Neretina, I. P. Grabarnik, S. V. Gubin, T. A. Vishnivetskaya, T. C. Onstott, and E. M. Rivkina. 2018. "Viable Nematodes from Late Pleistocene Permafrost of the Kolyma River Lowland." *Doklady Biological Sciences: Proceedings of the Academy of Sciences of the USSR, Biological Sciences Sections / Translated from Russian* 480 (1): 100–102.
- Shears, Rebecca K., Allison J. Bancroft, Catherine Sharpe, Richard K. Grencis, and David J. Thornton. 2018. "Vaccination Against Whipworm: Identification of Potential Immunogenic Proteins in Trichuris Muris Excretory/Secretory Material." *Scientific Reports* 8 (1): 4508.
- Shen, Xiang Jun, John F. Rawls, Thomas Randall, Lauren Burcal, Caroline N. Mpande, Natascha Jenkins, Biljana Jovov, Zaid Abdo, Robert S. Sandler, and Temitope O. Keku. 2010. "Molecular Characterization of Mucosal Adherent Bacteria and Associations with Colorectal Adenomas." *Gut Microbes* 1 (3): 138–47.
- Shih, Pei-Yin, James Siho Lee, Ryoji Shinya, Natsumi Kanzaki, Andre Pires-daSilva, Jean Marie Badroos, Elizabeth Goetz, Amir Sapir, and Paul W. Sternberg. 2019. "Newly Identified Nematodes from Mono Lake Exhibit Extreme Arsenic Resistance." *Current Biology: CB* 29 (19): 3339–44.e4.
- Shivakumara, Tagginahalli N., Vishal Singh Somvanshi, Victor Phani, Sonam Chaudhary, Alkesh Hada, Roli Budhwar, Rohit Nandan Shukla, and Uma Rao. 2019. "Meloidogyne Incognita (Nematoda: Meloidogynidae) Sterol-Binding Protein Mi-SBP-1 as a Target for Its Management." *International Journal for Parasitology* 49 (13-14): 1061–73.
- Silverman, P. H., and J. A. Campbell. 1959. "Studies on Parasitic Worms of Sheep in Scotland. I. Embryonic and Larval Development of Haemonchus Contortus at Constant Conditions." *Parasitology* 49 (1-2): 23–38.
- Singh, Santosh Kumar, L. SaiSree, Ravi N. Amrutha, and Manjula Reddy. 2012. "Three Redundant Murein Endopeptidases Catalyse an Essential Cleavage Step in Peptidoglycan Synthesis of Escherichia Coli K12." *Molecular Microbiology* 86 (5): 1036–51.
- Sizova, Maria V., Paul Muller, Nicolai Panikov, Manolis Mandalakis, Tine Hohmann, Amanda Hazen, William Fowle, Tanya Prozorov, Dennis A. Bazylinski, and Slava S. Epstein. 2013. "Stomatobaculum Longum Gen. Nov., Sp. Nov., an Obligately Anaerobic Bacterium from the Human Oral Cavity." *International Journal of Systematic and Evolutionary Microbiology* 63 (Pt 4): 1450–56.
- Smallwood, Taylor B., Paul R. Giacomini, Alex Loukas, Jason P. Mulvenna, Richard J. Clark, and John J. Miles. 2017. "Helminth Immunomodulation in Autoimmune Disease." *Frontiers in Immunology* 8 (April): 453.
- Smith, David, Daniel R. G. Price, Alison Burrells, Marc N. Faber, Katie A. Hildersley, Cosmin Chintoan-Uta, Ambre F. Chapuis, et al. 2021. "The Development of Ovine Gastric and Intestinal Organoids for Studying Ruminant Host-Pathogen Interactions." *Frontiers in Cellular and Infection Microbiology* 11 (September): 733811.
- Smits, Hermelijn H., Bart Everts, Franca C. Hartgers, and Maria Yazdanbakhsh. 2010. "Chronic Helminth Infections Protect Against Allergic Diseases by Active Regulatory Processes." *Current Allergy and Asthma Reports*. <https://doi.org/10.1007/s11882-009-0085-3>.

- Søe, Martin Jensen, Peter Nejsum, Brian Lund Fredensborg, and Christian Moliin Outzen Kapel. 2015. "DNA Typing of Ancient Parasite Eggs from Environmental Samples Identifies Human and Animal Worm Infections in Viking-Age Settlement." *The Journal of Parasitology* 101 (1): 57–63.
- Soloviev, Alexander, Joseph Gallagher, Aline Marnef, and Patricia E. Kuwabara. 2011. "C. Elegans Patched-3 Is an Essential Gene Implicated in Osmoregulation and Requiring an Intact Permease Transporter Domain." *Developmental Biology* 351 (2): 242–53.
- Soo, Rochelle Melissa. 2015. "In Search of Non-Photosynthetic Cyanobacteria." PhD, University of Queensland. https://www.researchgate.net/profile/Karen-Darbinyan/post/In-what-particular-environments-are-Non-photosynthetic-cyanobacteria-most-likely-to-be-found/attachment/5c800aa83843b034242eddd0/AS%3A733515813494786%401551895206587/download/s42780928_phd_submission.pdf.
- Sorek, Rotem, Yiwen Zhu, Christopher J. Creevey, M. Pilar Francino, Peer Bork, and Edward M. Rubin. 2007. "Genome-Wide Experimental Determination of Barriers to Horizontal Gene Transfer." *Science* 318 (5855): 1449–52.
- Spring, Stefan, Boyke Bunk, Cathrin Spröer, Peter Schumann, Manfred Rohde, Brian J. Tindall, and Hans-Peter Klenk. 2016. "Characterization of the First Cultured Representative of Verrucomicrobia Subdivision 5 Indicates the Proposal of a Novel Phylum." *The ISME Journal* 10 (12): 2801–16.
- Sprouffske, Kathleen, and Andreas Wagner. 2016. "Growthcurver: An R Package for Obtaining Interpretable Metrics from Microbial Growth Curves." *BMC Bioinformatics* 17 (April): 172.
- Stamatakis, Alexandros. 2014. "RAxML Version 8: A Tool for Phylogenetic Analysis and Post-Analysis of Large Phylogenies." *Bioinformatics* 30 (9): 1312–13.
- Steimle, Alex, Alessandro De Sciscio, Mareike Neumann, Erica T. Grant, Gabriel V. Pereira, Hiroshi Ohno, Eric C. Martens, and Mahesh S. Desai. 2021. "Constructing a Gnotobiotic Mouse Model with a Synthetic Human Gut Microbiome to Study Host–microbe Cross Talk." *STAR Protocols* 2 (2): 100607.
- Stein, Kathryn K., and Andy Golden. 2018. "The C. Elegans Eggshell." *WormBook: The Online Review of C. Elegans Biology* 2018 (August): 1–36.
- Sun, Jun, and Pradeep K. Dudeja. 2018. *Mechanisms Underlying Host-Microbiome Interactions in Pathophysiology of Human Diseases*. Springer.
- Sykes, Megan, and David H. Sachs. 2019. "Transplanting Organs from Pigs to Humans." *Science Immunology* 4 (41). <https://doi.org/10.1126/sciimmunol.aau6298>.
- Takehara, M., F. Ling, S. Izawa, Y. Inoue, and A. Kimura. 1995. "Molecular Cloning and Nucleotide Sequence of Purine Nucleoside Phosphorylase and Uridine Phosphorylase Genes from Klebsiella Sp." *Bioscience, Biotechnology, and Biochemistry* 59 (10): 1987–90.
- Tamburini, E., and G. Mastromei. 2000. "Do Bacterial Cryptic Genes Really Exist?" *Research in Microbiology* 151 (3): 179–82.
- Tang, Qiang, Ge Jin, Gang Wang, Tianyu Liu, Xiang Liu, Bangmao Wang, and Hailong Cao. 2020. "Current Sampling Methods for Gut Microbiota: A Call for More Precise Devices." *Frontiers in Cellular and Infection Microbiology*. <https://doi.org/10.3389/fcimb.2020.00151>.
- Taylor, D. P. 1962. "Effect of Temperature on Hatching of Aphelenchus Avenae Eggs." *Proceedings of the Helminthological Society of Washington* 29 (1): 52.
- Team, R. Core. 2020. "R: A Language and Environment for Statistical Computing. R Foundation for Statistical Computing [Internet]." *Vienna, Austria*.
- Telford, John L., Michèle A. Barocchi, Immaculada Margarit, Rino Rappuoli, and Guido Grandi. 2006. "Pili in Gram-Positive Pathogens." *Nature Reviews. Microbiology* 4 (7): 509–19.
- Thapa, Sita, Jayna A. Patel, Ursula Reuter-Carlson, and Nathan E. Schroeder. 2017. "Embryogenesis in the Parasitic Nematode Heterodera Glycines Is Independent of Host-Derived Hatching Stimulation." *BMC Developmental Biology* 17 (1): 2.

- Tiersch, K. M., G. Daş, G. V. Samson-Himmelstjerna, and M. Gauly. 2013. "The Role of Culture Media on Embryonation and Subsequent Infectivity of *Capillaria Obsignata* Eggs." *Parasitology Research* 112 (1): 357–64.
- Topalović, Olivera, and Mette Vestergård. 2021. "Can Microorganisms Assist the Survival and Parasitism of Plant-Parasitic Nematodes?" *Trends in Parasitology* 37 (11): 947–58.
- Torres-Morquecho, A., A. Rivera-Tapia, F. González-Velazquez, J. Torres, B. Chávez-Munguia, L. Cedillo-Ramírez, and Silvia Giono-Cerezo. 2010. "Adherence and Damage to Epithelial Cells of Human Lung by *Ureaplasma Urealyticum* Strains Biotype 1 and 2." *African Journal of Microbiology Research* 4 (6): 480–91.
- Traore, Sory Ibrahima, Esam Ibraheem Azhar, Muhammad Yasir, Fehmida Bibi, P-E Fournier, Asif Ahmad Jiman-Fatani, Jeremy Delerce, Frédéric Cadoret, J-C Lagier, and Didier Raoult. 2017. "Description of 'Blautia Phocaeensis' Sp. Nov. and 'Lachnoclostridium Edouardi' sp. Nov., Isolated from Healthy Fresh Stools of Saudi Arabia Bedouins by Culturomics." *New Microbes and New Infections* 19: 129–31.
- Trapnell, Cole, Lior Pachter, and Steven L. Salzberg. 2009. "TopHat: Discovering Splice Junctions with RNA-Seq." *Bioinformatics* 25 (9): 1105–11.
- Uniprot. 2021. "ATP-Dependent Clp Protease Proteolytic Subunit." 2021. <https://www.uniprot.org/uniprot/A0A2I8THN4>.
- Uritskiy, Gherman V., Jocelyne DiRuggiero, and James Taylor. 2018. "MetaWRAP—a Flexible Pipeline for Genome-Resolved Metagenomic Data Analysis." *Microbiome* 6 (1): 158.
- Vacca, Mirco, Giuseppe Celano, Francesco Maria Calabrese, Piero Portincasa, Marco Gobbetti, and Maria De Angelis. 2020. "The Controversial Role of Human Gut Lachnospiraceae." *Microorganisms*. <https://doi.org/10.3390/microorganisms8040573>.
- Van Gundy, Seymour D. 1965. "Factors in Survival of Nematodes." *Annual Review of Phytopathology* 3 (1): 43–68.
- Vejzagić, Nermina, Roberto Adelfio, Jennifer Keiser, Helene Kringel, Stig Milan Thamsborg, and Christian M. O. Kapel. 2015. "Bacteria-Induced Egg Hatching Differs for *Trichuris Muris* and *Trichuris Suis*." *Parasites & Vectors*. <https://doi.org/10.1186/s13071-015-0986-z>.
- Vejzagić, Nermina, Helene Kringel, Johan Musaeus Bruun, Allan Roepstorff, Stig Milan Thamsborg, Anette Blak Grossi, and Christian M. O. Kapel. 2016. "Temperature Dependent Embryonic Development of *Trichuris Suis* Eggs in a Medicinal Raw Material." *Veterinary Parasitology* 215 (January): 48–57.
- Vejzagić, Nermina, Stig Milan Thamsborg, Helene Kringel, Allan Roepstorff, Johan Musaeus Bruun, and Christian M. O. Kapel. 2015. "In Vitro Hatching of *Trichuris Suis* Eggs." *Parasitology Research*. <https://doi.org/10.1007/s00436-015-4476-1>.
- Venzon, Mericien, Ritika Das, Daniel J. Luciano, Hyun Shin Park, Eric T. Kool, Joel G. Belasco, E. Jane Albert Hubbard, and Ken Cadwell. 2021. "Microbial Byproducts Determine Reproductive Fitness of Free-Living and Parasitic Nematodes." *bioRxiv*. <https://doi.org/10.1101/2021.08.02.454806>.
- Viney, M. E. 1994. "A Genetic Analysis of Reproduction in *Strongyloides Ratti*." *Parasitology* 109 (Pt 4) (November): 511–15.
- Vries, Stefan P. W. de, Aileen Linn, Kareen Macleod, Amanda MacCallum, Simon P. Hardy, Gill Douce, Eleanor Watson, et al. 2017. "Analysis of *Campylobacter Jejuni* Infection in the Gnotobiotic Piglet and Genome-Wide Identification of Bacterial Factors Required for Infection." *Scientific Reports* 7 (March): 44283.
- Wagner, Michael, and Matthias Horn. 2006. "The Planctomycetes, Verrucomicrobia, Chlamydiae and Sister Phyla Comprise a Superphylum with Biotechnological and Medical Relevance." *Current Opinion in Biotechnology* 17 (3): 241–49.
- Wakelin, D. 1965. "Experimental Studies on the Biology of *Capillaria Obsignata* Madsen, 1945, a Nematode Parasite of the Domestic Fowl**." *Journal of Helminthology* 39 (4): 399–412.
- . 1967. "Acquired Immunity to *Trichuris Muris* in the Albino Laboratory Mouse." *Parasitology* 57 (3): 515–24.

- . 1969. "The Development of the Early Larval Stages of *Trichuris Muris* in the Albino Laboratory Mouse." *Journal of Helminthology* 43 (3): 427–36.
- Waller, P. J. 1971. "Structural Differences in the Egg Envelopes of *Haemonchus Contortus* and *Trichostrongylus Colubriformis* (Nematoda: Trichostrongylidae)." *Parasitology* 62 (1): 157–60.
- Wang, Jianbin, Julianne Garrey, and Richard E. Davis. 2014. "Transcription in Pronuclei and One- to Four-Cell Embryos Drives Early Development in a Nematode." *Current Biology: CB* 24 (2): 124–33.
- Wang, J. T., S. C. Chang, Y. C. Chen, and K. T. Luh. 2000. "Comparison of Antimicrobial Susceptibility of *Citrobacter Freundii* Isolates in Two Different Time Periods." *Journal of Microbiology, Immunology, and Infection = Wei Mian Yu Gan Ran Za Zhi* 33 (4): 258–62.
- Wang, Mei, and Sharon M. Donovan. 2015. "Human Microbiota-Associated Swine: Current Progress and Future Opportunities." *ILAR Journal / National Research Council, Institute of Laboratory Animal Resources* 56 (1): 63–73.
- Ward, Jordan D. 2015. "Rendering the Intractable More Tractable: Tools from *Caenorhabditis Elegans* Ripe for Import into Parasitic Nematodes." *Genetics* 201 (4): 1279–94.
- Ward, K. A., and D. Fairbairn. 1972. "Chitinase in Developing Eggs of *Ascaris Suum* (Nematoda)." *The Journal of Parasitology* 58 (3): 546–49.
- Wehr, Everett Elmer. 1939. *Studies on the Development of the Pigeon Capillarid, Capillaria Columbae*. U.S. Department of Agriculture.
- Wesemael, Wim, Roland Perry, and Maurice Moens. 2006. "The Influence of Root Diffusate and Host Age on Hatching of the Root-Knot Nematodes, *Meloidogyne Chitwoodi* and *M. Fallax*." *Nematology: International Journal of Fundamental and Applied Nematological Research* 8 (6): 895–902.
- Wharton, D. 1980. "Nematode Egg-Shells." *Parasitology* 81 (2): 447–63.
- Wharton, D. A., and T. Jenkins. 1978. "Structure and Chemistry of the Egg-Shell of a Nematode (*Trichuris Suis*)." *Tissue & Cell* 10 (3): 427–40.
- White, Emily C., Ashley Houlden, Allison J. Bancroft, Kelly S. Hayes, Marie Goldrick, Richard K. Grencis, and Ian S. Roberts. 2018. "Manipulation of Host and Parasite Microbiotas: Survival Strategies during Chronic Nematode Infection." *Science Advances* 4 (3): eaap7399.
- Wilkinson, David A., Andrew J. O'Donnell, Rukhshana N. Akhter, Ahmed Fayaz, Hamish J. Mack, Lynn E. Rogers, Patrick J. Biggs, Nigel P. French, and Anne C. Midwinter. 2018. "Updating the Genomic Taxonomy and Epidemiology of *Campylobacter Hyointestinalis*." *Scientific Reports* 8 (1): 2393.
- Wood, Derrick E., Jennifer Lu, and Ben Langmead. 2019. "Improved Metagenomic Analysis with Kraken 2." *Genome Biology* 20 (1): 257.
- WormBase ParaSite. 11-Apr-2019. "Trichuris Muris strain:Edinburgh- PRJEB126." 11-Apr-2019. <https://www.ncbi.nlm.nih.gov/bioproject/PRJEB126>.
- . 2014a. "Trichuris Trichiura -prjeb535." 2014. https://parasite.wormbase.org/Trichuris_trichiura_prjeb535/Info/Index.
- . 2014b. "Trichuris Suis- prjna179528." May 2014. https://parasite.wormbase.org/Trichuris_suis_prjna179528/Info/Index.
- . 2019. "Trichuris Muris- prjeb126." April 11, 2019. https://parasite.wormbase.org/Trichuris_muris_prjeb126/Info/Index.
- Wu, Yu-Wei, Blake A. Simmons, and Steven W. Singer. 2016. "MaxBin 2.0: An Automated Binning Algorithm to Recover Genomes from Multiple Metagenomic Datasets." *Bioinformatics* 32 (4): 605–7.
- Xiang, Yunqing, Hui Wen, Yue Yu, Mingqiang Li, Xiongfei Fu, and Shuqiang Huang. 2020. "Gut-on-Chip: Recreating Human Intestine in Vitro." *Journal of Tissue Engineering* 11 (January): 2041731420965318.
- Xiong, Ronglu, Daodong Pan, Zhen Wu, Yuxing Guo, Xiaoqun Zeng, and Liwei Lian. 2018. "Structure and Immunomodulatory Activity of a Recombinant Mucus-Binding Protein of

- Lactobacillus Acidophilus." *Future Microbiology* 13 (December): 1731–43.
- Yamamoto, Natsuko, Kenji Nakahigashi, Tomoko Nakamichi, Mihoko Yoshino, Yuki Takai, Yae Touda, Akemi Furubayashi, et al. 2009. "Update on the Keio Collection of Escherichia Coli Single-Gene Deletion Mutants." *Molecular Systems Biology* 5 (1): 335.
- Yang, Guodong, Baoli Zhou, Xinyu Zhang, Zijun Zhang, Yuanyuan Wu, Yiming Zhang, Shuwen Lü, Qingdao Zou, Yuan Gao, and Long Teng. 2016. "Effects of Tomato Root Exudates on Meloidogyne Incognita." *PloS One* 11 (4): e0154675.
- Yang, Jianyi, Renxiang Yan, Ambrish Roy, Dong Xu, Jonathan Poisson, and Yang Zhang. 2015. "The I-TASSER Suite: Protein Structure and Function Prediction." *Nature Methods* 12 (1): 7–8.
- Yarbrough, Victoria L., Sean Winkle, and Melissa M. Herbst-Kralovetz. 2015. "Antimicrobial Peptides in the Female Reproductive Tract: A Critical Component of the Mucosal Immune Barrier with Physiological and Clinical Implications." *Human Reproduction Update* 21 (3): 353–77.
- Zhang, Jianbo, Yu-Ja Huang, Jun Young Yoon, John Kemmitt, Charles Wright, Kirsten Schneider, Pierre Sphabmixay, et al. 2021. "Primary Human Colonic Mucosal Barrier Crosstalk with Super Oxygen-Sensitive Faecalibacterium Prausnitzii in Continuous Culture." *Med (New York, N.Y.)* 2 (1): 74–98.e9.
- Zheng, Leon, Caleb J. Kelly, and Sean P. Colgan. 2015. "Physiologic Hypoxia and Oxygen Homeostasis in the Healthy Intestine. A Review in the Theme: Cellular Responses to Hypoxia." *American Journal of Physiology. Cell Physiology* 309 (6): C350–60.
- Zou, Yuanqiang, Wenbin Xue, Guangwen Luo, Ziqing Deng, Panpan Qin, Ruijin Guo, Haipeng Sun, et al. 2019. "1,520 Reference Genomes from Cultivated Human Gut Bacteria Enable Functional Microbiome Analyses." *Nature Biotechnology* 37 (2): 179–85.
- Zugasti, Olivier, Jeena Rajan, and Patricia E. Kuwabara. 2005. "The Function and Expansion of the Patched- and Hedgehog-Related Homologs in C. Elegans." *Genome Research* 15 (10): 1402–10.